

**Mechanisms influencing the sensitivity of *Alternaria solani* causing
Early Blight on potato towards demethylation inhibitors**

Dissertation

**zur Erlangung des
Doktorgrades der Naturwissenschaften (Dr. rer. nat.)**

der

Naturwissenschaftlichen Fakultät III
Agrar- und Ernährungswissenschaften,
Geowissenschaften und Informatik



**MARTIN-LUTHER-UNIVERSITÄT
HALLE-WITTENBERG**

vorgelegt von

Frau M. Sc. Ana Carolina Schröder

Halle (Saale), 14.10.2024

Erster Gutachter: Prof. Dr. Holger B. Deising

Zweiter Gutachter: Prof. Dr. Ralf Vögele

Tag der Verteidigung: 10.03.2025

Diese Arbeit wurde unterstützt und finanziert durch die BASF SE, Unternehmensbereich Pflanzenschutz, Forschung Fungizide, Limburgerhof.

Table of contents

1	Introduction	1
1.1	<i>Solanum tuberosum</i> and early blight.....	1
1.2	<i>Alternaria</i> spp.....	2
1.2.1	Relevance.....	2
1.2.2	Taxonomy	2
1.2.3	Disease cycle, infection process and epidemiology	3
1.3	Disease control of early blight	5
1.3.1	Chemical control of <i>A. solani</i> and an introduction to fungicides.....	7
1.3.2	Demethylation inhibitors (DMIs)	9
1.4	Fungicide resistance.....	11
1.4.1	Fungicide resistance to demethylation inhibitors.....	14
1.4.2	Fungicide resistance in <i>A. solani</i>	16
1.5	Objectives	17
2	Material and Methods	19
2.1	Software and bioinformatic analyses.....	19
2.2	Fungal isolates.....	20
2.2.1	Cultivation of <i>A. solani</i> isolates.....	20
2.2.2	Long term storage and recultivation of isolates	20
2.2.3	Obtaining field isolates	21
2.2.4	Generation of single spore isolates	21
2.3	<i>Escherichia coli</i>	21
2.4	Cultivation of tomato plants for greenhouse tests	22
2.5	Potato cultivars for field trials.....	22
2.6	Molecular biological methods	22
2.6.1	Isolation of genomic DNA and RNA.....	22
2.6.2	Reverse transcription of RNA in cDNA	23
2.6.3	Polymerase chain reaction (PCR)	23
2.6.4	Cloning of PCR fragments.....	26
2.6.5	Gel electrophoresis.....	28
2.6.6	PCR clean-up	28
2.6.7	Sequencing.....	29
2.6.8	Pyrosequencing	29
2.6.9	Targeted mutagenesis of <i>A. solani</i>	31
2.6.10	Southern-Blot-hybridization	32
2.7	Fungicide sensitivity tests.....	35
2.7.1	Microtiter tests	35
2.8	Fungicide sensitivity tests in the greenhouse with targeted mutation strains of <i>A. solani</i>	37
2.8.1	Fungicide application	37
2.8.2	Inoculation	38

2.8.3	Evaluation	38
2.9	Efficacy of fungicides in field trials	38
2.9.1	Disease scoring	40
2.9.2	Sampling and isolation of <i>A. solani</i>	40
2.10	Competitiveness and vitality of <i>A. solani</i> haplotypes.....	41
2.10.1	<i>In vivo</i> competition studies in the greenhouse	41
2.10.2	Spore morphology	42
2.10.3	Quantification of spores	42
2.10.4	Infection rate	43
2.10.5	Determination of vegetative growth	43
2.11	Verification of multicellular spores for genetic identity	43
2.12	Homology modelling	44
3	Results	45
3.1	Verification of multicellular spores for genetic identity.....	45
3.2	Identification and characterization of <i>CYP51</i> haplotypes in <i>A. solani</i>	47
3.2.1	First detection of <i>CYP51</i> mutations	47
3.2.2	Molecular characterization of amino acid alterations in the Cyp51 enzyme	49
3.2.3	Alignment of <i>CYP51</i> sequences from different phytopathogenic fungi	51
3.3	Competitiveness and vitality of <i>A. solani</i> haplotypes.....	53
3.3.1	<i>In vivo</i> competition studies with <i>CYP51</i> mutants.....	53
3.3.2	Spore morphology and quantification	54
3.3.3	Infection rate	56
3.3.4	Determination of vegetative growth	56
3.4	Impact of new <i>CYP51</i> alterations on DMI sensitivity in <i>A. solani</i>	58
3.5	Evaluation of cross-resistance between different DMIs in <i>A. solani</i>	59
3.6	Multiple resistance	61
3.6.1	Multiple resistance between Qols and DMIs	61
3.6.2	Multiple resistance between SDHs and DMIs	63
3.7	Efficacy of DMIs in the field	64
3.7.1	Disease assessment.....	64
3.7.2	Composition of <i>CYP51</i> haplotypes in <i>A. solani</i> populations in field trials	66
3.8	Generation of L143F, G446S and L143F+G446S replacement constructs.....	69
3.9	DMI sensitivity of targeted mutation strains of <i>A. solani</i> with mutation L143F, G446S or L143F+G446S	72
3.10	Efficacy of DMIs on targeted mutation strains of <i>A. solani</i> in the greenhouse	75
4	Discussion.....	77
4.1	Confirmation of genetic identity of <i>A. solani</i> multicellular spores	78
4.2	Sequence analysis of <i>CYP51</i> show amino acid alterations	78
4.3	Distribution of <i>CYP51</i> mutation in <i>A. solani</i>	81
4.4	Competitiveness and vitality of <i>A. solani</i> haplotypes.....	82
4.5	<i>In vitro</i> effects of <i>CYP51</i> haplotypes on sensitivity to DMIs in <i>A. solani</i>	85

4.6	Mutations in <i>CYP51</i> in <i>A. solani</i> and their effects on DMIs	87
4.7	Incomplete cross-resistance of <i>A. solani</i> to different DMIs	90
4.8	Multiple resistance	92
4.9	Field efficacy of different DMIs in current <i>A. solani</i> population.....	93
4.10	Prospects for future DMI use	96
5	Summary.....	99
6	Literature	101
7	Appendix	116
7.1	Supplementary tables and figures	116
7.2	List of figures	130
7.3	List of tables.....	131
7.4	Technical Equipment	132
7.5	Fungicides	134
7.6	Chemicals and consumable	136
7.7	Buffers, solutions and growth media	137
7.8	Vectors.....	139
7.9	Oligonucleotides	139
7.10	Abbreviations	143
7.11	Curriculum vitae.....	145
7.12	Danksagung.....	147
7.13	Eidesstattliche Erklärung	149

1 Introduction

1.1 *Solanum tuberosum* and early blight

After wheat and rice, potatoes rank as the third most important crop for human consumption on a global scale (Camire et al. 2009; Barrell et al. 2013). According to the Food and Agriculture Organization Corporate Statistical Database (2022) (FAO 2024), production of potatoes worldwide exceeds 374 million tons per year, with an estimated harvested area for potato cultivation of around 17 million hectares in 2022. With an annual production of over 73 million tons, China is the top producer of potatoes worldwide followed by India, Russia, and the United States. Germany ranks in seventh place with an annual production of 11 million tons (FAO 2024). In terms of protein yield per hectare, potatoes are second to soybeans, with the major storage protein patatin - one of the most nutritionally balanced plant proteins (Liedl et al. 1987). Potatoes are a significant source of starch, protein, antioxidants, and vitamins in the global diet and serve as a storage organ and a vegetative propagation system for the plant (Burlingame et al. 2009).

The cultivated potato (*Solanum tuberosum*) and its wild relatives originated from various Southern American countries and can be classified in four species: *S. tuberosum*, *S. ajanhuiri*, *S. juzepczukii* and *S. curtilobum* with a number of chromosomes set of diploid, triploid, tetraploid or pentaploid (Spooner et al. 2007). Since the end of the 17th century, different varieties have been developed by crossing potato species with the aim to expand genetic valuable traits, such as resistance to pests and disease, tolerance to abiotic stress and others (Plaisted and Hoopes 1989). Early blight can infect members of the Solanaceae like potato, tomato (*Lycopersicon esculentum* Mill.) and others (Pscheidt 1985). Until now, no commercially available potato cultivars exhibit resistance to early blight (Ding et al. 2019), as resistant cultivars do not possess the desired agronomic and commercial traits (Boiteux et al. 1995). In addition to *A. solani*, *Phytophthora infestans*, the causal agent of late blight, is one of the most common diseases on potato, which led to the potato famine in Ireland and still has the potential to cause substantial yield loss (Fry and Goodwin 1997; Abuley and Hansen 2021). Another important disease on potato, is black scurf and stem canker caused by *Rhizoctonia solani*. Black scurf and stem canker have multiple inoculum sources and occur worldwide in potato growing regions (Tsror 2010).

1.2 *Alternaria* spp.

1.2.1 Relevance

Certain *Alternaria* pathogens are prevalent in nearly all countries, whereas others are limited to specific regions. Although the agricultural impact of *A. solani* in different regions varies, this pathogen is recorded in every potato growing region worldwide. Its distribution reaches from Iceland over Europe to equatorial areas in South America, Africa, southern Chile and Argentina (Rotem 1994). In Germany and other countries, yield losses can reach up to 50% depending on environmental conditions, potato varieties and agricultural practices including crop rotation, tillage, and choice of cultivar (Harrison and Venette 1970; Christ and Maczuga 1989; van der Waals et al. 2003; Leiminger and Hausladen 2014; Hausladen et al. 2024).

1.2.2 Taxonomy

The genus *Alternaria* was established in 1817 by Nees, with *Alternaria tenuis* as the type species (Rotem 1994; Thomma 2003). Since then, more than 100 species of *Alternaria* have been described worldwide (Simmons 1992), these can infect a variety of host plants, such as apple, broccoli, cauliflower, carrot, Chinese cabbage, citrus fruit, ornamentals, potato, tomato and weeds (Simmons 1992; Mamgain et al. 2013). The species *A. solani* was first described by Paul Sorauer in 1896, who did not distinguish between *A. solani* and *A. tenuis* (Foolad et al. 2008). However, variability of morphology, which can be influenced by intrinsic and environmental conditions, lead to errors in the taxonomy of *Alternaria* species (Thomma 2003). Consequently, single species have been misleadingly divided into several in the past (Rotem 1994). In the past years, the genus *Alternaria* was divided into 24 sections, based on molecular and morphological data (Woudenberg et al. 2013). The largest section is represented by *Alternaria* sect. *Porri*, including species with large spores with long beaks, such as *A. bataticola*, *A. porri*, *A. solani* and *A. tomatophila*. A molecular approach that used a multi-locus sequence analysis, divided the species in the section *Porri* into 63 morphospecies, including *A. solani*, *A. portenta* and *A. grandis* (Woudenberg et al. 2014). To classify the small-spored *Alternaria* species, Woudenberg et al. (2014) performed further analyses (whole-genome sequencing, transcriptome analysis and multi-gene sequencing) and could identify 11 species, including *A. alternata*, *A. longipes* and *A. gossypina*. It was claimed that *A. alternata* and *A. solani* are the predominant species that cause early blight on tomato (Landschoot et al. 2017a). Interestingly, it was shown that the large spore species *A. solani* is highly virulent on potatoes, whereas *A. alternata* is a rather secondary saprophyte (Stammler et al. 2014). Table 1 presents an overview of the taxonomic classification of the pathogen according to the EPPO code.

Table 1: Taxonomy of *Alternaria solani* (EPPO 2024).

Classification	Name
Kingdom	Fungi
Phylum	Ascomycota
Subphylum	Pezizomycotina
Class	Dothideomycetes
Subclass	Pleosporomycetidae
Order	Pleosporales
Family	Pleosporaceae
Genus	<i>Alternaria</i>
Species	<i>Alternaria solani</i>

1.2.3 Disease cycle, infection process and epidemiology

A. solani overwinters on infected plant material or potato tubers as mycelium or conidia in soil which serve as primary sources of inoculum. Melanin, which is present in the walls of the conidia cells, allows spores to survive for long periods (Pscheidt 1985; Rotem 1994). Because of the short disease cycle of *A. solani*, it tends to be a polycyclic pathogen, where many cycles of infection can occur (Zhang et al. 2018). Moreover, no sexual stages have been reported for the majority of *Alternaria* species, including *A. solani* (Rotem 1994). Typical conidia are brown to black and grow either individually or in small clusters. The morphology differs between various strains within one species and growth media. The length of conidiophores of *A. solani* ranges from 30 to 200 µm and transverse septa vary from three to 14. Sporulation is a two-phase process and near-ultraviolet wavelength radiation (310 - 400 nm) is favorable to induce conidiophore production. Conidiophores are formed in the first phase (inductive phase). Subsequently, conidia are formed on conidiophores in the absence of light and germinate (terminal phase). Spores are distributed by wind, insects, or rain splash from the ground to the lower leaves (Rotem 1994). Infection process is triggered by alternating cycles of wet and dry conditions and cause a reduction of photosynthetic potential due to destruction of the host tissue (Pscheidt 1985; Thomma 2003). After one to three hours, the germ tube emerges from the inner layer of the spore wall and penetration of the plant tissue occurs after two to three hours after formation of the germ tube and appressoria. The pathogen breaches the epidermis and establishes an intercellular presence within the mesophyll tissue where the cells become deformed leading to cell death (Rotem 1994). The disease cycle of early blight is shown in Figure 1 (Agrios 2005).

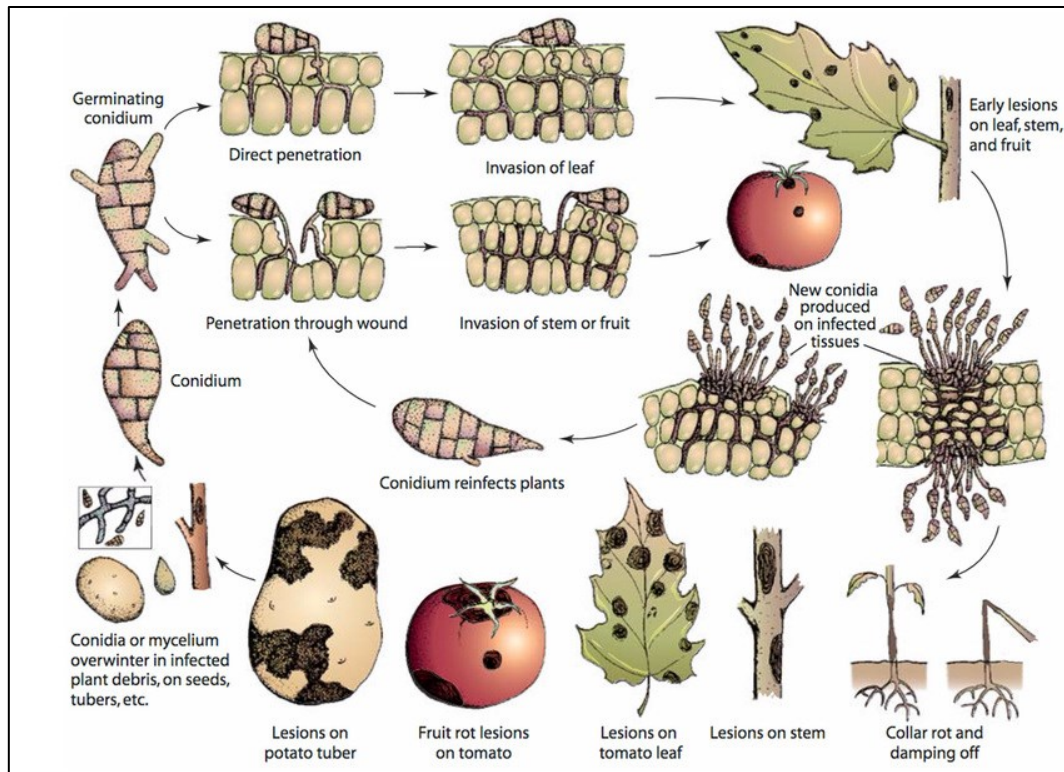


Figure 1: Disease cycle of *Alternaria solani* causing early blight on tomato (Agris, 2005).

Early blight, with its necrotrophic lifestyle, develops an infection of the foliage, this leads to leaf necrosis and complete premature defoliation of plants (Lawrence et al. 2000). In general, tissues are more susceptible to infection when weakened due to stresses, senescence, or wounds (Thomma 2003). It has been reported that resistance to early blight is influenced by the plants' age, with older leaves being more susceptible while on younger leaves low values of early blight severity have been recorded (Dita Rodriguez et al. 2006; Odilbekov et al. 2014). Occasionally, stem infections can occur, symptoms are similar to those on the leaves (Hausladen and Leiminger 2007). Lesions show characteristic concentric rings that appear dark surrounded by a chlorotic halo. The formation of these characteristic rings is attributed to day-night temperature fluctuations, radiation, and leaf moisture (Pscheidt 1985). The chlorotic halo arises because of the non-host-specific toxins, alternaric acid and zinniol that are produced by *A. solani* (Maiero et al. 1991; Lawrence et al. 2000). Many other non-host-specific toxins have been identified in *Alternaria* like brefeldin A (dehydro-)curvularin, tenuazonic acid and tentoxin, the precise function of which is not fully understood (Thomma 2003). Infection on tubers is rare and leads to a dry rot with characteristic dark, irregular, sunken lesions on the surface (Pscheidt 1985). Typical symptoms of *A. solani* and spores are shown in Figure 2.

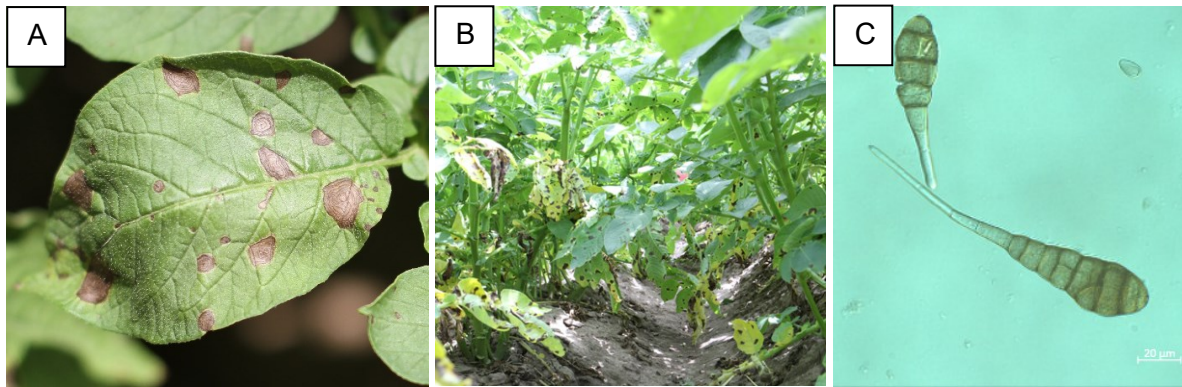


Figure 2: Disease symptoms of *A. solani*.

Symptoms of *A. solani* on a potato leaf showing necrotic lesions with concentric rings (A), front view of *A. solani* infection on potato (B) and *A. solani* spores under the microscope, scale: 50 μm (C).

Spore production is induced during spring season when temperature ranges between 5 and 30°C. Infection can take place at a minimum temperature of 10°C and a maximum of 35 °C, whereat the optimum ranges between 20 and 30°C (Rotem 1994). It has been reported that 8°C is the minimum temperature for spore production. Temperatures below reduces the spread of disease, even when relative humidity is high (van der Waals et al. 2003). Depending on the cultivar, a minimum four hours of leaf wetness is required to initiate infection but an increase above 24 hours, does not result in further infection of leaves (Vloutoglou and Kalogerakis 2000). Moreover, interrupted wetting periods are an important factor for spore formation and their dispersal (van der Waals et al. 2003).

1.3 Disease control of early blight

Controlling early blight requires a combination of agronomical measures, such as crop rotation, sanitation, elimination of infected plants and sustaining host vigor through appropriate nitrogen and phosphorus fertilization, use of resistant cultivars and fungicide treatment (Rotem 1994; Dorrance and Inglis 1997; Chaerani and Voorrips 2006; Rodríguez et al. 2007; Foolad et al. 2008). Further, biocontrol agents can be an alternative to chemical fungicides. However, the effectiveness of biocontrol agents tends to be variable due to weather conditions, plant physiology and genetical status (Ons et al. 2020). Considering that organic farming is lower yielding on average than conventional agriculture, it does not seem realistic to provide sustainable food security for the world's population with organic plant protection (Meemken and Qaim 2018). Nevertheless, the options of fungicide use are limited due to increasing resistance, regulatory for new chemistry and costs. Hence, it is necessary to search for new control strategies (Lucas et al. 2015).

Historical catastrophes, such as the Irish potato famine caused by *P. infestans* from 1845-1849 (Fry and Goodwin 1997) and the Bengal rice famine caused by *Cochliobolus miyabeanus*

(brown spot) of 1943 (Padmanabhan 1973), have shown how devastating fungal pathogens can be. Although those humanitarian events are unlikely to occur nowadays, the potential of fungal pathogens to reduce yield loss should not be overlooked. Yield losses of crops, such as wheat, rice, maize, barley, and potatoes caused by pests and diseases vary from 26-40% depending on the crop, of these, pathogens contribute to 15% of the yield losses (Oerke and Dehne 2004). Future challenges, that include the expanding world population expected to reach 9.7 billion by 2050 and 19.9 billion by 2100, demonstrate the need of effective control strategies (Nations 2019). Additionally, the impact of climate change on crop yield and rural livelihoods are progressively increasing, and if the current situation does not change, food crisis is expected to increase in the future (FAO 2022). Moreover, the relative abundance of soil-borne plant pathogens, such as *A. solani*, will increase with warmer temperatures (Delgado-Baquerizo et al. 2020).

As *A. solani* overwinters in plant debris and soil as mycelia or conidia (Pscheidt 1985; Rotem 1994), it is crucial to compromise primary infections by soil-borne inoculum. It has been reported that a continuous potato system contributes to higher early blight infection compared to other cropping systems, due to the permanent availability of host tissue (Olanya et al. 2009). To delay the occurrence of early blight, a two-year interval between subsequent plantings of potatoes in a crop rotation cycle is necessary (Abuley et al. 2018). The intercropping of marigolds and plastic mulching can also reduce *A. solani* infection, due to a change in the microclimate (Gómez-Rodríguez et al. 2003; Jambhulkar et al. 2012).

Host nutrition, especially nitrogen, is a key component to prevent early blight infections (Barclay et al. 1973; Soltanpour and Harrison 1974; MacKenzie 1981; Miller and Rosen 2005; Mittelstrass et al. 2006). Studies have reported that plants exhibit reduced susceptibility to early blight when nitrogen (N) was supplied (Mittelstrass et al. 2006). However, it is not only the quantity of N that is crucial, but also the timing of fertilization (Rens et al. 2016; Abuley et al. 2019). Interestingly, it was reported that a reduction in phosphorus also led to a reduction in the severity of early blight, and when combined with high N treatment, the infection rate was further reduced (Barclay et al. 1973).

Until now, no reports of any potato cultivar exhibiting complete resistance to early blight are known. Nevertheless, different cultivars show varying levels of disease intensity and show partially resistance (Holley et al. 1983; Christ 1991; Boiteux and Reifschneider 1993; Duarte et al. 2014; Odilbekov et al. 2019; Ding et al. 2019). Moreover, susceptibility is related to foliage maturity of the cultivar, since late maturing cultivars are less susceptible than early maturing cultivars (Christ 1991; Duarte et al. 2014). It was further reported that the number of lesions increased in the lower parts of the plant and decreased in the upper part, indicating that older leaves are more susceptible than younger leaves (Dita Rodriguez et al. 2006).

As an alternative to chemical fungicides, biological control agents are currently under investigation. Studies have shown that *Trichoderma* spp. have the potential to control early blight by different mechanisms (Vinale et al. 2008; Adnan et al. 2019; Metz 2021). Fungi within the genus *Trichoderma* have the ability to parasitize other fungi, have a competitive advantage over other plant pathogens due to fast growing, and can produce antimicrobial substances (Vinale et al. 2008; Adnan et al. 2019). However, the potential of *Trichoderma* spp. as biological control agents have not been fully investigated and further research is necessary (Metz and Hausladen 2022). *Bacillus subtilis*, another biocontrol agent, produces antibiotics which exhibit a broad-spectrum activity against plant pathogens. Alone and in combination with plant nutrients, *Bacillus subtilis* has the potential to control early blight (Awan and Shoaib 2019; Awan et al. 2023). Further, inoculation with the arbuscular mycorrhizal fungus *Funneliformis mosseae* can enhance resistance to early blight by inducing defense-related enzymes and genes in the plant leaves (Song et al. 2015).

1.3.1 Chemical control of *A. solani* and an introduction to fungicides

Several factors that complement and supplement each other play a role in effectively controlling early blight, but the primary method of managing infection remains the application of foliar fungicides (Hausladen and Leiminger 2007; Lucas et al. 2015). The use of pesticides, such as fungicides, herbicides, insecticides, rodenticides, and others, ensure disease control, higher yields, and improved food quality. Since the establishment of pesticides and other agronomical measures, food production has increased significantly in the last decades. Especially pesticides improved pest control to maintain food quality and quantity (Evenson and Gollin 2003; Aktar et al. 2009; Qaim 2017). Fungicides have been in use for over 200 years against fungal pathogens. Since the Second World War, there has been a dramatic increase in the number of crops and crop diseases treated, the variety of available chemicals, the frequency and area of their usage, and the effectiveness of treatments (Brent and Hollomon 2007).

Copper based formulations and sulfur are long established products that are still in use. However, since the late 1960s and 1970s, several more effective fungicides with novel structures were developed. These include sterol demethylation inhibitors, benzimidazoles, dicarboxamides, quinone outside inhibitors, anilinopyrimidines, phenylpyrroles and succinate dehydrogenase inhibitors (Brent and Hollomon 2007; Oliver and Hewitt 2014). To date, there are at least 45 different modes of action described which can be distinguished in groups according to their biochemical mode of action in plant pathogens (Hollomon 2015; FRAC 2024d). Fungicides can be classified as single-site fungicides, targeting a specific enzyme or protein in a metabolic pathway, or multi-site fungicides effecting different metabolic pathways

within the pathogen. Single-site inhibitors are often less phytotoxic and can exhibit systemic properties, whereas multi-site inhibitors act as contact fungicides and do not exhibit systemic activity (Oliver and Hewitt 2014). Quinone outside inhibitors, benzimidazoles and phenylamides are examples of single-site inhibitors, whereas multi-site fungicides are represented, for example, by the dithiocarbamates (Brent and Hollomon 2007; Deising et al. 2008). In addition to the classification between single-site and multi-site, as well as systemic and non-systemic, fungicides can also be categorized as protective, curative, or eradicated based on their modes of action (Oliver and Hewitt 2014). A non-systemic fungicide functions only in a preventive way, acting on the applied surface, as they are not distributed in plant tissues. Consequently, several applications during the season are needed for complete coverage of the target plant. Often, multi-site inhibitors are non-systemic fungicides. On the other hand, systemic fungicides penetrate plant tissues, providing protection against infection in untreated plant parts, and are less susceptible to being washed away by rainfall. Through distribution in the plant, newly formed parts can be protected and fungi infesting the xylem can be controlled. Systemic fungicides can often act as protectant and curative inhibitors, and as single-site mode of action. Therefore, systemic fungicides, which have been developed since the late 1960s, offer greater flexibility in their application (Edgington et al. 1980; Oerke 2005; Deising et al. 2008; Oliver and Hewitt 2014; Hollomon 2015).

Because of the polycyclic nature of early blight and its ability to produce high amounts of secondary inoculum, several fungicide applications per season are required to reduce infection and to avoid significant yield loss (Rosenzweig et al. 2008; Abuley et al. 2018). Nowadays, several fungicide classes are used to control early blight, such as quinone outside inhibitors (QoIs), succinate dehydrogenase inhibitors (SDHIs) and C-14 demethylation inhibitors (DMIs).

QoIs, or so called strobilurins, are an important class of agricultural fungicides that have been derived from the natural compound Strobilurin A (Krämer and Schirmer 2007). QoIs are able to block the mitochondrial respiration by binding to the Q_o site of cytochrome bc_1 in the mitochondrial electron transport complex III (Bartlett et al. 2002). Kresoxim-methyl and azoxystrobin were the first QoIs to be introduced to control early blight which showed excellent inhibition of infection (Pasche et al. 2004; Rosenzweig et al. 2008).

SDHIs are another class of fungicides impacting the pathogen by inhibiting the enzyme succinate ubiquinone reductase (complex II) in the mitochondrial electron transport chain (Kuhn 1984; Keon et al. 1991). The target gene consists of four subunits: *SDH A*, *B*, *C* and *D*. Subunit *A* is a flavoprotein and plays a role in the conversion of succinate to fumarate and subunit *B* is an iron protein that contains three iron-sulfur clusters and facilitates the transfer of electrons from succinate to ubiquinone. *SDH C* and *SDH D* represent two membrane anchor

subunits that hold the heme b molecule that is located between two antiparallel helices of two subunits (Hägerhäll 1997; Glättli et al. 2011). Among these subunits, the fungicides binding site is highly conserved and formed by subunits *B*, *C* and *D* (Horsefield et al. 2006; Stammler et al. 2007). Although SDHs and Qols both inhibit respiration by binding at the ubiquinone binding sites in complex II and III, respectively, and therefore have a similar mode of action, they do not show cross-resistance. This makes it possible to alternate or combine these fungicides to delay the development of fungicide resistance (Avenot et al. 2008) and to increase control efficiency.

Further, C-14-demethylase inhibitors (DMIs), belonging to the sterol biosynthesis inhibitors (SBIs), are a group of fungicides registered for the control of early blight. SBIs are clustered in four subgroups: demethylation inhibitors, amines, keto-reductase inhibitors (KRIs) and squalene-epoxidase inhibitors. Squalene-epoxidase inhibitors stand out as the class that is currently not utilized as agricultural fungicides. The fungal sterol biosynthesis pathway is targeted by all subgroups of inhibitors, however, DMIs represent the largest number of fungicidal compounds and the most extensive range of activity (FRAC 2024a). Since the focus of this study is on the fungicide class of DMIs, their mode of action and other characteristics will be elaborated in the following chapter.

1.3.2 Demethylation inhibitors (DMIs)

SBIs are widely distributed not only in agriculture, but also in human and veterinary medicine in the treatment of fungal infections. SBIs were introduced for agricultural use in the 1970s (Vanden Bossche et al. 2003; Ma and Michailides 2005; Gisi 2013; Jørgensen and Heick 2021). Among the SBIs, the DMIs represent the largest group which is further divided in piperazines, pyridines, pyrimidines, imidazoles, triazole and triazolinthiones. However, the most important group with respect to the commercial relevance and the number of compounds, are the triazoles (Oliver and Hewitt 2014; FRAC 2024a). Among the different DMIs, some are effective against foliar diseases and are therefore used as foliar fungicides, others are effective against seed-borne diseases and are used as seed treatments, and some can be used for both. Further, certain DMIs have growth-regulating properties or are applied as wood preservation agents (Jørgensen and Heick 2021). In the late 1970s, imazalil was registered as one of the first DMIs, followed by many more in the subsequent decades (Cools et al. 2013; Jørgensen and Heick 2021). Examples of DMIs to control fungal pathogens include cyproconazole, difenoconazole, epoxiconazole, fenbuconazole, metconazole, myclobutanil, penconazole and tebuconazole (Bowyer and Denning 2014; FRAC 2024b). After a period of more than a decade without launch of a new DMI, the novel compound mefentrifluconazole, belonging to the triazoles, was registered in 2020 (Strobel et al. 2020).

DMIs inhibit the fungal growth by interfering with the biosynthesis of ergosterol, this leads to a dysfunction of the cell membrane (Becher and Wirsel 2012). The antifungal effect originates from the interference with the sterol 14 α -demethylase (*CYP51* or *ERG11*), a cytochrome P450 monooxygenase. The enzyme is located on the outer membrane of the endoplasmic reticulum and catalyzes the removal of the C14-methyl group or 24-methylendihydrolanosterol. The binding of DMIs to the *CYP51* is non-competitive. It leads to a reduction in the production of ergosterol and accumulation of precursor sterols, which cause disruption of the cell membrane and inhibition of fungal growth (Siegel 1981; Vanden Bossche 1985; Gisi et al. 2002). Precursor sterols influence the constitution of the plasma membrane and lead to compromised rigidity and increased fluidity (Abe et al. 2009). Ergosterol is the major sterol in higher fungi, such as Basidiomycetes, Ascomycetes, but not in Oomycetes. It is crucial for the permeability and fluidity of the cell membrane (Siegel 1981; Douglas and Konopka 2014). Oomycetes differ from real fungi in many ways, such as physiology, biochemistry, and genetics. In contrast to real fungi, oomycetes do not have an ergosterol biosynthesis pathway and are therefore not affected by DMIs (Griffith et al. 1992; Latijnhouwers et al. 2003).

The Cyp51 protein is commonly found in animals, fungi, and plants (Rezen et al. 2004). Rezen et al. (2004) designed a phylogenetic tree indicating that Cyp51 is clustered in different types and subtypes by different fungal species. Within different fungal species, the number of *CYP51* genes differs and up to three clades, named *CYP51A*, *CYP51B* and *CYP51C* could be identified (Becher et al. 2011; Becher and Wirsel 2012). The analysis showed that most of the investigated Pezizomycotina harbored two or three clades of the Cyp51 protein and those species encoding for one copy were solely found in clade B. *Fusarium graminearum* harbors three *CYP51* paralogs (Becher et al. 2011). Further, in some species of *Magnaporthe*, *Penicillium*, *Pyrenophora*, *Trichoderma* and *Fusarium* *CYP51A* and *B* have been described. *Aspergillus fumigatus* and *Aspergillus nidulans* possess type *A* and *B*, whereas in *Aspergillus flavus* and *Aspergillus oryzae* the *CYP51A* is duplicated, and *CYP51B* in *Aspergillus terreus* (Becher et al. 2011; Becher and Wirsel 2012). However, Becher and Wirsel (2011) did not include *Alternaria* species in their research and no other studies have been found which reports of *CYP51* paralogous in *A. solani*.

1.4 Fungicide resistance

The increase of the global population is associated with crop cultivation which fosters plant diseases. In order to secure high quality and quantity food, the use of fungicides is indispensable. Therefore, it is unnegotiable to delay fungicide resistance with help of correct resistance management (Deising et al. 2008).

In the 1970s, fungicide resistance had become a relevant problem in agriculture with the introduction of single site inhibitors, such as benzimidazoles (Kiebacher and Hoffmann 1976). It was reported that after intensive use of benzimidazoles, resistance developed within two years. On the other hand, multi-site fungicides, such as copper, sulfur or dithiocarbamates, have maintained their full effectiveness, despite their long-term use over many decades (Brent and Hollomon 2007; Deising et al. 2008). As fungicide resistance had been an increasing problem in food production, the Fungicide Resistance Action Committee (FRAC) was founded in 1981 to provide information and recommendations on how emergence of fungicide resistance can be managed. FRAC provides various publications on the risk of resistance development by pathogens, fungicidal mode of action and agronomy measures, as well as information on the current resistance situation for many pathogens and modes of action, and resistance management strategies. Such recommendations include different strategies to minimize fungicide resistance development (FRAC 2024d).

Resistance towards single-site inhibitors occur due to changes in a single-target protein, whereas multi-site inhibitors act on various cellular processes, and changes in multiple targets are required to develop resistance. Therefore, resistance to single-site inhibitors is more likely (Deising et al. 2008; Lucas et al. 2015). The emergence of resistant populations has been already documented for antibacterial drugs, such as penicillin or streptomycin, and insecticides (Brent and Hollomon 2007; Deising et al. 2008). The risk of phytopathogenic fungi developing resistance depends on multiple factors. These include the chemical class of fungicides, biochemical and epidemiological processes, pathogen, crop type and region (Brent and Hollomon 2007a). Integrated disease management including resistant crop cultivars, agronomic measurements, crop hygienic measures and biological fungicides are an important contribution to reduce infection and delay fungicide resistance (Hollomon 2015). Further strategies to minimize selection pressure can be the consideration of application dose, number of applications, use of mixtures or alteration of different modes of action and timing of applications (Brent and Hollomon 2007; van den Bosch et al. 2014; Hollomon 2015). Especially pathogens that have short generation time, high spore production and a rapid and long-distance dispersal of spores are more likely to develop resistance (Brent and Hollomon 2007; He et al. 2019; Jørgensen and Heick 2021).

Fungal pathogens can mainly evolve four different mechanisms to overcome lethal effect of fungicide applications: (1) target site mutations leading to an altered binding of the fungicide; (2) overexpression of the target enzyme due to an upregulation of the target gene; (3) increased efflux by transporter proteins to reduce intracellular fungicide concentration; and (4) detoxification through metabolization of the compound. However, the most important resistance mechanism in phytopathogenic fungi is the alteration of the binding site due to target site mutations in the target gene of the fungicide (Ma and Michailides 2005; Brent and Hollomon 2007; Cools et al. 2013; Lucas et al. 2015).

When the target gene is mutated, the binding site is altered and the inhibition of the protein is reduced. Fungicide applications of the same fungicide favor the selection of mutants by decreasing the number of wildtype (WT) individuals and results in a resistant population. Throughout the selection process, the individuals show either a sensitive or a resistant phenotype (Deising et al. 2008). In general, pathogens evolving a target site mutation exhibit cross-resistance between compounds with the same mode of action (FRAC group). As a prominent example serves the cross-resistance between QoI fungicides caused by the target site mutation G143A (Sierotzki et al. 2000; Bolton et al. 2012). However, exceptions of cross-resistance exist in many modes of action groups. Negative cross-resistance is less common and describes the resistance to one fungicide, which leads to improved sensitivity to another and is known for some target site mutations of tubulin inhibitors (Brent and Hollomon 2007; Hollomon 2015). In the absence of fungicides, resistant genotypes are often linked with a reduced competitiveness in a population with sensitive genotypes. Therefore, resistant individuals are not able to survive without selection pressure of fungicides (Ma and Michailides 2005).

Another resistance mechanism of less importance than target site mutations, is the overexpression of the target enzyme due to the upregulation of the encoding gene (Ma and Michailides 2005; Lucas et al. 2015). An increase of the target enzyme favors the binding of the natural substrate thus cellular processes can persist to a certain degree (FRAC 2024c). It has been reported, that changes in the promotor region of the target gene may result in its overexpression (Hamamoto et al. 2000). Overexpression leading to a reduced fungicide sensitivity has been described for several pathogens, such as *Blumeriella jaapii*, *Venturia inaequalis*, *Cercospora beticola* and *Zymoseptoria tritici* (Schnabel and Jones 2001; Ma et al. 2006; Nikou et al. 2009; Cools et al. 2012).

An additional mechanism, which was described for *Botrytis cinerea*, *Z. tritici* and *Pyrenophora tritici-repentis*, is represented by the active efflux of fungicidal compounds. This leads to a reduced accumulation in the fungus and subsequently compromises their effectiveness to certain levels (Reimann and Deising 2005; Kretschmer et al. 2009; Grabke and Stammler 2015; Omrane et al. 2015; FRAC 2024c). This mechanism is also known as multi-drug

resistance (MDR) and is mediated by the membrane bound transporters ATP-binding cassette (ABC) or major facilitator superfamily (MFS). ABC and MFS transporters are overexpressed which leads to a decrease in fungicide at the target site inside the cells (de Waard 1997; de Waard et al. 2006). Whereas in agriculture the increased efflux activity in phytopathogenic fungi has limited relevance, MDR is commonly known in human fungal pathogens, such as *Candida albicans* and *Candida glabrata*, bacteria and human cancer cells (Del Sorbo et al. 2000; de Waard et al. 2006; Perez-Tomas 2006; Morschhäuser 2010; Bassetti et al. 2013). Further, the detoxification by metabolism of fungicides can confer resistance in fungal pathogens (Ma and Michailides 2005). The production of metabolic enzymes, such as glutathione transferase, esterases or cytochrome P450s, is increased and catalyze the degradation of toxic compounds in organisms (Leroux et al. 2002; Lucas et al. 2015). Metabolism-based resistance is most problematic in weeds and insects and seems to be less common in fungi (Puinean et al. 2010; Lucas et al. 2015; Cummins et al. 2013). However, metabolism of fungicides has been described for a few fungal pathogens, such as *F. graminearum*, *V. inaequalis* and *B. cinerea* (Jabs et al. 2001; Leroux et al. 2002; Sevastos et al. 2017).

Different resistance mechanisms cause different levels of resistance. A rough differentiation was made between qualitative and quantitative resistance by Brent and Hollomon (1998; 2007a). Characteristic for a qualitative resistance is that it occurs rapidly after the fungicide's commercialization and is caused by a single mutation in the target gene (Brent and Hollomon 1998). Benzimidazole resistance, caused by the target site mutation E198A in the beta tubulin gene, or QoI resistance caused by G143A in the *CYTB* gene, are prominent examples for qualitative resistance in various fungal pathogens (Kiebacher and Hoffmann 1976; Koenraadt et al. 1992; Sierotzki et al. 2000; Gisi et al. 2002; Fisher and Meunier 2007; Bolton et al. 2012; Olaya et al. 2017). In contrast, quantitative resistance evolves slowly and is caused by mutations in several genes (polygenic) or several mutations within a target site (polyallelic). This leads to a gradual and variable emergence of resistance. Further mechanisms for "quantitative" resistance may be enhanced efflux transporters or overexpression (Brent and Hollomon 2007; Cools and Fraaije 2008; Deising et al. 2008; He et al. 2019). Fitness penalties accompanied with some of these resistance mechanisms can lead to a shift back to higher sensitivities in the pathogen population when there is no or low fungicide selection pressure (Brent and Hollomon 1998; 2007a). As the individuals in a population have different levels of tolerance, the term resistance might not be appropriate for the shifting of a sensitive population towards a decrease of sensitivity (Deising et al. 2008). Quantitative resistance towards DMIs has been described, e.g., for *Z. tritici*, *V. inaequalis* or *Phakopsora pachyrhizi* (Cools and Fraaije 2008; Schmitz et al. 2014; Hoffmeister et al. 2021). The differentiation between qualitative and quantitative resistance was mainly driven by the experience gained from

benzimidazoles and QoI resistance, as examples for qualitative resistance, and SBI adaptation for quantitative resistance. However, this differentiation does not fit with the evolution of SDHI resistance in several pathogens, such as *Z. tritici*, *Pyrenophora teres*, *Ramularia collo-cygni* and many others. Here, various single target site mutations can be found with different resistance phenotypes with low to moderate or high resistance levels towards different SDHIs and partially lacking cross-resistance between SDHIs. Their properties and fitness penalties for various of these target site mutations determine the frequency of resistance phenotypes in the pathogen populations (Stammler et al. 2015; Rehfus et al. 2016; Rehfus 2018; Rehfus et al. 2019; Klappach and Stammler 2019).

1.4.1 Fungicide resistance to demethylation inhibitors

In the 1970s, imidazoles and triazoles were introduced and they represent the largest group of DMI fungicides (Cools et al. 2013). During the last decades, resistance to DMIs has been known to emerge in different fungal pathogens. Multiple mutations can accumulate so that a gradually loss of efficacy is observed. This refers to the quantitative development of resistance towards DMIs, which occurs stepwise (chapter 1.4). For the groups of fungicides within the SBIs, the resistant risk for amines and KRIs is considered to be low to medium, and for DMIs medium (FRAC 2024a). Members of the DMIs, amines and KRIs exhibit cross-resistance within the same group, but no cross-resistance has been observed between members of different groups. Hence, cross-resistance is incomplete within the SBI mode of action group (Cools et al. 2013; FRAC 2024a). The most important resistance mechanisms for DMIs are (1) target-site mutations in the *CYP51* gene, leading to a decreased binding of the protein for inhibitors, (2) enhanced efflux activity, due to membrane-bound transporters and (3) increased expression of the *CYP51* gene, often as a result of insertions in the promotor region (Cools et al. 2013). Resistance levels are often the result of a combination of the three different resistance mechanisms, e.g., in *Z. tritici* (Cools and Fraaije 2013; Huf 2021).

However, the most common resistance mechanism for DMIs is target site alterations in the *CYP51* gene. Several fungal pathogens have evolved target site mutations which have been described to influence the sensitivity towards DMIs (Huf et al. 2018; Rehfus et al. 2019; Hoffmeister et al. 2021; Muellender et al. 2021; Glaab et al. 2024). In different plant and human pathogens, some mutations were detected at homologous positions in the *CYP51* gene, e. g., mutation Y137F in *Z. tritici* in *Erysiphe necator*, *Puccinia triticina*, *C. albicans* and *Blumeria graminis* f. sp. *hordei/tritici* (Délye et al. 1997; Stammler et al. 2009; Becher and Wirsal 2012). One mutation alone often confers low levels of resistance, which is increased when various mutations or mutations with other resistance mechanisms are combined (Wyand and Brown 2005; Rehfus et al. 2019; Glaab et al. 2024).

Another resistance mechanism which contributes to DMI resistance, is the overexpression of the target gene. Often, *CYP51* is overexpressed when insertions in the predicted promotor regions are present (Schnabel and Jones 2001; Cools et al. 2013). This mechanism has been described for different fungal pathogens, such as *Venturia inaequalis*, *P. triticina*, *Monilinia fructicola* and *Z. tritici* (Schnabel and Jones 2001; Luo and Schnabel 2008; Stammler et al. 2009; Cools et al. 2012; Glaab et al. 2024). In contrast to alterations in *CYP51*, which might affect sensitivity to various DMIs differently, overexpression of *CYP51* confers reduced sensitivity to all DMIs (Cools et al. 2013).

Enhanced efflux activity is a resistance mechanism which is commonly known in human pathogens, but less in plant pathogens (Morschhäuser 2010; Cools et al. 2013). In fungal plant pathogens, an enhanced efflux was described for *Z. tritici*, *B. cinerea* and *Oculimacula yallundae* (Kretschmer et al. 2009; Stammler and Semar 2011; Leroux et al. 2013; Grabke and Stammler 2015; Omrane et al. 2015; Glaab et al. 2024). Insertions in the promotor region or mutations in transcriptions factors lead to overexpression of ABC or MFS-type transporter genes, hence an increased efflux activity (Kretschmer et al. 2009; Omrane et al. 2015; Glaab et al. 2024).

Several *CYP51* copies could be identified in different plant pathogens, which may lead to an advantage under selection pressure by DMIs. An unchanged enzyme with WT activity could compensate any trade-offs associated with changes or overexpression of the paralogs (Cools et al. 2013). The reason for the presence of paralogous *CYP51* genes within a single species and their functions are still not fully understood. It has been suggested that the *CYP51* paralogs in a species may have evolved from the duplication of an ancestral gene, which evolved to differ in function and structure (Mellado et al. 2001; Yin et al. 2023). Such a case has been confirmed for *Rhynchosporium graminicola* after genome screening of 125 isolates from across the world. With genome-wide association studies a segmental duplication of *CYP51A* could be identified, affecting the development of DMI resistance in *R. graminicola* (Stalder et al. 2023). However, further research is needed as there is only little known about the function of multiple *CYP51* paralogs (Liu et al. 2010; Yin et al. 2023).

Copies of *CYP51* genes, which differ only in target site mutations causing lower DMI sensitivity, have been reported for *P. pachyrhizi* (Schmitz et al. 2014; Stilgenbauer 2022; Stilgenbauer et al. 2023). It is interesting to note that DMI-adapted *P. pachyrhizi* isolates with mutations in *CYP51*, always possess WT alleles of *CYP51*. This was suggested to ensure higher effective enzymatic metabolic processes in situations without DMI exposure (Stilgenbauer et al. 2023). Another adaptation mechanism has recently been reported for *C. beticola*, which is a silent mutation in *CYP51* gene. Different codon usages for E170 led to different sensitivities to various DMIs (Spanner et al. 2021; Hoffmeister et al. 2024). However, the mechanism causing lower DMI sensitivity by this silent mutation is so far not fully understood. Further, the same

authors reported about an effect of the usage of two different codons for the L144F mutation, which affected DMI sensitivity of *C. beticola* differently (Spanner et al. 2021; Hoffmeister et al. 2024). In *F. graminearum* it was shown that a SNP in transcription factor Azr1 confers DMI adaptation. The transcription factor Azr1 has an effect on the regulation of ergosterol biosynthesis genes and, therefore, mutations in this gene can influence DMI adaptation. Such isolates with mutation in *AZR1* gene did not show fitness penalties and were as viable as the WT isolates (Eisermann 2023).

1.4.2 Fungicide resistance in *A. solani*

The pathogen associated risk for *A. solani* to develop fungicide resistance was categorized as medium (FRAC 2019). QoIs, SDHIs and DMIs are the major fungicides used to control this pathogen. For QoIs and SDHIs, a sensitivity loss in *A. solani* has been observed in the field some years after market introduction of the relevant mode of action (Pasche et al. 2004; Pasche et al. 2005; Rosenzweig et al. 2008; Leiminger et al. 2014; Mallik et al. 2014; Landschoot et al. 2017; Metz et al. 2019; Einspanier et al. 2022). To date however no field adaptation has been reported for DMIs (He et al. 2019; Yang et al. 2019).

QoI resistance in many pathogens is linked to mutation G143A in the cytochrome *b* (*CYTB*) gene leading to high resistance levels (Gisi et al. 2002; Fraaije et al. 2002; Grasso et al. 2006; Hausladen and Leiminger 2015). In *A. solani*, target site mutation G143A has never been reported. An intron directly after the codon for glycine at position 143 inhibits the occurrence of point mutations in this codon. The WT codon for glycine is mandatory for a correct splicing. Therefore, the amino acid (aa) alteration from glycine to alanine would result in incorrect mRNA maturation and lethal for such pathogens which harbor an intron directly after codon 143 (Grasso et al. 2006; Deising et al. 2008). An alternative resistance mechanism for such pathogens, is often mutation F129L, which confers a reduced sensitivity towards QoIs and has also been found in *A. solani* (Pasche et al. 2004; Rosenzweig et al. 2008; Leiminger et al. 2014). The effect of mutation F129L is pronounced heterogenous in different fungicides, as target site mutation F129L affects azoxystrobin more than pyraclostrobin or trifloxystrobin (Pasche et al. 2004). Moreover, two versions of mitochondrial *CYTB* gene in *A. solani* have been reported, that differ in the presence or absence of an intron. Genotype I consists of five exons and four introns, whereas in genotype II one intron is missing. The mutation F129L was detected only in genotype II in almost all isolates investigated by Leiminger et al. (2014). Genotype I was the predominant type and found in 63% of the isolates (Leiminger et al. 2014). Newer studies from 2019 in Germany reported that a shift from the predominant genotype I to genotype II has been observed and that mutation F129L has also been detected in genotype I, indicating a progression of the resistance (Nottensteiner et al. 2019). Nevertheless, an intron

is located directly after codon 143 in both genotypes, which makes the occurrence of G143A in *A. solani* unlikely. A long-term study from Sweden confirmed the occurrence of target site mutation F129L in most investigated isolates (Edin et al. 2019). FRAC (2024f) reported, that in the past years, resistance caused by mutation F129L in *A. solani* was detected in high frequency in Belgium, Germany, Netherlands and Sweden, and in moderate frequency in France, Latvia and Poland.

For SDHI fungicides, a reduced sensitivity in *A. solani* is known, caused by different target site mutations in *SDH* subunits *B*, *C* and *D*. Previous research has shown that mutation *B*-H278R/Y, *C*-N75S, *C*-H134R, and *D*-D123E confer reduced susceptibility. Mutations exhibit varying levels of resistance and an increase in mutations present in subunit *C* has been observed (Mallik et al. 2014; Landschoot et al. 2017; Metz et al. 2019; Einspanier et al. 2022). Nowadays, mutation H134R in subunit *C* is predominant (Landschoot et al. 2017; Metz et al. 2019). A study from Belgium monitored the *A. solani* population in 2014 and 2015, where 70% of the investigated isolates revealed aa substitutions in *SDH* subunits and 40% had the aa alteration F129L in *CYTB*, leading to a dual fungicide resistance (Landschoot et al. 2017). Correspondingly, *A. solani* isolates in Germany exhibited SDH mutations in combination with QoI mutations thus conferring resistance to both fungicide classes (Nottensteiner et al. 2019). In the past years, different target site mutations in subunit *B*, *C* and *D* have been detected over various European countries in low to high frequencies. In 2022, low frequencies of mutations *B*-H278R/Y, *C*-H134R, *D*-D123E in combination with *B*-H278Y and *C*-H134R in Norway, and high frequencies in Denmark were detected (FRAC 2024g).

1.5 Objectives

The use of fungicides is an essential agronomical method to ensure the health and productivity of crops. However, excessive application with the same mode of action can lead to emergence of fungicide resistance. Fungicide resistance monitoring is an important tool to detect and examine resistance mechanisms, for the establishment of strategies, to delay resistance in phytopathogenic fungi. Since resistance mechanisms in *A. solani* towards DMIs has not yet been described, the aim of this study was to investigate and evaluate the resistance mechanisms responsible for a sensitivity loss to demethylation inhibitors. To this end, isolates were obtained from field samples and single spore isolates were generated. Additionally, targeted mutagenesis of the *CYP51* of *A. solani* was conducted. Since aa alterations in the target gene are the major resistance mechanisms in fungi, the focus of this work was concentrated on the target site mutation in the *CYP51* gene. The following aspects were addressed:

- Determination of the current DMI sensitivity of field isolates of *A. solani* from different regions
- Evaluation of mechanisms responsible for reduced DMI sensitivity by sequencing of the *CYP51* gene for detection of target site mutations
- Evaluation of the effects of *CYP51* haplotypes on DMI sensitivity
- Transformation of the *CYP51* gene from different haplotypes with subsequent sensitivity tests to proof if target site mutations are the responsible mechanisms for DMI sensitivity reduction
- Analysis of cross-resistance between different DMIs
- Determination of fitness and vitality associated with reduced DMI sensitivity
- Development of a reliable quantification assay for detection of *CYP51* mutations in the field
- Evaluation of field performance of DMIs and selection of *CYP51* haplotypes by different DMI treatment.

2 Material and Methods

2.1 Software and bioinformatic analyses

Software used during the present work is listed in Table 2. For the design of PCR oligonucleotides, Geneious Prime[®] was utilized, while Pyrosequencing Assay Design software was additionally used for the design of pyrosequencing oligonucleotides. For alignments and comparison of multiple nucleotide and amino acid (aa) sequences, as well as prediction of the full length transformation cassette, Geneious Prime[®] from was also used. For microtiter tests the net optical density (OD) was measured by Magellan[™] and E-WorkBook Suite/Labbooq was used to calculate the EC₅₀ values. Fungicide efficacy in sensitivity tests in the greenhouse was also calculated using E-WorkBook Suite/Labbooq. For documentation and to edit Southern Blot results Image Lab[™] software was used. The locations of the collection sites were visualized using Tableau software.

The software Graphpad prism (version 8.0.2) was used for statistical analyses. Significant differences of DMI sensitivity obtained from microtiter tests between different haplotypes were calculated with Kruskal-Wallis-Test ($p=0.05$) for data that are not normally distributed. Kruskal-Wallis-Test ($p=0.05$) was further utilized for determining significant differences between fungicide efficacy in greenhouse tests between the efficacies for mutated single spore isolates and WT single spore isolates. The correlation was calculated with EC₅₀ values resulting from microtiter tests for all isolates for tested DMIs. T-test (Mann-Whitney test; $p=0.05$) was performed to determine significant differences for two unpaired groups in competition studies and to analyze significant differences of DMI sensitivity, obtained from microtiter test, between targeted mutation strains with more than one repetition. Further, t-test (Mann-Whitney test; $p=0.05$) was used to determine significant differences for spore morphology of different *CYP51* haplotypes. Tukey's test ($p=0.05$) was carried out to compare the mean values of the different groups represented by the treatment's efficacy in the field trials from 2023. Further, Kruskal-Wallis-Test ($p=0.05$) was used to compare the mean values of spore quantitate among single spore isolates with and without *CYP51* mutations.

Table 2: Software used in this work.

Name	Company
E-WorkBook Suite/Labbooq	IDBS, Guildford, UK
Geneious Prime®	Biomatters, Auckland, NZ
GraphPad Prism	GraphPad Software Inc., Boston, US
Image Lab™	Bio-Rad Laboratories Inc., Hercules, US
Microsoft 365 Office	Microsoft, Redmond, US
Molecular Operating Environment (MOE)	Chemical Computing Group Inc., Montreal, CA
Magellan™	TECAN Group, AG Männerdorf, CH
Tableau	Salesforce Inc., Seattle, US

2.2 Fungal isolates

Field isolates and single spore isolates were generated from infected potato leaves which had been collected from potato fields from 2020 to 2022 from different regions. This included commercial sites and trial sites in Germany (2021, 2022, 2023) and the Netherlands (2021, 2022). Additionally, isolates from 2020 and 2022 from the Netherlands and isolates from 2022 from Sweden have been provided by the external cooperator Biotransfer (Montreuil, France). Australian isolates from 2018 were recultivated from long-term storage in BASF. The single spore isolates Ms 1092 and Ms 1030 were used to mount the transformation cassette.

2.2.1 Cultivation of *A. solani* isolates

A. solani isolates and single spore isolates were cultivated on 2% (w/v) malt extract medium amended with 30 ppm streptomycin sulphate (AppliCHem GmbH, Darmstadt, Germany) in an incubation chamber at 18°C with a 12 h photoperiod. Isolates were cultivated for 12 days before they were used for further experiments. All 2% (w/v) malt agar plates used in this work contained 30 ppm streptomycin sulphate (AppliCHem GmbH, Darmstadt, Germany) to prevent contaminations with bacteria.

2.2.2 Long term storage and recultivation of isolates

Long-term storage of single spore isolates and field isolates was performed as spore suspension at -80°C. Therefore, isolates were cultivated for 12 days, and fungal material was transferred with a sterile cotton swab (Deltalab S.L., Barcelona, Spain) in 1 ml of 2% (w/v) malt extract medium with 15% (w/v) glycerol. For recultivation, the thawed suspension was transferred onto 2% (w/v) malt extract agar plates and incubated as described in chapter 2.2.1.

2.2.3 Obtaining field isolates

Twenty infected potato leaves from each plot were collected to obtain five field isolates each. The surface of infected leaves with typical early blight symptoms were disinfected with 20% (v/v) sodium hypochlorite for 30 seconds and washed twice with sterile water, once for 30 seconds, subsequently for 5 min. Lesions were cut out and placed onto 2% (w/v) malt extract agar plates. Outgrowing mycelium was transferred to new agar plates. Cultivation is carried out as described in chapter 2.2.1.

2.2.4 Generation of single spore isolates

A spore suspension was prepared from each isolate by wiping spores from 2% (w/v) malt extract agar plates with a cotton swab (Deltalab S.L., Barcelona, Spain) and mixing it with 600 µl deionized water in a 1.5 mL Eppendorf tube. After mixing for 30 seconds, 50-100 µl of the spore suspension was spread over 2% (w/v) malt extract agar plates by using a sterile disposable drygalski spatula (VWR International GmbH, Darmstadt, Germany). Single spores were picked with a sterile needle and transferred to a new 2% (w/v) malt extract agar plate using the five-point-inoculation method, transferring five single spores separately onto one plate. After two to four days, germinated spores were transferred onto new 2% (w/v) malt extract agar plates and placed for 12 days in an incubation chamber with same conditions as described in chapter 2.2.1. Single spore isolates are marked with "Ms" and a BASF internal isolate number.

2.3 *Escherichia coli*

For cultivation of plasmids, *E. coli* strain X-L1-Blue (Agilent Technologies Inc, Santa Clara, United States) was used. Chemically competent cells were prepared after Chung et al. (1989) with minor adjustments. In a 50 mL Eppendorf flask 5 mL Super Optimal broth with Catabolite repression (SOC) medium and 100-200 µL bacteria were incubated for an overnight culture at 37°C and 200 rpm in a culture incubation shaker. The next day, 400 µL were transferred to 50 mL SOC medium for incubation at 37°C and 200 rpm. When the OD₆₀₀ reached a value between 0.4 and 0.6, cells were centrifuged at 4°C and 1000 g and resuspended in 5 mL cold transformation and storage-solution (TSS) buffer. Aliquots of 100 µL were prepared in 1.5 mL Eppendorf tubes, either for storage at -80°C or direct use for transformation (chapter 2.6.4.2). *E. coli* strains with plasmids for ampicillin resistance were propagated in LB liquid medium with 100 mg/L antibiotic at 37°C and 200 rpm in an incubation shaker. LB liquid medium was inoculated with a single colony.

2.4 Cultivation of tomato plants for greenhouse tests

Fungicide sensitivity studies with *A. solani* were performed in the greenhouse with the tomato variety “Goldene Königin” (ENZA Zaden GmbH & Co. KG, Dannstadt-Schauernheim, Germany). Tomato plants were cultivated in seed trays (Schmidhuber e. K., Welzheim, Germany) for 7 days at 22°C and minimum 30% humidity in the greenhouse. On day eight, seedlings were placed into pots (ø8 cm) (Raiffeisen eG, Mannheim, Germany) and temperature were changed to 18.5°C until growth stage BBCH 13. Before application of fungicide the plants were fertilized with Kamasol® Brillant blau (Raiffeisen eG, Mannheim, Germany) and watered as necessary. Reason for use of tomatoes instead of potatoes were that growth of tomato plants is quicker, needs less space and is established as the test plant with reliable results for *A. solani* infections in BASF.

2.5 Potato cultivars for field trials

Potato cultivars “Kuras” and “Gala” were used for the field experiments in 2022 and 2023. “Kuras” is a late-maturing starch cultivar (Europlant 2023) and “Gala” is an early-maturing potato cultivar (Bundessortenamt 2011). Based on empirical data collected during prior trial implementations conducted by BASF SE, varieties “Kuras” and “Gala” and were chosen due to their high susceptibility to *A. solani*.

2.6 Molecular biological methods

2.6.1 Isolation of genomic DNA and RNA

For DNA- and RNA-isolation of field isolates and single spore isolates, fungal material from 12 days old agar plates were transferred with a sterile needle to a 2 mL Eppendorf tube. For extraction of DNA of field samples, the infection sites caused by *A. solani* were excised from the potato leaves and placed into a 2 mL Eppendorf tube. A metal bead with a diameter of 5 mm was added and the fungal material was frozen for 30-60 min on dry ice. Afterwards, the frozen fungal material was homogenized in an oscillating mill (MM200, Retsch GmbH, Haan, Germany) for 1-2 min at 20 Hz. Genomic DNA was extracted using the NucleoSpin Plant II mini Kit or NucleoSpin 96 Plant II mini Kit (depending on the number of samples) (Macherey-Nagel GmbH & Co. KG, Düren, Germany) following the manufacturer’s instructions for DNA from plants. RNA was extracted using RNeasy Plant Mini (Qiagen GmbH, Hilden, Germany) and On-Column DNase Digest Set (Sigma Aldrich, St. Louis, United States) following the manufacturer’s instruction. Before start of RNA extraction, the work surface, and all used equipment, such as pipettes and needles, were cleaned with RNase Away® spray. Concentration of extracted RNA was determined using the Qubit™ RNA HS Assay Kit (Thermo Fisher Scientific Inc., Waltham, United States) according to the manufacturer’s protocol and a

Qubit Flex fluorometer (Thermo Fisher Scientific Inc., Waltham, United States). RNA was stored at -20°C, while DNA was stored at 4°C for short-term usage and at -20°C for long-term usage.

For DNA extraction for the Southern Blots, targeted mutation strains were cultivated in 50 mL of 2% (w/v) malt extract medium with nourseothricin (WERNER BioAgents GmbH, Jena, Germany) as selection marker. After 12 days in a culture incubation shaker (Infors HT Multitron, Infors AG, Bottmingen, Switzerland) at 24°C and 110 rpm, fungal material was dried on paper towels and transferred to a 2 mL Eppendorf tube with a 5 mm diameter metal bead, frozen for 30-60 min on dry ice and homogenized as described before. Genomic DNA was extracted using the NucleoSpin Plant II midi Kit (Macherey-Nagel GmbH & Co. KG, Düren, Germany) following the manufacturer's instructions for DNA from plants for higher DNA yield. Purity and concentration of extracted DNA was determined using a Nanodrop2000 (Thermo Fisher Scientific Inc., Waltham, United States) photometrically. For short-term usage DNA was stored at 4°C and for long-term usage at -20°C.

2.6.2 Reverse transcription of RNA in cDNA

Reverse transcription of RNA into cDNA was performed using the Verso cDNA Kit (Thermo Fisher Scientific Inc., Waltham, United States) according to the manufacturer's instructions. For each reaction 50 ng of RNA were used, for short-term usage cDNA was stored at 4°C, while long-term storage was done at -20°C.

2.6.3 Polymerase chain reaction (PCR)

2.6.3.1 Standard-PCR

For amplification of target DNA or cDNA sequences PCR reactions were performed. In Table 28 (chapter 7.9), the used oligonucleotides are listed and in Table 3, components of PCR reactions with a final volume of 25 µL are shown. To avoid contaminations, PCR reactions were prepared in a clean bench and for control of absence of contaminations a no-template control (NTC) was included, in which target DNA or cDNA was replaced with diethyl pyrocarbonate (DEPC)-water (Ambion Inc., Austin, United States) was included.

Table 3: Components of PCR reactions.

Component	Volume (μL)
2 x Master Mix (DreamTaq/Phusion)	12.50
DEPC-water	7.50
Forward primer (10 pmol/ μL)	1.25
Reverse primer (10 pmol/ μL)	1.25
Template DNA or cDNA (10-50 ng)	2.50

Based on the purpose of the experiment, different DNA polymerases were used. Phusion™ Hot Start II, High-Fidelity PCR Mastermix (Thermo Fisher Scientific Inc., Waltham, United States), which shows proofreading activity, was utilized for amplification and sequencing of *CYP51* and the gene construct for targeted mutagenesis. However, DreamTaq™ Hot Start Taq polymerase (Thermo Fisher Scientific Inc., Waltham, United States) was used for pyrosequencing and test-PCR for subsequent Southern-Blot-hybridization. A schematic procedure of a standard PCR reaction is illustrated in Table 4.

Table 4: Schematic procedure of a standard PCR reaction program.

Phusion™ Hot Start II, High-Fidelity PCR Mastermix or DreamTaq™ Hot Start Taq polymerase were used. Annealing temperature and elongation time were adjusted depending on the pair of oligonucleotides and DNA polymerase used.

Function	Temperature Phusion/DreamTaq	(°C)	Time (s) Phusion/DreamTaq	Cycles
Initial denaturation	98/95		30/240	1
Denaturation	98/95		10/30	
Annealing	50-72		30/30	30-35
Elongation	72		15 per kb/60 per kb	
Final elongation	72		300/600	1
Cooling	4		∞	1

2.6.3.2 Double-Joint-PCR

Double-Joint-PCR (DJ-PCR) following Yu et al. (2004) consisting of three sequential reactions was used to generate the DNA constructs for the targeted mutagenesis with slight modifications. First, three sub-fragments with determined overhangs were generated by standard PCR, which facilitated the fusion of the fragments in the subsequent PCR reaction (Table 4, 5). In the second reaction, the three sub-fragments were joined to form one product. For this reaction, no primers were required due to the complementary overhangs at the fusion sites of the sub-fragments acting as self-primers (Table 6,7). In the final reaction (*Nested-PCR*), the second reaction was interrupted after 10 cycles to add the *Nested*-primers (Table 28,

chapter 7.9) that bind slightly inward from the outer regions of the fused product (Table 6,7). The aim of the third reaction was to amplify the joined construct for higher yield and to eliminate side products.

For all steps the Phusion™ High-Fidelity Polymerase (Thermo Fisher Scientific Inc., Waltham, United States) was used. The oligonucleotides added to the first reaction are shown in Table 28 (chapter 7.9) and the components are listed in Table 5. The standard PCR was conducted according to the instructions in Table 4 in chapter 2.6.3.1.

Table 5: Components of first reaction.

Component	Volume (µL)
DEPC-water	8.8
HF Buffer (5 x)	4
dNTPs (10 mM)	2
Forward primer (10 pmol/µL)	2
Reverse primer (10 pmol/µL)	2
DNA (10-50 ng)	1
Phusion DNA-Polymerase (2 U/mL)	0.2

PCR-products were purified using the GeneJET Gel Extraction Kit (Thermo Fisher Scientific Inc., Waltham, United States) as described in chapter 2.6.6. The DJ-PCR was combined with the *Nested*-PCR in 50 µL reaction with the components listed in Table 6.

Table 6: Components of second and third reaction.

Component	Volume (µL)
DEPC-water	Filled up to 50
Phusion DNA-Polymerase	0.6
DNA product of first reaction (10 ng, 20 ng, 10 ng)	1:2:1 (molar ratio)
Forward Primer (10 pmol/µL)	1
Reverse Primer (10 pmol/µL)	1
Buffer HF (5 x)	10
dNTPs (10 mM)	1.25

The construct was assembled via combination of DJ- and *Nested*-PCR with primer pair KES 2660 and KES 2658 for cassette harboring mutation G446S ($T_M=63^\circ\text{C}$), KES 2657 and KES 2658 for mutation L143F+G446S ($T_M=64^\circ\text{C}$) and KES 2662 and KES 2658 (oligonucleotides from Table 28, chapter 7.9) for mutation L143F ($T_M=62^\circ\text{C}$) following the procedure described in Table 7.

Table 7: Schematic procedure of a DJ-Nested-PCR reaction program.

Phusion™ High-Fidelity-Polymerase was used. Annealing temperature was adjusted depending on the oligonucleotide pair, elongation time were equivalent for all pair of oligonucleotides.

Function	Temperature (°C)	Time (s)	Cycles
Initial denaturation	98	30	1
Denaturation	98	15	10
Annealing	60	20	
Elongation	72	60	
Final elongation	4	∞	1
Add 1 µL of each <i>Nested</i> -primer (10 pmol/µL)			
Initial denaturation	98	preheat to favored temperature	1
Denaturation	98	15	35
Annealing	62-64	20	
Elongation	72	120	
Final Elongation	72	10	1
Cooling	4	∞	1

2.6.4 Cloning of PCR fragments

After successful joining of the sub-fragments and amplification of the replacement construct, the DNA construct was cloned in *Escherichia coli* DH5α and stored at -80°C. This step was necessary to have a long-term back up of the sequence and to have the appropriate concentration for further steps. The procedure for the cloning is described in the following chapters.

2.6.4.1 Ligation

After DJ-Nested-PCR the product was ligated into pJET 1.2/blunt cloning vector using the CloneJET PCR cloning Kit (Thermo Fisher Scientific Inc., Waltham, United States). Because Phusion™ High-Fidelity-Polymerase (Thermo Fisher Scientific Inc., Waltham, United States) generated blunt ends, due to its proofreading activity, the blunt-end cloning kit was utilized in this work. The compounds of the ligation with a final volume of 10 µL are listed in Table 8. After adding all compounds, the mixture was centrifuged and incubated at room temperature for 30 min.

Table 8: Components of Ligation.

Components	Volume (μL)
reaction buffer (2 x)	5
PCR-product (120 ng)	4
pJet 1.2/blunt cloning vector (25 ng/ μL)	0.5
T ₄ DNA-ligase	0.5

2.6.4.2 Transformation of *Escherichia coli*

The ligated plasmid was transformed in competent cells of *E. coli*. Therefore, competent cells were thawed on ice and 50 μL of bacteria suspension were transferred into cooled 1.5 mL Eppendorf tubes. Five μL of ligation reaction was added and incubated for 30 min on ice. A heat shock was conducted by placing the Eppendorf tubes into a 42°C water bath for 50 s, afterwards, the tubes were put back on ice for 2 min. Then, each bacteria culture was mixed with 900 μL of SOC medium in a 15 mL culture tube and placed in a shaking incubator at 37°C and 200-250 rpm. After one hour, the culture tubes were centrifuged at low rotation, 700 μL of the supernatant was discarded and cells were gently homogenized. 100 μL of concentrated suspension was spread on SOC plates containing 100 mg/L ampicillin and incubated at 37°C for 16 h.

2.6.4.3 Verification of the transformation and plasmid preparation

The colonies of transformed cells that grew on agar plates were individually picked using a sterile pipette tip under the laminar airflow bench and dipped into a reaction tube for a colony-PCR (Table 28, chapter 7.9, KES 2736 and 2737) to determine the presence or absence of inserted DNA. PCR reaction was performed following the instructions in Table 4 (chapter 2.6.3.1) for DreamTaq™ Hot Start Taq polymerase (Thermo Fisher Scientific Inc., Waltham, United States). For amplification the pipette tip was placed into a culture tube with 4 mL of SOC medium and 100 mg/L ampicillin. The culture tube was incubated in an incubation hood (CERTOMAT®H, Sartorius AG, Göttingen, Germany) at 37°C and 200-250 rpm for 16 h. When a 500 kb band was observed in a gel electrophoresis using 1% (w/v) TAE-agarose gel (chapter 2.6.5), the insertion of the DNA fragment was successful, and the colonies were used for plasmid extraction using the GeneJET Plasmid Miniprep Kit (Thermo Fisher Scientific Inc., Waltham, United States) following the manufacturer's instructions. In the PCR-reaction plasmid Ec47 (provided by Alan de Oliveira Silva, Martin-Luther-University Halle-Wittenberg, Germany) containing the nourseothricin gene was used as positive control. Plasmid DNA was stored at -20°C.

2.6.5 Gel electrophoresis

To separate amplified DNA fragments and visualize the exact size, agarose gel electrophoresis was performed. To prepare 1% (w/v) agarose gel, 2 g of agarose was dissolved in 200 mL TAE-buffer, by heating the mixture in an Erlenmeyer flask in the microwave. After short cool down 15 μ L of DNA-dye (peqGreen) (VWR International GmbH, Darmstadt, Germany) was added and gel was poured and solidified for 30 min. Of each PCR-reaction 5 μ L was mixed with 5 μ L Orange DNA loading dye (6x) (Thermo Fisher Scientific Inc., Waltham, United States) before loading the gel. The separation of the amplicons was performed at 120 V for approximately 45 min and the results were documented using the EasyDoc plus gel documentation system (Herolab GmbH Laborgeräte, Wiesloch, Germany). A 1 kb GeneRuler (Fermentas GmbH, St. Leon-Rot, Germany) was used as a size standard. Remaining 20 μ L amplified DNA fragments were used for subsequent clean-up and Sanger sequencing (chapter 2.6.6 and 2.6.7).

To visualize the size of the newly assembled cassettes for targeted mutagenesis of *A. solani* and to check if the DNA for Southern-Blot-hybridization was properly digested a 0.7% (w/v) agarose gel was prepared by dissolving 1.4 g of agarose in 200 mL TAE-buffer in an Erlenmeyer flask and heating the mixture in a microwave. Gel was poured and solidified for 30 min. 2 μ L of PCR-reaction was mixed with 1 μ L Orange DNA loading dye (6x) (Thermo Fisher Scientific Inc., Waltham, United States) to load the gel. The separation of the amplicons was performed at 70-80 V for 1-2 h. Before visualization of the results using the UVsolo TS Imaging System the gel was placed in 0.15% (v/v) ethidium bromide (Carl Roth GmbH & CO. KG., Karlsruhe, Germany) for 15-20 min. A 1 kb GeneRuler (Fermentas GmbH, St. Leon-Rot, Germany) was used as a size standard. Correct assembled and amplified DNA fragments were excised from the gel and transferred to a 2 mL Eppendorf tube for subsequent clean-up and sequencing. DNA was further utilized for the process of Southern-Blot-hybridization.

2.6.6 PCR clean-up

After separation of DNA fragments by gel electrophoresis, amplified DNA fragments were purified before sequencing. Remaining 20 μ L DNA fragments were solved in 80 μ L DEPC-water (Ambion Inc., Austin, United States) and depending on number of samples NucleoSpin® Gel and PCR Clean-up Kit or NucleoSpin® 96 PCR Clean-up Kit (Macherey-Nagel GmbH & Co. KG, Düren, Germany) was used according to the manufacturer's protocol. PCR products were eluted in 50 μ L elution buffer NE after following the manufacturer's protocol for centrifuge processing with slight adjustment of centrifuge speed to 2250 rcf.

Excised agarose gel slices were purified using the GeneJET Gel Extraction Kit (Thermo Fisher Scientific Inc., Waltham, United States) according to the manufacturer's protocol. PCR products were eluted in 30 µL elution buffer.

2.6.7 Sequencing

Sequencing via Sanger sequencing of purified PCR products was outsourced to the company Microsynth Seqlab (Göttingen, DE). To identify mutations in *CYP51*, the 1702 bp gene was sequenced using the oligonucleotides which were used for the respective PCR reaction (Table 28, chapter 7.9, KES 2539 and KES 2592). To sequence the transformation constructs from plasmid DNA harboring the respective mutations, nine different sequencing primers were utilized to ensure full coverage of the complete sequences (Table 28, chapter 7.9, pJET1.2F, KES 2660, KES 2736, KES 2737, KES 2658, KES 2895, KES 2893, KES 2894 and pJET1.2R), which were 4644 bp long for sequence of strain with mutation L143F+G446S, 4611 bp long for sequence of strains with L143F and 4497 bp long for sequence of strains with mutation G446S. Sequence analyses was performed with the Geneious Prime[®] software by generating contigs of two reads to compare to a *A. solani* WT sequence and identify SNPs (single nucleotide polymorphism) in the *CYP51* gene and therefore different *CYP51*-haplotypes. Contigs of nine reads were generated to align with a predicted sequence of the transformation construct to analyze the transformed gene with the mutations of interest.

2.6.8 Pyrosequencing

Pyrosequencing is a method to detect known mutations (SNPs) in a target sequence by enabling real-time sequencing of up to 30 bp during DNA synthesis. It is based on an enzyme mix (DNA-polymerase, ATP sulfurylase, luciferase and apyrase) and a substrate mix (adenosine phosphosulfate (APS) and D-luciferin), where one of the four deoxyribonucleoside triphosphates (dNTPs (A, T, C, G)) is sequentially added to the template DNA. A specific sequencing primer initializes the starting point for the DNA-polymerase. Each dNTP is added one at a time. When a dNTP forms a base pair with the template DNA and therefore is incorporated into the newly synthesized DNA strand, pyrophosphate (PPi) is released, which is converted to adenosine triphosphate (ATP) by ATP sulfurylase, and the APS present in the enzyme mix. ATP is a substrate for luciferase which generates a quantifiable light signal and is proportional to the incorporated dNTPs. Not incorporated dNTPs and excessive ATP between the additions of different bases are degraded by apyrase (Ahmadian et al. 2000; Ahmadian et al. 2006).

In this work two pyrosequencing assays were established to quantify the double mutation L143F+G446S in *CYP51* in *A. solani* after conducting competition studies in the greenhouse

(chapter 2.10.1). Additionally, a pyrosequencing assay were established to quantify the single mutation G462S. Mutations L143F+G446S and G462S were used for quantification of mutations in a DNA pool from field trials in 2022 and 2023 (chapter 2.9). Within the *CYP51* gene 957 bp separate mutation L143F and G446S from each other. As one pyrosequencing assay can only cover a sequence of around 30 bp, a respective assay hat to be developed for each mutation of the double mutation. Further, pyrosequencing was used in this study to investigate whether the cells in the multicellular spores of *A. solani* are clones or differ genetically (chapter 2.11). Therefore, pyrosequencing assays for the *SDH* mutations B-H278Y and C-H134R were used. Moreover, a pyrosequencing assay to quantifying mutations C-H134R in the *SDH* gene and F129L in the *CYTB* gene was used to analyze multiple resistance in isolates from field trials in 2022 and 2023. The pyrosequencing assay for mutations in *SDH* and *CYTB* genes were already established internally in BASF SE before this work.

For pyrosequencing, a PCR-reaction with a 5'biotin-oligonucleotid and an oligonucleotide without biotin was conducted with gDNA of the region of interest and DreamTaq™ polymerase (Thermo Fisher Scientific Inc., Waltham, United States) (oligonucleotides in Table 28, chapter 7.9, PCR-reaction in Table 4, chapter 2.6.3.1). Afterwards, PCR-products were immobilized on streptavidin-coated sepharose beads by incubating them with binding buffer and streptavidin sepharose (GE Healthcare GmbH, Buckinghamshire, United Kingdom) for at least 15 min at room temperature and 1400 rpm on a microplate shaker. Reaction compounds are shown in Table 9 (Immobilization of DNA-template during pyrosequencing). With help of the PyroMark® Q96 vacuum station (Qiagen GmbH, Hilden, Germany), the gDNA was absorbed, washed in 70% (v/v) ethanol, denaturized with 0.2 M NaOH and neutralized with 1x wash buffer, leaving a single stranded DNA bound to the streptavidin sepharose (GE Healthcare GmbH, Buckinghamshire, United Kingdom). The DNA was then transferred to low plates (96-well) with annealing buffer (Qiagen GmbH, Hilden, Germany) and sequencing primer and incubated for 3 min at 80°C on a thermoblock for denaturation. Respective sequencing primers are listed in Table 28, chapter 7.9 and volumes of the compounds are represented in Table 9 (Preparation of DNA-template for pyrosequencing).

Table 9: Components for pyrosequencing.

Compounds	Volume in µL per reaction	Notes
PCR-reaction	25	Immobilization of DNA-template during pyrosequencing
Binding buffer	37	
Streptavidin sepharose	3	
Annealing buffer	38.75	Preparation of DNA-template for pyrosequencing
Sequencing primer	1.25	

After cooling down to room temperature the templates were sequenced in the pyro sequencer (Qiagen GmbH, Hilden, Germany). The PyroMark Q96 MA software (Qiagen GmbH, Hilden, Germany) was used to calculate the volumes of enzyme mix, substrate mix and dNTPs required for filling the reagent cartridge (Qiagen GmbH, Hilden, Germany) following the manufacturer's instructions. The assays to quantify the *CYP51* mutations were developed using the Pyrosequencing assay design software. DNA mixtures were prepared for validation of the assays. DNA solutions from a WT isolate (100% sensitive) and from a mutated isolate (100% mutation of interest) were adjusted to a concentration of 1 ng/μL. DNA mixtures were prepared in different ratios: 95/5, 90/10, 75/25, 50/50, 25/75, 10/90 and 5/95 (% DNA WT isolate / % DNA mutated isolate). Two positive controls (100% and 0% mutation) and a NTC were included. The DNA mixtures were used for assay validation, while the NTC and the positive controls were included in each run for reference. For validation and measurement of the isolates, all reactions were set up as duplicates. As the pyrosequencing method has a detection accuracy tolerance of approximately 5%, accordingly values <5% were considered below that limit and values >95% were interpreted as 100%.

2.6.9 Targeted mutagenesis of *A. solani*

A protocol for transformation of *A. solani* was established following the method described for *A. alternata* by Pruß et al. (2014) with modifications. Spores were harvested by floating an overgrown 2% (w/v) malt extract agar plate with 5 mL Richard's liquid medium and incubated in a digital platform shaker with incubation hood (CERTOMAT[®]H, Sartorius AG, Göttingen, DE) at 30°C and 130 rpm in a 100 mL Erlenmeyer flask. After 19-24 h the culture was filtered through double-layered cheese cloth (VWR International GmbH, Darmstadt, Germany) and washed with 0.7 M NaCl to remove residues of medium. A kitalase solution was prepared, where fungal material was digested at 30°C with gentle agitation at 90 rpm. After 45 min incubation protoplast quality and quantity were observed by microscope. By filtering through double-layered cheese cloth (VWR International GmbH, Darmstadt, Germany), protoplasts were separated from cell fragments. The kitalase solution was discarded, and protoplasts were centrifuged in cold (4°C) sorbitol-tris-calcium chloride (STC) for 10 min at 800 g and 4°C followed by a second washing step. Protoplasts were resuspended in 250 μL STC to which the transformation cassette (5000 ng DNA) was added and incubated on ice for 30 min. Subsequently, 1 mL polyethylenglycol (PEG) solution was added, carefully inverted, and incubated at room temperature. After 20 min, 12 mL of 0.6% (w/v) liquid regeneration medium at 45°C was carefully mixed with transformed protoplasts and poured onto selection plates containing 1.5% (w/v) regeneration medium and 100 μg/mL nourseothricin. This ensured that the protoplasts had enough time to develop a cell wall before the antibiotic diffuses into the superior layer of the regeneration medium. Plates were incubated at 25°C for three to five

days, as soon as growing colonies were visible, they were transferred to 12-well PDA plates containing 50 µg/mL nourseothricin as selection marker. To obtain homokaryotic targeted mutation strains, single spore isolates were generated on 2% (w/v) malt agar plates with 25 µg/mL nourseothricin, as described in chapter 2.2.4.

2.6.10 Southern-Blot-hybridization

The concept of Southern Blot relies on the separation of digested DNA through gel electrophoresis, followed by a DNA transfer onto a positively charged membrane to detect DNA fragments using a specific probe (Southern 1975). This method was used to verify correct integration of transformed gene cassettes in *A. solani*, according to Southern (1975) with modifications.

After DNA isolation of targeted mutation single spore isolates (chapter 2.6.1) a test-PCR was conducted (Table 4, chapter 2.6.3.1) with primer pair KES 2653 and 2737 (Table 28, chapter 7.9) to have a first indication for homologous transformation. The forward primer was chosen to anneal upstream of the *Nested-Primer* and the reverse primer annealing to the sequence of the nourseothricin acetyltransferase gene (*NAT1*) (Malonek et al. 2004). However, it was not possible to ensure whether the construct had been integrated in its entirety or fragmented elsewhere into the genome. Therefore, Southern-Blot-hybridizations were performed additionally on clones to identify strains with homologous integration of the new gene.

2.6.10.1 Preparation of digoxigenin-labeled probes

The amplification of probes, which are specific for *CYP51* or *NAT1*, was executed by a PCR-reaction with digoxigenin (DIG)-labeled dNTPs. Therefore, a DIG-dNTP-labeling mix (Merck KGaA, Darmstadt, Germany) containing 1 mM of dATP, dCTP, dGTP and 0.65 mM dTTP, as well as 0.35 mM DIG-dUTP was used. Since DIG-labeled dNTPs are light-sensitive, all following steps were performed under light reduced conditions. The reaction was set up on ice, the pipette scheme is shown in Table 10 with a final volume of 20 µL and the PCR conditions are shown in Table 11. For the amplification of the *CYP51* probe primer pair KES 2749 and 2750 (Table 28, chapter 7.9) was used, whereas primer pair KES 2736 and 2737 (Table 28, chapter 7.9) were added to the reaction for amplification of *NAT1* probe. Taq DNA Polymerase with ThermoPol® Buffer (M0267) (New England BioLabs GmbH, Frankfurt am Main, Germany) was used for amplification. Annealing temperature was adjusted depending on the primer used.

Table 10: Components of PCR reaction for probes.

Component	Volume (μL)
Taq DNA-Polymerase	0.5
DEPC-water	11.5
Forward primer (10 pmol/ μL)	1
Reverse primer (10 pmol/ μL)	1
ThermoPol Reaction Buffer (10x)	2
DIG DNA labeling mix	2
Template Plasmid DNA (max. 10 ng)	2

Table 11: Schematic procedure of a PCR reaction program for amplification of probes.

Taq DNA Polymerase with ThermoPol® Buffer (M0267) was used, annealing temperature was adjusted depending on the primer used.

Function	Temperature ($^{\circ}\text{C}$)	Time (s)	Cycles
Initial denaturation	95	300	1
Denaturation	95	45	30-35
Annealing	x	60	
Elongation	72	60 per kb	
Final elongation	72	600	1
Cooling	4	∞	1

A reaction with standard dNTPs were performed which serves as control. The successful incorporation of DIG-dUTPs was verified by gel electrophoresis (chapter 2.6.5) and amplified probes were purified using NucleoSpin® Gel and PCR Clean-up Kit (Macherey-Nagel GmbH & Co. KG, Düren, Germany) as described in chapter 2.6.6. PCR products were eluted in 30 μL elution buffer NE. Concentration of extracted DNA was determined using a Nanodrop2000 (Thermo Fisher Scientific Inc., Waltham, United States) photometrically and storage was done at -20°C in darkness. Before utilizing the probe, it was denatured for a duration of 5 min at 99°C .

2.6.10.2 Digestion of DNA with restriction enzymes

Concentration of isolated gDNA from targeted mutation strains of *A. solani* was adjusted to 125-250 ng/ μl in 40 μl volume. Afterwards, DNA were digested overnight with 30 Units of restriction enzyme and subsequent inactivation following the manufacturer's protocol for *Eco147I* or *Bsp119I* (Thermo Fisher Scientific Inc., Waltham, United States). Afterwards, a 0.7% (w/v) agarose gel electrophoresis was performed with an aliquot (chapter 2.6.5) to examine whether the DNA was properly digested. To visualize the fragments 15 μL of DNA-

dye (peqGreen) (VWR International GmbH, Darmstadt, Germany) was added to the gel and the EasyDoc plus gel documentation system (Herolab GmbH Laborgeräte, Wiesloch, Germany) was used.

2.6.10.3 Fixation, hybridization and detection

Digested DNA was mixed with 5 μ L of orange loading dye (Thermo Fisher Scientific Inc., Waltham, United States) and then loaded onto a 1 cm thick 0.7 % (w/v) agarose gel to separate the fragments. After 2 h at 60 V the gel was incubated at gentle agitation on a 3D digital shaker with 0.25 M HCl for 15 min for depurination of DNA. This led to partial fragmentation of the DNA to facilitate the transfer onto the Hybond™ -N+ membrane (Thermo Fisher Scientific Inc., Waltham, United States). Agarose gel was washed in demineralized water (VE) for 5 min and agitated in 0.4 M NaOH for 30 min to denature the DNA. After a second washing step the DNA was transferred onto a membrane overnight. The setup for the transfer of the denatured DNA fragments on a positively charged membrane was carried out. A stack of dry paper towels was placed on an elevated surface, on top of which three filter papers (Grade MN 68, Altmann Analytik GmbH & Co. KG, Munich, Germany) slightly larger than the gel were placed, followed by the membrane in the size of the gel, the gel itself and three filter papers of the same size as the gel. The gel was placed with the loading wells facing upwards. A length of filter paper was positioned on top the setup, with the left and right sides immersed in a tray containing 20x SSC solution. All filter papers and the membrane were soaked in 20x SSC and carefully placed on top of each other, avoiding trapping air bubbles, to ensuring an even transfer. 20x SSC solution permeates through the gel, drawn by the filter paper and dry paper towels, and carries the DNA molecules, effectively immobilizing them within the membrane. The set-up is left overnight.

At the end of the transfer, the membrane was carefully placed in between to filter papers to let it dry before it was placed in a UVP crosslinker to immobilize the DNA by irradiating twice with 120 mJ/cm². To confirm the successful transfer of DNA, the gel was exposed to the EasyDoc plus gel documentation system (Herolab GmbH Laborgeräte, Wiesloch, Germany). Pre-hybridization and hybridization were performed in a thermoblock to ensure a temperature of 68°C. After crosslinking the DNA to the membrane, a pre-hybridization was carried out to block non-specific binding of the probe. Therefore, 2 mL of 10x blocking reagent was mixed with 18 mL hybridization buffer, pre-heated to 68°C and filled in a plastic bag where the membrane was positioned carefully. The plastic bag was sealed with an impulse sealer. A small aperture was created at one corner of the plastic bag to allow substitution of buffers and solutions during the subsequent stages. After addition of the following solution the aperture was resealed. From this point forward, it must be ensured that the membrane remained drenched during the next stages. After 2 h at 68°C of pre-hybridization, a concentration of 5-25 ng/mL denatured probe

was added and left overnight at 68°C for hybridization. Unless otherwise specified, the following washing steps for detection were performed at room temperature with gentle agitation. A temperature of 68°C was maintained using a thermoblock. For each washing steps, 20 mL of the following solutions and buffers were sequentially added and discarded from the plastic bag: two times wash solution 2x for 5 min, wash solution 0.5x for 15 min at 68°C, wash solution 0.25x for 15 min at 68°C, wash solution 0.1x for 15 min at 68°C, wash buffer M for 1 min and blocking solution for 60 min. Then, 2 µL Anti-DIG (Merck KGaA, Darmstadt, Germany) was added and incubated for 30 min. This was followed by three washing steps with 20 mL wash buffer M for 10 min, to remove non-specific binding and non-binding antibodies. After washing, membrane was incubated with detection buffer for 2 min. Membrane was then positioned on filter paper for drying, before placing it in a plastic envelope for a 5 min incubation period with chemiluminescence substrate for phosphate detection (CSPD) (Merck KGaA, Darmstadt, Germany) in darkness. Afterwards, membrane was transferred to a fresh plastic envelope and incubated for another 5 min with the remaining CSPD (Merck KGaA, Darmstadt, Germany) on its surface. During these steps, it was necessary to ensure that no air bubbles were trapped. The extinction of the membrane was executed using the ChemiDoc™ imaging system and Image Lab™ software. The exposure times was determined by the signal strength of the DNA fragments and ranged from 5-25 min. The membrane was continuously exposed, and pictures were captures at 30-seconds intervals.

2.7 Fungicide sensitivity tests

2.7.1 Microtiter tests

The EC₅₀ values of *A. solani* were determined *in vitro* for various fungicides. EC₅₀ values represent the effective concentration of a substance that leads to inhibition of 50% of fungal growth, germination of fungal development (depending on the test method) when compared to the untreated control. Commercial formulations of azoxystrobin, mefentrifluconazole, difenoconazole and prothioconazole were used to assess the sensitivity of isolates of *A. solani* in 96-well microtiter plates. To determine the sensitivity of targeted mutation strains of *A. solani*, commercial formulations of mefentrifluconazole and difenoconazole were used. Seven concentrations of each fungicide were selected and tested based on their intrinsic activity. The method is based on “SEPTTR microtiter monitoring method BASF 2009 V1” (FRAC 2024e) with some minor changes for *A. solani* and was performed in a clean bench. Commercial formulations were dissolved in sterile deionized water, to prepare a 10,000 mg/L stock solution. Afterwards, a 20 mg/L, 60 mg/L and 200 mg/L solution were diluted in a 15 mL Eppendorf falcon to use for a fungicide dilution series in a 48-deep-well plate (Table 12). In 96-well microtiter plates 50 µL of double-concentrated fungicide and 50 µL of spore suspension was mixed for a ratio of 1:1 resulting in the following concentrations: 0, 0.003, 0.01, 0.03, 0.1, 0.3,

1, and 3 mg/L, prothioconazole was tested in the following concentrations: 0, 0.01, 0.03, 0.1, 0.3, 1, 3 and 10 mg/L (Table 12). Sterile deionized water was used as negative control.

Table 12: Preparation of fungicide dilutions.

Dilution (concentration in fungicide dilution (mg/L))	Final concentration in microtiter plate (mg/L)
9.8 mL water+0.2 mL 10,000 mg/L solution (200)	(100)
7 mL water+3 mL 200 mg/L solution (60)	(30)
9 mL water+1 mL 200 mg/L solution (20)	10
4.5 mL water+0.5 mL 60 mg/L solution (6)	3
4.5 mL water+0.5 mL 10,000 mg/L solution (2)	1
4.5 mL water+0.5 mL 6 mg/L solution (0.6)	0.3
4.5 mL water+0.5 mL 10,000 mg/L solution (0.2)	0.1
4.5 mL water+0.5 mL 0.6 mg/L solution (0.06)	0.03
4.5 mL water+0.5 mL 10,000 mg/L solution (0.02)	0.01
4.5 mL water+0.5 mL 0.06 mg/L solution (0.006)	0.003
4.5 mL water	0

Isolates of *A. solani* were grown for 12 days before preparing the spore suspension. One to two agar plates of each isolate were grown to obtain enough spores to test with different fungicides. Agar plates were flooded with 5-8 mL YBA double-concentrated (d. c.) and the surface of plates were suspended with a drygalski spatula (VWR International GmbH, Darmstadt, Germany). To separate the spores from the mycelium, the respective suspension was filtered through double-layered cheese cloth (VWR International GmbH, Darmstadt, Germany). The filtered suspension was pre-diluted with 5-8 mL YBA d. c. medium in a 50 mL Eppendorf falcon. The number of spores was then counted twice microscopically in a disposable haemocytometer (Neubauer Improved) (NanoEnTek Inc., Seoul, South Korea) and their density adjusted to 10^4 spores/mL by dilution in a 15 mL Eppendorf falcon with 15 mL YBA d. c. medium. Fifty μ L spore suspension and 50 μ L double-concentrated fungicide was mixed in a 96-well microtiter plate, where one well represents one replication. For each fungicide dilution, four replicants of each isolate were prepared. The average of the four replicants were calculated to determine the EC_{50} values. YBA d. c. medium without spores were mixed with the fungicide dilutions to generate a blank to serve as control and to measure the net OD. The set-up is illustrated in Figure 3.

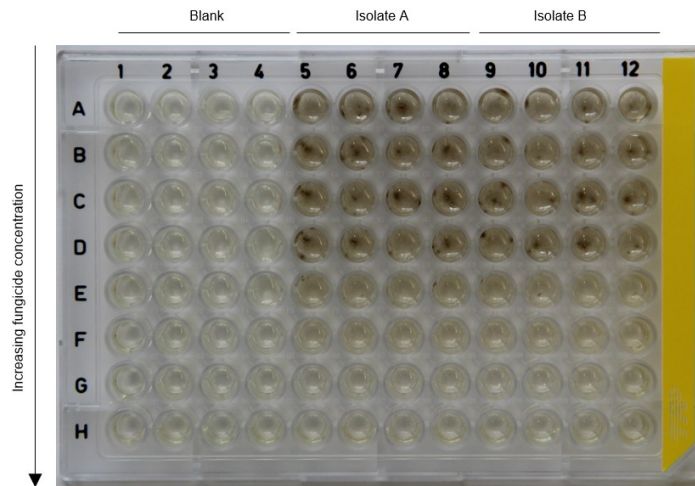


Figure 3: Experimental set up of a microtiter plate assay.

Water control without fungicide in row A. Increasing fungicide concentration in rows B-H. Columns 1-4 are blank controls with fungicide and medium without spores. Columns 5-12 show inoculated wells with the same number of spores in each well.

Afterwards, the microtiter plates were wrapped in plastic bags to reduce evaporation and incubated at 18°C and darkness. After six days, growth was measured in a photometer (96-well reader) at 405 nm and OD values were transferred into an excel spreadsheet using the software Magellan™ (version 7.3). Subsequently, EC₅₀ values were calculated using E-WorkBook Suite/Labbooq.

2.8 Fungicide sensitivity tests in the greenhouse with targeted mutation strains of *A. solani*

Fungicide sensitivity tests were conducted to investigate the *in vivo* effects of different DMIs towards targeted mutation strains in the greenhouse. For this purpose, strains with mutation L143F, G446S, L143F+G446S and two strains with ectopic integration were selected. Two individual greenhouse tests were performed.

2.8.1 Fungicide application

Fungicides were applied three-days prior to inoculation (preventive) in a spray chamber (SK06) (BASF SE, Ludwigshafen, Germany) with a water volume corresponding to 1000 L/ha. Tomato plants were cultivated according to chapter 2.4 and sprayed with 33 g active ingredient (a.i.)/ha and 100 g a.i./ha for the solo-formulated products mefentrifluconazole (Revysol®) and difenoconazole (Score®). Metiram (Polyram WG®) was included as a standard fungicide in every greenhouse test with 1260 g a.i./ha. Untreated plants served as control (UTC) to confirm the infection success for each isolate and trial. Water was used for dilution of formulated products. Per treatment and fungicide concentration three replicants were included.

2.8.2 Inoculation

Spore suspensions of *A. solani* were initially prepared in 2% (v/v) malt extract medium and then diluted to 0.2% (v/v). Spores from isolates (targeted mutation strains or field isolates) were harvested from culture grown for 12 days on agar plates by washing off the spores by flooding the agar plate with 5-8 mL 0.2% (v/v) malt extract medium and suspended with a drygalski spatula (VWR International GmbH, Darmstadt, Germany). Spores were filtered through double-layered cheese cloth (VWR International GmbH, Darmstadt, Germany) and spore density was determined by counting spores in a haemocytometer (Neubauer Improved) (NanoEnTek Inc., Seoul, South Korea) under the light microscope. The spore concentration was adjusted in a 300 mL Erlenmeyer flask to 10^4 spores/mL in a final volume of 200 mL. To prevent germination, spores were stored at 4°C until needed. Before inoculation of tomato plants with an airbrush (0.8 mm nozzle size) (SATA GmbH & Co. KG, Kornwestheim, Germany), greenhouse trolleys were covered with wet fleece and a semipermeable foil. Inoculation was performed until a homogenous coverage of spore suspension droplets were visible on the first two developed leaves, without running off. To avoid cross contamination only plants inoculated with the same isolate were placed on one greenhouse trolley. Greenhouse trolleys were covered with a light permeable plastic box to keep humid microclimate around the inoculated leaves, slowing down drying out of the spore suspension and allow *A. solani* to penetrate the leaves. After each isolate the airbrush (SATA GmbH & Co. KG, Kornwestheim, Germany) was cleaned once with 70% (v/v) ethanol and twice with water to avoid cross contamination. Inoculated plants were cultivated for four days in a greenhouse chamber at 21°C with 80-90% humidity. The lid of the plastic box was removed after one day.

2.8.3 Evaluation

Infection was visually rated five days after infection (5 dpi) in diseased leaf area (%). Therefore, tomato leaves that were available at the time of fungicide application and inoculation were evaluated, but no leaves that evolved after. Data of diseased leaf area were transferred to the software E-WorkBook Suite/Labbooq where the efficacy of fungicides was calculated as followed:

$$\% \text{ efficacy} = 100 - \frac{\text{average (treated sample)}}{\text{average (untreated sample)}} \times 100$$

2.9 Efficacy of fungicides in field trials

The purpose of the field trials in 2022 and 2023 was to analyze the current field population of *A. solani* on the trial sites and to investigate if target site mutations in *CYP51* are selected by DMI fungicides. Therefore, the potato varieties “Gala” and “Kuras”, which are highly susceptible

to early blight were planted. A complete randomized block design with six plots and three replicants per plot (Figure 4) were designed for both years in different locations.

1	2	3	4	5	6
1	2	3	4	5	6
6	2	5	4	3	1
12	11	10	9	8	7
3	5	1	2	6	4
13	14	15	16	17	18

Figure 4: Map with completely randomized plots.

Bold numbers represent the treatment number, regular number represent the replicants. Untreated control is marked in orange.

Trials included five treated plots and a fully untreated control with unrestricted development of *A. solani* infection to compare disease severity. In 2022, the location for the field trial was at the experimental station of BASF SE in Limburgerhof (Rhineland-Palatinate, Germany) where both potato varieties were planted in direct neighborhood. In 2023 variety “Kuras” was planted in Böhl-Iggelheim (Rhineland-Palatinate) and “Gala” in Ruchheim (Rhineland-Palatinate, Germany). Trial fields in Böhl-Iggelheim and Ruchheim are situated in representative potato growing regions of the Palatinate area and were chosen to portray the current *A. solani* population in southern Germany. Three to four fungicide treatments with tested products, depending on disease incidence and disease progress, with a spray interval of 10-14 days in 2022 and 14-21 days in 2023 were applied. One plot of the size of 2 m x 7 m represented one replicate of treatment. Solo formulations and fungicide mixtures were dissolved in water with an application rate of 400 L/ha as commercially available formulations and registered application rate (Table 13). All fields were infected by natural inoculum of early blight.

Table 13: Fungicide treatments, product rate and active ingredient rate.

Treatment	Product	Active ingredient	Product rate (L/ha)	Active ingredient rate (g/ha)
1		untreated control		
2	Revysol®	Mefentrifluconazole	1.25	93.8
3	Score®	Difenoconoazole	0.5	125
4	Proline®	Prothioconazole	0.2	96
5	Signum®	Boscalid+Pyraclostrobin	0.25	66.7+16.75
6	Vendetta®	Fluazinam+Azoxystrobin	0.5	188+75

In 2022, potato varieties were planted on 6th April in Limburgerhof in clayey sandy soil which was fertilized with 5 dt/ha ENTEC[®] 26 (equivalent to 130 kg N/ha) (Raiffeisen eG, Mannheim, Germany). Whereas in 2023 potatoes were planted on 19th April in silty clay (Böhl-Iggelheim) and sand/clay (Ruchheim) and fertilized with 5.5 dt/ha ENTEC[®] perfect (equivalent 83 kg N/ha) (Raiffeisen eG, Mannheim, Germany). To control infections with *P. infestans* (late blight) one application with Polyram WG[®] (Limburgerhof, 1.8 kg/ha; Böhl-Iggelheim/Ruchheim, 1.6 kg/ha) and three applications with Ranman Top[®] (0.5 L/ha) Revus[®] (0.6 L/ha) were carried out alternately in both years and all locations. Further in both years and all locations, SpinTor[®] (0.05 L/ha) and Mospilan[®] (0.125 L/ha) were utilized to control *Leptinotarsa decemlineata* (Colorado potato beetle). In Böhl-Iggelheim and Ruchheim additionally four applications with SpinTor[®] (0.05 L/ha) were conducted. For weed control, Bandur[®] (3 L/ha) with Sencor Liquid[®] (0.5 L/ha) were used in all three locations and two applications with Cato[®] (0.03 L/ha) were carried out in 2023 in Böhl-Iggelheim.

2.9.1 Disease scoring

The progress of infection of *A. solani* was observed in frequent time intervals of one or two weeks. Disease severity was assessed from beginning of July until mid-September by percent of infection of the leaf area which showed necrotic early blight spots. The efficacy (%) of the fungicide treatment was calculated as described in chapter 2.8.3 for evaluation of fungicide efficacy in the greenhouse. Each plot of each treatment was evaluated separately, and the average was calculated. One evaluation date was selected for each trial, where a sufficient infestation was determined, and on which a good differentiation of the different treatments was possible.

2.9.2 Sampling and isolation of *A. solani*

Potato leaflets with typical *A. solani* lesions were collected in all untreated and treated plots. Leaf samples of all three replicants were collected randomly across the plots and pooled for isolation of *A. solani* isolates. One sample included a minimum of 20 *A. solani* lesions, each from a different infected potato leaf, collected randomly in the plots. DNA was extracted from 20 *A. solani* lesions of these leaves and subsequently analyzed with a pyrosequencing assay. To calculate the frequency of the sensitive alleles (WT), the frequency of the different resistance alleles was added and subtracted from 100%. Further, collected leaves were used for isolation of isolates and generation of single spore isolates.

In 2022, leaf samples from variety “Gala“ were collected on 18th July and samples from “Kuras” on 24th August and 12th September. In 2023, infected leaves from “Gala“ were collected on 1st September and from “Kuras” on 11th September.

2.10 Competitiveness and vitality of *A. solani* haplotypes

The competitiveness of WT and L143F+G446S single spore isolates were determined by performing competition studies in the greenhouse, to observe the development of DMI adaptation in *A. solani* over time. Further, vitality of *CYP51* haplotypes was analyzed by observing spore morphology, spore quantity, infection rate, and vegetative growth.

Therefore, 10 isolates were selected from a limited region in northern Netherlands to reduce genetic background heterogeneity between the isolates, except for the *CYP51* mutations. Five single spore isolates harboring the double mutation L143F+G446S and five WT single spore isolates were used for the competition studies and determination of vitality of different *CYP51* haplotypes (Table 14).

Table 14: Single spore isolates used in competition studies of different *CYP51* haplotypes.

The mixture contained 10 single spore isolates, five mutated and five sensitive. The table shows the percentage of the mutations, the respective haplotypes and the origin of the single spore isolates.

Isolate	Origin	Mutation in <i>CYP51</i> (%)		<i>CYP51</i> haplotype
		L143F	G446S	
Ms 1076	NL (Valthermond)	100	100	L143F+G446S
Ms 1077	NL (Valthermond)	100	100	L143F+G446S
Ms 1080	NL (Valthermond)	100	100	L143F+G446S
Ms 1085	NL (Valthermond)	100	100	L143F+G446S
Ms 1088	NL (Valthermond)	100	100	L143F+G446S
Ms 1035	NL (Emmeloord)	0	0	WT
Ms 1036	NL (Emmeloord)	0	0	WT
Ms 1037	NL (Emmeloord)	0	0	WT
Ms 1038	NL (Emmeloord)	0	0	WT
Ms 1039	NL (Emmeloord)	0	0	WT

2.10.1 *In vivo* competition studies in the greenhouse

The single spore isolates were used to prepare three mixtures. The first mixture consisted of spores from five sensitive isolates (wildtype-mixture), while the second mixture consisted of spores from five mutated isolates (mutant-mixture). The third mixture consisted of spores from all five WT and all five mutated isolates (wildtype-mutant-mixture). All isolates for all mixtures were adjusted to 10^4 spores/mL. Spore suspensions of single spore isolates were prepared, as described in chapter 2.8.2 in a final volume of 50 mL. Each mixture (wildtype/mutant/wildtype-mutant-mixture) was inoculated onto three tomato plants. Tomato plants were inoculated and incubated using the same procedure as described in chapter 2.8.2.

After four to six days of incubation, leaves with 80-90% diseased leaf area were placed on 2% (w/v) malt extract medium plates in an incubation chamber at 18°C with a 12 h photoperiod to improve sporulation. After two days spores were washed off of the leaves with 100 mL of 0.2% (v/v) malt extract medium to release spores. This mixture was stirred approximately every 5 min for an incubation period of 30 min and filtered through double-layered cheese cloth (VWR International GmbH, Darmstadt, Germany). The resulting spore suspensions were used to inoculate new leaves, starting a new disease cycle. After every disease cycle an aliquot of 25 mL of each spore suspension was centrifuged, supernatant discarded, and the remaining spores were stored at -20°C for DNA extraction. The objective of this test system was to cover all stages of the infection cycle including spore germination, infection, growth, sporulation, spore production, and release, to assess the competitive ability of the isolates. The wildtype-mutant-mixture was included to monitor the prevalence of mutated isolates throughout the cycles, while the wildtype-mixture and mutant-mixture were used to confirm their infectivity on tomato plants. Additionally, these mixtures served as positive and negative controls for the genetic analysis. This experiment was terminated after five cycles and the experiment was conducted twice. To quantify the frequency of mutations in the population, pyrosequencing assay was done after every disease cycle as described in chapter 2.6.8.

2.10.2 Spore morphology

To identify if there are differences in spore morphology between WT and mutants, spores of different haplotypes were harvested by flooding a 2% (w/v) malt agar plate with 12 day old cultures (chapter 2.2.1) with 5-8 ml 2% (w/v) malt extract medium and suspended with a drygalski spatula (VWR International GmbH, Darmstadt, Germany) over the surface. Subsequently, the spore suspension was filtered through double-layered cheese cloth (VWR International GmbH, Darmstadt, Germany) to remove mycelia debris, pipetted onto an object slide and covered with a cover glass. The length and width of spores were observed and measured under a light microscope and compared between the haplotypes. For each, WT and double mutation L143F+G446S, five biological replicants were included, and for each single spore isolate 100 spores were examined.

2.10.3 Quantification of spores

Spores of single spore isolates were quantified to observe potential differences in spore production of WT and haplotype L143F+G446S. Therefore, 2% (w/v) malt agar plates were inoculated by placing 10 µl of a spore suspension, which was prepared as described in chapter 2.7.1 with 10⁵ spores/mL and 2% (w/v) malt extract medium, in the center of the agar plate. When the mycelium of the single spore isolates was 1 cm away from the border of the petri dish, spores were washed off with 3 ml 2% malt extract medium and suspended with a

drygalski spatula (VWR International GmbH, Darmstadt, Germany). Subsequently, spores were separated from mycelium by filtering the suspension through double-layered cheese cloth (VWR International GmbH, Darmstadt, Germany). The number of spores was then counted twice microscopically in a disposable haemocytometer (Neubauer Improved) (NanoEnTek Inc., Seoul, South Korea). Based on the number of spores counted, the total number of spores in the 3 ml suspension was calculated. Five biological replicants and three technical replicants for WT and haplotype L143F+G446S were included, respectively.

2.10.4 Infection rate

For determination of infection rate and inhibition by DMIs, greenhouse sensitivity tests were conducted as described in chapter 2.8. Two single spore isolates with double mutation L143F+G446S and two WT single spore isolates were tested in two independent experiments with DMI fungicide application of mefentrifluconazole (Revysol®) and difenoconazole (Score®). Infection rate was visually rated in diseased leaf area (%).

2.10.5 Determination of vegetative growth

Vegetative growth of *A. solani* haplotype L143F+G446S and WT were determined by incubating single spore isolates on 2% (w/v) malt agar plates as described in chapter 2.2.1. Agar plates were amended with mefentrifluconazole and difenoconazole in following concentrations: 0, 0.01, 0.03, 0.1, 0.3, 1, 3 and 10 mg/L. Moreover, agar plates without fungicides were included as control. Inoculation of agar plates were conducted as described in chapter 2.10.3 with 10⁵ spores/mL. Agar plates used in this experiment did not contain streptomycin sulphate (AppliCHem GmbH, Darmstadt, Germany). Two biological replicants and three technical replicants per haplotype were performed. The radial growth was measured using a ruler when the mycelium of the single spore isolates at 0 mg/L was 1 cm away from the border of the petri dish. The diameter was measured twice per plate, with the two measuring lines at a 90° angle to each other. The growth was calculated in cm.

2.11 Verification of multicellular spores for genetic identity

The isolate 744 exhibits varying quantities of SDHI mutations (83% *SDH B*-H1278Y; 9% *SDH C*-H134R) and was chosen to prove that the cells in the multicellular spores of *A. solani* are genetically identical. The isolate was recultivated from long-term storage (chapter 2.2.2) and single spore isolates were generated as described in chapter 2.2.4. Afterwards, quantification of mutations in each single spore isolate was performed by pyrosequencing (chapter 2.6.8).

2.12 Homology modelling

The software Molecular Operating Environment (MOE) with standard settings (version 2020-09) was used by Dr. Ian Craig of BASF SE, to perform the homology modelling of the Cyp51 protein of *A. solani*. Due to no availability of a crystal structure of *A. solani* Cyp51 protein, the Cyp51 from *A. fumigatus* (PDB ID: 6CR2) was used as a template because of the high sequence identity with *A. solani* Cyp51 of 64%. To aid visualization of the binding site, the pharmaceutical DMI analog bound to *A. fumigatus* Cyp51 in the template protein structure (VNI; (2,4-dichlorophenyl) 2-(1H-imidazol-1-yl)-4-(5-phenyl-1,3,4-oxadiazol-2-yl)benzamide) (Friggeri et al. 2018) was implemented in the final model of *A. solani* Cyp51.

3 Results

In this work, samples were collected from different countries to monitor the sensitivity of *A. solani* to different DMIs. Therefore, isolates and single spore isolates were obtained from infected leaves from different regions, years, and fields with different fungicide background. Single spore isolates and isolates were obtained to elucidate whether the population of *A. solani* developed resistance mechanisms to DMIs. Because no resistance mechanisms for DMIs were known so far, single spore isolates were generated, since these isolates originate from a single spore and bear only the genetic information of one individual. The genetic uniformity of the single spore isolates should simplify the molecular detection of potential aa alterations in the sequence of the *CYP51* gene. To prove the genetical uniformity pyrosequencing for different *SDH* mutations was conducted. While the parental isolate showed varying quantities of *SDH* mutations, the single spore isolates should show either 0% or 100% of the respective mutation. With single spore isolates, resistance mechanisms could be detected and examined. New *CYP51* mutations were characterized by testing different haplotypes for their effect on DMI sensitivity. Further, a protein model was designed to indicate the positions of new detected mutations, that lead to aa alterations in the Cyp51 enzyme. Additionally, field trials were conducted with infection by natural inoculum of the current *A. solani* population to examine, whether DMI treatments select mutations in the *CYP51* gene and to evaluate the efficacy of DMIs in the field with presence or absence of mutants in the population. Competition tests were performed in the greenhouse to determine potential fitness costs associated with the L143F+G446S haplotype and vitality of *CYP51* WT and L143F+G446S was analyzed. Moreover, targeted mutagenesis was conducted to prove, that the target site mutations detected in the *CYP51* gene are the reason for DMI adaptation and to investigate the effect of artificially generated haplotypes on DMI sensitivity. To verify successful homologous transformation of *CYP51* and to exclude strains with ectopic integration, a Southern Blot was performed. Targeted mutation strains of *A. solani* were used for *in vitro* sensitivity tests with DMIs. Further, greenhouse studies were performed, to test the effect of *CYP51* mutations introduced through targeted mutagenesis on DMI performance on the plant and predict their impact on the field efficacy.

3.1 Verification of multicellular spores for genetic identity

In order to determine the genetic variability of multicellular spores in *A. solani*, 20 single spore isolates were generated (chapter 2.2.4) from isolate 744 exhibiting varying quantities of *SDH* mutations. Isolate 744 represented a population and was recultivated from internal BASF storage originally provided by Biotransfer (Montreuil, France) in 2018. This parental isolate revealed 83% mutation H278Y in *SDH B* and 9% mutation H134R in *SDH C* gene. Rates of mutations in single spore isolates were subsequently analyzed by pyrosequencing. The

resulting mutation frequencies for mutation *B*-H278Y and *C*-H134R are represented in Table 15. Single spore isolates generated from 744 showed either 0% or 100% mutation. Consequently, it can be inferred that the multicellular spores of *A. solani* are genetically identical and therefore single spore isolates are clones.

Table 15: Confirmation of the genetic identity of multicellular spores of *A. solani* through determination of quantitative mutation proportion (%).

Single spores were generated and gDNA was extracted for subsequent pyrosequencing for identification of mutations frequency. The parent of the single spore isolates represents the reference isolate and frequency of mutation *B*-H1278 and *C*-H134R for all isolates are listed. Since the detection accuracy of pyrosequencing is 5%, all values <5% were considered as 0% and all values above 95% can be interpreted as 100%.

Isolate	Mutation (%) in gDNA	
	<i>SDH B</i> -H278Y	<i>SDH C</i> -H134R
744 ^a	83	9
Ms 744-021	0	100
Ms 744-022	100	0
Ms 744-023	100	0
Ms 744-024	100	0
Ms 744-025	100	0
Ms 744-026	100	0
Ms 744-027	100	0
Ms 744-028	100	0
Ms 744-029	0	100
Ms 744-030	0	100
Ms 744-031	100	0
Ms 744-032	100	0
Ms 744-033	0	100
Ms 744-034	0	100
Ms 744-035	100	0
Ms 744-036	0	100
Ms 744-037	0	100
Ms 744-038	100	0
Ms 744-039	100	0
Ms 744-040	0	100

^a reference isolate = parent of single spore isolates

3.2 Identification and characterization of *CYP51* haplotypes in *A. solani*

3.2.1 First detection of *CYP51* mutations

A total of 261 field isolates and 235 single spore isolates were obtained from samples from different countries and collected in 2018, 2020, 2021, 2022 and 2023. The *CYP51* gene of all isolates was amplified and sequenced. Sequences were then aligned to a WT cDNA obtained in this work, to analyze mutations leading to aa alterations resulting in different *CYP51* haplotypes. The gene has 1673 nucleotides with two introns at positions 245-293 and 492-540. Three aa alterations (Table 16) have been found in *CYP51* across all investigated *A. solani* isolates and single spore isolates.

Table 16: *CYP51* alterations found in *A. solani*.

Detected mutations in *CYP51* are listed, along with the WT codon and corresponding aa, as well as the mutated codon and aa of the mutation.

Mutation	WT		Mutant	
	Codon	Amino acid	Codon	Amino acid
L143F	CTC	Leucin	TTC	Phenylalanine
G446S	GGC	Glycine	AGC	Serin
G462S	GGC	Glycine	AGC	Serin

Isolates with mutation L143F, a nucleotide substitution from cytosine to thymine, by a change of the aa at position 143 from leucine to phenylalanine, reveal a co-existing aa change at position 446 from glycine to serine (G446S), caused by a nucleotide substitution from guanine to adenine. The mutation L143F has been exclusively found in combination with the mutation G446S. In contrast, mutation G462S was detected solely and is caused due to a nucleotide substitution from guanine to adenine, by a change of the aa at position 462 from glycine to serine. This mutation was identified as a single mutation, without any co-occurring mutations. In Figure 5, both introns (49 bp) are highlighted, and positions of detected mutations are named. Mutation L143F is located between intron I (codon 83-98) and II (codon 165-181), whereas mutation G446S and G462S are located after the second intron.



Figure 5: Point mutations detected in *CYP51* gene of *A. solani*.

Introns I and II are marked with a line segment, highlighting its position within the gene. Detected single point mutations are highlighted in red with nucleotide substitutions.

Across all isolates two *CYP51* haplotypes with mutations were identified and described for the first time. Isolates originated from Sweden (n=6), the Netherlands (n=106), Germany (n=317) and Australia (n=67) (Figure 6). Isolates carrying the double mutation L143F+G446S were found in Australian isolates from 2018 (n=42), in Dutch isolates from 2020 (n=20), 2021 (n=9) and 2022 (n=18) and in German isolates from 2022 (n=1) and 2023 (n=42). Additionally, single mutation G462S was detected in Germany in 2022 (n=2) and 2023 (n=4). Among all isolates investigated, the WT was the predominant haplotype and present in Australia in 2018 (n=25), the Netherlands in 2021 (n=36) and 2022 (n=23), Sweden in 2022 (n=6) and Germany in 2021 (n=4), 2022 (n=96) and 2023 (n=168). When *CYP51* genotype data from all regions and years collected were pooled, double mutation L143F+G446S (n=132) were more common than single mutation G462S (n=6), but most of the population carried no target site mutations (n=358). No isolates were detected carrying mutation G462S and L143F or G446S simultaneously.

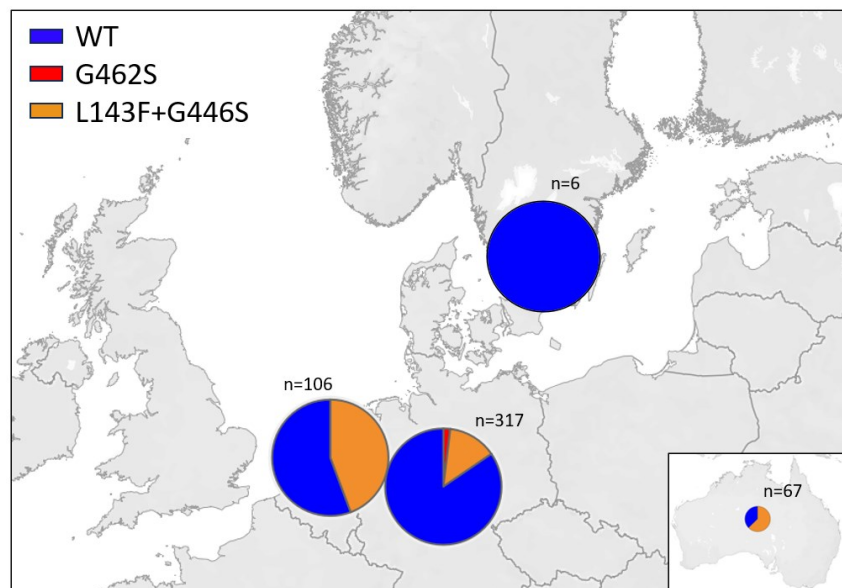


Figure 6: Collection sites of *A. solani* isolates.

Collection sites of isolates from Germany (n=317), the Netherlands (n=106), Sweden (n=6) and Australia (n=67) and respective *CYP51* mutations are shown. WT is illustrated in blue, mutation G462S in red and double mutation L143F+G446S in orange.

3.2.2 Molecular characterization of amino acid alterations in the Cyp51 enzyme

The Cyp51 protein model, designed by Dr. Ian Craig (BASF SE), was utilized to identify the location of the detected mutations in relation to the prosthetic heme group of the protein. The positions of the target site mutations are important to investigate and explain the altered aa effect on DMI binding and sensitivity. As no crystal structure of *A. solanis* Cyp51 is currently available, the model is based on an experimental structure of the Cyp51 from *A. fumigatus* (PDB ID: 6CR2). For demonstrational purpose, an analog DMI structure derived from the pharmaceutical compound VNI (2,4-dichlorophenyl) 2-(1H-imidazol-1-yl)-4-(5-phenyl-1,3,4-oxadiazol-2-yl)benzamide) was implemented. The prosthetic heme group represents the binding site for DMIs and is indicated in light blue, while the analog DMI is shown in pink. Mutations L143F+G446S and G462S are marked in yellow (Figure 7A). In Figure 7B the binding site with the surrounding mutations is shown in a close-up view. Position of aa G446 (11 Å) is the one furthest away from the heme group, whereas L143 (6.6 Å) and G462 (3.9 Å) are positioned in proximity of the binding site. As the aa alteration L143F and G446S always emerge in combination, it can be assumed that the effect on DMIs is more severe than the effect of the single mutation G462S, despite the proximity of the single mutation to the prosthetic heme (3.9 Å).

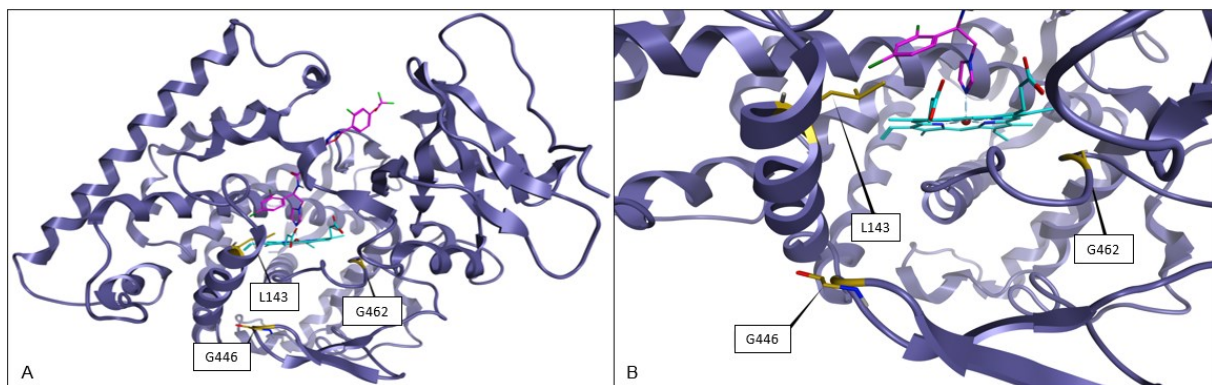


Figure 7: Homology model of *A. solanis* sterol 14- α demethylase enzyme (Cyp51) representing the location of the WT amino acid identified as positions of new alterations.

The protein model is based on Cyp51 from *A. fumigatus* (PDB ID: 6CR2), the heme group is illustrated in light blue and indicates the DMI binding site. The WT aa positions to be identified as new alterations (L143F, G446S, G462S) are indicated in yellow, the analog DMI is painted in pink. An overview of all positions at which new aa alterations were identified (A) and a close-up on the surrounding positions of aa alterations of the heme group (B) were indicated.

Closer inspection of the mutation L143F shows a formation of an aromatic ring when the aa is altered from leucin to phenylalanine (Figure 8A). The aromatic ring is in proximity to the carboxylate group of the prosthetic heme. A steric clash would create an energetically unfavorable state and is expected to induce a change of neighboring heme and protein atoms.

Mutation G446S is further away from the heme and therefore, the site where the DMI binds. No steric clash with the heme is observed when glycine is altered to serine at position 446 (Figure 8B). Figure 8C illustrates, that at position 462 the mutated serine has an additional hydroxy (OH)-group compared to the WT glycine, which aligns well between a backbone NH and one of the carboxylate groups on the heme, forming hydrogen bonds.

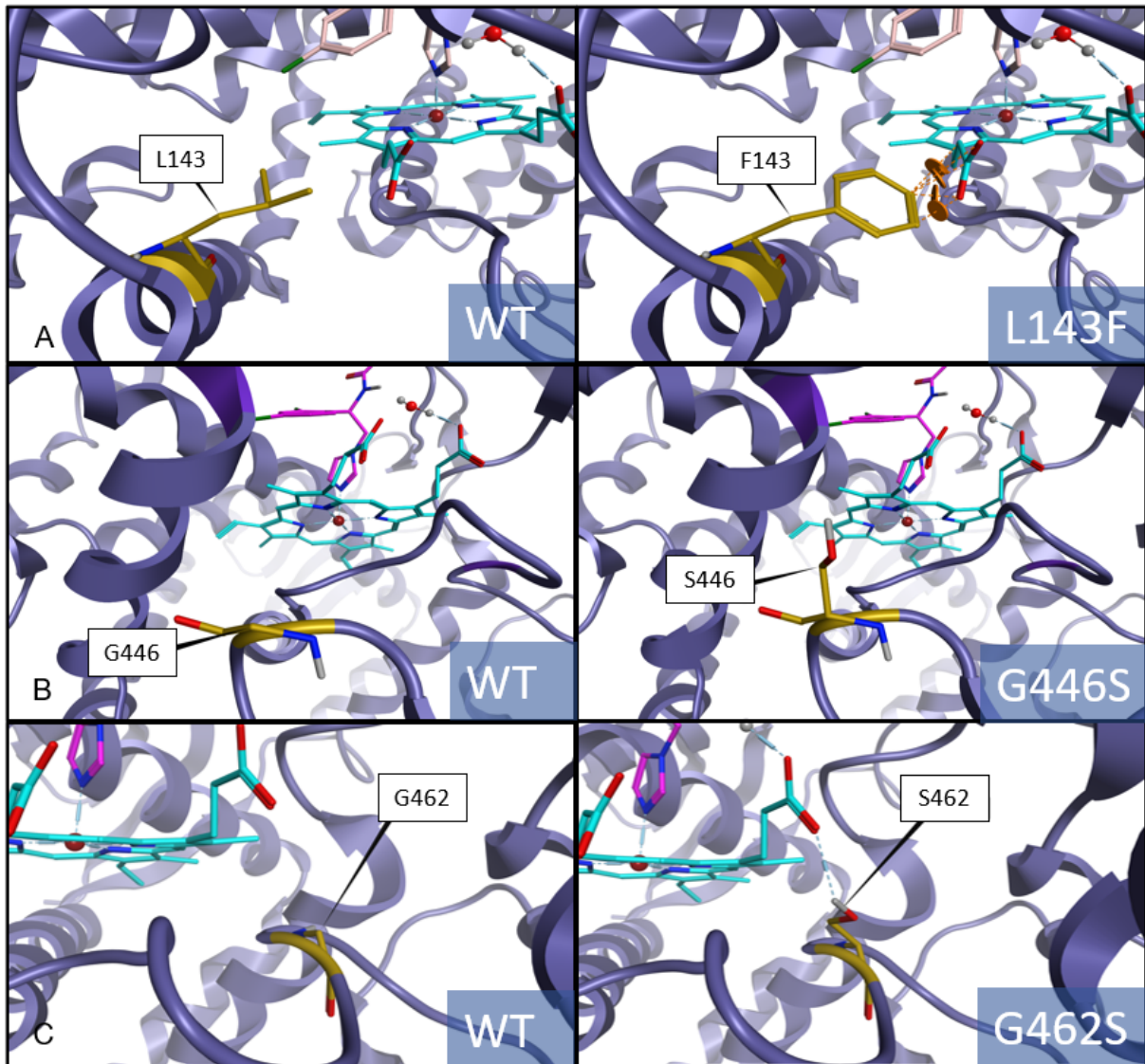


Figure 8: Homology model of *A. solanis* Cyp51 representing the location L143, G446 and G462.

The aa positions identified as a subject of new alterations are highlighted in yellow and the heme group is indicated in light blue. The WT aa position L143 and mutated F143 (A), the WT aa position G446 and mutated S446, as well as the WT aa position G462 and mutated S462 are shown.

3.2.3 Alignment of *CYP51* sequences from different phytopathogenic fungi

Newly detected aa alterations in *A. solani* are homologous to mutations in other phytopathogenic fungi, that are known to influence the DMI sensitivity. A multiple alignment was used to compare the nucleotide and aa sequence of the *CYP51* gene of different phytopathogenic fungi to *A. solani*. The included fungi are plant pathogens that cause severe damage to the production of specialty (e.g., fruit, vegetables) and arable (e.g., potatoes, sugar beet) crops and oilseed rape. The *A. solani* sequence was obtained in the present study, sequences of *V. inaequalis*, *C. beticola* and *M. fructicola* were extracted from National Centre for Biotechnology Information (NCBI) or from internal sequences from BASF database. *P. brassicae* sequence was kindly provided by Diana E. Bucur (Teagasc Crop Science Department, Oak Park, Carlow, Ireland). The WT cDNA sequence of *A. solani* was used as reference and was aligned to other fungi, evolving homologues mutations, in Geneious Prime[®] software using Clustal Omega-Alignment. Pathogens aligned to *A. solani* with respective homologous mutations are listed in Table 17.

Table 17: Phytopathogenic fungi and point mutations in target gene *CYP51* responsible for sensitivity losses towards DMIs.

Pathogens are listed with corresponding mutations and describing literature.

Species	Mutation in target gene <i>CYP51</i>	Literature
<i>Alternaria solani</i>	L143F	
<i>Cercospora beticola</i>	L144F	Muellender et al. (2021)
<i>Venturia inaequalis</i>	L140F	Hoffmeister et al. (2021)
<i>Alternaria solani</i>	G446S	
<i>Venturia inaequalis</i>	G444S	Hoffmeister et al. (2021)
<i>Alternaria solani</i>	G462S	
<i>Monilinia fructicola</i>	G461S	Lichtemberg et al. (2017)
<i>Pyrenopeziza brassicae</i>	G460S	Carter et al. (2014)

All fungal pathogens listed in Table 17, belong to the Ascomycota and are therefore genetically closely related. Further, *A. solani*, *C. beticola* and *V. inaequalis* are classified as Dothideomycetes, whereas *M. fructicola* and *P. brassicae* classify as Leotiomycetes (EPPO 2024). *V. inaequalis* reveals mutation L140F, which is homologous to mutation L143F in *A. solani* and mutation G444S, which is homologous to G446S. In contrast to double mutation L143F+G446S, in *V. inaequalis* mutations L140F and G444S do not occur in combination, nevertheless L140F is found, so far, only in combination with M141V (Hoffmeister et al. 2021). Muellender et al. (2021) described a mutation at position 144 which consequently alters the aa from leucine to phenylalanine in *C. beticola*. This aa alteration is equivalent to L143F in *A.*

solani and often evolved in combination with mutation I309T in *C. beticola*. Further, *M. fruticola* developed mutation G461S (Lichtemberg et al. 2017) and *P. brassicae* developed mutation G460S (Carter et al. 2014), which are homologous to mutation G462S in *A. solani*. *P. brassicae* emerged mutation G460S as single mutation or in combination with S508T (Carter et al. 2014; Bucur et al. 2022). Additionally, *Z. tritici* and *R. collo-cygni* developed mutation G460D at position YGY (459-461), with the WT aa being homologous to G446 in *A. solani* (Stammler et al. 2008; Rehfus et al. 2019). Both pathogens belong to the Ascomycota and the class of Dothideomycetes.

All mentioned aa alterations affect the binding of DMIs to the heme group in *CYP51*. Due to deletions and insertions in the sequence, positions of aa alterations shift (Table 17). The extend of genetic similarity can also be observed in the alignment of the cDNA (Figure 9), where aa 134-155 and 442-463 with regions of mutations are pictured and aa agreements are highlighted in color.

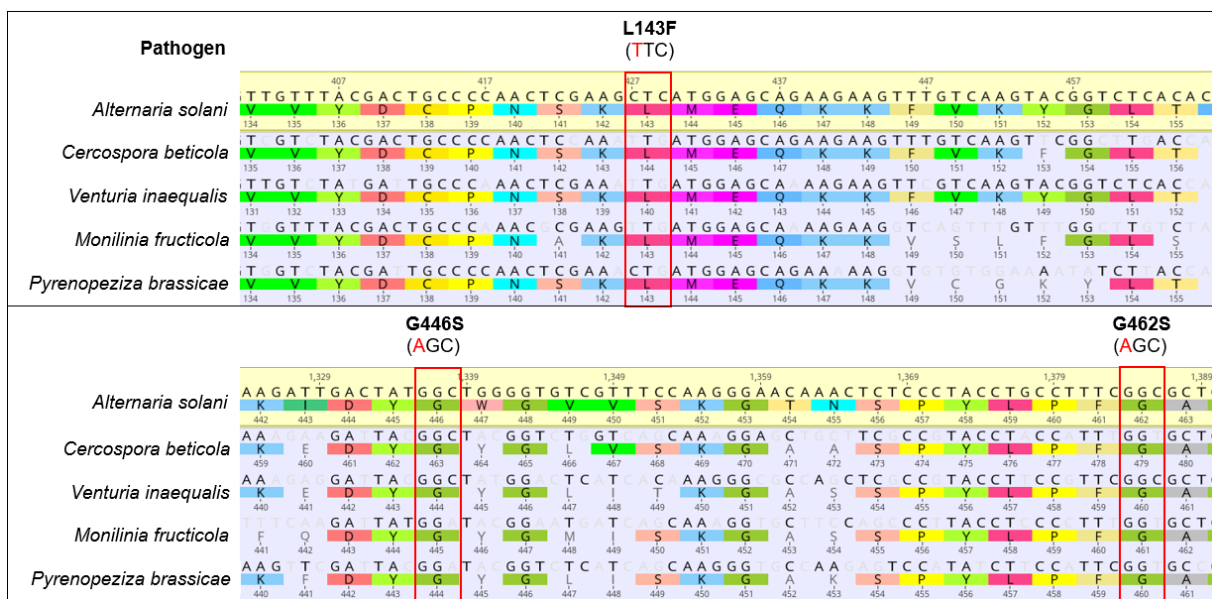


Figure 9: Cutout of the alignment of nucleotide and amino acid sequences from *A. solani* and other phytopathogenic fungi.

The WT cDNA sequences of *A. solani*, *C. beticola*, *M. fruticola*, *P. brassicae* and *V. inaequalis* were aligned using *A. solani* WT as reference strain. Agreements in aa of included pathogens are highlighted multicolored, agreements in nucleotides are pictured in black letters. Detected mutations with altered nucleotides are marked with red boxes. Position L143, as well as position G446 and G462 in *A. solani* WT are marked.

What stands out in Figure 9, is the dominance of similarity around the mutated regions. It can be seen, that mutations L143F, G446S and G462S all occur in regions conserved over the different fungi. Slight disagreements in nucleotides are visible, but the aa sequence remains conserved. This observation implies that these regions play a role in either determining the proteins three dimensional structure or the creation of binding sites essential for substrate and

fungicide interaction. Mutation G446S occurs in a region, so called YGY, and is known to be conserved over many fungal species.

3.3 Competitiveness and vitality of *A. solani* haplotypes

3.3.1 *In vivo* competition studies with *CYP51* mutants

Competition studies in the greenhouse were carried out to determine the stability of double mutation L143F+G446S in the *CYP51* gene when no selection pressure due to fungicide applications was present. Therefore, a mixture of mutants and wildtype single spore isolates were prepared. The following competition study focused on the L143F+G446S mutations since they were more frequent in populations analyzed in this work than single mutation G462S. Additionally, to its dominance, this aa alterations in general showed higher resistance levels for DMIs than single mutation G462S (chapter 3.4). The mixture of sensitive and mutated single spore isolates was inoculated on tomato plants for several infection cycles. The procedure was repeated in two independent experiments and two quantitative pyrosequencing assays after each cycle were used for evaluation of the quantity of mutations within the mixture. Figure 10 provides the frequency of double mutation L143F+G446S and WT in the infection cycles. The initial mixture of wildtype and mutant contained around 50% of the L143F+G446S mutation in both trials. A significant decrease of the isolates with *CYP51* mutations can be observed in the mixture after the fourth cycle ($p < 0.05$). Single spore isolates with double mutation L143F+G446S decreased after the first infection cycle from a mean of 50% to a mean of 21%, after the second cycle decreased further to a mean of 15%, in cycle three mutations are present at mean of 4% and in cycle four and five WT dominates with a mean of 100%. This indicates a disadvantage of the L143F+G446S haplotype in the greenhouse when there is no DMI application, and that the WT showed a higher competitiveness. Wildtype-mixture and mutant-mixture of isolates showed stable mean values during the infection cycles of either 0% or 100% of mutation L143F+G446S.

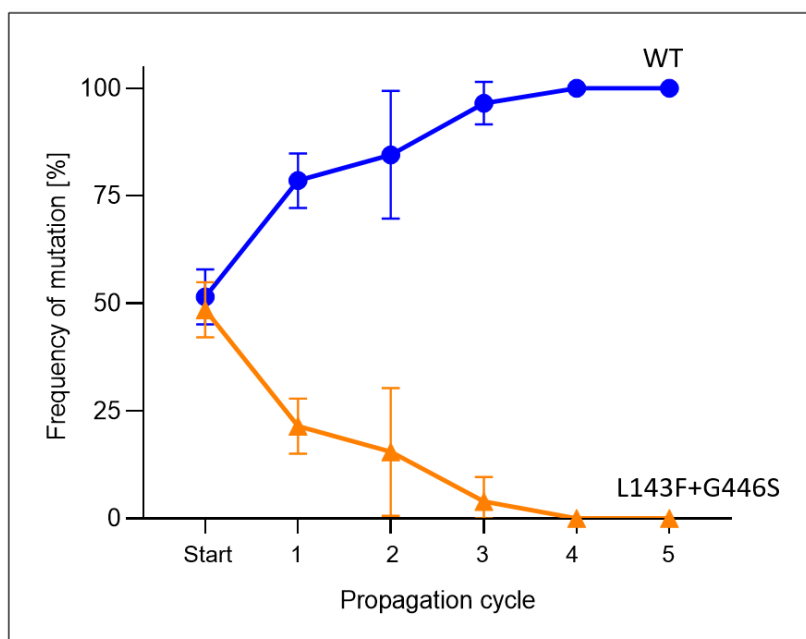


Figure 10: *In vivo* competition studies of *CYP51* haplotype L143F+G446S and WT of *A. solani* under non-selective conditions.

A wildtype-mutant mixture of five WT single spore isolates and five single spore isolates carrying double mutation L143F+G446S was used to analyze the competitiveness of different haplotypes when propagated together over several infection cycles on tomato plants without fungicide application. Frequency of *CYP51* haplotype L143F+G446S is indicated with blue dots, and *CYP51* sensitive haplotype (WT) is indicated with orange triangles. Vertical lines indicate the standard error of the mean. Spore suspension after every cycle was used for subsequent analysis by pyrosequencing.

3.3.2 Spore morphology and quantification

Spore morphology was determined under the light microscope, by measuring length and width of *A. solani* spores with *CYP51* double mutation and WT. Spores of five WT single spore isolates (n=500) and five single spore isolates with double mutation L143F+G446S (n=500) were observed to determine differences in morphology. Spores of WT and L143F+G446S were then washed off with 3 ml 2% malt extract medium from 2% (w/v) malt agar plates to quantify the sporulation.

Figure 11A pictures spores of Ms 1088, which exhibits mutation L143F+G446S in the *CYP51* gene and spores of WT Ms 1036. When comparing these two haplotypes no differences in shape or septation was observed. Further, no significant difference was observed in length or width of spores with or without mutation in the *CYP51* gene (Figure 11B). The length of WT spores of five different isolates varied from 72.7 μm to 351.1 μm with a mean of 157.7 μm , whereas the length of spores harboring mutation L143F+G446S varied from 91.7 μm to 281.8 μm with a mean of 160.4 μm . The width in WT spores ranged from 12.7 μm to 32.8 μm with a mean of 20.72 μm and the width in spores with mutation L143F+G446S varied from 13.80 μm to 31.20 μm with a mean of 20.81 μm .

In Figure 11C the sporulation is illustrated. The number of spores of the WT isolates varied from 40^4 to 285^4 with a mean of 101^4 spores. The single spore isolate Ms 1036 showed a significant higher number of spores compared to all other isolates. Spores of isolates carrying mutation L143F+G446S varied from 15^4 to 65^4 with a mean of 41^4 . No significant difference was observed between number of spores from WT and L143F+G446S haplotype.

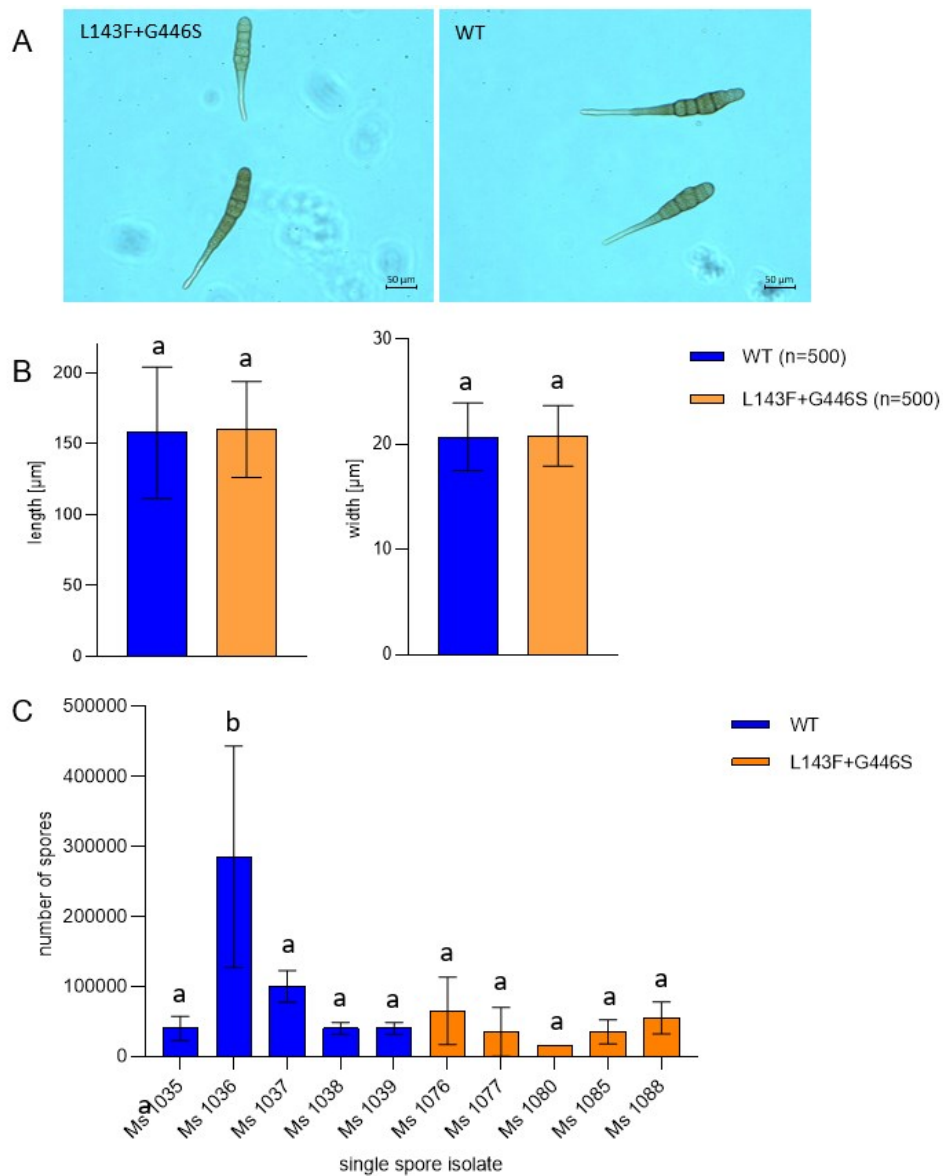


Figure 11: *A. solani* spore morphology and quantification of different *CYP51* haplotypes.

A: Spores of Ms 1088 carrying double mutation L143F+G446S and Ms 1036 without mutation in *CYP51*, scale: 50 μm.

B: Spore length and width of five WT isolates (n=500) and five isolates harboring double mutation L143F+G446S (n=500) were measured. The y-scale for length was adjusted to 200 μm and for width to 30 μm. Blue color indicates the WT and orange color indicates double mutation L143F+G446S. Same letters indicate no significant differences in means at alpha 0.05 according to Mann-Whitney test.

C: Spores of isolates were counted under the light microscope and calculated for 3 mL total volume. Ms 1035, 1036, 1037, 1038 and 1039 represent the *CYP51* WT and Ms 1076, 1077, 1080, 1085 and 1088 carry double mutation L143F+G446S. Blue color indicates the WT and orange color indicates double mutation L143F+G446S. Different letters denote significant differences in means at alpha 0.05 according to Tukey's test. Same letters indicate no significant differences between treatments.

3.3.3 Infection rate

Single spore isolates without mutation (n=2) and with mutation L143F+G446S (n=2) were inoculated on tomato plants in the greenhouse and treated with DMIs mefentrifluconazole and difenoconazole to observe infection. Figure 12 provides pictures of the infection of WT and L143F+G446S haplotype on treated (33 g a.i./ha and 100 g a.i./ha) and UTC tomato plants. No infection on mock control leaves is visible, whereas clear infection symptoms are visible on the UTC. Mefentrifluconazole and difenoconazole showed good efficacy with both application rates, and 100 g a.i./ha of both compounds showed less symptoms when compared to leaves treated with 33 g a.i./ha. Leaves treated with difenoconazole showed more severe symptoms than leaves treated with mefentrifluconazole.

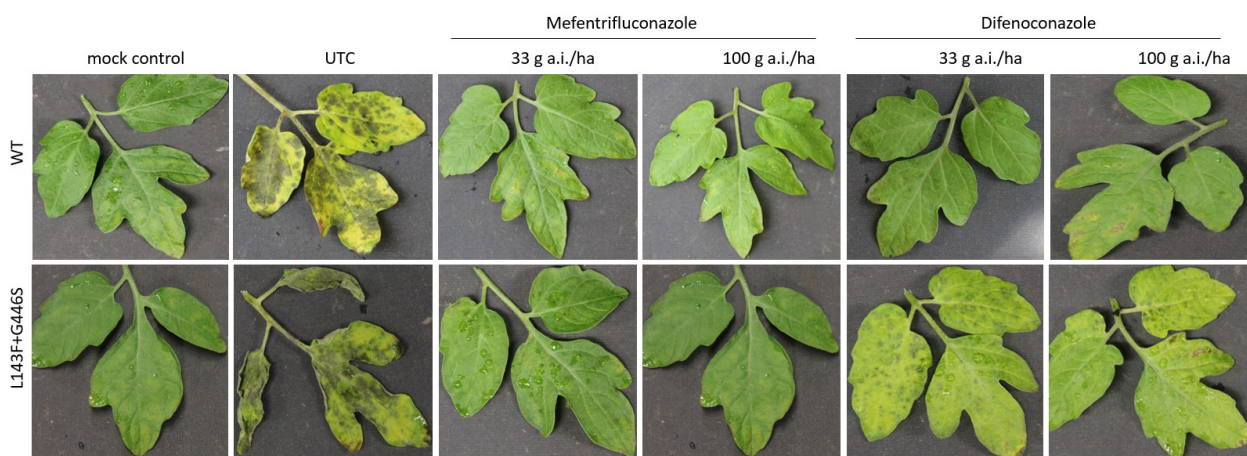


Figure 12: A. solani infection of WT and haplotype L143F+G446S on treated and non-treated tomato leaves.

Tomato plants were inoculated with WT single spore isolates (n=2) and single spore isolates harboring mutation L143F+G446S (n=2) in three independent experiments. Mefentrifluconazole and difenoconazole were applied ten days preventive as solo-formulated products with 33 g a.i./ha and 100 g a.i./ha.

3.3.4 Determination of vegetative growth

The radial growth of *CYP51* WT and L143F+G446S was observed on agar plates amended with different concentrations of mefentrifluconazole and difenoconazole, additional plates without fungicides served as UTC. The vegetative growth of fungal mycelium was measured 9 dpi in cm. As can be seen from Figure 13 growth of single spore isolates harbouring double mutation L143F+G446S and WT did not differ on UTC agar plates. Compared to the UTC, growth of WT isolates for both fungicides were fully inhibited at 0.3 mg/L, whereas mutated isolates were almost fully controlled at 3 mg/L mefentrifluconazole and difenoconazole.

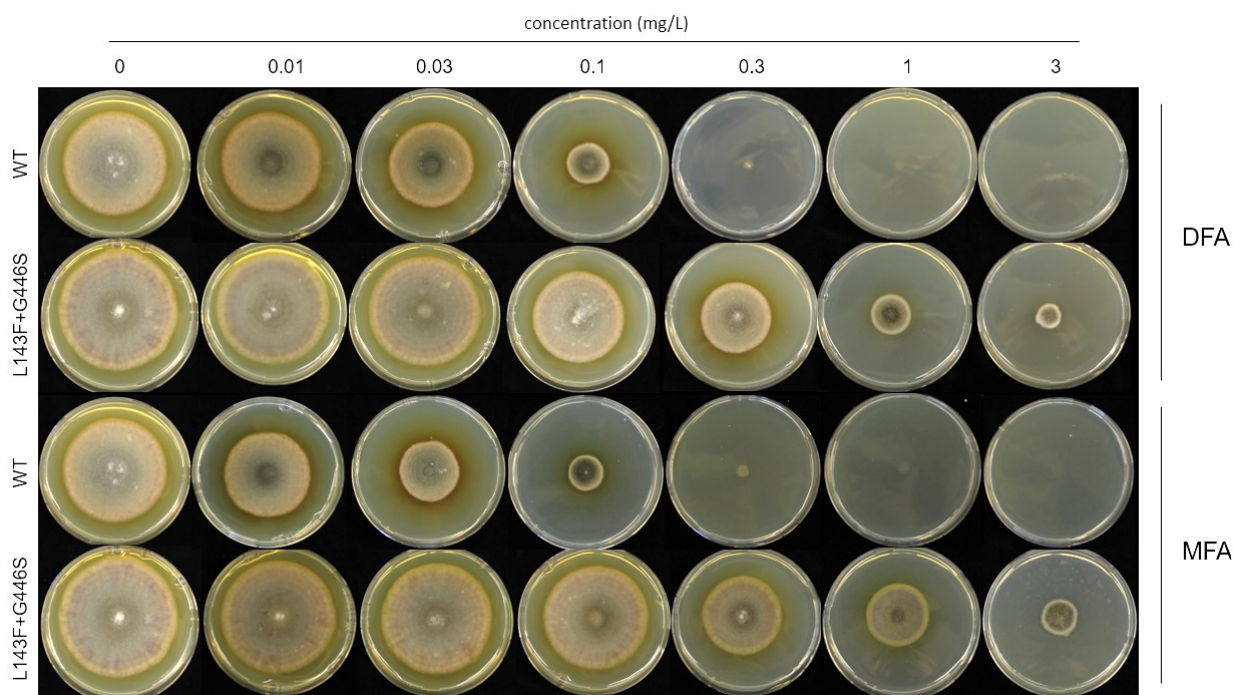


Figure 13: Inhibition of vegetative growth of *CYP51* haplotypes by mefentrifluconazole and difenoconazole.

Representative sensitive (Ms 1036; WT) and mutated (Ms 1088; L143F+G446S) single spore isolate on 2% (w/v) malt agar plates amended with 0 mg/L (UTC), 0.01 mg/L, 0.03 mg/L, 0.1 mg/L, 0.3 mg/L, 1 mg/L and 3 mg/L difenoconazole (DFA) and mefentrifluconazole (MFA).

EC₅₀ values for sensitive isolates were 0.032 mg/L mefentrifluconazole and ranged from 0.051 to 0.055 mg/L difenoconazole with a mean of 0.054 mg/L. For mutated isolates EC₅₀ values ranged from 0.884 to 0.858 mg/L mefentrifluconazole with a mean of 0.871 mg/L, and 0.421 to 0.401 mg/L difenoconazole with a mean of 0.411 mg/L (Table 18).

Table 18: EC₅₀ values of *CYP51* haplotypes tested with difenoconazole and mefentrifluconazole in sensitivity agar plate tests.

Isolate	<i>CYP51</i> haplotype	MFA	DFA
Ms 1036	WT	0.032	0.055
Ms 1039	WT	0.032	0.051
Ms 1077	L143F+G446S	0.884	0.421
Ms 1088	L143F+G446S	0.858	0.401

3.4 Impact of new *CYP51* alterations on DMI sensitivity in *A. solani*

The EC_{50} values of all isolates (n=496) were determined for mefentrifluconazole, difenoconazole, and prothioconazole by microtiter tests. To analyze the impact of new *CYP51* aa alterations on DMI sensitivity, isolates carrying the double mutation L143F+G446S, single mutation G462S and WT were tested with seven fungicide concentrations. Microtiter tests were evaluated six days after incubation by determining the optical density (OD) with a photometer. Figure 14 provides an overview of the sensitivity in different *A. solani* haplotypes to DMIs. EC_{50} values for WT isolates tested with mefentrifluconazole ranged from 0.003 to 0.039 mg/L, with a mean of 0.013 mg/L, isolates carrying the G462S mutation showed EC_{50} values from 0.030 to 0.081 mg/L, with a mean of 0.048 mg/L and for double mutation L143F+G446S the values ranged from 0.040 to 0.367 mg/L, with a mean of 0.164 mg/L. WT isolates and isolates harboring the mutation L143F+G446S or G462S showed significant differences in EC_{50} values for mefentrifluconazole.

The EC_{50} values for WT tested with difenoconazole varied from 0.005 mg/L to 0.078 mg/L, with a mean of 0.033 mg/L and the double mutation L143F+G446S from 0.036 mg/L to 0.256 mg/L, with a mean of 0.133 mg/L. Significant differences could be observed within the haplotypes. Isolates evolving single mutation G462S provided for WT isolates EC_{50} values ranging from 0.033 mg/L to 0.073 mg/L, with a mean of 0.047 mg/L. Isolates tested with mefentrifluconazole and difenoconazole showed a reduced sensitivity when double mutation L143F+G446S is present and slightly enhanced values for isolates carrying mutation G462S.

For prothioconazole EC_{50} values for WT isolates ranged from 0.237 mg/L to >10 mg/L, with a mean of 0.341 mg/L. For isolates harboring mutation G462S from 9.235 mg/L to >10 mg/L, with a mean of 9.844 mg/L and for isolates harboring double mutation L143F+G446S from 0.442 mg/L to 6.482 mg/L, with a mean of 2.348 mg/L. EC_{50} values for all three groups differ significantly. Of interest are the overall much higher EC_{50} values for prothioconazole than for mefentrifluconazole and difenoconazole: Furthermore, a significant decrease of EC_{50} values to prothioconazole when mutation L143F+G446S is present, and a significant loss of sensitivity when single mutation G462S is developed.

Altogether, double mutation L143F+G446S showed higher adaptation for mefentrifluconazole and difenoconazole whereas prothioconazole was most effected by the single mutation G462S.

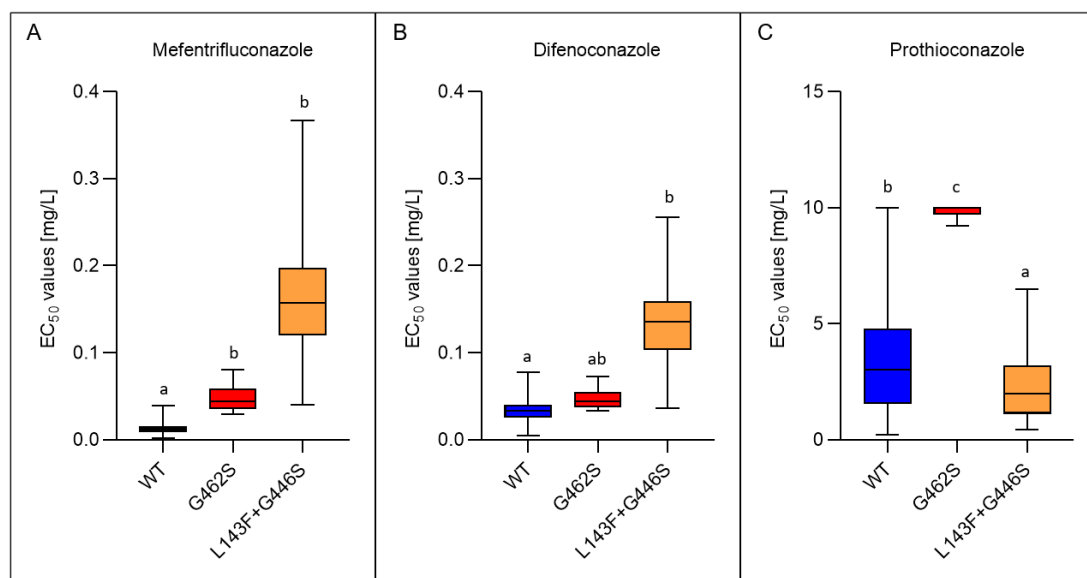


Figure 14: DMI sensitivity in different *A. solani* CYP51 haplotypes.

The EC₅₀ values for different haplotypes detected in *A. solani* isolates are plotted for mefentrifluconazole (A), difenoconazole (B) and prothioconazole (C). For A and B, the y-scale was adjusted to 0,4 mg/L, for C to 15 mg/L. Groups with different letters denote significant differences in means at alpha 0.05. Blue boxes indicate WT isolates (n=358; prothioconazole n=334), red boxes indicate isolates with mutation G462S (n=6), and orange boxes indicate isolates with double mutation L143F+G446S (n=132; prothioconazole n=73), respectively.

3.5 Evaluation of cross-resistance between different DMIs in *A. solani*

To determine if *A. solani* isolates show cross-resistance between DMIs, the correlation of the sensitivity to DMIs resulting from microtiter tests was analyzed. EC₅₀ values of all investigated isolates were determined for mefentrifluconazole (n=496), difenoconazole (n=494) and prothioconazole (n=413) with help of microtiter tests and plotted against each other. The results of the correlational analyses of EC₅₀ values for different haplotypes and tested DMIs are presented in Figure 15, 16 and 17. For all tested isolates, EC₅₀ values ranged from 0.003 to 0.367 mg/L mefentrifluconazole, 0.005 to 0.256 mg/L difenoconazole and 0.237 to >10 mg/L prothioconazole. The highest EC₅₀ values with the widest range were determined for prothioconazole. A very strong correlation of the EC₅₀ values (r=0.8706) of all haplotypes was observed for mefentrifluconazole and difenoconazole (Figure 15). The results of the analyses showed very weak correlation for mefentrifluconazole and prothioconazole (r=0.03946) (Figure 16), and difenoconazole and prothioconazole (r=0.06042) (Figure 17).

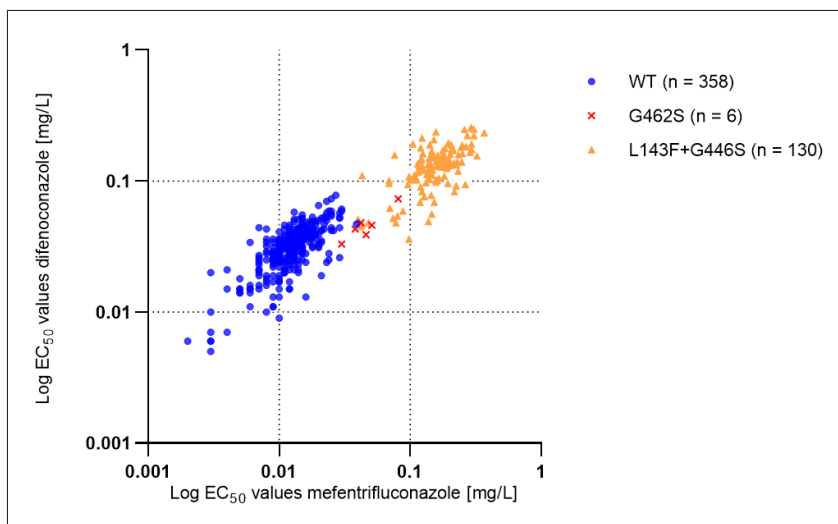


Figure 15: Correlation of EC₅₀ values of *A. solani* haplotypes (WT, G462S, L143F+G446S) for mefentrifluconazole and difenoconazole.

To calculate the correlation ($r=0.8706$), the log transformed EC₅₀ values of all isolates were used. EC₅₀ values for difenoconazole and mefentrifluconazole available are plotted in the diagram and the number of isolates is shown.

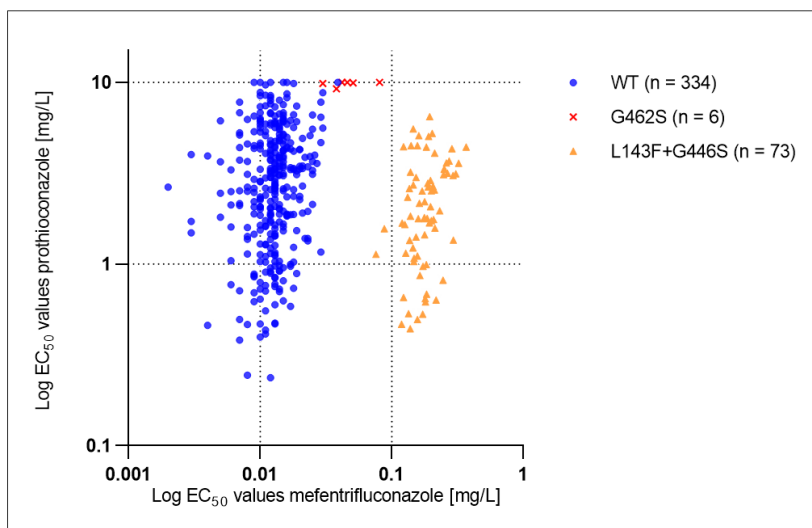


Figure 16: Correlation of EC₅₀ values of *A. solani* haplotypes (WT, G462S, L143F+G446S) for mefentrifluconazole and prothioconazole.

To calculate the correlation ($r=0.03946$), the log transformed EC₅₀ values of all isolates were used. EC₅₀ values for mefentrifluconazole and prothioconazole available are plotted in the diagram and the number of isolates is shown.

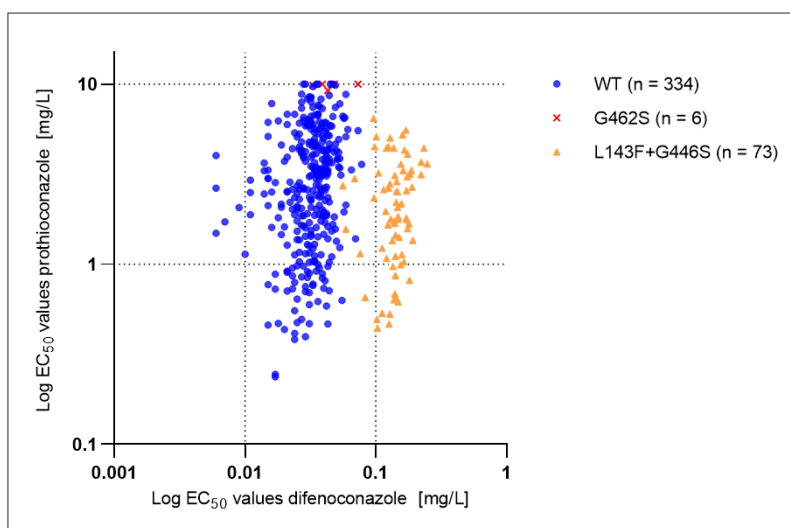


Figure 17: Correlation of EC₅₀ values of *A. solani* haplotypes (WT, G462S, L143F+G446S) for difenoconazole and prothioconazole.

To calculate the correlation ($r=0.06042$), the log transformed EC₅₀ values of all isolates were used. EC₅₀ values for difenoconazole and prothioconazole available are plotted in the diagram and the number of isolates is shown.

3.6 Multiple resistance

In previous studies multiple resistance in *A. solani* was observed for QoI and SDHI fungicides (Gudmestad et al. 2013; Landschoot et al. 2017; Metz et al. 2019; Nottensteiner et al. 2019; Mostafanezhad et al. 2021). Therefore, in this chapter isolates with available data for SDHI and QoI resistance (chapter 7.1, Table 22) were used to determine if multiple resistance with DMIs is present. Pyrosequencing was used to quantify mutation H134R in *SDH C* gene conferring SDHI adaptation (chapter 2.6.8). For QoI adaptation mutation F129L in the *CYT B* gene was quantified. Additionally, EC₅₀ values were determined (chapter 2.7). DMI adaptation in *A. solani* was firstly described in this work. Thus, information about *CYP51* mutations, conferring DMI adaptation, was provided via Sanger sequencing.

3.6.1 Multiple resistance between QoIs and DMIs

To determine resistance for QoIs azoxystrobin was used, since this compound is more affected by mutation F129L than other relevant QoIs, such as pyraclostrobin and trifloxystrobin (Pasche et al. 2004). EC₅₀ values for tested isolates ($n=380$) ranged from 0.006 mg/L to 1.660 mg/L azoxystrobin, with a mean of 0.338 mg/L. In Figure 18, 19 and 20 the distribution of the EC₅₀ values for azoxystrobin and different DMIs of analyzed isolates are pictured. Of interest here is the combined adaptation of DMI and QoI. In all isolates with mutated *CYP51* haplotype, reduced sensitivity to azoxystrobin was observed. No isolates with solely reduced sensitivity to DMIs were detected. However, isolates sensitive to DMIs but azoxystrobin-adapted have been found in high frequency.

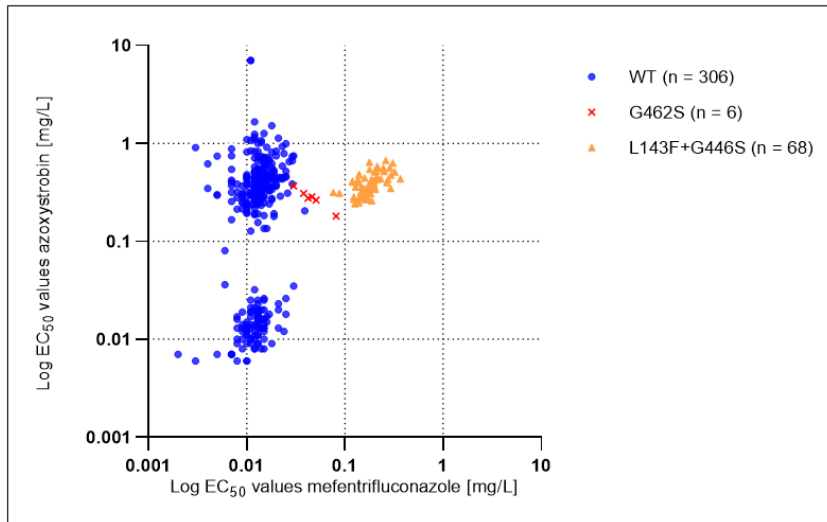


Figure 18: Distribution of EC₅₀ values of *A. solani* haplotypes (WT, G462S, L143F+G446S) for azoxystrobin and mefenfluconazole.

EC₅₀ values for mefenfluconazole and azoxystrobin available are plotted in the diagram and the number of isolates is shown.

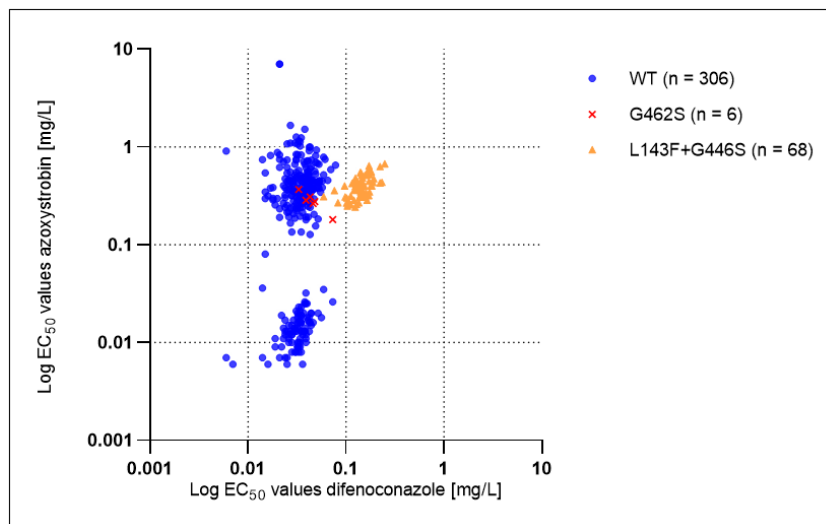


Figure 19: Distribution of EC₅₀ values of *A. solani* haplotypes (WT, G462S, L143F+G446S) for azoxystrobin and difenoconazole.

EC₅₀ values for difenoconazole and azoxystrobin available are plotted in the diagram and the number of isolates is shown.

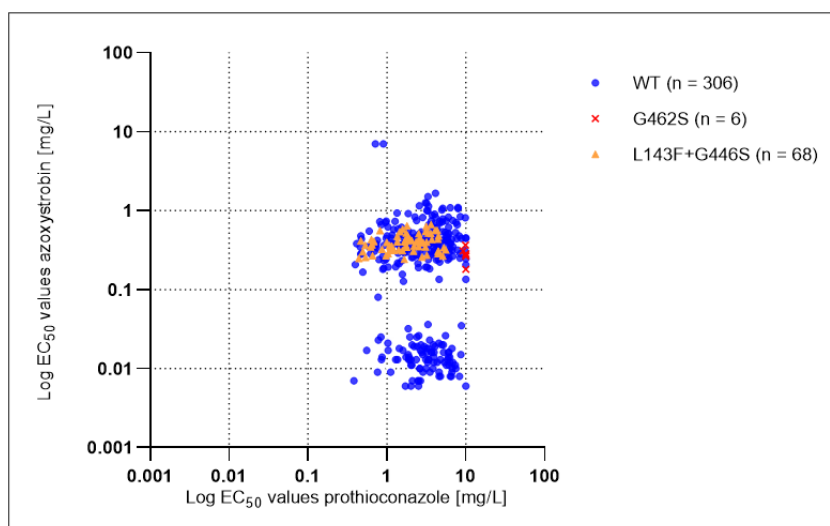


Figure 20: Distribution of EC₅₀ values of *A. solani* haplotypes (WT, G462S, L143F+G446S) for azoxystrobin and prothioconazole.

EC₅₀ values for prothioconazole and azoxystrobin available are plotted in the diagram and the number of isolates is shown.

Table 19 provides an overview of different *CYP51* haplotypes and their sensitivity to azoxystrobin. Mutation G462S and L143F+G446S are considered adapted to DMIs. Sensitivity to azoxystrobin is referred to EC₅₀ values <0.100 mg/L and reduced sensitivity to azoxystrobin is referred to EC₅₀ values >0.100 mg/L. It was shown that isolates with EC₅₀ values >0.100 mg/L carry mutation F129L (BASF internal data). A major part of the analyzed isolates (n=210) exhibited reduced sensitivity to azoxystrobin and 96 isolates were azoxystrobin sensitive.

Table 19: Sensitivity of *CYP51* haplotypes to azoxystrobin.

Number of *CYP51* haplotypes are listed, along with the respective azoxystrobin sensitivity.

		Sensitive to azoxystrobin	Resistant to azoxystrobin
<i>CYP51</i> haplotype	WT	96	210
	L143F+G446S	0	68
	G462S	0	6

3.6.2 Multiple resistance between SDHs and DMIs

Sensitivity to fluopyram is referred to *SDH C* WT gene and resistance was expected to be present, in particular, when mutation C-H134R was detected, since relevant mutations in subunit *B* or *D*, e.g., B-H278Y, show minor effects on fluopyram (BASF internal data). In Table 20 an overview of different *CYP51* haplotypes and their sensitivity to fluopyram is shown. A major part of the isolates (n=188) were sensitive to DMIs and fluopyram and most DMI adapted isolates showed adaptation to fluopyram (n=27). However, isolates adapted to DMIs but not to fluopyram, and *vice versa*, were observed.

Table 20: Sensitivity of CYP51 haplotypes to fluopyram.

Number of *CYP51* haplotypes are listed, along with the respective fluopyram sensitivity.

		Sensitive to fluopyram	Resistant to fluopyram
<i>CYP51</i> haplotype	WT	188	52
	L143F+G446S	10	27
	G462S	4	0

3.7 Efficacy of DMIs in the field

3.7.1 Disease assessment

Field trials were conducted in 2022 and 2023 to analyze the *A. solani* population and the DMI efficacy in the field. Therefore, one trial with variety "Gala" and one trial with variety "Kuras" were performed each year. Samples were collected and isolates were obtained. The *CYP51* gene was sequenced and the *in vitro* sensitivity to DMIs was determined.

In 2022, both varieties were planted in Limburgerhof (Rhineland Palatinate, Germany) where first infections on lower leaves were observed on 6th July in "Gala" and "Kuras". In this season, the incidence of infection was too low to determine the efficacy of the different treatments. Nevertheless, samples in all plots have been selected and isolates were obtained for *in vitro* analysis. In both varieties over all untreated and treated plots 99 isolates were generated. Among these, 96 isolates did not show any aa alteration in the *CYP51* gene. One isolate revealed double mutation L143F+G446S and two revealed mutation G462S. During this field trials mutation G426S in *CYP51* gene was detected for the first time.

In 2023 "Kuras" was cultivated in Böhl-Iggelheim (Rhineland Palatinate, DE) where first infections were visible on 14th August and "Gala" was planted in Ruchheim (Rhineland Palatinate, DE) where first infections were observed on 4th August. In both locations, 214 isolates in total were obtained, where 168 did not show any aa alteration in the *CYP51* gene, 42 developed double mutation L143F+G446S and four developed mutation G462S. Variety "Gala" developed in the untreated control a frequency of infection of 15%, and "Kuras" up to 35%.

The efficacy (%) was used as a measure for the effectiveness of the fungicide treatment. Figure 21 provides an overview of the efficacy of different fungicides as solo formulation or in mixtures on variety "Kuras". The comparison of the DMI treatments as solo formulation showed for mefentrifluconazole (94%) and difenoconazole (91%) the best efficacy, followed by the SDHI and QoI mixture with boscalid+pyraclostrobin (83%). The treatment prothioconazole and the

mixture of fluazinam+azoxystrobin were roughly on a par with 56% and 66% efficacy, respectively. The efficacy of prothioconazole was significantly compromised compared to mefentrifluconazole and difenoconazole.

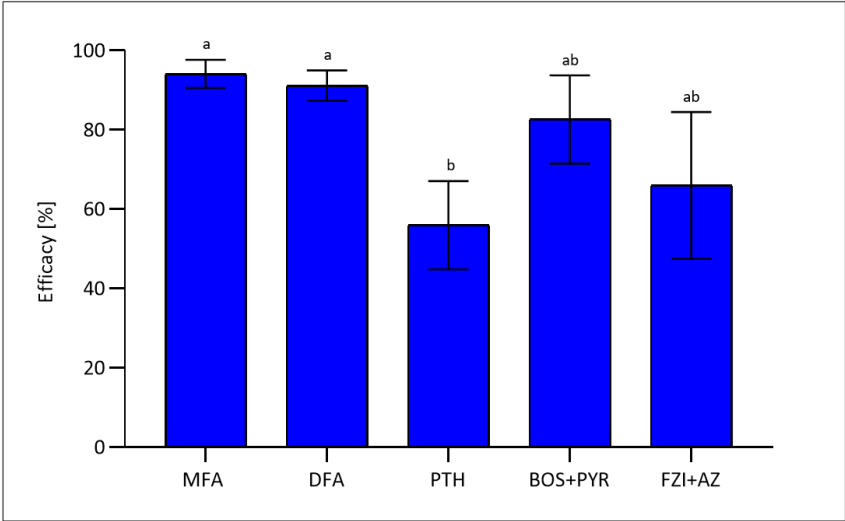


Figure 21: Fungicide efficacy of different compounds for *A. solani* population in 2023 on potato variety “Kuras”.

The treatments were performed with commercially available formulation of mefentrifluconazole (MFA), difenoconazole (DFA), prothioconazole (PTH), boscalid+pyraclostrobin (BOS+PYR) and fluazinam+azoxystrobin (FZI+AZ) at registered application rate for each compound. Each fungicide application was replicated in three randomized plots. Efficacy is given in percentage. Error bars show the standard deviation. Groups with different letters denote significant differences in means at alpha 0.05 according to Tukey’s test. Same letters indicate no significant differences between treatments.

Figure 22 illustrates the efficacy of different fungicide treatments against *A. solani* infection on potato variety “Gala”. Mefentrifluconazole showed the best efficacy (82%), followed by difenoconazole (68%) and prothioconazole (66%). The treatment mixtures boscalid+pyraclostrobin, and fluazinam+azoxystrobin were roughly on a par with 55% and 61% efficacy, respectively. Statistically, the different treatments belonged to one significant group (a), with no significant difference among each other.

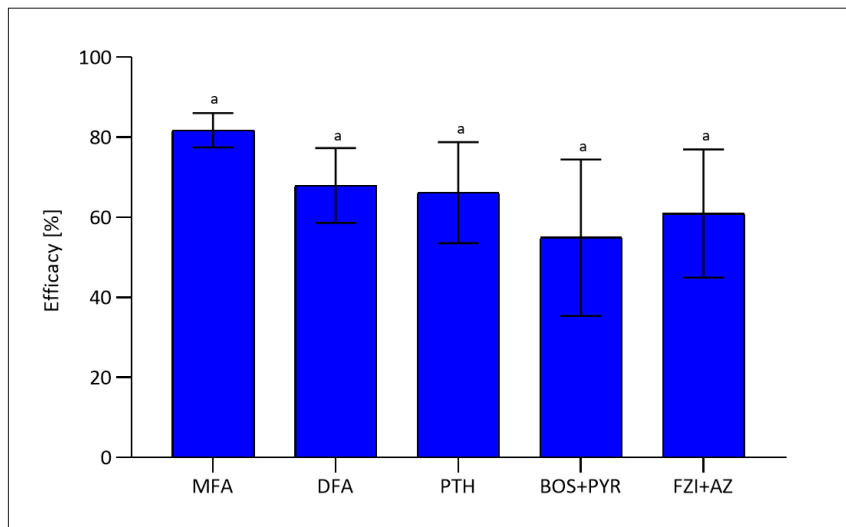


Figure 22: Fungicide efficacy of different compounds for *A. solani* population in 2023 on potato variety “Gala”.

The treatments were performed with commercially available formulation of mefenftrifluconazole (MFA), difenoconazole (DFA), prothioconazole (PTH), boscalid+pyraclostrobin (BOS+PYR) and fluazinam+azoxystrobin (FZI+AZ) at registered application rate for each compound. Each fungicide application was replicated in three randomized plots. Efficacy is given in percentage. Error bars show the standard deviation. Groups with different letters denote significant differences in means at alpha 0.05 according to Tukey’s test. Same letters indicate no significant differences between treatments.

The results showed that the efficacies of the same treatments were higher in variety “Kuras” (56-94%) than in “Gala” (55-82%). It must be considered that the infection of the untreated control in “Kuras” was 20% higher than in “Gala” and this might have led to a more pronounced efficacy. Isolates generated from field trials in 2022 and 2023 were included in this study.

3.7.2 Composition of *CYP51* haplotypes in *A. solani* populations in field trials

To clarify if DMI treatments have an influence on the development of mutations in the *CYP51* of *A. solani* field populations, the incidence of mutations L143F, G446S, and G462S within the population were quantified by pyrosequencing assays. The aim was to determine the frequency of alleles leading to DMI adaptation in infected leaf samples from *A. solani* populations in 2022 and 2023.

Figure 23 provides an overview of the frequencies of *CYP51* haplotypes in plots treated with different fungicides. One sample includes a pool of 20 *A. solani* lesions.

Locations in 2022 and 2023 were all located in Rhineland Palatinate in proximity to each other. In both years the WT was the predominant haplotype in treated and untreated plots. In 2022, haplotype G462S was marginal detected after treatment of the population in Limburgerhof with DMIs (10%). After non-DMI treatments no mutations in *CYP51* were detected. The double mutation L143F+G446S was not detected in leaf samples in year 2022 (Figure 23A). The

following year, haplotype G462S and L143F+G446S was detected in all treated plots in low frequencies in Ruchheim and Böhl-Iggelheim. In 2023, after non-DMI treatments, mutation G462S was detected at a level of 2% and double mutation L143F+G446S at 6%. After DMI treatment mutation G462S was detected at a level of 3% and mutation L143F+G446S at 8%. Haplotype G462S was found in lower frequency than haplotype L143F+G446S (Figure 23B). It is also worth noting that despite the fact that haplotypes with *CYP51* mutations slightly increased from 2022 to 2023 in the palatine population, a major part of the population in all investigated plots was sensitive in both years. Taken together both years, one can observe that after DMI application the sum of mutated *CYP51* haplotypes (G462S and L143F+G446S) were detected at a level of 10%, and after application of non-DMIs at 4% (Figure 23C).

The results indicated a slightly higher selection of mutated *CYP51* haplotypes after application with DMIs. After application with non-DMI fungicides, *CYP51* mutations have been selected, which could give a hint on multiple resistance. This will be further discussed in chapter 4.8.

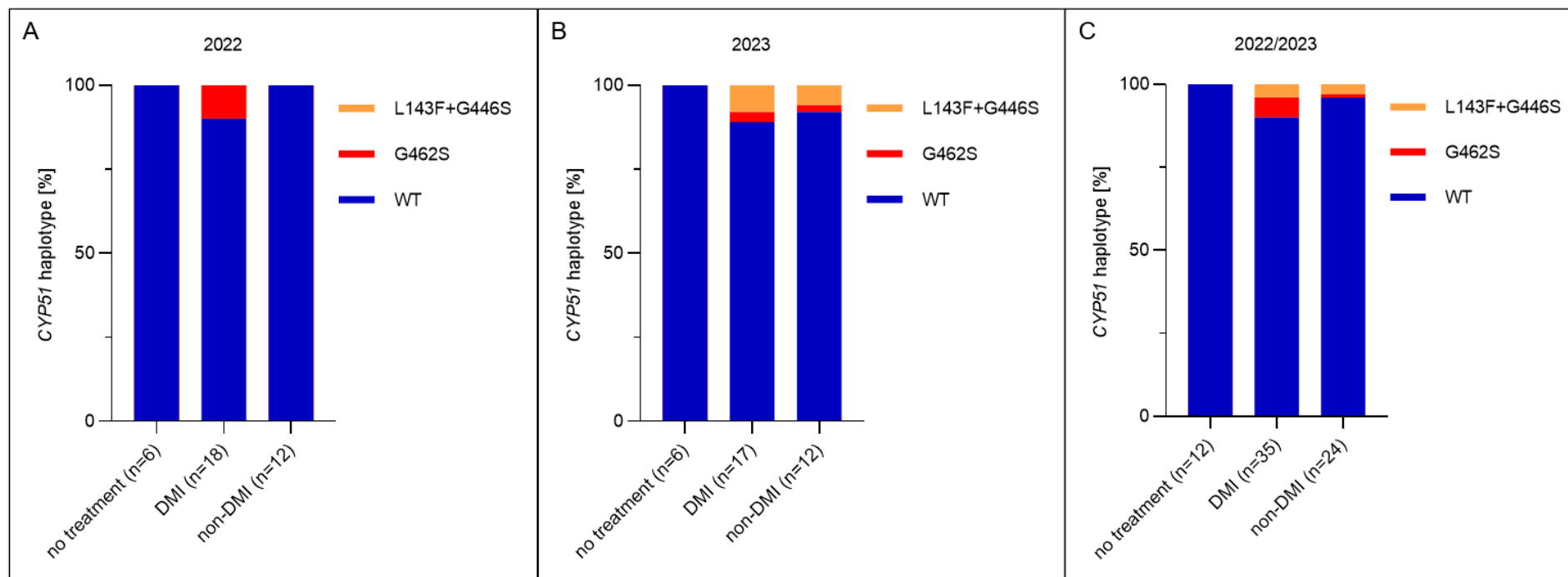


Figure 23: CYP51 haplotypes of *A. solani* and their relative frequency in field trials after application of fungicides.

Field trials were performed in 2022 and 2023 in Germany. Early blight infected leaves were taken in untreated, DMI (mefentrifluconazole, difenoconazole, prothioconazole), and non-DMIs (boscalid+pyraclostrobin, fluazinam+azoxystrobin.) treated plots. One sample includes a pool of 20 infected leaves randomly collected from one trial. DNA was extracted and frequency of DMI resistant allele was measured using quantitative pyrosequencing. For 2022 (A), 2023 (B) and both years (C) blue color indicates the sensitive alleles (WT), red color indicates mutation G462S, and orange color indicates double mutation L143F+G446S.

3.8 Generation of L143F, G446S and L143F+G446S replacement constructs

In order to analyze the influence of the double mutation L143F+G446S and the single mutations L143F and G446S on DMI sensitivity, three transformation constructs were generated in this study. In all cases, integration of the constructs at the target locus was achieved by homologous recombination. The targeted mutation strains were named AsL143F, AsG446S and AsL143F+G446S. For AsG446S and AsL143F+G446S the WT gene in isolate Li-0016 was replaced by the mutated allele from DMI adapted isolate Ms 1030-001. To substitute the WT gene in strain Li-0016 for the L143F mutation the cytosine was replaced by a thymine in WT isolate Ms 1092-001 during PCR reaction thus forcing aa alteration L143F to develop. For subsequent selection of successful transformation, each construct consisted of an *A. nidulans trpC* terminator and a following *NAT1* resistance gene (Nourseothricin-Acetyltransferase) from *Streptomyces noursei* under the control of the *A. nidulans oliC* promoter representing the middle part of the construct. The middle part of the construct was surrounded by approximately 1000 bp flanking sequences at each side, which were necessary to drive the homologous integration. The 5' flank consisted of the *CYP51* gene with respective mutations, while the 3' flank was represented by the *CYP51* terminator (Figure 24A). Described constructs were transformed into *A. solani* WT strain Li-0016 from which single spore isolates were generated for further analyses of integrated mutations.

After integration of the replacement construct (chapter 2.6.9), targeted mutation strains were used for test-PCR and Southern-Blot-hybridization. Forward primer for test-PCR was located in the *CYP51* gene and reverse primer was located in the *NAT1* resistance gene (Figure 24A). Targeted mutation strains with integrated replacement construct could be identified when showing a 3440 bp fragment, which is shown in Figure 24B.

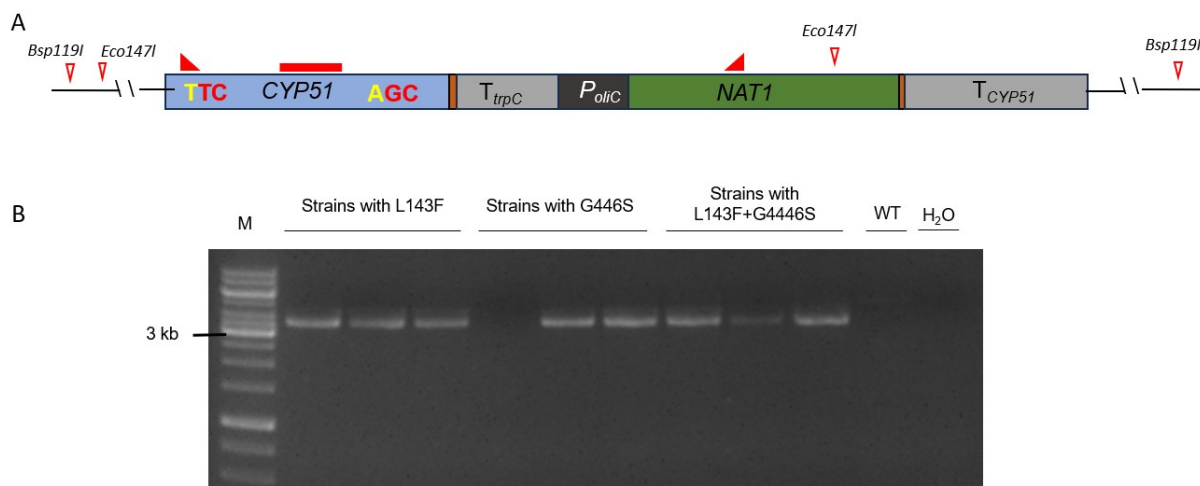


Figure 24: Verification of transformed replacement construct.

Targeted mutation strains showing a 3440 bp band in agarose gel. WT DNA as control and H₂O as no template control were included (A). Transformation construct with primers for test-PCR marked with red triangles, and red bar indicating the probe used for Southern-Blot-hybridization (B).

Subsequently, among these targeted mutation strains, those were selected through Southern-Blot-hybridization that possessed a single, homologous integration of the construct at the target locus. Transformation construct and Southern Blot are shown for mutation L143F in Figure 25A, for G446S in Figure 25B and for L143F+G446S in Figure 25C. Using the *CYP51* probe and enzyme *Bsp119I* (Thermo Fisher Scientific Inc., Waltham, United States) to digest genomic DNA, a single band at 8858 bp showed a homologous integration of the replacement cassette, while the WT showed a band at 6546 bp. With enzyme *Eco147I* (Thermo Fisher Scientific Inc., Waltham, United States) a single band at 6568 bp represented a homologous integration, while the WT showed a 4256 bp band. Targeted mutation strains with multiple bands indicated more than one integration resulting in a strain with ectopic integration.

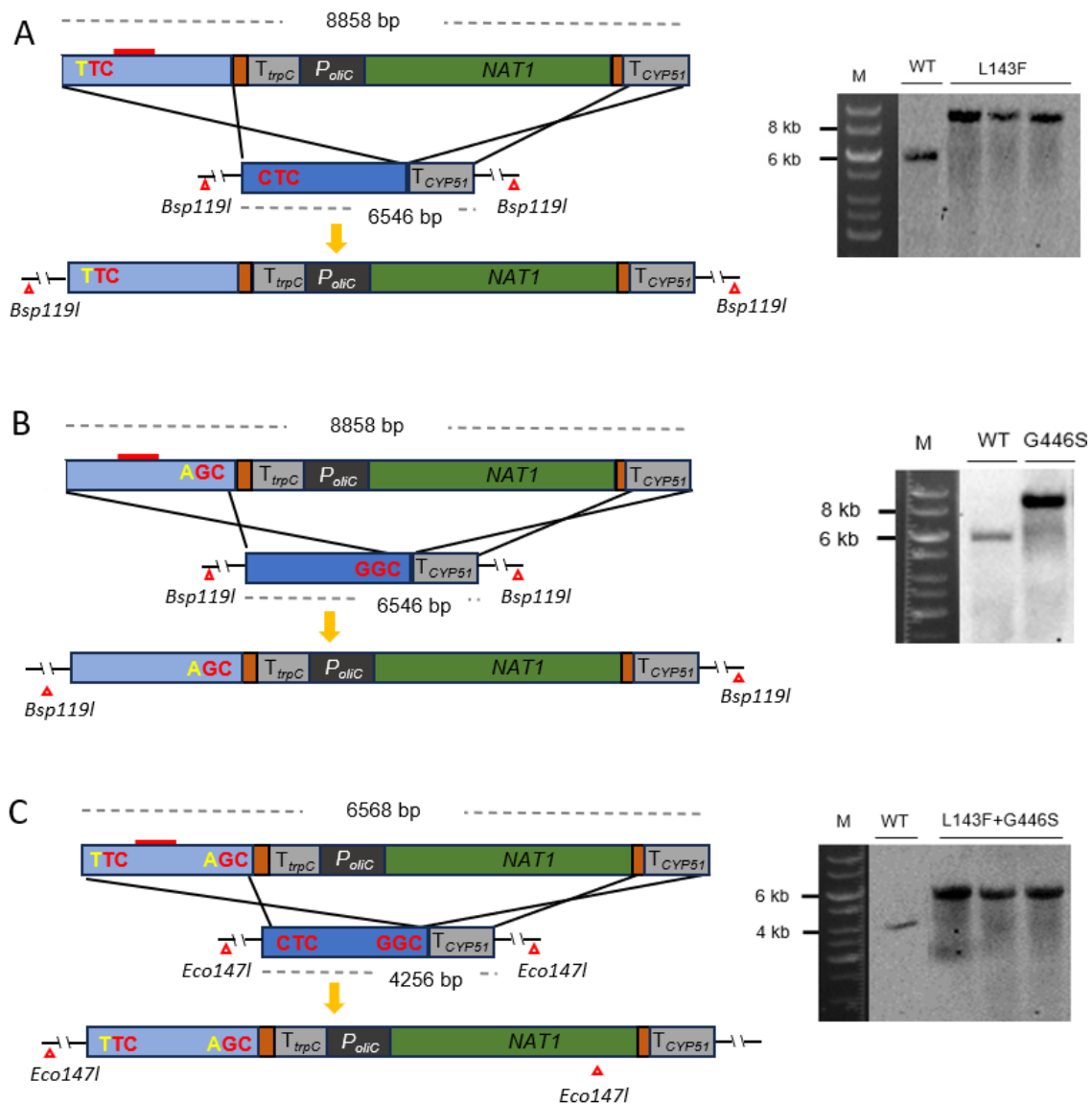


Figure 25: Verification of replacement cassettes containing respective substitutions.

Schematic scheme of transformation construct with mutation L143F (A), G446S (B) and L143F+G446S (C) and Southern Blots are shown. The brown bars represent the matching tails added to the primers for fragments joining during PCR reaction. Double crossover integration of replacement construct at *CYP51* WT locus is shown. Red bars indicating the probe used for Southern-Blot-hybridization, restriction sites of the restriction endonuclease *Bsp119I* and *Eco147I* are marked with red arrows. Integrated cassettes with respective substitutions are illustrated.

Figure 26 shows mutation L143F, G446S and L143F+G446S for targeted mutagenesis of *A. solani*. After targeted mutagenesis of the WT isolate Li-0016, 120 targeted mutation strains could be generated containing the new cassette with either single mutation L143F, G446S or double mutation L143F+G446S. Out of these targeted mutation strains, single spore isolates were generated. Six single spore isolates with mutation L143F, one with mutation G446S and four with double mutation L143F+G446S were verified to have a single, homologous integration at the target locus. To exclude undesired mutations in the targeted mutation strains and to confirm the introduced mutations, Sanger sequencing was performed for the full replacement construct.

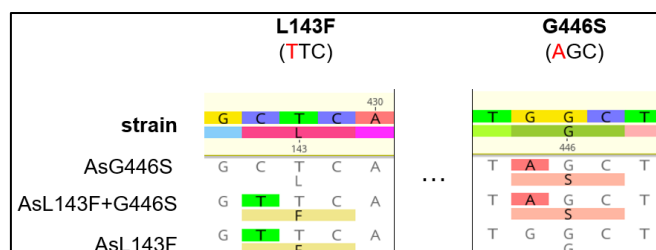


Figure 26: Cutout of the alignment of mutations introduced into *A. solani* WT.

Sequences from replacement cassettes with mutation L143F, G446S and L143F+G446S were aligned using *A. solani* WT as reference strain. Disagreements in aa and nucleotides are highlighted in multicolor. Alignments were generated in Geneious Prime® software.

3.9 DMI sensitivity of targeted mutation strains of *A. solani* with mutation L143F, G446S or L143F+G446S

Targeted mutation strains with homologous integration, the WT parent isolate and a strain with ectopic integration were used for microtiter tests to determine the *in vitro* sensitivity to mefentrifluconazole and difenoconazole with seven concentrations. Microtiter tests were evaluated after six days of incubation by determining the OD with a photometer. One strain with ectopic integration was included as control, one targeted mutation strain with mutation G446S, six with mutation L143F and four with double mutation L143F+G446S were verified with Southern-Blot-hybridization to have a single, homologous integration and were therefore used for further experiments. The EC₅₀ values were determined to analyze the impact of the introduced mutations. In Figure 27 the sensitivity of targeted mutation strains is illustrated. EC₅₀ values for the parental strain were determined at 0.006 mg/L for mefentrifluconazole and 0.016 mg/L for difenoconazole. For the strain with ectopic integration the EC₅₀ value assigned for mefentrifluconazole (0.006 mg/L) and difenoconazole (0.013 mg/L) were in the same range as the WT EC₅₀ values. EC₅₀ values for strains with mutation L143 tested with mefentrifluconazole ranged from 0.009 to 0.029 mg/L, with a mean of 0.019 mg/L. For strains with mutation L143 tested with difenoconazole EC₅₀ values ranged from 0.023 mg/L to 0.053 mg/L, with a mean of 0.039 mg/L. For the targeted mutation strain with mutation G446S EC₅₀ values of 0.016 mg/L for mefentrifluconazole and 0.036 mg/L for difenoconazole were determined. EC₅₀ values for strains with double mutation L143F+G446S tested with mefentrifluconazole ranged from 0.017 mg/L to 0.027 mg/L, with a mean of 0.021 mg/L and for difenoconazole from 0.074 mg/L to 0.099 mg/L, with a mean of 0.084 mg/L. What stands out in Figure 27 is that EC₅₀ values for targeted mutation strains tested with difenoconazole are higher than for mefentrifluconazole. EC₅₀ values of difenoconazole strains with L143F+G446S are significantly higher than strains with mutation L143. Statistical significance could not be detected for groups with no biological replicates.

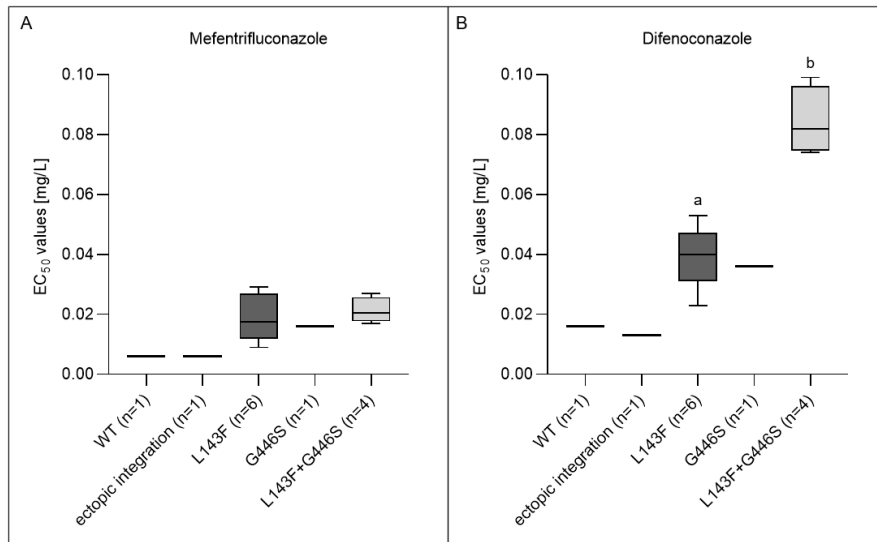


Figure 27: DMI sensitivity of targeted mutation strains of *A. solani* carrying different mutations in *CYP51* gene.

The EC₅₀ values of the parental WT isolate (n=1), strain with ectopic integration (n=1), L143F (n=6), G446S (n=1), and L143F+G446S (n=4) are plotted for mefentrifluconazole (A) and difenoconazole (B). Groups with different letters denote significant differences in means at alpha 0.05.

Figure 28 illustrates the EC₅₀ values of field isolates with double mutation L143F+G446S and the mean EC₅₀ values of targeted mutation strains with double mutation for mefentrifluconazole and difenoconazole. For mefentrifluconazole the adaptation of the targeted mutation strains is lower than for field isolates with L143F+G446S. The mean EC₅₀ values for WT field isolates tested with mefentrifluconazole were 0.013 mg/L and for difenoconazole 0.033 mg/L. EC₅₀ values for the parental strain was determined at 0.006 mg/L for mefentrifluconazole and 0.016 mg/L for difenoconazole.

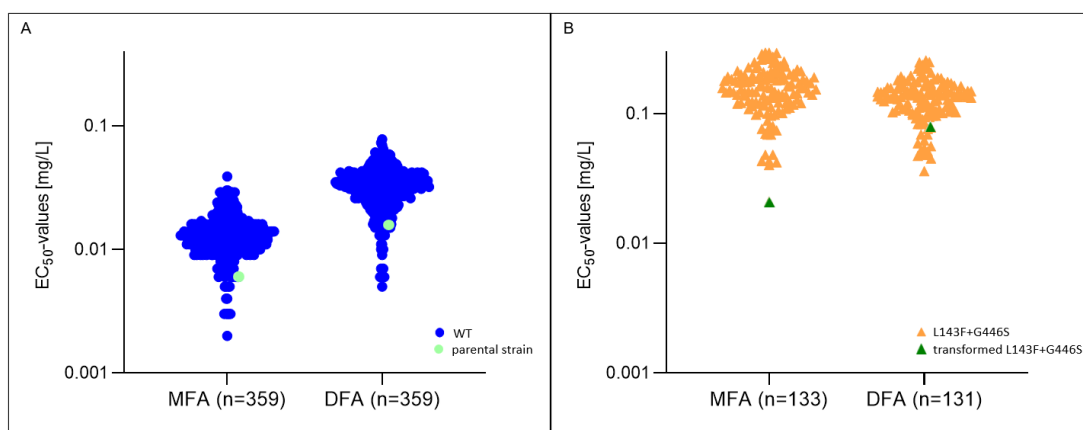


Figure 28: Distribution of EC₅₀ values in *CYP51* haplotype L143F+G446S and WT in *A. solani*.

Blue circles indicate WT field isolates (mefentrifluconazole n=358; difenoconazole n=358) and light green circles indicate mean EC₅₀ values of parental WT isolate (mefentrifluconazole n=1; difenoconazole n=1) (A). The EC₅₀ values for haplotype L143F+G446S detected in *A. solani* are plotted for mefentrifluconazole (n=133) and difenoconazole (n=131). Orange triangles indicate field isolates harboring mutation L143F+G446S (mefentrifluconazole n=132; difenoconazole n=130) and dark green triangles indicate mean EC₅₀ values for targeted mutation strains harboring L143F+G446S (mefentrifluconazole n=1; difenoconazole n=1) (B).

Additionally, the resistance factors (RFs) for mefentrifluconazole and difenoconazole were calculated as the ratio of the mean EC₅₀ values of targeted mutation strains carrying the respective mutations, to the EC₅₀ value of the parent WT isolate. The RFs are represented in Table 21. As one isolate was used as parent for the targeted mutagenesis of *A. solani* the EC₅₀ value for this WT isolate is also depicted. Across different haplotypes RFs ranged from two to five for difenoconazole and mefentrifluconazole. RFs for both compounds are relatively low and in the same range through all the haplotypes.

Table 21: RFs of targeted mutation strains of *A. solani* for mefentrifluconazole and difenoconazole.

RFs were calculated for mefentrifluconazole and difenoconazole as ratio of the mean EC₅₀ value of targeted mutation strains to EC₅₀ value of the parental WT strain. EC₅₀ values of targeted mutation strains and a parental WT isolate were used for determination in microtiter tests.

Isolate	<i>CYP51</i> mutations	Mefentrifluconazole RFs	Difenoconazole RFs
AsL143F (n=6)	L143F	3	2
AsG446S (n=1)	G446S	3	2
AsL143F+G446S (n=4)	L143F+G446S	4	5
parent	WT	0.006	0.016

In Figure 29 vegetative growth of targeted mutation strains and the WT are visible. No difference can be observed for different targeted mutations in the *CYP51* gene and the WT.

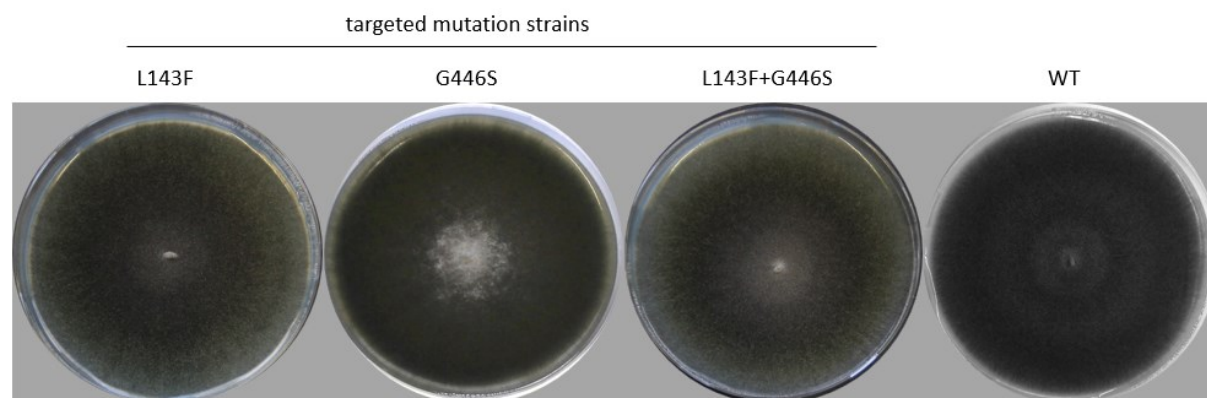


Figure 29: Vegetative growth of targeted mutation strains.

Representative targeted mutation strains of *A. solani* with different *CYP51* mutations (L143F, G446S, L143F+G446S) and parental WT strain cultivated on 2% (w/v) malt agar plates (12 dpi).

3.10 Efficacy of DMIs on targeted mutation strains of *A. solani* in the greenhouse

In vitro tests confirmed a slightly reduced sensitivity to the tested DMIs for targeted mutation strains. Therefore, DMI efficacies were tested in the greenhouse for better understanding of the effects of the individual mutations and mutations in combination in *A. solani*. Greenhouse experiments allow more realistic conditions to study the pathogen in interaction with the host plant. The parental isolate and two targeted mutation strains with ectopic integration were included. Further, strains with mutation L143F (n=2), G446S (n=1) and double mutation L143F+G446S (n=2) were tested. Mefentrifluconazole (Revysol®), difenoconazole (Score®) and metiram (Polyram®) were applied as solo formulations three-days preventive. Mefentrifluconazole and difenoconazole are commercially available DMIs used in specialty crops and cereal crops, whereas metiram was used as a standard multisite fungicide. Diseased leaf area was assessed visually 5 dpi when 80-100% of the control plants were infected, and the efficacy (inhibition %) of fungicides was calculated. The greenhouse test with the same isolates and fungicides was repeated in two independent experiments.

Figure 30 provides the data on the inhibition of mefentrifluconazole, difenoconazole and metiram in the greenhouse for the tested strains. No statistical differences between the inhibition for the strains could be observed with Kruskal-Wallis test ($p < 0.05$). Across all tested compounds, a very good inhibition of around 100% was observed. Strains with mutation L143F, G446S and L143F+G446S, as well as the parental isolate and the strain with ectopic integration were fully controlled by mefentrifluconazole, difenoconazole and metiram.

In vitro sensitivity tests with targeted mutation strains showed slight adaptation to mefentrifluconazole and difenoconazole. The *in vivo* impact of *CYP51* mutations introduced through targeted mutagenesis on DMIs, did not distinguish from each other.

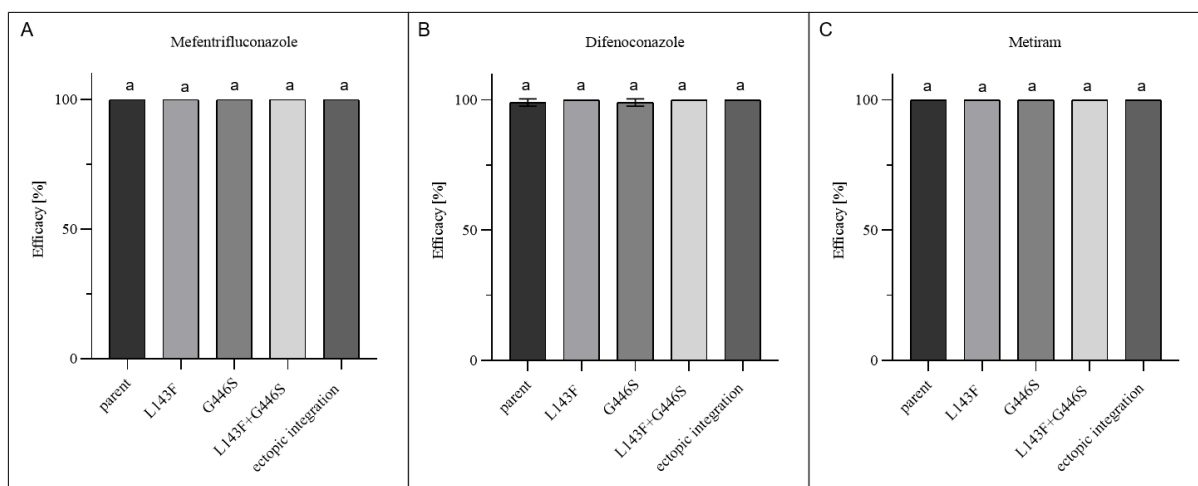


Figure 30: Efficacy of mefentrifluconazole (Revysol®), difenoconazole (Score®) and metiram (Polyram®) on targeted mutation strains of *A. solani* in greenhouse experiments.

Mefentrifluconazole (A), difenoconazole (B) and metiram (C) were applied three-days preventive in three replicants. Targeted mutation strains with *CYP51* mutation L143F, G446S and L143F+G446S were tested. Additionally, the parental strain and two strains with ectopic integration were included.

In Figure 31 infected tomato leaves from greenhouse trials are shown. Representative leaves treated with difenoconazole are shown, since different treatments did only differ marginally. Mock control did not show any symptoms, whereas infection of UTC was clearly visible. Less infection for strains with mutation L143F were observed on the UTC.

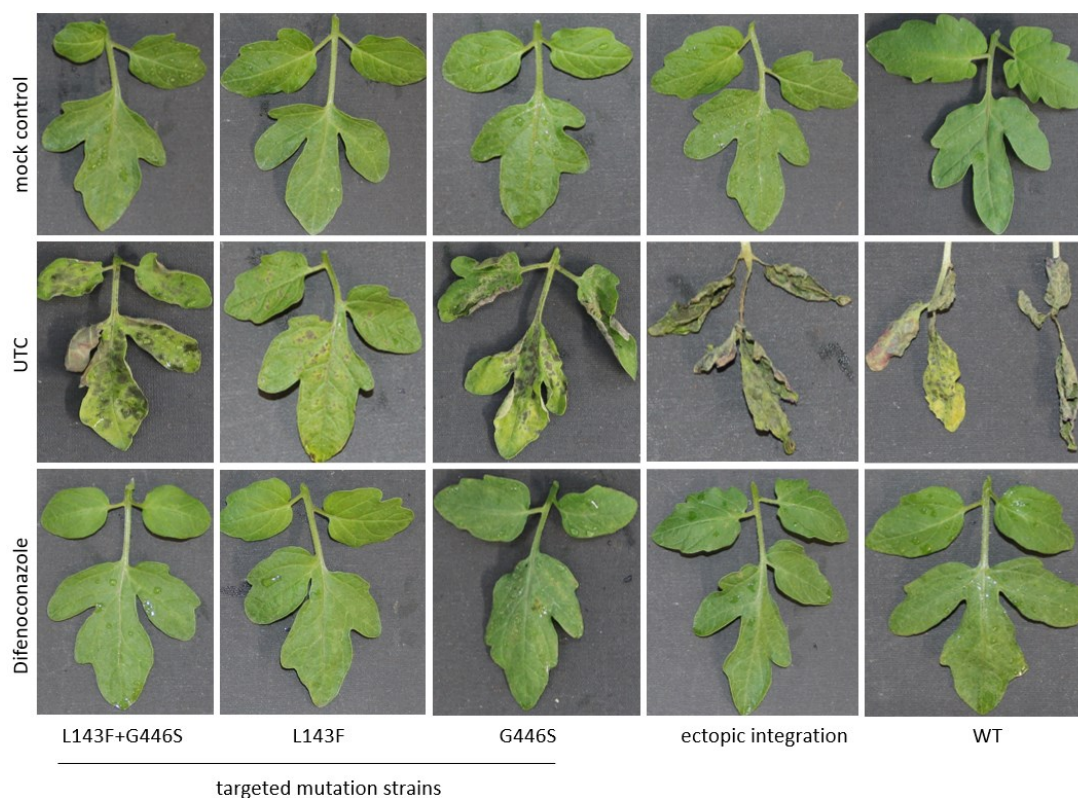


Figure 31: Infection of targeted mutation strains of *A. solani* in the greenhouse.

Representative targeted mutation strains of *A. solani* with different *CYP51* mutations (L143F+G446, L143F, G446S) inoculated on tomato plants in the greenhouse. Parental WT isolate and strains with ectopic integration were included as control.

4 Discussion

A. solani, the causal agent of early blight, has established in every potato growing region worldwide (Rotem 1994). The most effective strategy for controlling early blight infections continues to be the application of foliar fungicides (Hausladen and Leiminger 2007; Lucas et al. 2015). QoIs, SDHIs and DMIs are three important fungicide groups to control early blight and an intensive use of QoIs and SDHIs over many years led to fungicide resistance in *A. solani* (Pasche et al. 2005; Rosenzweig et al. 2008; Metz et al. 2019; Einspanier et al. 2022). However, no shift to a reduced sensitivity in *A. solani* population for DMIs has been observed (He et al. 2019; Yang et al. 2019), making DMIs the main fungicides to control early blight. Therefore, it is crucial to determine the adaptation in *A. solani* to DMIs.

An initial objective of this work was to identify target site mutations reducing the sensitivity in *A. solani* to DMIs, by collecting field samples from different regions, years and fungicide treatments. To detect and assess the impact of mutations in *CYP51* on DMI fungicide efficacy, single spore isolates were generated. Single spore isolates originate from one single spore and therefore their genetic material originates from one source and the obtained cultures represent genetically identical clones. As no resistance mechanisms to DMIs were known in *A. solani*, this method was advantageous, as it provides best possible method to minimize genetic variability within the fungi. It facilitated the study of the individual resistance mechanism by eliminating the potential effects from mixed genotypes. Genetically identical single spore isolates allowed direct comparability of the EC_{50} values resulting from sensitivity studies across multiple experiments. Due to their genetic stability, single spore isolates can be used to compare and evaluate the efficacy of known and new fungicides among each other. Throughout the course of this work, it was observed that isolates derived from a single leaf lesion maintained genetic uniformity and comparability, just as single spore isolates. Therefore, isolates, as well as single spore isolates were used for subsequent stages of this study.

In the following chapter, the sequence of *CYP51* in *A. solani* isolates, and the effect of point mutations on the sensitivity to DMIs are discussed. Cross-resistance patterns of different DMIs are evaluated in terms of future fungicide use. Selection of mutations in *CYP51* by the application of different DMIs are elucidated and efficacy of DMIs on current *A. solani* population in the field is discussed. Competitiveness and vitality of different *CYP51* haplotypes is examined. Further, the discussion revolves around the impact of mutations introduced through targeted mutagenesis in the *CYP51* gene influencing the sensitivity in *A. solani* to DMIs.

4.1 Confirmation of genetic identity of *A. solani* multicellular spores

To answer the question, if multicellular conidia of *A. solani* differ in their genetic, single spore isolates were generated from an isolate with varying *SDH* mutations. Resistance to SDHI fungicides, represented by target site mutations in the target gene, can develop in subunit *B*, *C* and *D* of the *SDH* gene (Horsefield et al. 2006; Stammler et al. 2007). In this study, single spore isolates were generated from *A. solani* isolate 744 to produce genetic identical spores. Isolate 744 represented a population with 83% mutation *B*-H278Y and 9% mutation *C*-H134R. By generation of single spore isolates from an isolate with varying frequencies of mutations, mutation frequencies result in either 0% or 100% (Table 15). This indicated that multicellular spores of *A. solani* are genetically identical and that the initial isolate 744 represented a population. There are similarities between these results and those described by Louw (1976), where it was reported that vegetative mycelium and multicellular conidia of *A. alternata* were predominantly monokaryotic. He also showed that few conidia contained cells with up to four nuclei, and sometimes various cells without nuclei. Sand (2011) reported about transformed *A. alternata* isolates showing constantly WT and transformed DNA, after a protoplast transformation of a deletion cassette. The possibility of non-homologous integration of the transformed DNA as well as the existence of multiple WT gene copies was ruled out by Southern Blot analysis. By successful isolation of single protoplasts after transformation the possibility of a diploid chromosome set and the transformation of only one allele was ruled out. Therefore, she postulated the presence of heterokaryotic conidia in *A. alternata*. Many years ago, Stall (1958) reported that cells of *A. solani* were observed to have multiple nuclei. Overall, very little was found in the literature on the question if the multicellular spores of *A. solani* are genetically identical. The results of this work indicated that multicellular spores in *A. solani* may not differ genetically between different cells within the spore and multicellular spores can be regarded as clones. Additionally, it was observed that isolates originating from one early blight lesion had either 0 or 100% of *CYP51* mutations, which indicate that these isolates are clones.

4.2 Sequence analysis of *CYP51* show amino acid alterations

Fungal pathogens show different resistance mechanisms to overcome lethal effects of fungicide applications (Ma and Michailides 2005). SNPs in the target gene represent the major mechanism leading to compromised sensitivity to fungicides (Brent and Hollomon 2007). To detect SNPs within the *CYP51*, the gene in *A. solani* was sequenced and aligned to a WT cDNA. To date, no aa alterations were detected for *A. solani* conferring compromised DMI

sensitivity (He et al. 2019; Yang et al. 2019). This is the first study reporting about adaptation caused by SNPs in the *CYP51* gene in *A. solani* (Table 16).

A total of 496 isolates and single spore isolates originated from Germany, Sweden, the Netherlands, and Australia were analyzed in this work. Across all isolates, aa alterations at position 143, 446 and 462 were detected. Mutation L143F, where a substitution of leucine (CTC) to phenylalanine (TTC) occurs at position 143, was only detected in combination with mutation G446S, which is represented by a substitution of glycine (GGC) to serine (AGC) at position 446. Additionally, single mutation G462S was observed solely, involving a substitution of glycine (GGC) to serine (AGC) at position 462. Within the investigated isolates, L143F+G446S mutations were the most frequent alteration over the years (n=132).

DMIs bind to the *CYP51* by direct adherence with the prosthetic heme group, which is located within the protein's interior. Decreased susceptibility is often caused through target site mutations in the coding region of the *CYP51* gene (Becher and Wirsal 2012). Structural analysis of the Cyp51 protein was performed, and the distances of the detected mutations were measured from the alpha carbon of each mutated position to the closest heavy (non-hydrogen) atom in the heme group, for better understanding of the effect on the fungicides binding. The protein model revealed that mutation L143F have emerged in proximity (6.6 Å) to the binding site represented by the heme group. When aa at position 143 is altered, a steric clash between the aromatic ring of the phenylalanine and the carboxylate group of the binding site is indicated (Figure 8A). Hence, it was suggested that the resulting changes in positions of surrounding protein and heme atoms may influence DMI binding affinity. Mutation G446S is located 11 Å away from the binding site and therefore the relevance of this alteration may consider to be minor, as there seem to be no steric clashes with the heme (Figure 8B). Considering the short distance of 3.9 Å between mutation G462S and the binding site, it can be inferred that this mutation exhibits a significant impact on DMI binding. In fact, the mutated serine has an additional OH-group compared to the WT aa glycine. The OH-group of the serine fits very well between a backbone NH and one of the carboxylate groups on the heme, making hydrogen bonds with both, avoiding major steric clashes with other positions of the heme (Figure 8C). Therefore, it can be assumed that the effect on the DMI sensitivity is rather low.

Prior studies have shown that other fungal pathogens developed homologous target site mutations to mutations detected in *A. solani*. G462S in *A. solani* is homologous to mutation G461S in *M. fructicola* and G460S in *P. brassicae*, which are linked to reduced DMI sensitivity (Carter et al. 2014; Lichtemberg et al. 2018). Mutation G460S in *P. brassicae* was firstly described as single mutation in 2014 with low to moderate effect on the DMI sensitivity (RFs 10-33) (Carter et al. 2014). Newer studies reported about mutation G460S detected

additionally in combination, showing higher adaptation when found with mutation S508T and/or inserts in the promotor region, then occurring as single mutation (Bucur et al. 2022). In the study from Bucur et al. (2022) it was obvious that isolates with single mutation G460S were less frequent (n=61) than isolates with this mutation in combination with S508T and/or different inserts (n=288). Interestingly, also the number of inserts in the promotor region have increased during the years from three to 11 (Bucur et al. 2022). This states, that the potential in other pathogens to develop additional resistance mechanisms in combination with mutation G460S, which is homologous to mutation G462S in *A. solani*, is present. As mutation G462S was detected for the first time in 2022 and 2023, it is possible that in future additional resistance mechanisms evolve, due to the relatively high genetic diversity in *A. solani* (van der Waals et al. 2004) and the fungicide selection pressure in the fields. Mutations homologous to L143F are associated with reduced sensitivity to DMIs as well and are described in *C. beticola* and *V. inaequalis* (Shrestha et al. 2020; Hoffmeister et al. 2021; Muellender et al. 2021). In *A. solani* mutation G446S is located in a conserved region of fungal pathogens (YGY) (Figure 9). In these conserved domains mutations are known to mediate DMI adaptation, and were detected e.g., in *Z. tritici*, *R. collo-cygni* or *V. inaequalis* (Stammler et al. 2008; Rehfus et al. 2019; Hoffmeister et al. 2021). It is very clear that in all investigated isolates mutation L143F and G446S were detected only in combination. In *V. inaequalis* the homologous mutation L144F was detected exclusively in combination with mutation M141V, but mutation M141V could be also found alone (Hoffmeister et al. 2021). In *C. beticola* homologous mutation L144F can develop as single mutation, but more preferably as double mutation with I309T (Muellender et al. 2021; Hoffmeister et al. 2024). The combination of mutation L143F and G446S in *A. solani* may be due to different reasons. On the one hand, it could be assumed that one mutation occurred alone causing a slight sensitivity shift and the second mutation developed through fungicide evolution and added higher adaptation to the population. Such additive effect on the sensitivity was observed for mutation S524T in *Z. tritici*. Several *CYP51* haplotypes showed an increased adaptation to epoxiconazole and prothioconazole, when developing mutations in combination with S524T (Huf et al. 2018). Therefore, it could be assumed that due to excessive DMI use the accumulation of *CYP51* mutations may play a crucial role in the gradual development of resistant phenotypes in *A. solani*. An alternative hypothesis could be that mutation L143F or G446S can only exist with the other mutation in combination, because of lethal effects when occurring alone. This case was shown for *Z. tritici*. Cools et al. (2010) reported that during complementation studies with *Saccharomyces cerevisiae* mutation I381V alone prevents the capacity of the *Z. tritici* Cyp51 protein to function in *S. cerevisiae*, but function is partially restored when mutation I381V is introduced in combination with mutations at position YGY (aa 459-461). This indicated that mutation I381V alone has a lethal effect in *Z. tritici* and can only exist with and additional mutation in the conserved domain between Y459

and Y461. Mutation I381V is nowadays present in most *Z. tritici* isolates in Europe (Stammler et al. 2008; Cools et al. 2013; Jørgensen et al. 2021; Glaab et al. 2024) and therefore plays a crucial role in the evolution of DMI adaptation. From the results shown by Cools et al. (2010) it can be concluded that the conserved domain Y459 to Y461 was necessary to develop mutation I381V, which indicates the importance of region Y459 to Y461 in fungal pathogens to maintain the function of the enzyme activity of Cyp51. The importance of this position for aa exchanges implies the importance of mutation G446S for development of L143F. This hypothesis will be further discussed in chapter 4.6.

4.3 Distribution of *CYP51* mutation in *A. solani*

According to this work the double mutation L143F+G446S was detected for the first time in isolates from 2018 on. The fact that the same *CYP51* haplotype were detected in Australia and Europe, leads to the suggestion, that the mutations arose individually and independently in each region, rather than being spread through wind or global transportation of contaminated plants or propagation material. Such independent and parallel DMI adaptation with the same mechanisms (target site mutations) has been found also in other pathogens, especially in *Z. tritici* and *C. beticola* (Stammler et al. 2008; Taher et al. 2014; Hartmann et al. 2020; Spanner et al. 2021; Hoffmeister et al. 2024).

Einspanier et al. (2022) performed a whole-genome sequencing for several *A. solani* isolates from different regions in Europe with mutations in the *SDH* gene. The authors concluded that the mutations in the *SDH* complex arose in non-admixed genetic backgrounds. Although *A. solani* is known to be windborne, it is very unlikely that *A. solani* spores spread over continents through wind and distributed mutation L143F+G446S in Europe. Additionally, it is likely that mutation L143F+G446S developed at least twice in Europe, since the mutation was detected in Dronten (the Netherlands) and Palatinate are (Germany), which are over 490 km apart from each other. The theory of the independent evolution of resistance mechanisms in *A. solani* is supported by QoI resistance development. Leiminger et al. (2014) suggested that mutation F129L in *A. solani* occurred minimum twice in the USA, since the substitution was found in isolates of genotype I and II. In Germany the authors detected the mutation in locations relatively wide apart (180 km), indicating an independent selection. The fact that two different codons for leucin at position F129L have been detected (CTC and TTA) is further a strong argument for frequent independent evolution of fungicide resistance (BASF internal studies) in *A. solani*. According to these findings, it is likely that selective pressure exerted by fungicide application in different locations led to the individual emergence of haplotype L143F+G446S. When fungicides are applied those individuals with lower sensitivity can survive and reproduce in the regions. This could lead to a gradual shift to a population with less sensitive isolates pushed by local factors, such as fungicide treatment.

Furthermore, mutation L143F+G446S was dominantly detected in field trials in the Netherlands. There are two possible explanations for this result. Trial sites are exposed to increased selection and disease pressure over the years since trials for efficacy evaluation and regulatory purposes are not following resistance management strategies. Additionally various measures are used to keep high disease pressure (environmental conditions (e. g. irrigation), susceptible varieties, inoculation etc.). A diverse range of fungal strains with varying genetic background may have accumulated at such sites, increasing the probability of occurring and reproduction of adapted isolates. Secondly, a prior study has noted, that although *A. solani* is an asexually reproducing fungi, the genetic diversity is relatively high. It was suggested that the natural chance of mutations and the ability of producing high number of spores in a short time, leads to this phenomenon (van der Waals et al. 2004). Consequently, the risk of random development of mutations could be higher, as a result of the greater number of spores, propagation cycles per season and high selection pressure. The risk for *A. solani* to develop fungicide resistance was classified by FRAC as "medium" (FRAC 2019), mainly base on the current experience on fungicide development in the past and in comparison with other species (Stammler, pers. communication). This is in line with our findings, that the majority of the isolates analyzed did not show *CYP51* mutations and maintained their high sensitivity to DMIs, even if many from them were collected in trial sites.

4.4 Competitiveness and vitality of *A. solani* haplotypes

In the simplest form, fitness defines the ability of an organism to survive and reproduce in an environment (Sober 2001; Orr 2009). Decades ago, it was reported that DMI adapted fungal isolates are associated to fitness penalties (Fuchs and de Waard 1982). Spore production, spore dispersal, infection efficiency, ability to survive between seasons and other characteristics are stages of the life cycle, which represent the fitness of a fungal pathogen (Mikaberidze and McDonald 2015).

A mixture of WT single spore isolates and single spore isolates harboring double mutation L143F+G446S was inoculated on tomato plants and incubated in the greenhouse. Different single spore isolates from one region (North Netherlands) and the same year were chosen to minimize the varying genetic background between the haplotypes. Since field experiments are time and cost consuming, and are influenced by uncontrollable environmental factors, the competition studies were conducted in the greenhouse. The aim of this experiment was to include the whole infection cycle for the pathogen, such as spore germination, infection, growth, sporulation, spore production and release, to cover as many stages as possible, with which a pathogen must undergo in the field. The results, of the *in vivo* fitness studies, indicated

fitness costs for haplotype L143F+G446S by significant reduction of L143F+G446S frequency (Figure 10). Double mutation L143F+G446S could lead to structural rearrangements of the enzyme and consequently lower the efficiency of it. Fitness penalties of isolates with lower DMI sensitivity are known from other fungal plant pathogens (Karaoglanidis et al. 2001; Chen et al. 2013; Lichtemberg et al. 2018; Li et al. 2023). Li et al. (2023) generated lab-mutants by fungicide adaptation. While the generated mutated strains were cultured over ten cycles on fungicide free PDA media, the RFs decreased, indicating a fitness penalty of adapted individuals. Karaoglanidis et al. (2001) described fitness penalties in DMI adapted isolates of *C. beticola* by inoculating field trials with different ratios of resistant and sensitive strains. Additionally, growth chamber experiments including inoculation onto whole plants were performed. The results of the different conducted fitness tests indicated that mutations are likely to be associated with compromised fitness. To determine the fitness in DMI adapted *P. pachyrhizi* isolates, mixtures of different haplotypes were prepared and inoculated onto treated and non-treated soybean leaves. Frequency of isolates linked to reduced DMI sensitivity, such as haplotype F120L+Y131H, decreased and WT isolates increased (Klosowski et al. 2016). However, recent studies suggested that mutation I145V in the *CYP51* gene of *P. pachyrhizi* could potentially confer fitness advantages (Stilgenbauer 2022). A new haplotype F120L+Y131H+I145V exhibiting identical effect on sensitivity compared to the haplotype F120L+Y131H was documented. Therefore, it was hypothesized that the I145V mutation showed little to no effect on DMI adaptation. Furthermore, an alignment with the Basidiomycota *Puccinia recondita* and different Ascomycota species, such as *Z. tritici*, *C. beticola* and *R. collo-cygni*, demonstrated that aa valine at position 145 is coded in the WT sequence. Thus, it was suggested that the aa alteration I145V in *P. pachyrhizi* is associated with a structural change in the Cyp51 protein, which exerts a positive effect on the involved metabolic processes and could be an indication for a protective mechanism in the fungi (Stilgenbauer 2022). Not all plant pathogens exhibit fitness disadvantages in isolates displaying reduced DMI sensitivity. In *P. teres* the latent period and sporulation were determined, but no evidence for fitness costs linked to DMI resistance was observed (Peever and Milgroom 1994). Cox et al. (2007) compared sporulation and conidial germination, as well as incubation and latent periods of sensitive and resistant *M. fructicola* isolates. No correlation between DMI resistance and fitness was obtained. However, different mutations occurring simultaneously on different genes within an isolate can have varying effects on the fitness. While in *P. pachyrhizi* isolates with mutations in *CYP51* showed compromised competitiveness, isolates with mutation F129L in *CYTB* gene did not correlate with fitness costs compared to the WT isolates. A mixture of *CYP51* haplotype F120L+Y131H, and *CYP51* haplotype F120L+Y131H with *CYTB* haplotype F129L showed competitive advantage of the isolate developing mutation on both genes. Therefore, it was suggested that the F129L mutation in *CYTB* is not associated with reduced

fitness. This is in line with the fact that since more than 10 years the majority of the Brazilian *P. pachyrhizi* population carries the F129L mutation (Klosowski et al. 2016; Stilgenbauer 2022).

Considering this fact, it would be of interest to perform fitness studies with isolates differing solely in *CYP51* mutations. The targeted mutation strains of *A. solani* harboring the double mutation and the parental strain could be used for such experiments. This would ensure a defined genetic background with determination of the effect of the introduced mutations in *CYP51*. Further, targeted mutation strains with only mutation L143F or G446S can be included to elucidate the effect of the single mutations on the competitiveness in *A. solani*. The advantage of using targeted mutation strains would be the precise assessment of the effects of the SNPs in the *CYP51* gene itself. This would help to ensure that the observed differences in viability are not confounded by variations in other genes. However, the introduced *NAT1* gene in the transformation cassette could affect the fitness of targeted mutation strains. Therefore, a method to generate mutants with identical genetic background would be the generation of *in vitro* mutants on fungicide amended agar plates. DMIs are characterized by a quantitative resistance (Brent and Hollomon 2007) what could lead to difficulties for this method as mutations in *CYP51* gene usually show stepwise adaptation. In this work the fitness in *A. solani* was studied *in vivo* with single spore isolates generated from field samples. When looking at other studies, it was shown that many methods to analyze the competitiveness of resistant isolates exist. On the one hand, *in vivo* competition studies in the greenhouse are limited by time and effort and do not allow high throughput, compared to *in vitro* experiments. On the other hand, *in vivo* experiments represent a more realistic environment and the study of the infections on the host plant.

Additionally, spore morphology of strains with WT and mutated *CYP51* gene were observed to identify potential variations. The results showed no significance differences in terms of their spore length, width or septation between the two haplotypes (Figure 11A, B). Sporulation of WT and spores carrying mutation L143F+G446S was variable. However, no differences in quantity of spores from the WT or the L143F+G446S haplotype was detected (Figure 11C). Single spore isolate Ms 1036 showed significant increased spore production compared to all other single spore isolates. As no other single spore isolate showed enhanced spores, Ms 1036 might be attributed as outlier. Additionally, spore morphology of this single spore isolate was observed exclusively and did not show any differences in width, length or septation of spores. These findings indicated that mutation in *CYP51* gene do not affect growth or sporulation under the tested conditions. Further infection rate of WT and haplotype L143F+G446S on the untreated tomato plants were at the same range and DMIs were able to control infection. Vegetative growth of WT and *CYP51* haplotype L143F+G446S did not differ.

This interesting finding may be attributed to the low effects of mutations in *CYP51* gene showed, which are not strong enough to influence vitality of haplotype L143F+G446S. Understanding the emergence and spread of adapted isolates in plant pathogens is crucial for effective disease management and prediction on how resistance will develop in the fields.

Considering the obvious fitness disadvantageous of haplotype L143F+G446S *in vivo* it would be interesting to investigate the vitality of mutated isolates in a DMI driven environment, and of adapted isolates with single mutation G462S. However, it is likely that mutated isolates with such fitness penalties will not survive in the absence of fungicide selection pressure as they have to compete with more fit sensitive individuals. This information is valuable for assessing the rate of occurrence and spread of resistant individuals of *A. solani* in the field and implementing appropriate management strategies to counteract it.

4.5 *In vitro* effects of *CYP51* haplotypes on sensitivity to DMIs in *A. solani*

Besides other fungal compounds, such as QoIs or SDHIs, DMIs are the favored class of fungicides because of their high efficacy against a wide spectrum of fungal strains (Price et al. 2015). For various pathogens reduced sensitivity to DMIs, due to target site mutations, have been described (Huf et al. 2018; Rehfus et al. 2019; Hoffmeister et al. 2021; Muellender et al. 2021). Therefore, it is necessary to assess the *CYP51* haplotypes detected in this work to implement future resistance management strategies. *In vitro* sensitivity tests were performed to determine the effect of different *CYP51* haplotypes in *A. solani* on DMIs.

In vitro sensitivity tests (microtiter tests) with isolates from different regions, years and fungicide applications revealed different haplotypes with mutations in *CYP51* gene showing slightly increased EC_{50} values for difenoconazole, mefentrifluconazole and prothioconazole when compared to the WT. WT isolates could be effectively controlled by mefentrifluconazole and difenoconazole, whereas values for prothioconazole showed a great span. Since prothioconazole is a pro-drug fungicide, EC_{50} values ranged from 0.646 mg/L to >10 mg/L and it was observed, that the EC_{50} values of the double mutation L143F+G446S were similar to the EC_{50} values of the WT. Double mutation L143F+G446S revealed higher EC_{50} values for mefentrifluconazole and difenoconazole, whereas prothioconazole was more affected by single mutation G462S. EC_{50} values for prothioconazole reached up to >10 mg/L, for mefentrifluconazole and difenoconazole the highest value was 0.367 mg/L. Mefentrifluconazole and difenoconazole belong to the triazoles and have therefore a similar chemical structure (FRAC 2024). Prothioconazole is a triazolinethione derivate introduced in 2002 (Price et al. 2015). The characteristic of prothioconazole is the need of metabolization to

its desthio form to evolve full fungicidal effect. In studies with *C. albicans* it was reported that the antifungal effect of the pro-drug fungicide prothioconazole is attributed to prothioconazole-desthio. Hence, it can be estimated that prothioconazole is metabolized to the more active prothioconazole-desthio in fungal cells (Parker et al. 2013). Since prothioconazole showed variable EC₅₀ values for WT and double mutation L143F+G446S, and no significant difference for those haplotypes, results might be attributed to the need of metabolization to prothioconazole-desthio.

One unexpected finding was that prothioconazole was more affected by the single mutation G462S than by the double mutation L143F+G446S. It is therefore likely that the chemical structure of prothioconazole is of disadvantage when mutation G462S is present so that it favors steric clash with the heme, despite the beneficial location within the protein explained in chapter 3.2.2. Because of the proximity of the single mutation G462S to the binding site, the altered serine may interfere with the binding of prothioconazole leading to a decreased susceptibility. In contrast, the chemical structure of prothioconazole is favorable when double mutation L143F+G446S is present. It is likely that the position of these mutations allows the fungicide to interact with the binding site or form alternative interactions which leads to inhibition of the fungal growth. It is difficult to explain this result, but it might be related to findings in other fungal species, where *CYP51* mutations have also different effects on different DMIs. Y137F in *Z. tritici* and the homologous Y136F in *Erysiphe necator* confers adaptation to triadimenol, but not to most other DMIs including prothioconazole or mefentrifluconazole (Cools et al. 2011; Zito et al. 2024). On the other hand, the homologous mutation Y131F in combination with F120L+V130A in *P. pachyrhizi* seems to have a stronger effect on prothioconazole than to tebuconazole and the combination of F120L+Y131H+I145V *vice versa* (Stilgenbauer et al. 2023). Due to the distance of mutation G446S to the active site, it is plausible that prothioconazole might not interact with the mutated position and therefore show low effect on sensitivity. In *Z. tritici* it was reported that isolates developing mutation Y461S, showed reduced sensitivity to different DMIs except prothioconazole (Cools et al. 2011). Mutation Y461S is located in the same YGY region as G446S in *A. solani*. An alteration of the aa to serine in this position seems to have a marginal influence on resistance to prothioconazole compared to the WT. Nevertheless, to develop a full picture of the efficacy of prothioconazole on single mutation G462S and double mutation L143F+G446S, additional studies will be needed.

Isolates developing double mutation L143F+G446S expressed higher adaptation for mefentrifluconazole and difenoconazole when compared to the WT and G462S haplotype. For several fungal pathogens it was reported that additional mutations in combination further

decrease the sensitivity to fungicides. For example, in *Z. tritici* mutations in combination with S524T showed higher adaptation to epoxiconazole and prothioconazole than single mutations (Huf et al. 2018). In *R. collo-cygni* it was observed that haplotypes with three mutations (e.g., haplotype I381T+I384L+Y461H) showed the highest adaptation to DMIs compared to haplotypes with one mutation (e.g., haplotype Y461) (Rehfus et al. 2019). When multiple mutations occur together, they show combined impact with further decreasing effectiveness of the fungicide, resulting in higher level of adaptation. Single mutation G462S was first detected in year 2022, whereas haplotype L143F+G446S have been detected in Australian isolates from 2018. This occurrence could be evidence for the stepwise resistance, characteristic for the quantitative resistance of DMIs (Brent and Hollomon 2007). Therefore, the results presented in this work are crucial to delay future resistance development in *A. solani* by appropriate resistance management.

4.6 Mutations in *CYP51* in *A. solani* and their effects on DMIs

In the past it was reported that in some fungal pathogens, such as *C. albicans*, *P. pachyrhizi* or *Z. tritici*, a combination of resistance mechanisms led to DMI adaptation (Sanglard et al. 1998; Cools and Fraaije 2008; Cools et al. 2012; Huf 2021; Stilgenbauer 2022). It is also known that higher resistance levels usually arise through combination of mutations, such as the additional mutation K147Q in *B. graminis* or S524T in *Z. tritici* (Wyand and Brown 2005; Huf 2021). After characterization of the detected mutations in *A. solani*, a WT isolate was transformed with three replacement constructs containing single mutation L143F, G446S or the double mutation L143F+G446S to study their effects and to prove, if the detected double mutation is the reason for the slight DMI shift.

Targeted mutation strains of *A. solani* with single mutation L143F or G446S, and double mutation L143F+G446S could be selected and were vital. The *CYP51* function was not fully destroyed as it was shown for mutation I381V in *Z. tritici* (Cools et al. 2010). *In vitro* sensitivity tests showed slightly increased EC₅₀ values for difenoconazole and mefentrifluconazole of targeted mutation strains with mutation L143F or G446S when compared to the WT (Figure 27). For the target mutation strains with double mutation L143F+G446S, a 3.5-fold higher adaptation for mefentrifluconazole and a 5-fold higher adaptation for difenoconazole was observed when compared to the parental WT isolate. Further, the RFs for double mutation introduced through targeted mutagenesis were in the same range as for the field double mutation (Table 21). These results proved that mutations L143F and G446S in the *CYP51* gene in *A. solani* are the reason for reduced DMI sensitivity. Similar results were recently shown for *C. beticola* where mutation L144F and silent mutation E170 in *CYP51* confer adaptation towards DMIs (Bolton et al. 2024; Hoffmeister et al. 2024). This was confirmed by

targeted mutagenesis where the native *CYP51* gene was replaced by different haplotypes (Bolton et al. 2024).

While it has been demonstrated that the detected double mutation in *A. solani* represent the underlying resistance mechanisms for DMI adaptation, it is important to note that other resistance mechanisms might be involved. EC₅₀ values of field isolates with double mutation L143F+G446S and the mean EC₅₀ values of targeted mutation strains with double mutation for mefentrifluconazole and difenoconazole showed, that the adaptation of the targeted mutation strains with the double mutation was lower than for naturally mutated field isolates. An implication of these findings described is the possibility of additional resistance mechanisms with low effect (Yin et al. 2023), to mitigate the lethal effect of repeated DMI application in the field. The parental isolate was isolated in 1977 and the isolates analysed in this work were from 2018 to 2023. Since the 1970s many DMIs have been developed and used in agricultural plant protection and since then, resistance mechanisms started to evolve (Brent and Hollomon 2007). In this work, no other resistance mechanisms, such as overexpression, increased efflux or metabolization, were investigated for *A. solani*, however, higher EC₅₀ values for WT field strains from current populations may be an indication for other unknown resistance mechanisms evolved in the last decades. Such an accumulation of so far not identified resistance mechanisms in the current population might be the reason why the parental isolate from 1977 itself is higher sensitive to DMIs than the current population. Further, this might be the reason for the lower EC₅₀ values for the targeted mutation strains compared to the field mutants. Nevertheless, RFs for targeted mutation strains and field strains were in the same range, which showed that the adaptation is caused by the detected mutations in the *CYP51* gene.

After targeted mutagenesis of the WT parental isolate, 120 targeted mutation strains could be generated containing the new cassette with desired mutations. Of these 120 targeted mutation strains, six strains with mutation L143F and four with double mutation L143F+G446S could be isolated, whereas only one strain with mutation G446S was generated. Although the individual mutations may not be lethal, it is plausible that mutation G446S solely is somehow disadvantageous. As mentioned in the literature, mutations in the conserved domain Y459 to Y461 are important to develop mutation I381V in *Z. tritici* (Cools et al. 2010), in *A. solani* it may be *vice versa*. It seems possible that mutation G446S in the conserved region preferably evolve when mutation L143F is present. This would indicate, that in case the second mutation evolved due to selection pressure of DMIs, mutation G446S followed the development of mutation L143F to overcome lethal effects of DMIs and to confer stronger adaptation. Since DMI resistance develops gradually over time (Brent and Hollomon 2007), in this case it could be

assumed that individuals with double mutation L143F+G446S reproduced in the past and suppressed individuals with single mutation G446S or L143F due to more pronounced fitness costs of isolates with single mutations. Prior studies about *C. beticola* have noted that mutation L144F develops frequent in combination with other mutations, e. g., M145L, H306R, I309T or I387M (Muellender et al. 2021; Hoffmeister et al. 2024). Further, mutation L144F in *C. beticola* was found as single mutation, supporting the assumption that mutation L143F in *A. solani* is necessary for development of mutation G446S during the emergence of adaptation driven by use of DMI fungicides (Muellender et al. 2021; Hoffmeister et al. 2024).

The positions of the mutations in *CYP51* indicate that mutation L143F might have a greater impact on the DMI binding due to steric clashes with the heme. Mutation G446S is located 11 Å away from the heme and does not show steric clash with the heme (Figure 8). Therefore, the effect on DMI bindings is approximately low. In fact, the data demonstrated the same RFs for strains with single mutation L143F and G446S, leading to the suggestion that mutation L143F and G446S might have the same impact on resistance to DMIs. However, in recent studies it was reported that isolates carrying mutation L144F in *C. beticola* have increased EC₅₀ values and show the strongest adaptation to DMIs when compared to other mutations (e. g., I387M or Y464S) and the highest adaptation when mutation L144F is present in combination with I309T (Hoffmeister et al. 2024). This is in accordance with higher EC₅₀ values in *A. solani* strains carrying mutation L143F in combination with G446S than for strains with solely mutation G462S (chapter 3.4). These findings and the proximity of mutation L143F to the binding site support the assumption that *A. solani* evolved mutation G446S in addition to L143F in consequence of intense DMI treatment.

Moreover, it was not possible to generate more than one strain with mutation G446S. More than one strain is necessary to eliminate experimental error and variability. Further work with multiple strains with single mutation G446S is needed to enhance the reliability of the *in vitro* tests and to fully determine the effect of this mutation. Despite the small sampling size of strains with G446S the effect of both single mutations seems to have a cumulative effect on the sensitivity to mefentrifluconazole and difenoconazole.

In vivo tests in the greenhouse proved that targeted mutation strains with mutations L143F, G446S and L143F+G446S are able to infect tomato plants. Infection on control plants with no DMI application reached up to 90%, which is comparable to infection rates of field isolates (80-100%). Mefentrifluconazole, difenoconazole and the reference fungicide metiram showed 100% efficacy on the targeted mutation strains. As mentioned before, the results lead to the suggestion, that *A. solani* may developed other resistance mechanisms in combination with mutations in *CYP51* gene, which are now missing in the targeted mutation strains with the

genetic background of the sensitive WT strain from the 1970s. Combinations of resistance mechanisms are not unusual and were reported for *Z. tritici* or *P. pachyrhizi* and is one of the major characteristics of DMI shifting (Wyand and Brown 2005; Brent and Hollomon 2007; Cools and Fraaije 2013; Rehfus et al. 2019; Huf 2021; Stilgenbauer 2022).

4.7 Incomplete cross-resistance of *A. solani* to different DMIs

Generally, compounds with the same mode of action are considered to be cross-resistant with each other. However, not all DMIs show complete cross-resistance (FRAC 2024a), which was also shown in *A. solani* (chapter 3.5). For example, in *Z. tritici* isolates related to mutations in the target gene *CYP51*, show incomplete cross-resistance between DMIs (Stammler et al. 2008; Jørgensen et al. 2018; Jørgensen et al. 2021).

Correlation between mefentrifluconazole, difenoconazole and prothioconazole were determined. There was a high correlation of the *in vitro* sensitivity across all investigated isolates, between mefentrifluconazole and difenoconazole ($r=0.8706$), while correlation with prothioconazole and both other DMIs was nearly absent. This result is consistent with those of Li et al. (2023) for *A. alternata* who showed cross-resistance for difenoconazole and mefentrifluconazole. It may be possible that no cross-resistance between difenoconazole or mefentrifluconazole and prothioconazole was observed, since prothioconazole belongs chemically to the triazolinethiones, and mefentrifluconazole and difenoconazole to the triazoles (FRAC 2024a). The similar chemical structure may also be the reason for the high correlation of mefentrifluconazole and difenoconazole. As difenoconazole is used for many years in potato, it is likely that the exposure to this fungicide supported the evolution of the slight adaptation to mefentrifluconazole as well.

Further, the reason for the lack of cross-resistance to prothioconazole could be the weak effect of the detected mutations on DMIs. In the present study the resistance levels were comparatively low for haplotype G462S and L143F+G446S, indicating low adaptation in *A. solani*. Moreover, prothioconazole was more affected by single mutation G462S and less by double mutation L143F+G446S, and difenoconazole and mefentrifluconazole were more affected by the double mutation than by the single mutation. This may also play a role in the incomplete cross-resistance in *A. solani*. The low effect implies that a small amount of compound is necessary to overcome resistance. Therefore, it is unlikely that cross-resistance between fungicides will occur. It has been reported that other pathogens such as *P. pachyrhizi*, *Z. tritici* or *C. beticola* show higher resistance levels and exhibit RFs >100 (Stilgenbauer 2022; Huf 2021; Kumar et al. 2021) with a greater effect on DMI sensitivity *in vitro*. Considering the high RFs for other pathogens, it is more likely that cross-resistance will develop due to the

robust and effective resistance mechanisms, which can cause reduced sensitivity to several fungicides within one chemical group. For example, in *P. pachyrhizi* high RFs (>100) for tebuconazole and metconazole in haplotype F120L+Y131H (+I145V/F154Y) showed a nearly perfect correlation ($R^2=0.99$) (Stilgenbauer 2022).

Additionally, a previous study evaluating different *SDH* haplotypes in *Z. tritici*, reported about varying RFs for haplotype C-H152R. Some isolates with mutation C-H152R were linked to fitness penalties and showed lower RFs, others had competitive advantages and revealed higher RFs (Rehfus 2018). The author assumed that the isolates vigor might influence the RFs, although further research is needed on this topic. Nevertheless, in *A. solani* a weak impact on adaptation for haplotype L143F+G446S was obtained from microtiter tests and a fitness penalty was observed in the greenhouse. Additionally, the frequency of mutation in *CYP51* gene in the field was minor (chapter 3.7.2). Since in *A. solani* the fitness of isolates developing mutation L143F+G446S was obviously reduced, it may be assumed, that this fitness disadvantage is also pronounced under DMI treatment after several propagation cycles, as the selection pressure is relatively weak. Low resistance levels are a result of a low degree of sensitivity loss, which might be due to low vitality of mutated individuals leading to incomplete cross-resistance. It could be suggested that the viability of an individual may also influence the EC_{50} values *in vitro*. In field experiments in 2022 and 2023 it was shown, that *CYP51* haplotype L143F+G446S and G462S represent a minority proportion within the *A. solani* population. These results could be potentially attributed to the weak adaptation, resulting from low selection pressure of fungicide treatments. Even though relative frequencies of resistant alleles in the population were low it was observed that individuals with L143F+G446S and G462S mutations preferably survived after DMI treatment.

In further studies, it would be interesting to analyze the competitiveness in *A. solani* haplotypes under fungicide treatments to investigate if prothioconazole selects for mutation G462S and difenoconazole and mefentrifluconazole for mutation L143F+G446S. For such studies, field isolates, as well as targeted mutation strains of *A. solani* can be included to determine the effect of the mutations with defined genetic background. Additionally, since haplotype G462S is also characterized by low effects on DMIs and incomplete cross-resistance, this haplotype could be included in future fitness studies without fungicide treatment to determine the vitality of the single mutation. Knowledge about the selection patterns of different DMIs, may help to slow down further adaptation in *A. solani*. Van den Bosch et al. (2014) suggested that the density of sensitive strain is reduced when the fungicide dose increases. This may lead to less competition, hence providing resistant individuals the potential to establish. Information about

competitiveness and selection patterns of *CYP51* haplotypes could help to estimate the potential of future increase or decrease of adapted individuals leading to adaptation.

In conclusion, the cross-resistance patterns in *A. solani*, indicate a low effect on DMIs of detected mutations and incomplete cross-resistance within the DMIs. This advantage can be used to manage DMI adaptation in *A. solani* in the field. Application of DMIs on early blight that show incomplete cross-resistance pattern in mixtures or alternation is suggested to be suitable for anti-resistance management. Li et al. (2023) claimed that due to positive cross-resistance it is not advisable to mix or alternate difenoconazole and mefentrifluconazole on *A. alternata* which can be transferred to *A. solani*.

4.8 Multiple resistance

Multiple resistance describes the development of different resistance mechanisms e.g., mutations on separate genes, to two or more fungicides with different modes of action (Brent and Hollomon 2007).

Previous results showed that *A. solani* is able to develop multiple resistance to fungicides with different modes of action (Gudmestad et al. 2013; Landschoot et al. 2017; Metz et al. 2019; Nottensteiner et al. 2019; Mostafanezhad et al. 2021). For example, in a Swedish population it was shown that isolates possessing either *SDH B*-H278Y or *SDH C*-H134R mutation also harbored the F129L substitution in *CYTB* (Mostafanezhad et al. 2021). Multiple resistance can limit the effectiveness of available fungicides, making it challenging to control early blight thus regular monitoring and early detection of resistant populations are crucial to enable appropriate anti-resistant management strategies.

In this work some isolates showed multiple resistance to QoIs, SDHIs and adaptation to DMIs. When mutation L143F+G446S or G462S in *CYP51* gene were present, mutation F129L in *CYTB* gene was always detected. A possible explanation for this might be the fitness costs when mutation L143F+G446S is present (chapter 3.3.1). It was reported that in *P. pachyrhizi* mutation F129L does not cause fitness penalties and that isolates developing mutations in *CYP51* and *CYTB* gene showed competitive advantageous compared to isolates with solely mutation in *CYP51* gene (Klosowski et al. 2016). Hence, it can conceivably be hypothesized that mutation F129L in *A. solani* has the same positive effect when mutation L143F+G446S develops, especially under field conditions and QoI exposure.

Competition studies, as well as investigation of vitality and infection of *CYP51* mutants, were performed with isolates from the Netherlands to find out if mutations in the *CYP51* gene confer fitness penalties or are less fit than the WT. No insights into the fitness of individuals with DMI

and QoI resistance were obtained in the present work. Therefore, in further studies the competitiveness of single spore isolates with mutation F129L alone and in combination with L143F+G446S or G462 might be investigated.

4.9 Field efficacy of different DMIs in current *A. solani* population

Besides QoIs and SDHIs, DMIs play a crucial role in controlling early blight and other fungal pathogens (Price et al. 2015). In the past, mutated *A. solani* genotypes were identified being associated with a compromised QoI and SDHI efficacy (Rosenzweig et al. 2008; Leiminger et al. 2014; Metz et al. 2019). Until now, DMIs have demonstrated high efficacy in reducing *A. solani* infection. Nevertheless, the performance of DMIs in the field can vary due to disease pressure, potato variety, climate, and other reasons (Hausladen et al. 2024).

To evaluate the efficacy of DMIs on the current *A. solani* population and to get an overview of the frequency and distribution of detected mutations in the target gene *CYP51*, field trials in 2022 and 2023 were conducted in Germany. Infection in the field occurred by natural inoculum and varieties “Gala” and “Kuras” were used. DMIs were applied as solo products and SDHIs and QoIs were applied in mixtures. Samples were collected, and isolates were obtained. In this work, most isolates analyzed originated from these trial fields in Germany (n=313). While sequencing the *CYP51* gene, haplotypes G462S and L143F+G446S have been detected (additionally to the WT) and showed a slight effect on DMI sensitivity *in vitro* (chapter 3.4). The genotypes are described in chapter 3.2. In the following chapter, the impact of detected *CYP51* mutations in the field will be discussed.

In field trials from 2022 the infection rate was too low to determine the efficacy of different treatments. Several reasons could lead to this result. The trials were conducted in Limburgerhof, the experimental station of BASF SE. The location provides low disease pressure since the cultivated crops vary frequently depending on the trials and normally no potatoes or other host plants for *A. solani* are cultivated in proximity. In 2023 the locations were chosen to be in Böhl-Iggelheim and Ruchheim since these regions are more closely to commercial trials and therefore the amount of natural inoculum is higher. This favors the spread of *A. solani* and can increase the infection and disease development. To further increase the incidence of *A. solani* infection in 2023 the same potato varieties (“Gala” and “Kuras”) were planted almost two weeks later. Especially “Gala” is an early-maturing cultivar (Bundessortenamt 2011) and it was observed that in 2022 senescence and maturing of the potato plants hindered the identification of *A. solani* lesions, although it was reported that, the plants age is associated with increased early blight infection (Dita Rodriguez et al. 2006). However, the incidence of other pathogens also increased in the course of the growing season. Confounding effects of *P. infestans* and other infections, as well as senescence leaves,

complicated the identification of *A. solani* lesions which led to a smaller number of collected samples. Therefore, in 2023, potatoes were planted two weeks later, resulting in an extended growing period during which the pathogen was able to infect the green foliage. This facilitated recognition of *A. solani* infection on the potato plants. Further, in 2023 the application interval was extended to 14-21 days to promote the outbreak of *A. solani* infection and to facilitate the collection of leaves with visible *A. solani* infections. These measures could have contributed to a higher infection rate in 2023 and consequently the efficacy of the applications could be evaluated. Also, environmental conditions could play a role in disease occurrence and severity. Thus, a higher number of isolates were gained in 2023.

Figure 23A and B showed that in samples collected in 2022 haplotype G462S was detected in low frequencies and no double mutation L143F+G446S, whereas in 2023 the double mutation and single mutation G462S were rarely present in all treated plots. In both years, the relative frequency of mutated haplotypes is very low, and a major part of the population consists of sensitive individuals. The infrequent occurrence may be explained by the weak impact on DMI adaptation determined *in vitro*. Thus, these mutations may not provide a strong enough selective advantage for the fungi to develop these mutations as it was shown that mutation L143F+G446S showed fitness disadvantages. However, isolates with double mutation L143F+G446S were slightly more adapted than isolates with mutation G462S, what could lead to the assumption that the double mutation is the preferred mechanism to overcome the lethal effect of DMI applications. In *A. solani* it was shown, that highly SDHI adapted isolates occur more often than moderately adapted isolates (Gudmestad et al. 2013; Metz et al. 2019) what could explain why mutation G462S was rarely found in the course of this work (n=6).

Further, it could be interpreted that the relative frequency of mutated haplotypes slightly increased from 2022 to 2023 (Figure 23). DMI adaptation is characterized by a gradually shift over time and is variable in degree (Brent and Hollomon 2007). The interpretation of the increase of mutated haplotypes in 2023 may be somewhat limited by the low incidence of infection in 2022. A larger sample size in 2022 would have provided more accurate results. Further, field trials over several growing seasons would be necessary to obtain the development of resistance in *A. solani*. In general, the low effect of L143F+G446S and G462S on DMI adaptation observed *in vitro* and the fitness penalties of individuals with mutations in *CYP51* gene could be an explanation for the low frequencies detected in the field. However, it is important to note that results illustrated in chapter 3.7.2 represent relative frequencies of *CYP51* haplotypes obtained from different number of leaf samples randomly collected in the field trials from 2022 and 2023. Hence, the results do not reflect absolute numbers of individuals. The relative frequency expresses the ratio of sensitive and mutated haplotypes

within the investigated number of samples, therefore, indicating the proportion in the population. For example, in 2022 one isolates with mutation G462S could be obtained from the untreated plots. From the same untreated plots leaf samples were collected to determine the relative frequency of mutated alleles in the population. The results showed that 100% of the investigated population in these plots were sensitive and did not develop *CYP51* mutations. It can be speculated that the adaptation in *A. solani* to DMIs is at the beginning. During the initial stages of resistance evolution, levels of resistant individuals in a population are rather low, and therefore hard to detect (Brent and Hollomon 2007). This is in accordance with the results from *in vitro* and the good efficacy of DMIs shown in the fields.

Results based on the field trials in 2023 indicated that DMIs as solo products gave the best early blight control, although no significant differences were observed. In variety "Kuras" the efficacy of prothioconazole was significant reduced when compared to mefentrifluconazole and difenoconazole. *In vitro* sensitivity tests revealed highest EC₅₀ values for prothioconazole, which could be an indicator for the compromised efficacy in the field. Moreover, it was shown, that in 2022 and 2023 haplotype G462S and L143F+G446S were present in all treated plots. In this work multiple resistance was described for DMIs and Qols (chapter 3.6.1), what may be the explanation for DMI adapted individuals in plots treated with Qols and SDHIs. Isolates analyzed in this work with adaptation to DMIs always exhibit resistance to Qols by mutation F129L – thus, a DMI adapted population might be controlled by mixtures of different modes of action. This is shown by the good efficacy of the mixture of boscalid+pyraclostrobin in the variety "Kuras", which can effectively control early blight. Nowadays, mutation F129L in *CYTB* and mutation C-H134R in *SDH* are widespread in *A. solani* reducing sensitivity to Qols and SDHIs (Edin et al. 2019; FRAC 2024f, 2024g, BASF internal data). Because of the low frequency of *CYP51* haplotype L143F+G446S and G462S, it can be assumed, that mutations in *CYTB* or *SDH* lead to compromised efficacy of fungicides rather than mutation in *CYP51* gene. Metz et al. (2019) reported that in Germany mutation H134R is the predominant mutation, whereas Mallik et al. (2014) showed that in the US mutation H278R used to dominate the population. In the Belgium *A. solani* population mutations in subunit *B* and *C* occurred often in combination (Landschoot et al. 2017). Further it was shown that the frequency of mutation F129L in *CYTB* and mutation H134R in *SDH* subunit *C* are nowadays the dominating mutations conferring Qol and SDHI resistance, respectively, and as it was mentioned in previous chapter 4.8 *A. solani* is capable of developing multiple resistance (Gudmestad et al. 2013; Landschoot et al. 2017; Metz et al. 2019; Nottensteiner et al. 2019; Mostafanezhad et al. 202). Therefore, it is likely that adaptation to fungicides in *A. solani* is mostly driven by mutations in *CYTB* and *SDH* genes. SDHI and Qol adaptation in *A. solani* is known for many years. Due to rather low frequency and low effect of *CYP51* mutations, it seems possible that adaptation in *A. solani* to

DMIs is starting to emerge. For other fungal pathogens undergoing selection pressure for several decades, such as *C. beticola*, *V. inaequalis*, *R. collo-cygni*, or *Z. tritici*, it was reported that a major part of the population is adapted to DMIs (Huf et al. 2018; Rehfus et al. 2019; Hoffmeister et al. 2021; Hoffmeister et al. 2024). This is in contrast with results shown in this work for *A. solani*. Taken all results from *in vitro* sensitivity tests, incomplete cross-resistance, competition studies and field trials into account, it could conceivably be hypothesized that mutation in *CYP51* will not strongly emerge in the future and until now, the effect is rather low. Regarding the obvious fitness disadvantage of mutation L143F+G446S and the low frequency of adapted haplotype L143F+G446S and G462S it can be suggested that appropriate resistance strategies can reduce the speed of emerging adaptation. By regularly monitoring of the population, proper strategies can be implemented to delay the sensitivity shift of fungal populations. Therefore, it is of importance to further investigate the impact of *CYP51* mutations in *A. solani*.

4.10 Prospects for future DMI use

FRAC classified the risk for *A. solani* to develop fungicide resistance as medium (FRAC 2019) and the resistant risk for DMIs was categorized low to medium (FRAC 2024a). In this work, adaptation in *A. solani* to DMIs has been firstly described, resulting in low resistance levels *in vitro* and in the field. Nevertheless, development of fungicide resistance could pose a challenge in the future, and it is crucial to optimize resistance management with this knowledge.

In the past, DMIs have shown to have good efficacy despite their extensive use. Mutations in *CYP51* gene generally cause a low magnitude decrease in sensitivity to DMIs resulting in relatively low DMI adaptation and incomplete cross-resistance between different DMIs (Cools et al. 2013) what is in accordance to the results in this work. The *CYP51* haplotype L143F+G446S and G462S in *A. solani* detected in Europe and Australia are marginal distributed and haplotype L143F+G446S showed significant fitness costs when compared to the WT. Mutated isolates were detected, but without significant effect on product performance in the field. As mutation G462S have been identified only six times in investigated isolates and effects were minor, the practical relevance of this mutation needs further investigation. Based on the result of this work the developing resistance risk of *A. solani* is speculated to be low for DMIs and it seems likely that DMIs can still contribute to early blight control in the future. However, resistance management strategies must be followed to ensure the effectiveness of DMIs against fungal pathogens. Therefore, guidelines are proposed by FRAC and renewed at the annual FRAC meetings. Thus, the use of mixtures of fungicides contribute to an effective resistance management (van den Bosch et al. 2014a). Mixing a high-risk, single-site inhibitor with a low-risk, multisite inhibitor represents an intention to reduce fungicide selection (Lucas

et al. 2015). Alternation between DMI and non-DMI fungicides could be further employed to overcome fungicide resistance (van den Bosch et al. 2014). Moreover, the spray timing of fungicides resulted in an important factor for good disease control, focusing on preventive, rather than curative application (van den Berg et al. 2013). Also, lowering the number of fungicide applications reduces the risk of resistance (van den Bosch et al. 2014). Moreover, developing new modes of action, alternation and mixing modes of action and others, are examples for important tools to counteract resistance mechanisms. Understanding how the mechanisms of fungicide resistance evolve is a reasonable approach to tackle the problem of this issue.

The development of multiple resistance poses as challenge to the resistance management of fungal plant pathogens. In *A. solani* multiple resistance was shown and has to be considered to be a relevant aspect for future disease control of early blight. All adapted *CYP51* haplotype investigated here showed QoI adaptation. Pasche et al. (2004) reported that azoxystrobin is affected by mutation F129L in *CYTB* gene, but less to pyraclostrobin or trifloxystrobin. Therefore, one potential approach for controlling *A. solani* population developing multiple resistance to DMIs and QoIs could be the use of a combination of DMIs with either pyraclostrobin or trifloxystrobin.

In other phytopathogenic fungi homologous mutations to L143F, G446S and G462S detected in *A. solani* have been described recently (Carter et al. 2014; Lichtemberg et al. 2017; Hoffmeister et al. 2021; Muellender et al. 2021; Hoffmeister et al. 2024). In *V. inaequalis* the newly introduced DMI mefentrifluconazole can effectively counter reduced DMI sensitivity caused by *CYP51* mutations (Hoffmeister et al. 2021). In *M. fructicola* mutation G461S is related to tebuconazole resistance (Lichtemberg et al. 2017). For *P. brassicae* it was proposed that different resistance mechanisms, including target site mutations G460S and S508T, may cause a reduced DMI efficacy in the field. However, *P. brassicae* showed additional resistance conferred by, e. g., promoter insertion and target protein variation, which may reduce field efficacy of DMIs (Carter et al. 2014). Also, Bucur et al. (2022) reports of additional resistance mechanisms influencing the sensitivity of *P. brassicae* to DMIs which emerged due to repeated DMI use. In *C. beticola* different *CYP51* haplotypes, including L144F alone and in combination, and induced overexpression were identified linked to reduced DMI sensitivity (Muellender et al. 2021; Hoffmeister et al. 2024). In summary, resistance mechanisms in those phytopathogenic fungi were mostly described *in vitro* and continued effort are needed to evaluate practical relevance of mutations homologous to mutations in *A. solani*. However, these studies show that pathogens with homologous *CYP51* mutations to mutations in *A. solani* are likely to develop several resistance mechanisms in combination. It should be taken into

account that in *A. solani* it could be possible that due to DMI selection pressure other resistance mechanisms may evolve in future as shown for these pathogens (Carter et al. 2014; Lichtemberg et al. 2017; Hoffmeister et al. 2021; Muellender et al. 2021; Hoffmeister et al. 2024). Other relevant resistance mechanisms influencing DMI efficacy, which were not investigated in this work, are overexpression of transporter genes and increased efflux. The knowledge of the effect of homologous mutations, and possibilities of combinations with other resistance mechanisms, in other fungal pathogens may help to estimate the resistance development of mutations L143F+G446S and G462S in the future and anti-resistance management strategies can be implemented to delay such scenarios in *A. solani*. Many other fungal pathogens develop a combination of various resistant mechanisms to DMIs. For example, *Z. tritici* and *B. cinerea* revealed an increased fungicide efflux activity against DMIs and other modes of action (Kretschmer et al. 2009; Stammler and Semar 2011; Omrane et al. 2015). Overexpression of the *CYP51* gene contributes to DMI adaptation and was described for several phytopathogenic fungi, such as *V. inaequalis*, *P. triticina*, *M. fructicola* and *Z. tritici* (Schnabel and Jones 2001; Stammler et al. 2009; Luo and Schnabel 2008; Cools et al. 2012). Also, *P. brassicae* developed additional mechanisms in form of inserts in the promotor region (Bucur et al. 2022).

It seems likely that *A. solani* is in an early phase of developing DMI adaptation. Slight adaptation was determined *in vitro*, but frequency of mutants (L143F+G446S, G462S) is low and also RFs. The field efficacy of DMIs on the current *A. solani* population is still stable and the significant fitness cost of mutation L143F+G446S may negatively influence the ability of *A. solani* to develop a stable DMI-resistance with higher resistance levels. Further monitoring is needed to observe the DMI sensitivity in *A. solani* populations in the main potato growing regions. With such programs, isolates with further DMI adaptation could be identified and characterized, which could lead to countermeasures in form of effective resistance management strategies. The 2024 initiative of the EuroBlight Group (EuroBlight 2024) on a common European sensitivity monitoring with subsequent *CYP51* sequencing and isolate characterization based on the data of this thesis is an important step for the sustainable use of fungicides for early blight control.

5 Summary

Early blight, caused by *A. solani*, is one of the major pathogens in potato and other Solanaceae and has the potential to reduce yield in potato production on a global scale. No potato cultivars resistant to *A. solani* are known, but susceptibility to early blight varies depending on cultivar and maturity. Besides agronomical measures, such as elimination of infected plants, crop rotation or appropriate nitrogen and phosphorus fertilization, early blight is controlled by chemical and biological foliar fungicides. Fungicides are used for over 200 years against phytopathogenic fungi and played a crucial role in improvement of food quality and quantity. The single-site fungicides QoIs, SDHIs and DMIs represent three major fungicide groups that are used to control early blight in potato. To overcome the lethal effect of fungicide use, plant pathogens are able to evolve resistance mechanisms. The most important are point mutations in the target gene, overexpression of the target enzyme, increased efflux, and metabolization of the fungicide. The focus of this work was placed on target site mutations, as they represent the principal mechanism underlying resistance in fungal plant pathogens.

A. solani has developed mutation F129L in *CYTB* gene leading to a reduced sensitivity to QoIs. Mutations that acquire resistance to SDHIs evolved in subunit *B*, *C* and *D* of the *SDH* gene in *A. solani*. Mutation *B*-H278R/Y, *C*-N75S, *C*-H134R and *D*-D123E confer varying levels of resistance. Further, DMIs play a crucial role in controlling *A. solani*. DMIs inhibit the sterol 14 α -demethylase (*CYP51*), a key enzyme in the fungal sterol biosynthesis pathway. However, to date, no resistance mechanisms have been detected. Therefore, the aim of this work was to determine and elucidate target site mutations in *CYP51* gene conferring DMI adaptation in *A. solani*.

In the course of this work, *CYP51* mutations L143F+G446S and G462S in *A. solani* have been detected and identified being responsible for reduced sensitivity to DMIs. A nucleotide substitution from cytosine to thymine leads to a change of the aa at position 143 from leucine to phenylalanine and results in mutation L143F. At positions 446 and 462 an aa change from glycine to serine is caused by a nucleotide substitution from guanine to adenine results in mutations G446S and G462S. Isolates were analyzed from different regions in Europe and from Australia, where L143F+G446S have been detected. Therefore, it can be suggested that the double mutation emerged independently at various locations, rather than a single mutated isolate spreading throughout different locations. In the investigated isolates, mutation L143F and G446S evolved always in combination, whereas mutation G462S was detected as single mutation. *In vitro* sensitivity tests showed slightly enhanced EC₅₀ values for difenoconazole and mefentrifluconazole and low resistance levels. Surprisingly, the single mutation G462S had a stronger effect on prothioconazole than double mutation L143F+G446S.

Mefentrifluconazole and difenoconazole were more affected by mutation L143F+G446S. The distinct chemical structure of triazolinethiones and triazoles seem to interact differently with the binding site when mutations are present, resulting in varying levels of effectiveness against different *CYP51* haplotypes.

Furthermore, a *CYP51* gene transfer achieved by protoplast transformation were performed, to examine whether the mutations found in combination are responsible for reduced sensitivity to DMIs. The L143F and G446S mutations showed slightly increased EC₅₀ values for difenoconazole and mefentrifluconazole when compared to the parent. The RFs of the double mutation introduced through targeted mutagenesis were similar to the RFs calculated for the double mutants from the field. Hence, it was proven that the detected target site mutations L143F and G446S are the reason for limited DMI shift in *A. solani*. It could be assumed that mutation G446S (or L143F) alone may influence the *CYP51* activity negatively but not lethally and that the second mutation restores this effect and adds additional DMI adaptation.

Moreover, *in vivo* greenhouse fitness tests were conducted without fungicide application to determine the mutations frequency after several infection cycles on tomato plants. After the first infection cycle the frequency of mutation L143F+G446S decreased in the initial *CYP51* haplotype mixture and was completely reduced after four cycles. This result led to the assumption that haplotype L143F+G446S is linked to significant fitness penalties. Hence, it can be assumed that detected mutations do not confer a loss of field efficacy which was additionally shown in the conducted field trials. Further, spore morphology and quantity did not differ from WT and L143F+G446S haplotype. Under this assumption, emergence of adaptation may be slowed down as mutated individuals have to compete with more fit sensitive individuals.

Field studies revealed that frequency of *CYP51* mutations in the population of 2022 and 2023 is very low and mutations were detected in DMI, and non-DMI treated plots. In isolates obtained from the field trials multiple resistance was detected to DMIs and Qols, but not for DMIs and SDHIs. Cross-resistance was determined for mefentrifluconazole and difenoconazole, but not for prothioconazole. Since difenoconazole was introduced few years prior to mefentrifluconazole, the exposure to difenoconazole may have influenced the sensitivity of the population to mefentrifluconazole.

The findings of this study have significant implications for the understanding of how target site mutations in *A. solani* influence the DMI efficacy. It can be expected that resistance management strategies which include practical measurements and biological and chemical foliar fungicide, with different modes of action, lead to a good control of early blight. Further monitoring studies are essential to assess the susceptibility to DMI fungicides and to adjust resistance managements recommendations in the case of any changes.

6 Literature

- Abe F, Usui K, Hiraki T (2009) Fluconazole modulates membrane rigidity, heterogeneity, and water penetration into the plasma membrane in *Saccharomyces cerevisiae*. *Biochemistry* 48 (36):8494-8504. doi:10.1021/bi900578y
- Abuley IK, Nielsen BJ, Hansen HH (2018) The influence of crop rotation on the onset of early blight (*Alternaria solani*). *Journal of Phytopathology* 167 (1):35-40. doi:10.1111/jph.12771
- Abuley IK, Nielsen BJ, Hansen HH (2019) The influence of timing the application of nitrogen fertilizer on early blight (*Alternaria solani*). *Pest Management Science* 75 (4):1150-1158. doi:10.1002/ps.5236
- Abuley IK, Hansen JG (2021) An epidemiological analysis of the dilemma of plant age and late blight (*Phytophthora infestans*) susceptibility in potatoes. *European Journal of Plant Pathology* 161 (3):645-663. doi:10.1007/s10658-021-02350-4
- Adnan M, Islam W, Shabbir A, Khan KA, Ghramh HA, Huang Z, Chen HYH, Lu GD (2019) Plant defense against fungal pathogens by antagonistic fungi with *Trichoderma* in focus. *Microbial Pathogenesis* 129:7-18. doi:10.1016/j.micpath.2019.01.042
- Agrios G (2005) *Plant Pathology*, vol 5. Elsevier Academic Press, San Diego, CA, United States
- Ahmadian A, Gharizadeh B, Gustafsson AC, Sterky F, Nyren P, Uhlen M, Lundeberg J (2000) Single-nucleotide polymorphism analysis by pyrosequencing. *Analytical Biochemistry* 280 (1):103-110. doi:10.1006/abio.2000.4493
- Ahmadian A, Ehn M, Hober S (2006) Pyrosequencing: history, biochemistry and future. *Clinica Chimica Acta* 363 (1-2):83-94. doi:10.1016/j.cccn.2005.04.038
- Aktar MW, Sengupta D, Chowdhury A (2009) Impact of pesticides use in agriculture: their benefits and hazards. *Interdisciplinary Toxicology* 2 (1):1-12. doi:10.2478/v10102-009-0001-7
- Avenot H, Morgan DP, Michailides TJ (2008) Resistance to pyraclostrobin, boscalid and multiple resistance to Pristine® (pyraclostrobin + boscalid) fungicide in *Alternaria alternata* causing alternaria late blight of pistachios in California. *Plant Pathology* 57 (1):135-140. doi:10.1111/j.1365-3059.2007.01701.x
- Awan ZA, Shoaib A (2019) Combating early blight infection by employing *Bacillus subtilis* in combination with plant fertilizers. *Current Plant Biology* 20:100125. doi:10.1016/j.cpb.2019.100125
- Awan ZA, Shoaib A, Schenk PM, Ahmad A, Alansi S, Paray BA (2023) Antifungal potential of volatiles produced by *Bacillus subtilis* BS-01 against *Alternaria solani* in *Solanum lycopersicum*. *Frontiers in Plant Science* 13:1089562. doi:10.3389/fpls.2022.1089562
- Barclay GM, Murphy HJ, Manzer FE, Hutchinson FE (1973) Effects of differential rates of nitrogen and phosphorus on early blight in potatoes. *American Potato Journal* 50 (2):42-48. doi:10.1007/bf02855367
- Barrell PJ, Meiyalaghan S, Jacobs JM, Conner AJ (2013) Applications of biotechnology and genomics in potato improvement. *Plant Biotechnology Journal* 11 (8):907-920. doi:10.1111/pbi.12099
- Bartlett DW, Clough JM, Godwin JR, Hall AA, Hamer M, Parr-Dobrzanski B (2002) The strobilurin fungicides. *Pest Management Science* 58 (7):649-662. doi:10.1002/ps.520
- Bassetti M, Merelli M, Temperoni C, Astilean A (2013) New antibiotics for bad bugs: where are we? *Annals of Clinical Microbiology and Antimicrobials* 12:22. doi:10.1186/1476-0711-12-22

- Becher R, Weihmann F, Deising HB, Wirsal SG (2011) Development of a novel multiplex DNA microarray for *Fusarium graminearum* and analysis of azole fungicide responses. *BioMed Central Genomics* 12:52. doi:10.1186/1471-2164-12-52
- Becher R, Wirsal SG (2012) Fungal cytochrome P450 sterol 14 α -demethylase (CYP51) and azole resistance in plant and human pathogens. *Applied Microbiology and Biotechnology* 95 (4):825-840. doi:10.1007/s00253-012-4195-9
- Boiteux LS, Reifschneider FJB (1993) Identification and field characterization of rate-reducing resistance to early blight disease (*Alternaria solani*) in potato (*Solanum tuberosum*) clones and cultivars. *Fitopatologia Brasileira* 18:86-86
- Boiteux LS, Reifschneider FJB, Fonseca MEN, Buso JA (1995) Search for sources of early blight (*Alternaria solani*) field resistance not associated with vegetative late maturity in tetraploid potato germplasm. *Euphytica* 83 (1):63-70. doi:10.1007/bf01677862
- Bolton MD, Rivera V, Secor G (2012) Identification of the G143A mutation associated with Qol resistance in *Cercospora beticola* field isolates from Michigan, United States. *Pest Management Science* 69 (1):35-39. doi:10.1002/ps.3358
- Bolton MD, Rangel L, Courneya I, Wyatt N, Secor G (2024) Unraveling the molecular basis of DMI resistance in *Cercospora beticola*. *Proceedings XX International Plant Protection Congress* (p. 108). Athens, Greece
- Bowyer P, Denning DW (2014) Environmental fungicides and triazole resistance in *Aspergillus*. *Pest Management Science* 70 (2):173-178. doi:10.1002/ps.3567
- Brent KJ, Hollomon DW (1998) Fungicide resistance: the assessment of risk. 2nd revised edition edn. Fungicide Resistance Action Committee, Brussels, Belgium
- Brent KJ, Hollomon DW (2007) Fungicide resistance in crop pathogens: how can it be managed? 2nd revised edition edn. Fungicide Resistance Action Committee, Brussels, Belgium
- Brent KJ, Hollomon DW (2007a) Fungicide resistance: the assessment of risk. 2nd revised edition edn. Fungicide Resistance Action Committee, Brussels, Belgium
- Bucur DE, Huang YJ, Fitt BDL, Kildea S (2022) Azole fungicide sensitivity and molecular mechanisms of reduced sensitivity in Irish *Pyrenopeziza brassicae* populations. *Pest Management Science* 80 (5):2393-2404. doi:10.1002/ps.7219
- Bundessortenamt (2022) Beschreibende Sortenliste Kartoffel 2022. https://www.bundessortenamt.de/bsa/media/Files/BSL/bsl_kartoffel_2022.pdf Accessed 15.11.2023
- Burlingame B, Charrondiere R, Mouille B (2009) Food composition is fundamental to the cross-cutting initiative on biodiversity for food and nutrition. *Journal of Food Composition and Analysis* 22 (5):361-365. doi:10.1016/j.jfca.2009.05.003
- Camire ME, Kubow S, Donnelly DJ (2009) Potatoes and Human Health. *Critical Reviews in Food Science and Nutrition* 49 (10):823-840. doi:10.1080/10408390903041996
- Carter HE, Fraaije BA, West JS, Kelly SL, Mehl A, Shaw MW, Cools HJ (2014) Alterations in the predicted regulatory and coding regions of the sterol 14 α -demethylase gene (CYP51) confer decreased azole sensitivity in the oilseed rape pathogen *Pyrenopeziza brassicae*. *Molecular Plant Pathology* 15 (5):513-522. doi:10.1111/mpp.12106
- Chaerani R, Voorrips RE (2006) Tomato early blight (*Alternaria solani*): the pathogen, genetics, and breeding for resistance. *Journal of General Plant Pathology* 72 (6):335-347. doi:10.1007/s10327-006-0299-3
- Chen F, Liu X, Schnabel G (2013) Field strains of *Monilinia fructicola* resistant to both MBC and DMI fungicides isolated from stone fruit orchards in the eastern United States. *Plant Disease* 97 (8):1063-1068. doi:10.1094/PDIS-12-12-1177-RE

- Christ BJ, Maczuga SA (1989) The effect of fungicide schedules and inoculum levels on early blight severity and yield of potato. *Plant Disease* 73 (8):695-698. doi:10.1094/pd-73-0695
- Christ BJ (1991) Effect of disease assessment method on ranking potato cultivars for resistance to early blight. *Plant Disease* 75 (4):353-356. doi:10.1094/pd-75-0353
- Chung CT, Niemela SL, Miller RH (1989) One-step preparation of competent *Escherichia coli*: Transformation and storage of bacterial cells in the same solution. *Proceedings of the National Academy of Sciences of the United States of America* 86 (7):2172-2175. doi:10.1073/pnas.86.7.2172
- Cools HJ, Fraaije BA (2008) Are azole fungicides losing ground against Septoria wheat disease? Resistance mechanisms in *Mycosphaerella graminicola*. *Pest Management Science* 64 (7):681-684. doi:10.1002/ps.1568
- Cools HJ, Parker JE, Kelly DE, Lucas JA, Fraaije BA, Kelly SL (2010) Heterologous expression of mutated eburicol 14 α -demethylase (CYP51) proteins of *Mycosphaerella graminicola* to assess effects on azole fungicide sensitivity and intrinsic protein function. *Applied and Environmental Microbiology* 76 (9):2866-2872. doi:10.1128/AEM.02158-09
- Cools HJ, Mullins JG, Fraaije BA, Parker JE, Kelly DE, Lucas JA, Kelly SL (2011) Impact of recently emerged sterol 14 α -demethylase (CYP51) variants of *Mycosphaerella graminicola* on azole fungicide sensitivity. *Applied and Environmental Microbiology* 77 (11):3830-3837. doi:10.1128/AEM.00027-11
- Cools HJ, Bayon C, Atkins S, Lucas JA, Fraaije BA (2012) Overexpression of the sterol 14 α -demethylase gene (*MgCYP51*) in *Mycosphaerella graminicola* isolates confers a novel azole fungicide sensitivity phenotype. *Pest Management Science* 68 (7):1034-1040. doi:10.1002/ps.3263
- Cools HJ, Fraaije BA (2013) Update on mechanisms of azole resistance in *Mycosphaerella graminicola* and implications for future control. *Pest Management Science* 69 (2):150-155. doi:10.1002/ps.3348
- Cools HJ, Hawkins NJ, Fraaije BA (2013) Constraints on the evolution of azole resistance in plant pathogenic fungi. *Plant Pathology* 62 (S1):36-42. doi:10.1111/ppa.12128
- Cox KD, Bryson PK, Schnabel G (2007) Instability of propiconazole resistance and fitness in *Monilinia fructicola*. *Phytopathology* 97 (4):448-453. doi:10.1094/PHYTO-97-4-0448
- Cummins I, Wortley DJ, Sabbadin F, He Z, Coxon CR, Straker HE, Sellars JD, Knight K, Edwards L, Hughes D, Kaundun SS, Hutchings SJ, Steel PG, Edwards R (2013) Key role for a glutathione transferase in multiple-herbicide resistance in grass weeds. *Proceedings of the National Academy of Science* 110 (15):5812-5817. doi:10.1073/pnas.1221179110
- de Waard MA (1997) Significance of ABC transporters in fungicide sensitivity and resistance. *Pesticide Science* 51 (3):271-275. doi:10.1002/(sici)1096-9063(199711)51:3<271::Aid-ps642>3.0.Co;2-%23
- de Waard MA, Andrade AC, Hayashi K, Schoonbeek HJ, Stergiopoulos I, Zwieters LH (2006) Impact of fungal drug transporters on fungicide sensitivity, multidrug resistance and virulence. *Pest Management Science* 62 (3):195-207. doi:10.1002/ps.1150
- Deising HB, Reimann S, Pascholati SF (2008) Mechanisms and significance of fungicide resistance. *Brazilian Journal of Microbiology* 39 (2):286-295. doi:10.1590/S1517-838220080002000017
- Del Sorbo G, Schoonbeek H, de Waard MA (2000) Fungal transporters involved in efflux of natural toxic compounds and fungicides. *Fungal Genetics and Biology* 30 (1):1-15. doi:10.1006/fgbi.2000.1206

- Delgado-Baquerizo M, Guerra CA, Cano-Díaz C, Egidi E, Wang J-T, Eisenhauer N, Singh BK, Maestre FT (2020) The proportion of soil-borne pathogens increases with warming at the global scale. *Nature Climate Change* 10 (6):550-554. doi:10.1038/s41558-020-0759-3
- Délye C, Laigret F, Corio-Costet MF (1997) A mutation in the 14 α -demethylase gene of *Uncinula necator* that correlates with resistance to a sterol biosynthesis inhibitor. *Applied and Environmental Microbiology* 63 (8):2966-2970. doi:10.1128/aem.63.8.2966-2970.1997
- Ding S, Meinholz K, Cleveland K, Jordan SA, Gevens AJ (2019) Diversity and virulence of *Alternaria* spp. causing potato early blight and brown spot in Wisconsin. *Phytopathology* 109 (3):436-445. doi:10.1094/PHYTO-06-18-0181-R
- Dita Rodriguez MA, Brommonschenkel SH, Matsuoka K, Mizubuti ESG (2006) Components of resistance to early blight in four potato cultivars: Effect of leaf position. *Journal of Phytopathology* 154 (4):230-235. doi:10.1111/j.1439-0434.2006.01089.x
- Dorrance AE, Inglis DA (1997) Assessment of greenhouse and laboratory screening methods for evaluating potato foliage for resistance to late blight. *Plant Disease* 81 (10):1206-1213. doi:10.1094/PDIS.1997.81.10.1206
- Douglas LM, Konopka JB (2014) Fungal membrane organization: the eisosome concept. *Annual Review of Microbiology* 68:377-393. doi:10.1146/annurev-micro-091313-103507
- Duarte HSS, Zambolim L, Rodrigues FA, Paul PA, Pádua JG, Ribeiro Júnior JI, N. Júnior AF, Rosado AWC (2014) Field resistance of potato cultivars to foliar early blight and its relationship with foliage maturity and tuber skin types. *Tropical Plant Pathology* 39 (4):294-306. doi:10.1590/s1982-56762014000400004
- Edgington LV, Martin RA, Bruin GC, Parsons IM (1980) Systemic fungicides: A perspective after 10 years. *Plant Disease* 64 (1):19-23. doi:10.1094/pd-64-19
- Edin E, Liljeroth E, Andersson B (2019) Long term field sampling in Sweden reveals a shift in occurrence of cytochrome *b* genotype and amino acid substitution F129L in *Alternaria solani*, together with a high incidence of the G143A substitution in *Alternaria alternata*. *European Journal of Plant Pathology* 155 (2):627-641. doi:10.1007/s10658-019-01798-9
- Einspanier S, Susanto T, Metz N, Wolters PJ, Vleeshouwers V, Lankinen A, Liljeroth E, Landschoot S, Ivanovic Z, Huckelhoven R, Hausladen H, Stam R (2022) Whole-genome sequencing elucidates the species-wide diversity and evolution of fungicide resistance in the early blight pathogen *Alternaria solani*. *Evolutionary Applications* 15 (10):1605-1620. doi:10.1111/eva.13350
- Eisermann I (2023) Ein einziger Aminosäureaustausch im Transkriptionsfaktor Azr1 erzeugt Azolresistenz in *Fusarium graminearum*. Dissertation, Martin-Luther-Universität Halle-Wittenberg, Germany
- EPPO (2024) Global database of European and Mediterranean Plant Protection Organization. <https://gd.eppo.int/> Accessed 19.01.2024
- EuroBlight (2024) EuroBlight: A potato late blight network for Europe. 20th EuroBlight Workshop. https://agro.au.dk/fileadmin/euroblight/Workshops/Netherlands/Presentations/Session6_Alternaria/Subgroup_Alternaria_EUROBLIGHT_2024.pdf Accessed 23.07.2024
- Europlant (2023) EUROPLANT Pflanzenzucht GmbH. <https://www.europlant.biz/sortiment/kuras/>. Accessed 15.11.2023
- Evenson RE, Gollin D (2003) Assessing the impact of the green revolution, 1960 to 2000. *Science* 300 (5620):758-762. doi:10.1126/science.1078710

- FAO (2022) The future of food and agriculture - Drivers and triggers for transformation., vol 3. Rome, Italy. doi:<https://doi.org/10.4060/cc0959en>
- FAO (2024) Food and Agriculture Organization of the United Nations. <https://www.fao.org/faostat/en/#data/QCL/visualize>. Accessed 02.02.2024
- Fisher N, Meunier B (2007) Molecular basis of resistance to cytochrome *bc*₁ inhibitors. *FEMS Yeast Research* 8 (2):183-192. doi:10.1111/j.1567-1364.2007.00328.x
- Foolad MR, Merk HL, Ashrafi H (2008) Genetics, genomics and breeding of late blight and early blight resistance in tomato. *Critical Reviews in Plant Sciences* 27 (2):75-107. doi:10.1080/07352680802147353
- Fraaije BA, Butters JA, Coelho JM, Jones DR, Hollomon DW (2002) Following the dynamics of strobilurin resistance in *Blumeria graminis* f.sp. *tritici* using quantitative allele-specific real-time PCR measurements with the fluorescent dye SYBR Green I. *Plant Pathology* 51 (1):45-54. doi:10.1046/j.0032-0862.2001.00650.x
- FRAC (2019) Pathogen Risk List. <https://www.frac.info/docs/default-source/publications/pathogen-risk/frac-pathogen-list-2019.pdf>. Accessed 02.02.2024
- FRAC (2024). <https://www.frac.info/frac-teams/working-groups/sdhi-fungicides/information>. Accessed 03.03.2024
- FRAC (2024a) Sterol biosynthesis inhibitor (SBI) Working Group. <https://www.frac.info/frac-teams/working-groups/sbi-fungicides/information>. Accessed 03.03.2024
- FRAC (2024b) Fungicide Resistance Action Committee. <https://www.frac.info/fungicide-resistance-management/by-fungicide-common-name>. Accessed 03.03.2024
- FRAC (2024c) Fungicide Resistance Action Committee. <https://www.frac.info/fungicide-resistance-management/background>. Accessed 25.04.2024
- FRAC (2024d) Fungicide Action Resistance Committee. <https://www.frac.info/home/about-frac>. Accessed 25.04.2024
- FRAC (2024e) Fungicide Resistance Action Committee. https://www.frac.info/docs/default-source/monitoring-methods/approved-methods/septr-monitoring-method-syngenta-2006-v1.pdf?sfvrsn=a899419a_4. Accessed 25.04.2024
- FRAC (2024f) Quinone 'outside' inhibitor (QoI) Working Group. https://www.frac.info/docs/default-source/working-groups/qol-fungicides/qoi-meeting-minutes/2024-qoi-wg-meeting-minutes-and-recommendations-17jan2024-and-24mar2024.pdf?sfvrsn=d4ec4e9a_2. Accessed 26.04.2024
- FRAC (2024g) Succinate Dehydrogenase Inhibitor (SDHI) Working Group. https://www.frac.info/docs/default-source/working-groups/sdhi-fungicides/sdhi-meeting-minutes/minutes-of-the-2024-sdhi-meeting-with-recommendations-for-2024-from-16-17th-jan-and-22nd-march-2024.pdf?sfvrsn=7ceb4e9a_2. Accessed 26.04.2024
- Friggeri L, Hargrove TY, Wawrzak Z, Blobaum AL, Rachakonda G, Lindsley CW, Villalta F, Nes WD, Botta M, Guengerich FP, Lepesheva GI (2018) Sterol 14 α -demethylase structure-based design of VNI ((R)- N-(1-(2,4-dichlorophenyl)-2-(1 H-imidazol-1-yl)ethyl)-4-(5-phenyl-1,3,4-oxadiazol-2-yl)benzamide)) derivatives to target fungal infections: synthesis, biological evaluation, and crystallographic analysis. *Journal of Medicinal Chemistry* 61 (13):5679-5691. doi:10.1021/acs.jmedchem.8b00641
- Fry WE, Goodwin SB (1997) Resurgence of the irish potato famine fungus. *BioScience* 47 (6):363-371. doi:10.2307/1313151
- Fuchs A, de Waard MA (1982) Resistance to ergosterol-biosynthesis inhibitors I. Chemistry and phenomenological aspects. Fungicide resistance in crop protection. Center for Agricultural Publishing and Documentation, Wageningen, The Netherlands

- Gisi U, Sierotzki H, Cook A, McCaffery A (2002) Mechanisms influencing the evolution of resistance to Qo inhibitor fungicides. *Pest Management Science* 58 (9):859-867. doi:10.1002/ps.565
- Gisi U (2013) Assessment of selection and resistance risk for demethylation inhibitor fungicides in *Aspergillus fumigatus* in agriculture and medicine: a critical review. *Pest Management Science* 70 (3):352-364. doi:10.1002/ps.3664
- Glaab A, Weilacher X, Hoffmeister M, Strobel D, Stammler G (2024) Occurrence and distribution of CYP51 haplotypes of *Zymoseptoria tritici* in recent years in Europe. *Journal of Plant Diseases and Protection* 131:1187-1194. doi:10.1007/s41348-024-00897-y
- Glättli A, Grote T, Stammler G (2011) SDH-Inhibitors: History, biological performance and molecular mode of action. In Dehne HW, Deising HB, Gisi U, Kuck KH, Russel PE, Lyr H (Eds.) *Modern Fungicides and Antifungal Compounds VI* (pp. 159-169). Deutsche Phytomedizinische Gesellschaft, Braunschweig, Germany
- Gómez-Rodríguez O, Zavaleta-Mejía E, González-Hernández VA, Livera-Muñoz M, Cárdenas-Soriano E (2003) Allelopathy and microclimatic modification of intercropping with marigold on tomato early blight disease development. *Field Crops Research* 83 (1):27-34. doi:10.1016/s0378-4290(03)00053-4
- Grabke A, Stammler G (2015) A *Botrytis cinerea* population from a single strawberry field in Germany has a complex fungicide resistance pattern. *Plant Disease* (8):1078-1086. doi:10.1094/PDIS-07-14-0710-RE
- Grasso V, Palermo S, Sierotzki H, Garibaldi A, Gisi U (2006) Cytochrome *b* gene structure and consequences for resistance to Qo inhibitor fungicides in plant pathogens. *Pest Management Science* 62 (6):465-472. doi:10.1002/ps.1236
- Griffith JM, Davis AJ, Grant BR (1992) Target sites of fungicides to control Oomycetes. *Target sites of fungicide action*, vol 1 CRC Press
- Gudmestad NC, Arabiat S, Miller JS, Pasche JS (2013) Prevalence and impact of SDHI fungicide resistance in *Alternaria solani*. *Plant Disease* 97 (7):952-960. doi:10.1094/PDIS-12-12-1176-RE
- Hägerhäll C (1997) Succinate: quinone oxidoreductases. Variations on a conserved theme. *Biochimica et Biophysica Acta* 1320 (2):107-141. doi:10.1016/s0005-2728(97)00019-4
- Hamamoto H, Hasegawa K, Nakaune R, Lee YJ, Makizumi Y, Akutsu K, Hibi T (2000) Tandem repeat of a transcriptional enhancer upstream of the sterol 14alpha-demethylase gene (*CYP51*) in *Penicillium digitatum*. *Applied and Environmental Microbiology* 66 (8):3421-3426. doi:10.1128/AEM.66.8.3421-3426.2000
- Harrison MD, Venette JR (1970) Chemical control of potato early blight and its effect on potato yield. *American Potato Journal* 47 (3):81-86. doi:10.1007/bf02864808
- Hartmann FE, Vonlanthen T, Singh NK, McDonald MC, Milgate A, Croll D (2020) The complex genomic basis of rapid convergent adaptation to pesticides across continents in a fungal plant pathogen. *Molecular Ecology* 30 (21):5390-5405. doi:10.1111/mec.15737
- Hausladen H, Leiminger J (2007) Potato early blight in Germany. Tenth Workshop of an European Network for development of an Integrated Control Strategy of potato late blight 12:189-193. Bologna, Italy
- Hausladen H, Leiminger J (2015) Evidence of strobilurine resistant isolates of *A. solani* and *A. alternata* in Germany. *Proceedings 15th EuroBlight Workshop* 17:93-100. Brasov, Romania
- Hausladen H, Abuley I, Kessel G, Hansen JG (2024) Late blight and early blight in Europe in 2022 & 2023. Presentation 19th EuroBlight Workshop. Lunteren, The Netherlands

- He MH, Wang YP, Wu EJ, Shen LL, Yang LN, Wang T, Shang LP, Zhu W, Zhan J (2019) Constraining evolution of *Alternaria alternata* resistance to a demethylation inhibitor (DMI) fungicide difenoconazole. *Frontiers in Microbiology* 10:1609. doi:10.3389/fmicb.2019.01609
- Hoffmeister M, Zito R, Böhm J, Stammler G (2021) Mutations in *Cyp51* of *Venturia inaequalis* and their effects on DMI sensitivity. *Journal of Plant Diseases and Protection* 128 (6):1467-1478. doi:10.1007/s41348-021-00516-0
- Hoffmeister M, Schorer J, Hinson A, Stammler G (2024) Alterations in CYP51 of *Cercospora beticola* and their effects on DMI sensitivity. *Journal of Plant Diseases and Protection*. doi:10.1007/s41348-024-00961-7
- Holley JD, Hall R, Hofstra G (1983) Identification of rate-reducing resistance to early blight in potato. *Canadian Journal of Plant Pathology* 5 (2):111-114. doi:10.1080/07060668309501637
- Hollomon DW (2015) Fungicide resistance: facing the challenge - a review. *Plant Protection Science* 51 (4):170-176. doi:10.17221/42/2015-pps
- Horsefield R, Yankovskaya V, Sexton G, Whittingham W, Shiomi K, Omura S, Byrne B, Cecchini G, Iwata S (2006) Structural and computational analysis of the quinone-binding site of complex II (succinate-ubiquinone oxidoreductase): a mechanism of electron transfer and proton conduction during ubiquinone reduction. *The Journal of Biological Chemistry* 281 (11):7309-7316. doi:10.1074/jbc.M508173200
- Huf A, Rehfus A, Lorenz KH, Bryson R, Voegelé RT, Stammler G (2018) Proposal for a new nomenclature for *CYP51* haplotypes in *Zymoseptoria tritici* and analysis of their distribution in Europe. *Plant Pathology* 67 (8):1706-1712. doi:10.1111/ppa.12891
- Huf A (2021) Characterisation of the sensitivity of *Zymoseptoria tritici* to demethylation inhibitors in Europe. Doctoral dissertation, Universität Hohenheim, Germany
- Jabs T, Cronshaw K, Freund A (2001) New strobilurin resistance mechanism in apple scab (*Venturia inaequalis*). *Phytoprotection* 3:15-16
- Jambhulkar PP, Meghwal ML, Kalyan RK (2012) Efficacy of plastic mulching, marigold intercropping and fungicidal spray against early blight of tomato caused by *Alternaria solani*. *The Bioscan* 7 (2):365-368
- Jørgensen LN, Matzen N, Hansen JG, Semaskiene R, Korbas M, Danielewicz J, Glazek M, Maumene C, Rodemann B, Weigand S, Hess M, Blake J, Clark B, Kildea S, Batailles C, Ban R, Havis N, Treikale O (2018) Four azoles' profile in the control of Septoria, yellow rust and brown rust in wheat across Europe. *Crop Protection* 105:16-27. doi:10.1016/j.cropro.2017.10.018
- Jørgensen LN, Heick TM (2021) Azole use in agriculture, horticulture, and wood preservation - Is it indispensable? *Frontiers in Cellular and Infection Microbiology* 11:730297. doi:10.3389/fcimb.2021.730297
- Jørgensen LN, Matzen N, Heick TM, Havis N, Holdgate S, Clark B, Blake J, Glazek M, Korbas M, Danielewicz J, Maumene C, Rodemann B, Weigand S, Kildea S, Bataille C, Brauna-Morževska E, Gulbis K, Ban R, Berg G, Semaskiene R, Stammler G (2021) Decreasing azole sensitivity of *Z. tritici* in Europe contributes to reduced and varying field efficacy. *Journal of Plant Diseases and Protection* 128 (1):287-301. doi:10.1007/s41348-020-00372-4
- Karaoglanidis GS, Thanassoulopoulos CC, Ioannidis PM (2001) Fitness of *Cercospora beticola* field isolates – resistant and – sensitive to demethylation inhibitor fungicides. *European Journal of Plant Pathology* 107 (3):337-347. doi:10.1023/a:1011219514343

- Keon JPR, White GA, Hargreaves JA (1991) Isolation, characterization and sequence of a gene conferring resistance to the systemic fungicide carboxin from the maize smut pathogen, *Ustilago maydis*. *Current Genetics* 19 (6):475-481. doi:10.1007/bf00312739
- Kiebacher H, Hoffmann GM (1976) Resistance against benzimidazole fungicide in *Venturia inaequalis*. *Journal of Plant Diseases and Protection* 83 (6):352-358
- Klappach K, Stammler G (2019) Resistance of plant pathogens to succinate dehydrogenase inhibitor (SDHI) fungicides (FRAC Code 7). In *Fungicide resistance in North America*. Stevensons KL, McGrath MT, Wyenandt CA (Eds.) APS (pp. 85-95)
- Klosowski AC, Brahm L, Stammler G, May De Mio LL (2016) Competitive fitness of *Phakopsora pachyrhizi* isolates with mutations in the CYP51 and CYTB genes. *Phytopathology* 106 (11):1278-1284. doi:10.1094/PHYTO-01-16-0008-R
- Koenraadt H, Somerville SC, Jones AL (1992) Characterization of mutations in the beta-tubulin gene of benomyl-resistant field strains of *Venturia inaequalis* and other plant pathogenic fungi. *Molecular Plant Pathology* 82:1348-1354
- Krämer W, Schirmer U (2007) *Modern crop protection compounds*, vol 3.
- Kretschmer M, Leroch M, Mosbach A, Walker AS, Fillinger S, Mernke D, Schoonbeek HJ, Pradier JM, Leroux P, de Waard MA, Hahn M (2009) Fungicide-driven evolution and molecular basis of multidrug resistance in field populations of the grey mould fungus *Botrytis cinerea*. *PLoS Pathogens* 5 (12). doi:10.1371/journal.ppat.1000696
- Kuhn PJ (1984) *Mode of action of carboxamides*. British Mycological Society Symposia Series. Elsevier, Amsterdam, The Netherlands
- Kumar R, Mazakova J, Ali A, Sur VP, Sen MK, Bolton MD, Manasova M, Rysanek P, Zouhar M (2021) Characterization of the molecular mechanisms of resistance against DMI fungicides in *Cercospora beticola* populations from the Czech Republic. *Journal of Fungi* 7 (12). doi:10.3390/jof7121062
- Landschoot S, Carrette J, Vandecasteele M, De Baets B, Höfte M, Audenaert K, Haesaert G (2017) Boscalid-resistance in *Alternaria alternata* and *Alternaria solani* populations: An emerging problem in Europe. *Crop Protection* 92:49-59. doi:10.1016/j.cropro.2016.10.011
- Landschoot S, Vandecasteele M, De Baets B, Hofte M, Audenaert K, Haesaert G (2017a) Identification of *A. arborescens*, *A. grandis*, and *A. protenta* as new members of the European *Alternaria* population on potato. *Fungal Biology* 121 (2):172-188. doi:10.1016/j.funbio.2016.11.005
- Latijnhouwers M, de Wit PJ, Govers F (2003) Oomycetes and fungi: similar weaponry to attack plants. *Trends in Microbiology* 11 (10):462-469. doi:10.1016/j.tim.2003.08.002
- Lawrence CB, Singh NP, Qiu J, Gardner RG, Tuzun S (2000) Constitutive hydrolytic enzymes are associated with polygenic resistance of tomato to *Alternaria solani* and may function as an elicitor release mechanism. *Physiological and Molecular Plant Pathology* 57 (5):211-220. doi:10.1006/pmpp.2000.0298
- Leiminger JH, Adolf B, Hausladen H (2014) Occurrence of the F129L mutation in *Alternaria solani* populations in Germany in response to QoI application, and its effect on sensitivity. *Plant Pathology* 63 (3):640-650. doi:10.1111/ppa.12120
- Leiminger JH, Hausladen H (2014) Untersuchungen zur Befallsentwicklung und Ertragswirkung der Dürffleckenkrankheit (*Alternaria* spp.) in Kartoffelsorten unterschiedlicher Reifegruppe. *Gesunde Pflanzen* 66 (1):29-36. doi:10.1007/s10343-014-0314-0
- Leroux P, Fritz R, Debieu D, Albertini C, Lanen C, Bach J, Gredt M, Chapeland F (2002) Mechanisms of resistance to fungicides in field strains of *Botrytis cinerea*. *Pest Management Science* 58 (9):876-888. doi:10.1002/ps.566

- Leroux P, Gredt M, Remuson F, Micoud A, Walker AS (2013) Fungicide resistance status in French populations of the wheat eyespot fungi *Oculimacula acufiformis* and *Oculimacula yallundae*. *Pest Management Science* 69 (1):15-26. doi:10.1002/ps.3408
- Li G, Li X, Zeng Y, Liao S, Chen Y, Miao J, Peng Q, Liu X (2023) Three point mutations in AaCYP51 combined with induced overexpression of AaCYP51 conferred low-level resistance to mefentrifluconazole in *Alternaria alternata*. *Pesticide Biochemistry and Physiology* 197:105677. doi:10.1016/j.pestbp.2023.105677
- Lichtemberg PSF, Luo Y, Morales RG, Muehlmann-Fischer JM, Michailides TJ, May De Mio LL (2017) The point mutation G461S in the *MfCYP51* gene is associated with tebuconazole resistance in *Monilinia fructicola* populations in Brazil. *Phytopathology* 107 (12):1507-1514. doi:10.1094/PHYTO-02-17-0050-R
- Lichtemberg PSF, Michailides TJ, Puckett RD, Zeviani WM, May De Mio LL (2018) Fitness costs associated with G461S mutants of *Monilinia fructicola* could favor the management of tebuconazole resistance in Brazil. *Tropical Plant Pathology* 44 (2):140-150. doi:10.1007/s40858-018-0254-9
- Liedl BE, Kosier T, Desborough SL (1987) HPLC isolation and nutritional value of a major tuber protein. *American Potato Journal* 64 (10):545-557. doi:10.1007/bf02853753
- Liu X, Yu F, Schnabel G, Wu J, Wang Z, Ma Z (2010) Paralogous *cyp51* genes in *Fusarium graminearum* mediate differential sensitivity to sterol demethylation inhibitors. *Fungal Genetics and Biology* 48 (2):113-123. doi:10.1016/j.fgb.2010.10.004
- Louw CD (1976) Nuclear distribution in *Alternaria tenuis*. *Mycopathologia* 58 (3):169-176. doi:10.1007/bf00496026
- Lucas JA, Hawkins NJ, Fraaije BA (2015) The evolution of fungicide resistance. *Advances in Applied Microbiology* 90:29-92. doi:10.1016/bs.aambs.2014.09.001
- Luo CX, Schnabel G (2008) The cytochrome P450 lanosterol 14 α -demethylase gene is a demethylation inhibitor fungicide resistance determinant in *Monilinia fructicola* field isolates from Georgia. *Applied and Environmental Microbiology* 74 (2):359-366. doi:10.1128/AEM.02159-07
- Ma Z, Michailides TJ (2005) Advances in understanding molecular mechanisms of fungicide resistance and molecular detection of resistant genotypes in phytopathogenic fungi. *Crop Protection* 24 (10):853-863. doi:10.1016/j.cropro.2005.01.011
- Ma Z, Proffer TJ, Jacobs JL, Sundin GW (2006) Overexpression of the 14 α -demethylase target gene (*CYP51*) mediates fungicide resistance in *Blumeriella jaapii*. *Applied and Environmental Microbiology* 72 (4): 2581-2585. doi:10.1128/AEM.72.4.2581-2585.2006
- MacKenzie DR (1981) Association of potato early blight, nitrogen fertilizer rate, and potato yield. *Plant Disease* 65 (7):575-577. doi: 10.1094/PD-65-575
- Maiero M, Bean GA, Ng TJ (1991) Toxin production by *Alternaria solani* and its related phytotoxicity to tomato breeding lines. *Phytopathology* 81 (9):1030-1033. doi:10.1094/Phyto-81-1030
- Mallik I, Arabiat S, Pasche JS, Bolton MD, Patel JS, Gudmestad NC (2014) Molecular characterization and detection of mutations associated with resistance to succinate dehydrogenase-inhibiting fungicides in *Alternaria solani*. *Phytopathology* 104 (1):40-49. doi:10.1094/phyto-02-13-0041-r
- Malonek S, Rojas MC, Hedden P, Gaskin P, Hopkins P, Tudzynski B (2004) The NADPH-cytochrome P450 reductase gene from *Gibberella fujikuroi* is essential for gibberellin biosynthesis. *Journal of Biological Chemistry* 279 (24):25075-25084. doi:10.1074/jbc.M308517200

- Mamgain A, Roychowdhury R, Tah J (2013) *Alternaria* pathogenicity and its strategic controls. *Research & Reviews: Journal of Biology* 1:1-9
- Meemken E-M, Qaim M (2018) Organic Agriculture, Food Security, and the Environment. *Annual Review of Resource Economics* 10 (1):39-63. doi:10.1146/annurev-resource-100517-023252
- Mellado E, Diaz-Guerra TM, Cuenca-Estrella M, Rodriguez-Tudela JL (2001) Identification of two different 14- α sterol demethylase-related genes (*cyp51A* and *cyp51B*) in *Aspergillus fumigatus* and other *Aspergillus species*. *Journal of Clinical Microbiology* 39 (7):2431-2438. doi:10.1128/JCM.39.7.2431-2438.2001
- Metz N, Adolf B, Chaluppa N, Huckelhoven R, Hausladen H (2019) Occurrence of *sdh* Mutations in German *Alternaria solani* Isolates and Potential Impact on Boscalid Sensitivity In Vitro, in the Greenhouse, and in the Field. *Plant Disease* 103 (12):3065-3071. doi:10.1094/PDIS-03-19-0617-RE
- Metz N (2021) Environment interaction, fungicide resistance and biological control of *Alternaria solani* on potato. Doctoral dissertation, Technische Universität München, Germany
- Metz N, Hausladen H (2022) *Trichoderma* spp. As potential biological control agent against *Alternaria solani* in potato. *Biological Control* 166 (1):104820. doi:10.1016/j.biocontrol.2021.104820
- Mikaberidze A, McDonald BA (2015) Fitness cost of resistance: Impact on management. In: *Fungicide Resistance in Plant Pathogens*:77-89. doi:10.1007/978-4-431-55642-8_6
- Miller JS, Rosen CJ (2005) Interactive effects of fungicide programs and nitrogen management on potato yield and quality. *American Journal of Potato Research* 82 (5):399-409. doi:10.1007/bf02871970
- Mittelstrass K, Treutter D, Plessl M, Heller W, Elstner EF, Heiser I (2006) Modification of primary and secondary metabolism of potato plants by nitrogen application differentially affects resistance to *Phytophthora infestans* and *Alternaria solani*. *Plant Biology* 8 (5):653-661. doi:10.1055/s-2006-924085
- Morschhäuser J (2010) Regulation of multidrug resistance in pathogenic fungi. *Fungal Genetics and Biology* 47 (2):94-106. doi:10.1016/j.fgb.2009.08.002
- Mostafanezhad H, Edin E, Grenville-Briggs LJ, Lankinen Å, Liljeroth E (2021) Rapid emergence of boscalid resistance in Swedish populations of *Alternaria solani* revealed by a combination of field and laboratory experiments. *European Journal of Plant Pathology* 162 (2):289-303. doi:10.1007/s10658-021-02403-8
- Muellender MM, Mahlein A-K, Stammler G, Varrelmann M (2021) Evidence for the association of target-site resistance in *cyp51* with reduced DMI sensitivity in European *Cercospora beticola* field isolates. *Pest Management Science* 77 (4):1765-1774. doi:10.1002/ps.6197
- Nations U (2019) Department of economic and social affairs, population division. *World Population Prospects*
- Nikou D, Malandrakis A, Konstantakaki M, Vontas J, Markoglou A, Ziogas B (2009) Molecular characterization and detection of overexpressed C-14 alpha-demethylase-based DMI resistance in *Cercospora beticola* field isolates. *Pesticide Biochemistry and Physiology* 95 (1):18-27. doi:10.1016/j.pestbp.2009.04.014
- Nottensteiner M, Absmeier C, Zellner M (2019) QoI fungicide resistance mutations in *Alternaria solani* and *Alternaria alternata* are fully established in potato growing areas in bavaria and dual resistance against SDHI fungicides is upcoming. *Gesunde Pflanzen* 71 (3):155-164. doi:10.1007/s10343-019-00475-5

- Odilbekov F, Carlson-Nilsson U, Liljeroth E (2014) Phenotyping early blight resistance in potato cultivars and breeding clones. *Euphytica* 197 (1):87-97. doi:10.1007/s10681-013-1054-4
- Odilbekov F, Edin E, Mostafanezhad H, Coolman H, Grenville-Briggs LJ, Liljeroth E (2019) Within-season changes in *Alternaria solani* populations in potato in response to fungicide application strategies. *European Journal of Plant Pathology* 155 (3):953-965. doi:10.1007/s10658-019-01826-8
- Oerke EC, Dehne HW (2004) Safeguarding production—losses in major crops and the role of crop protection. *Crop Protection* 23 (4):275-285. doi:10.1016/j.cropro.2003.10.001
- Oerke EC (2005) Crop losses to pests. *The Journal of Agricultural Science* 144 (1):31-43. doi:10.1017/s0021859605005708
- Olanya OM, Honeycutt CW, Larkin RP, Griffin TS, He Z, Halloran JM (2009) The effect of cropping systems and irrigation management on development of potato early blight. *Journal of General Plant Pathology* 75 (4):267-275. doi:10.1007/s10327-009-0175-z
- Olaya G, Stuermer C, Linley R, Edlebeck K, Torriani S (2017) Detection of the G143A mutation that confers resistance to QoI fungicides in *Alternaria tomatophila* from tomatoes. In Deising HB, Fraaije B, Mehl A, Oerke EC, Sierotzki H, Stammler G (Eds.) *Modern Fungicides and Antifungal Compounds* Modern Fungicides and Antifungal Compounds VIII (pp. 225-231). Deutsche Phytomedizinische Gesellschaft, Braunschweig, Germany
- Oliver RP, Hewitt HG (2014) *Fungicide in crop protection*, vol 2. CABI, Wallingford, United Kingdom
- Omrane S, Sghyer H, Audeon C, Lanen C, Duplaix C, Walker AS, Fillinger S (2015) Fungicide efflux and the MgMFS1 transporter contribute to the multidrug resistance phenotype in *Zymoseptoria tritici* field isolates. *Environmental Microbiology* 17 (8):2805-2823. doi:10.1111/1462-2920.12781
- Ons L, Bylemans D, Thevissen K, Cammue BPA (2020) Combining biocontrol agents with chemical fungicides for integrated plant fungal disease control. *Microorganisms* 8 (12). doi:10.3390/microorganisms8121930
- Orr HA (2009) Fitness and its role in evolutionary genetics. *Nature Review Genetics* 10 (8):531-539. doi:10.1038/nrg2603
- Padmanabhan SY (1973) The great bengal famine. *Annual Review of Phytopathology* 11:11-24. doi:10.1146/annurev.py.11.090173.000303
- Parker JE, Warrillow AG, Cools HJ, Fraaije BA, Lucas JA, Rigdova K, Griffiths WJ, Kelly DE, Kelly SL (2013) Prothioconazole and prothioconazole-desthio activities against *Candida albicans* sterol 14- α -demethylase. *Applied and Environmental Microbiology* 79 (5):1639-1645. doi:10.1128/AEM.03246-12
- Pasche JS, Wharam CM, Gudmestad NC (2004) Shift in sensitivity of *Alternaria solani* in response to Q(o)I fungicides. *Plant Disease* 88 (2):181-187. doi:10.1094/PDIS.2004.88.2.181
- Pasche JS, Piche LM, Gudmestad NC (2005) Effect of the F129L mutation in *Alternaria solani* on fungicides affecting mitochondrial respiration. *Plant Disease* 89 (3):269-278. doi:10.1094/PD-89-0269
- Peever TL, Milgroom MG (1994) Lack of correlation between fitness and resistance to sterol biosynthesis-inhibiting fungicides in *Pyrenophora teres*. *Phytopathology* 84 (5):515-519. doi:10.1094/Phyto-84-515
- Perez-Tomas R (2006) Multidrug resistance: retrospect and prospects in anti-cancer drug treatment. *Current Medicinal Chemistry* 13 (16):1859-1676. doi:10.2174/092986706777585077

- Plaisted RL, Hoopes RW (1989) The past record and future prospects for the use of exotic potato germplasm. *American Potato Journal* 66 (10):603-627. doi:10.1007/bf02853982
- Price CL, Parker JE, Warrilow AG, Kelly DE, Kelly SL (2015) Azole fungicides - understanding resistance mechanisms in agricultural fungal pathogens. *Pest Management Science* 71 (8):1054-1058. doi:10.1002/ps.4029
- Pruß S, Fetzner R, Seither K, Herr A, Pfeiffer E, Metzler M, Lawrence CB, Fischer R (2014) Role of the *Alternaria alternata* blue-light receptor LreA (white-collar 1) in spore formation and secondary metabolism. *Applied and Environmental Microbiology* 80 (8):2582-2591. doi:10.1128/AEM.00327-14
- Pscheidt JW (1985) Epidemiology and control of potato early blight, caused by *Alternaria solani*. PhD Thesis, University of Wisconsin-Madison, United States
- Puinean AM, Foster SP, Oliphant L, Denholm I, Field LM, Millar NS, Williamson MS, Bass C (2010) Amplification of a cytochrome P450 gene is associated with resistance to neonicotinoid insecticides in the aphid *Myzus persicae*. *PLoS Genetics* 6 (6):e1000999. doi:10.1371/journal.pgen.1000999
- PubChem (2023) National Center for Biotechnology Information. <https://pubchem.ncbi.nlm.nih.gov/> Accessed 01.03.2023
- Qaim M (2017) Globalisation of agrifood systems and sustainable nutrition. *Proceedings of the Nutrition Society* 76 (1):12-21. doi:10.1017/S0029665116000598
- Reimann S, Deising HB. Inhibition of efflux transporter-mediated fungicide resistance in *Pyrenophora tritici-repentis* by a derivative of 4'-hydroxyflavone and enhancement of fungicide activity. *Applied Environmental Microbiology* 71 (6):3269-3275. doi:10.1128/AEM.71.6.3269-3275.2005
- Rehfus A, Miessner S, Achenbach J, Strobel D, Bryson R, Stammler G (2016) Emergence of succinate dehydrogenase inhibitor resistance of *Pyrenophora teres* in Europe. *Pest Management Science* 72 (10):1977-1988. doi:10.1002/ps.4244
- Rehfus A (2018) Analysis of the emerging situation of resistance to succinate dehydrogenase inhibitors in *Pyrenophora teres* and *Zymoseptoria tritici* in Europe. Doctoral dissertation, Universität Hohenheim, Germany
- Rehfus A, Matusinsky P, Strobel D, Bryson R, Stammler G (2019) Mutations in target genes of succinate dehydrogenase inhibitors and demethylation inhibitors in *Ramularia collo-cygni* in Europe. *Journal of Plant Diseases and Protection* 126 (5):447-459. doi:10.1007/s41348-019-00246-4
- Rens L, Zotarelli L, Alva A, Rowland D, Liu G, Morgan K (2016) Fertilizer nitrogen uptake efficiencies for potato as influenced by application timing. *Nutrient Cycling in Agroecosystems* 104 (2):175-185. doi:10.1007/s10705-016-9765-2
- Rezen T, Debeljak N, Kordis D, Rozman D (2004) New aspects on lanosterol 14 α -demethylase and cytochrome P450 evolution: lanosterol/cycloartenol diversification and lateral transfer. *Journal of Molecular Evolution* 59 (1):51-58. doi:10.1007/s00239-004-2603-1
- Rodríguez NV, Kowalski B, Rodríguez LG, Carabaloso IB, Suárez MA, Pérez PO, Quintana CR, González N, Ramos RQ (2007) *In vitro* and *ex vitro* selection of potato plantlets for resistance to early blight. *Journal of Phytopathology* 155 (10):582-586. doi:10.1111/j.1439-0434.2007.01282.x
- Rosenzweig N, Atallah ZK, Olaya G, Stevenson WR (2008) Evaluation of QoI fungicide application strategies for managing fungicide resistance and potato early blight epidemics in Wisconsin. *Plant Disease* 92 (4):561-568. doi:10.1094/pdis-92-4-0561
- Rotem J (1994) The genus *Alternaria*. Biology, epidemiology and pathogenicity. American Phytopathological Society Press, St. Paul, Minnesota, United States

- Sand S (2011) Charakterisierung eines Blaulichtrezeptors in *Alternaria alternata*. Doctoral dissertation, Karlsruher Institut für Technologie, Germany
- Sanglard D, Ischer F, Koymans L, Bille J (1998) Amino acid substitutions in the cytochrome P-450 lanosterol 14 α -demethylase (*CYP51A1*) from azole-resistant *Candida albicans* clinical isolates contribute to resistance to azole antifungal agents. *Antimicrobial Agents and Chemotherapy* 42 (2):241-253. doi:10.1128/AAC.42.2.241
- Schmitz HK, Medeiros CA, Craig IR, Stammler G (2014) Sensitivity of *Phakopsora pachyrhizi* towards quinone-oxidase-inhibitors and demethylation-inhibitors, and corresponding resistance mechanisms. *Pest Management Science* 70 (3):378-388. doi:10.1002/ps.3562
- Schnabel G, Jones AL (2001) The 14 α -Demethylase(*CYP51A1*) gene is overexpressed in *Venturia inaequalis* strains resistant to myclobutanil. *Phytopathology* 91 (1):102-110. doi:10.1094/PHYTO.2001.91.1.102
- Sevastos A, Labrou NE, Flouri F, Malandrakis A (2017) Glutathione transferase-mediated benzimidazole-resistance in *Fusarium graminearum*. *Pesticide Biochemistry and Physiology* 141:23-28. doi:10.1016/j.pestbp.2016.11.002
- Shrestha S, Neubauer J, Spanner R, Natwick M, Rios J, Metz N, Secor GA, Bolton MD (2020) Rapid detection of *Cercospora beticola* in Sugar Beet and mutations associated with fungicide resistance using LAMP or probe-based qPCR. *Plant Disease* 104 (6):1654-1661. doi:10.1094/PDIS-09-19-2023-RE
- Siegel MR (1981) Sterol-inhibiting fungicides: Effects on sterol biosynthesis and sites of action. *Plant Disease* 65 (12):986-989. doi:10.1094/pd-65-986
- Sierotzki H, Parisi S, Steinfeld U, Tenzer I, Poirey S, Gisi U (2000) Mode of resistance to respiration inhibitors at the cytochrome bc1 enzyme complex of *Mycosphaerella fijiensis* field isolates. *Pest Management Science* 56 (10):833-841. doi:10.1002/1526-4998(200010)56:10<833::Aid-ps200>3.0.Co;2-q
- Simmons EG (1992) *Alternaria* taxonomy: current status, viewpoint, challenge. *Alternaria: biology, plant diseases and metabolites*. Elsevier Amsterdam, The Netherlands
- Sober E (2001) *The two faces of fitness. Thinking about Evolution: Historical, philosophical, and political perspectives*. Cambridge University Press, Cambridge, England
- Soltanpour PN, Harrison MD (1974) Interrelations between nitrogen and phosphorus fertilization and early blight control of potatoes. *American Potato Journal* 51:1-7. doi:10.1007/BF02852021
- Song Y, Chen D, Lu K, Sun Z, Zeng R (2015) Enhanced tomato disease resistance primed by arbuscular mycorrhizal fungus. *Frontiers in Plant Science* 6:786. doi:10.3389/fpls.2015.00786
- Southern EM (1975) Detection of specific sequences among DNA fragments separated by gel electrophoresis. *Journal of Molecular Biology* 98 (3):503-517. doi:10.1016/s0022-2836(75)80083-0
- Spanner R, Taliadoros D, Richards J, Rivera-Varas V, Neubauer J, Natwick M, Hamilton O, Vaghefi N, Pethybridge S, Secor GA, Friesen TL, Stukenbrock EH, Bolton MD (2021) Genome-wide association and selective sweep studies reveal the complex genetic architecture of DMI fungicide resistance in *Cercospora beticola*. *Genome Biology and Evolution* 13 (9). doi:10.1093/gbe/evab209
- Spooner DM, Núñez J, Trujillo G, Del Rosario Herrera M, Guzmán F, Ghislain M (2007) Extensive simple sequence repeat genotyping of potato landraces supports a major reevaluation of their gene pool structure and classification. *Proceedings of the National Academy of Sciences* 104 (49):19398-19403. doi:10.1073/pnas.0709796104

- Stalder L, Oggenfuss U, Mohd-Assaad N, Croll D (2023) The population genetics of adaptation through copy number variation in a fungal plant pathogen. *Molecular Ecology* 32 (10):2443-2460. doi:10.1111/mec.16435
- Stall RE (1958) An investigation of nuclear number in *Alternaria solani*. *American Journal of Botany* 45:657-659
- Stammler G, Brix HD, Glättli A, Semar M, Schoefl U (2007) Biological properties of the carboxamide boscalid including recent studies on its mode of action. *Proceedings XVI International Plant Protection Congress* (pp. 16-21). Glasgow, Scotland
- Stammler G, Carstensen M, Koch A, Semar M, Strobel D, Schlehuber S (2008) Frequency of different CYP51-haplotypes of *Mycosphaerella graminicola* and their impact on epoxiconazole-sensitivity and -field efficacy. *Crop Protection* 27 (11):1448-1456. doi:10.1016/j.cropro.2008.07.007
- Stammler G, Cordero J, Koch A, Semar M, Schlehuber S (2009) Role of the Y134F mutation in *cyp51* and overexpression of *cyp51* in the sensitivity response of *Puccinia triticina* to epoxiconazole. *Crop Protection* 28 (10):891-897. doi:10.1016/j.cropro.2009.05.007
- Stammler G, Semar M (2011) Sensitivity of *Mycosphaerella graminicola* (anamorph: *Septoria tritici*) to DMI fungicides across Europe and impact on field performance. *Bulletin OEPP/EPPO Bulletin* 41 (2):149-155. doi:10.1111/j.1365-2338.2011.02454.x
- Stammler G, Wolf A, Glaettli A, Klappach K (2015) Respiration Inhibitors: Complex II. In *Fungicide Resistance in Plant Pathogens* (eds. Ishii H, Hollomon D) (pp. 102-117) Springer Verlag. doi:10.1007/978-4-431-55642-8_8
- Stammler G, Böhme F, Philippi J, Miessner S, Tegge V (2014) Pathogenicity of *Alternaria*-species on potatoes and tomatoes. *Proceedings 14th EuroBlight Workshop* 16:85-96. Limassol, Cyprus
- Stilgenbauer SA (2022) Einsporisolate des Erregers des Asiatischen Sojabohnenrostes (*Phakopsora pachyrhizi*) zur Charakterisierung der Resistenz gegenüber Demethylierungsinhibitoren. Dissertation, Universität Bonn, Germany
- Stilgenbauer S, Simões K, Craig IR, Brahm L, Steiner U, Stammler G (2023) New CYP51-genotypes in *Phakopsora pachyrhizi* have different effects on DMI sensitivity. *Journal of Plant Diseases and Protection* 130 (5):973-983. doi:10.1007/s41348-023-00757-1
- Strobel D, Bryson R, Semar M, Stammler G, Kienle M, Smith J (2020) Mefentrifluconazole (REVYSOL®) - The first isopropanol-azole. In Deising HB, Fraaije B, Mehl A, Oerke EC, Sierotzki H, Stammler G (Eds.) *Modern Fungicides and Antifungal Compounds IX* (pp. 259-264). Deutsche Phytomedizinische Gesellschaft, Braunschweig, Germany
- Taher K, Grad S, Fakhfakh M, Salah HBH, Yahyaoui A, Rezgui S, Nasraoui B, Stammler G (2014) Sensitivity of *Zymoseptoria tritici* isolates from Tunisia to pyraclostrobin, fluxapyroxad, epoxiconazole, metconazole, prochloraz and tebuconazole. *Journal of Phytopathology* 162:442-448. doi: 10.1111/jph.12210
- Thomma BPHJ (2003) *Alternaria* spp.: from general saprophyte to specific parasite. *Molecular Plant Pathology* 4 (4):225-236. doi:10.1046/j.1364-3703.2003.00173.x
- Tsrer L (2010) Biology, epidemiology and management of *Rhizoctonia solani* on potato. *Journal of Phytopathology* 158 (10):649-658. doi:10.1111/j.1439-0434.2010.01671.x
- van den Berg F, van den Bosch F, Paveley ND (2013) Optimal fungicide application timings for disease control are also an effective anti-resistance strategy: A case study for *Zymoseptoria tritici* (*Mycosphaerella graminicola*) on wheat. *Phytopathology* 103 (12):1209-1219. doi:10.1094/phyto-03-13-0061-r
- van den Bosch F, Oliver R, van den Berg F, Paveley N (2014) Governing principles can guide fungicide-resistance management tactics. *The Annual Review of Phytopathology* 52:175-195. doi:10.1146/annurev-phyto-102313-050158

- van den Bosch F, Paveley N, van den Berg F, Hobbelen P, Oliver R (2014a) Mixtures as a fungicide resistance management tactic. *Phytopathology* 104 (12):1264-1273. doi:10.1094/phyto-04-14-0121-rvw
- van der Waals JE, Korsten L, Aveling TAS, Denner FDN (2003) Influence of environmental factors on field concentrations of *Alternaria solani* conidia above a South African potato crop. *Phytoparasitica* 31 (4):353-364. doi:10.1007/bf02979806
- van der Waals JE, Korsten L, Slippers B (2004) Genetic diversity among *Alternaria solani* isolates from potatoes in South Africa. *Plant Disease* 88 (9):959-964. doi:10.1094/pdis.2004.88.9.959
- Vanden Bossche H (1985) Biochemical targets for antifungal azole derivatives: hypothesis on the mode of action. *Current Topics in Medical Mycology* 313-351. doi:10.1007/978-1-4613-9547-8_12
- Vanden Bossche H, Engelen M, Rochette F (2003) Antifungal agents of use in animal health--chemical, biochemical and pharmacological aspects. *Journal of Veterinary Pharmacology and Therapeutics* 26 (1):5-29. doi:10.1046/j.1365-2885.2003.00456.x
- Vinale F, Sivasithamparan K, Ghisalberti EL, Marra R, Woo SL, Lorito M (2008) *Trichoderma*-plant-pathogen interactions. *Soil Biology and Biochemistry* 40 (1):1-10. doi:10.1016/j.soilbio.2007.07.002
- Vloutoglou I, Kalogerakis SN (2000) Effects of inoculum concentration, wetness duration and plant age on development of early blight (*Alternaria solani*) and on shedding of leaves in tomato plants. *Plant Pathology* 49 (3):339-345. doi:10.1046/j.1365-3059.2000.00462.x
- Woudenberg JH, Groenewald JZ, Binder M, Crous PW (2013) *Alternaria* redefined. *Studies in Mycology* 75 (1):171-212. doi:10.3114/sim0015
- Woudenberg JH, Truter M, Groenewald JZ, Crous PW (2014) Large-spored *Alternaria* pathogens in section *Porri* disentangled. *Studies in Mycology* 79:1-47. doi:10.1016/j.simyco.2014.07.003
- Wyand RA, Brown JK (2005) Sequence variation in the *CYP51* gene of *Blumeria graminis* associated with resistance to sterol demethylase inhibiting fungicides. *Fungal Genetics and Biology* 42 (8):726-735. doi:10.1016/j.fgb.2005.04.007
- Yang LN, He MH, Ouyang HB, Zhu W, Pan ZC, Sui QJ, Shang LP, Zhan J (2019) Cross-resistance of the pathogenic fungus *Alternaria alternata* to fungicides with different modes of action. *BMC Microbiology* 19 (1):205. doi:10.1186/s12866-019-1574-8
- Yin Y, Miao J, Shao W, Liu X, Zhao Y, Ma Z (2023) Fungicide Resistance: Progress in understanding mechanism, monitoring, and management. *Phytopathology* 113 (4):707-718. doi:10.1094/PHYTO-10-22-0370-KD
- Yu JH, Hamari Z, Han KH, Seo JA, Reyes-Dominguez Y, Scazzocchio C (2004) Double-joint PCR: a PCR-based molecular tool for gene manipulations in filamentous fungi. *Fungal Genetics and Biology* 41 (11):973-981. doi:10.1016/j.fgb.2004.08.001
- Zhang D, He JY, Haddadi P, Zhu JH, Yang ZH, Ma L (2018) Genome sequence of the potato pathogenic fungus *Alternaria solani* HWC-168 reveals clues for its conidiation and virulence. *BMC Microbiology* 18 (1):176. doi:10.1186/s12866-018-1324-3
- Zito R, Hoffmeister M, Kuehn A, Stammler G (2024) Current update on the fungicide sensitivity of *Erysiphe necator* (grape powdery mildew) in Europe. *Journal of Plant Disease and Protection* 131:1217-1223. doi: 10.1007/s41348-024-00893-2

7 Appendix

7.1 Supplementary tables and figures

Table 22: *A. solani* isolates used in this work, their origin, year and EC₅₀ values for different fungicides.

EC₅₀ values for mefentrifluconazole (MFA), difenoconazole (DFA), prothioconazole (PTH), azoxystrobin (AZ) are listed. Isolates not tested with respective fungicides are described with n.a..

Year	Country	Region	Isolate	<i>CYP51</i> haplotype	MFA	DFA	PTH	AZ
2018	Australia	Walkers Flat	Ms 730-001	WT	0.012	0.034	n.a.	n.a.
			Ms 730-002	WT	0.009	0.034	n.a.	n.a.
			Ms 730-003	WT	0.022	0.047	n.a.	n.a.
			Ms 730-004	WT	0.003	0.006	4.012	0.905
			Ms 730-005	WT	0.016	0.039	n.a.	n.a.
			Ms 749-001	L143F+G446S	0.147	0.111	n.a.	n.a.
			Ms 749-002	L143F+G446S	0.233	0.159	n.a.	n.a.
			Ms 749-003	L143F+G446S	0.114	0.135	n.a.	n.a.
			Ms 749-004	L143F+G446S	0.263	0.094	n.a.	n.a.
			Ms 749-005	L143F+G446S	0.178	0.158	n.a.	n.a.
			Ms 752-002	L143F+G446S	0.121	0.144	n.a.	n.a.
			Ms 752-003	L143F+G446S	0.145	0.078	n.a.	n.a.
			Ms 752-004	WT	0.029	0.052	n.a.	n.a.
			Ms 752-005	L143F+G446S	0.138	0.049	n.a.	n.a.
			Ms 753-001	WT	0.021	0.019	n.a.	n.a.
			Ms 753-002	WT	0.016	0.013	n.a.	n.a.
			Ms 753-003	WT	0.024	0.025	n.a.	n.a.
			Ms 753-004	WT	0.023	0.024	n.a.	n.a.
			Ms 753-005	WT	0.014	0.020	n.a.	n.a.
			Ms 757-001	WT	0.016	0.043	n.a.	n.a.
			Ms 757-002	WT	0.016	0.037	n.a.	n.a.
			Ms 757-003	WT	0.016	0.041	n.a.	n.a.
			Ms 757-004	WT	0.015	0.028	n.a.	n.a.
			Ms 757-005	WT	0.018	0.031	n.a.	n.a.
			Ms 758-001	L143F+G446S	0.048	0.048	n.a.	n.a.
			Ms 758-003	L143F+G446S	0.111	0.105	n.a.	n.a.
			Ms 758-004	L143F+G446S	0.074	0.052	n.a.	n.a.
			Ms 758-005	L143F+G446S	0.070	0.062	n.a.	n.a.
			Ms 762-001	L143F+G446S	0.108	0.112	n.a.	n.a.
			Ms 762-002	L143F+G446S	0.117	0.129	n.a.	n.a.
			Ms 762-003	L143F+G446S	0.101	0.104	n.a.	n.a.
			Ms 762-004	L143F+G446S	0.100	0.102	n.a.	n.a.
			Ms 762-005	L143F+G446S	0.115	0.117	n.a.	n.a.
			Ms 763-001	L143F+G446S	0.088	0.059	1.568	0.310
			Ms 763-002	L143F+G446S	0.069	0.096	n.a.	n.a.
			Ms 763-003	L143F+G446S	0.078	0.048	n.a.	n.a.
			Ms 763-004	L143F+G446S	0.042	0.045	n.a.	n.a.
			Ms 763-005	L143F+G446S	0.043	0.110	n.a.	n.a.
			Ms 765-001	WT	0.003	0.020	n.a.	n.a.
			Ms 765-002	WT	0.003	0.010	n.a.	n.a.
Ms 765-003	WT	0.004	0.007	n.a.	n.a.			

2020	Netherlands	Dronten	Ms 765-004	WT	0.003	0.005	n.a.	n.a.			
			Ms 765-005	WT	0.005	0.015	n.a.	n.a.			
			Ms 775-001	L143F+G446S	0.040	0.051	n.a.	n.a.			
			Ms 775-002	L143F+G446S	0.292	0.256	n.a.	n.a.			
			Ms 775-003	L143F+G446S	0.098	0.108	n.a.	n.a.			
			Ms 775-004	L143F+G446S	0.140	0.125	4.497	0.480			
			Ms 775-005	L143F+G446S	0.098	0.036	n.a.	n.a.			
			Ms 776-001	L143F+G446S	0.203	0.160	5.238	0.340			
			Ms 776-002	L143F+G446S	0.120	0.137	n.a.	n.a.			
			Ms 776-003	L143F+G446S	0.069	0.101	n.a.	n.a.			
			Ms 776-004	L143F+G446S	0.043	0.047	n.a.	n.a.			
			Ms 776-005	L143F+G446S	0.080	0.054	n.a.	n.a.			
			Ms 782-001	WT	0.011	0.020	n.a.	n.a.			
			Ms 782-002	WT	0.010	0.013	n.a.	n.a.			
			Ms 782-004	WT	0.012	0.030	n.a.	n.a.			
			Ms 782-005	WT	0.009	0.013	n.a.	n.a.			
			Ms 786-001	L143F+G446S	0.125	0.162	n.a.	n.a.			
			Ms 786-002	L143F+G446S	0.112	0.102	n.a.	n.a.			
			Ms 786-003	L143F+G446S	0.182	0.109	n.a.	n.a.			
			Ms 786-004	L143F+G446S	0.120	0.090	n.a.	n.a.			
			Ms 786-005	L143F+G446S	0.109	0.108	n.a.	n.a.			
			Ms 787-001	L143F+G446S	0.122	0.149	n.a.	n.a.			
			Ms 787-002	L143F+G446S	0.196	0.195	n.a.	n.a.			
			Ms 787-003	L143F+G446S	0.119	0.069	n.a.	n.a.			
			Ms 787-004	L143F+G446S	0.185	0.178	n.a.	n.a.			
			Ms 787-005	L143F+G446S	0.169	0.134	n.a.	n.a.			
			Ms 957-001	L143F+G446S	0.096	0.094	n.a.	n.a.			
			Ms 957-002	L143F+G446S	0.224	0.092	n.a.	n.a.			
			Ms 957-003	L143F+G446S	0.157	0.237	n.a.	n.a.			
			Ms 957-004	L143F+G446S	0.123	0.213	n.a.	n.a.			
			Ms 957-005	L143F+G446S	0.174	0.139	n.a.	n.a.			
			Ms 958-001	L143F+G446S	0.105	0.192	n.a.	n.a.			
			Ms 958-002	L143F+G446S	0.191	0.145	n.a.	n.a.			
			Ms 958-003	L143F+G446S	0.166	0.105	n.a.	n.a.			
			Ms 958-004	L143F+G446S	0.147	0.155	n.a.	n.a.			
			Ms 958-005	L143F+G446S	0.226	0.133	n.a.	n.a.			
			Ms 959-001	L143F+G446S	0.218	0.083	n.a.	n.a.			
			Ms 959-002	L143F+G446S	0.229	0.139	n.a.	n.a.			
			Ms 959-003	L143F+G446S	0.141	0.189	n.a.	n.a.			
			Ms 959-004	L143F+G446S	0.152	0.207	n.a.	n.a.			
			Ms 959-005	L143F+G446S	0.306	0.249	n.a.	n.a.			
			Ms 998-001	L143F+G446S	0.142	0.134	n.a.	n.a.			
			Ms 998-002	L143F+G446S	0.143	0.134	n.a.	n.a.			
			Ms 998-003	L143F+G446S	0.205	0.132	n.a.	n.a.			
			Ms 998-004	L143F+G446S	0.102	n.a.	n.a.	n.a.			
			Ms 998-005	L143F+G446S	0.048	n.a.	n.a.	n.a.			
			2021	Netherlands	Emmeloord	Ms 1015	WT	0.020	0.032	2.262	0.831
						Ms 1016	WT	0.021	0.034	3.357	1.132
						Ms 1017	WT	0.015	0.030	2.594	0.343
						Ms 1018	WT	0.026	0.042	3.987	0.310
Ms 1019	WT	0.014				0.021	0.918	0.233			

			Ms 1020	WT	0.013	0.025	2.720	0.538
			Ms 1021	WT	0.011	0.046	1.102	n.a.
			Ms 1022	WT	0.018	0.041	1.875	0.437
			Ms 1023	WT	0.029	0.057	6.446	0.384
			Ms 1024	WT	0.020	0.031	2.366	0.747
			Ms 1025	L143F+G446S	0.206	0.189	2.683	0.431
			Ms 1026	WT	0.025	0.042	3.283	0.991
			Ms 1027	WT	0.015	0.025	1.527	0.616
			Ms 1028	L143F+G446S	0.211	0.172	2.565	0.446
			Ms 1029	WT	0.018	0.041	2.571	0.505
			Ms 1030	L143F+G446S	0.146	0.056	2.730	n.a.
			Ms 1031	L143F+G446S	0.153	0.069	3.000	n.a.
			Ms 1032	WT	0.006	0.015	2.119	n.a.
			Ms 1033	WT	0.003	0.006	1.489	n.a.
			Ms 1034	WT	0.009	0.011	2.930	n.a.
			Ms 1035	WT	0.009	0.011	1.888	n.a.
			Ms 1036	WT	0.012	0.015	3.000	n.a.
			Ms 1037	WT	0.012	0.015	3.000	n.a.
			Ms 1038	WT	0.008	0.010	1.139	n.a.
			Ms 1039	WT	0.010	0.009	2.065	n.a.
			Ms 1040	WT	0.018	0.041	3.359	0.452
			Ms 1041	WT	0.021	0.042	1.910	0.013
			Ms 1042	WT	0.018	0.037	2.364	0.273
			Ms 1043	WT	0.017	0.043	0.973	0.241
	Germany	Limburgerhof	Ms 1075	WT	0.013	0.058	6.523	n.a.
			Ms 1076	L143F+G446S	0.191	0.129	5.041	n.a.
			Ms 1077	L143F+G446S	0.194	0.096	6.482	n.a.
			Ms 1078	WT	0.010	0.033	4.507	n.a.
			Ms 1079	WT	0.006	0.034	1.044	n.a.
			Ms 1080	L143F+G446S	0.250	0.187	3.333	n.a.
			Ms 1081	WT	0.012	0.039	1.856	0.032
			Ms 1082	WT	0.007	0.026	5.287	0.421
			Ms 1083	WT	0.005	0.014	3.657	0.742
			Ms 1084	WT	0.008	0.018	6.259	0.384
			Ms 1085	L143F+G446S	0.251	0.162	3.323	0.517
			Ms 1086	WT	0.005	0.014	2.454	0.007
			Ms 1087	WT	0.010	0.030	6.331	1.090
			Ms 1088	L143F+G446S	0.177	0.171	1.805	0.641
			Ms 1089	WT	0.013	0.032	6.083	0.016
			Ms 1090	WT	0.007	0.020	3.735	0.875
			Ms 1091	WT	0.009	0.024	5.366	0.301
			Ms 1092	WT	0.006	0.014	3.304	0.036
			Ms 1093	WT	0.010	0.017	2.843	0.818
			Ms 1094	WT	0.007	0.023	4.382	0.401
			Ms 1141	WT	0.029	0.053	7.786	0.662
			Ms 1143	WT	0.011	0.026	2.613	0.010
			Ms 1147	WT	0.008	0.043	0.466	0.280
			Ms 1148	WT	0.012	0.027	4.231	0.237
			Ms 1154	WT	0.002	0.006	2.650	0.007
			Ms 1156	WT	0.011	0.033	7.435	0.010
			Ms 1157	WT	0.025	0.054	3.122	0.453
	Netherlands	Valthermond						
2022	Germany	Limburgerhof						

Ms 1158	WT	0.014	0.042	3.093	0.300
Ms 1159	WT	0.015	0.047	1.664	0.295
Ms 1160	WT	0.012	0.027	7.962	1.093
Ms 1161	WT	0.011	0.031	8.508	0.840
Ms 1167	WT	0.010	0.032	8.449	0.249
Ms 1168	WT	0.007	0.021	6.817	0.746
Ms 1170	WT	0.011	0.021	1.277	n.a.
Ms 1171	WT	0.014	0.023	0.730	n.a.
Ms 1172	WT	0.006	0.016	1.603	n.a.
Ms 1173	WT	0.010	0.015	3.326	n.a.
Ms 1174	WT	0.010	0.027	8.805	0.445
Ms 1175	WT	0.009	0.019	1.461	n.a.
Ms 1177	WT	0.014	0.033	1.038	n.a.
Ms 1178	WT	0.009	0.017	0.882	n.a.
Ms 1179	WT	0.015	0.037	0.955	n.a.
Ms 1180	WT	0.011	0.020	0.434	n.a.
Ms 1181	WT	0.029	0.026	1.167	n.a.
Ms 1182	WT	0.010	0.024	6.811	0.012
Ms 1183	WT	0.010	0.027	7.362	n.a.
Ms 1184	WT	0.006	0.011	2.505	n.a.
Ms 1185	WT	0.008	0.017	0.245	n.a.
Ms 1187	WT	0.010	0.025	0.642	n.a.
Ms 1188	WT	0.013	0.032	2.284	n.a.
Ms 1189	WT	0.012	0.017	0.237	n.a.
Ms 1194	WT	0.015	0.039	3.827	0.010
Ms 1195	WT	0.005	0.015	6.146	0.296
Ms 1196	WT	0.012	0.036	7.636	0.441
Ms 1197	WT	0.007	0.016	7.804	0.316
Ms 1199	WT	0.019	0.042	6.087	0.511
Ms 1204	WT	0.015	0.035	3.146	0.016
Ms 1211	WT	0.012	0.036	6.806	0.264
Ms 1214	WT	0.012	0.032	8.483	0.284
Ms 1217	WT	0.011	0.033	9.697	0.313
Ms 1225	WT	0.012	0.030	8.282	0.008
Ms 1227	WT	0.010	0.032	6.212	0.014
Ms 1230	WT	0.014	0.032	7.984	1.063
Ms 1232	WT	0.007	0.015	5.134	0.542
Ms 1234	WT	0.013	0.030	0.845	0.662
Ms 1237	WT	0.019	0.039	0.889	0.180
Ms 1239	WT	0.013	0.033	0.777	0.023
Ms 1242	WT	0.014	0.035	0.916	0.364
Ms 1243	WT	0.013	0.031	0.468	0.480
Ms 1248	WT	0.015	0.041	0.811	0.723
Ms 1254	WT	0.017	0.036	0.999	0.477
Ms 1257	WT	0.013	0.029	0.752	0.420
Ms 1260	WT	0.013	0.031	0.597	0.550
Ms 1269	WT	0.017	0.042	0.586	0.352
Ms 1274	WT	0.011	0.024	0.413	0.381
Ms 1277	WT	0.013	0.039	0.839	0.025
Ms 1280	WT	0.010	0.026	1.035	0.193
Ms 1285	L143F+G446S	0.245	0.181	0.815	0.557

		Ms 1287	WT	0.018	0.044	1.027	0.623	
		Ms 1289	WT	0.023	0.050	1.341	0.930	
		Ms 1294	WT	0.022	0.043	1.384	0.289	
		Ms 1295	WT	0.014	0.034	4.962	1.017	
		Ms 1297	WT	0.014	0.029	0.706	0.352	
		Ms 1301	G462S	0.038	0.043	9.235	0.308	
		Ms 1302	WT	0.013	0.025	0.474	0.439	
		Ms 1305	WT	0.011	0.024	0.553	0.017	
		Ms 1306	WT	0.023	0.070	1.387	0.585	
		Ms 1310	WT	0.013	0.039	4.377	0.308	
		Ms 1313	WT	0.014	0.042	3.612	0.274	
		Ms 1317	WT	0.016	0.043	4.339	0.601	
		Ms 1319	WT	0.014	0.041	5.486	0.534	
		Ms 1324	WT	0.008	0.034	3.668	0.016	
		Ms 1358	WT	0.039	0.047	10.000	0.205	
		Ms 1359	WT	0.018	0.049	9.855	0.813	
		Ms 1360	WT	0.016	0.038	8.253	0.478	
		Ms 1361	WT	0.012	0.021	5.973	0.826	
		Ms 1362	G462S	0.081	0.073	10.000	0.181	
		Ms 1363	WT	0.016	0.044	8.655	0.015	
		Ms 1364	WT	0.009	0.026	4.331	0.012	
		Ms 1365	WT	0.015	0.037	7.535	0.708	
		Ms 1366	WT	0.019	0.049	7.422	0.529	
		Ms 1367	WT	0.013	0.038	2.600	0.335	
		Ms 1369	WT	0.014	0.043	3.328	0.360	
		Ms 1370	WT	0.015	0.045	10.000	0.451	
		Ms 1371	WT	0.012	0.046	5.836	0.456	
		Ms 1372	WT	0.013	0.037	2.953	0.344	
		Ms 1376	WT	0.015	0.047	6.606	0.434	
		Ms 1377	WT	0.016	0.045	5.886	0.416	
		Ms 1379	WT	0.016	0.045	4.408	0.382	
		Ms 1380	WT	0.015	0.036	6.820	0.351	
		Ms 1381	WT	0.014	0.036	6.706	0.316	
		Ms 1383	WT	0.016	0.040	4.995	0.717	
		Ms 1384	WT	0.015	0.039	5.144	0.423	
		Ms 1386	WT	0.012	0.025	1.738	0.363	
		Ms 1389	WT	0.021	0.042	2.689	0.431	
		Ms 1390	WT	0.013	0.035	4.113	0.827	
		Ms 1392	WT	0.014	0.037	2.128	0.326	
		Ms 1393	WT	0.020	0.050	4.282	0.436	
		Ms 1394	WT	0.022	0.053	3.867	0.448	
2022	Netherlands	Emmeloord	1425	WT	0.027	0.078	3.588	0.648
			1426	WT	0.012	0.041	3.782	0.513
			1427	L143F+G446S	0.157	0.102	0.496	0.300
			1428	WT	0.007	0.044	0.713	0.372
			1429	WT	0.016	0.048	1.835	0.375
		Dronten	1430	WT	0.023	0.053	3.433	0.431
			1431	L143F+G446S	0.294	0.192	1.357	0.473
			1432	WT	0.017	0.034	1.872	0.328
			1433	L143F+G446S	0.172	0.128	0.530	0.364
			1434	L143F+G446S	0.119	0.126	0.467	0.412

			1436	L143F+G446S	0.138	0.103	0.442	0.248	
		Valthermond	1437	WT	0.020	0.065	3.344	0.456	
			1438	WT	0.013	0.038	1.131	0.384	
			1439	WT	0.025	0.059	2.132	0.519	
			1440	WT	0.019	0.046	1.528	0.364	
			1441	WT	0.018	0.053	1.238	0.377	
			1442	WT	0.023	0.057	1.953	0.446	
		Dordrecht	1443	WT	0.015	0.055	0.629	0.344	
			1444	WT	0.013	0.031	1.270	0.730	
			1445	WT	0.013	0.040	1.469	0.349	
			1446	WT	0.009	0.036	0.621	0.284	
			1447	WT	0.010	0.029	0.397	0.207	
			1448	WT	0.007	0.024	0.382	0.007	
	Sweden	Lockarp	1455	WT	0.010	0.028	1.636	0.447	
				1456	WT	0.010	0.041	2.255	0.384
				1457	WT	0.021	0.052	4.927	0.020
				1458	WT	0.008	0.025	1.370	0.013
				1459	WT	0.014	0.035	2.022	0.013
				1460	WT	0.014	0.039	2.009	0.419
	Netherlands	Emmeloord	1461	L143F+G446S	0.148	0.121	1.077	0.361	
				1462	WT	0.024	0.059	5.109	0.785
				1463	L143F+G446S	0.137	0.134	1.352	0.405
				1464	WT	0.012	0.032	1.465	0.495
				1465	L143F+G446S	0.208	0.174	1.760	0.521
				1466	L143F+G446S	0.213	0.175	1.579	0.581
			Valthermond	1467	WT	0.012	0.035	3.171	1.240
				1468	WT	0.016	0.042	1.862	0.914
				1469	WT	0.012	0.033	2.569	1.153
				1470	L143F+G446S	0.178	0.142	1.451	0.542
				1471	L143F+G446S	0.193	0.139	1.688	0.415
				1472	L143F+G446S	0.157	0.141	1.108	0.346
			Dronten	1473	L143F+G446S	0.197	0.147	2.071	0.416
				1474	L143F+G446S	0.139	0.148	1.841	0.478
				1475	L143F+G446S	0.2	0.138	1.737	0.361
				1476	L143F+G446S	0.178	0.147	1.783	0.342
				1477	L143F+G446S	0.367	0.233	4.417	0.434
				1478	L143F+G446S	0.26	0.248	3.612	0.670
	Germany	Böhl-Iggelheim	1484	WT	0.008	0.016	2.519	0.006	
				1485	WT	0.010	0.026	2.300	0.460
				1486	WT	0.007	0.021	2.535	0.007
				1487	WT	0.013	0.043	3.196	1.000
				1488	WT	0.010	0.032	1.542	0.233
				1489	L143F+G446S	0.183	0.155	0.994	0.397
				1490	G462S	0.042	0.048	10.000	0.276
				1491	WT	0.009	0.028	2.621	0.010
				1492	L143F+G446S	0.170	0.147	2.527	0.349
				1493	WT	0.010	0.024	2.347	0.013
				1494	WT	0.003	0.007	1.718	0.006
				1495	WT	0.012	0.034	3.363	0.515
				1496	WT	0.010	0.022	2.863	0.009

1497	WT	0.015	0.041	4.245	0.559
1498	WT	0.015	0.031	4.780	0.013
1499	WT	0.007	0.019	2.153	0.255
1500	WT	0.013	0.036	4.468	0.242
1501	WT	0.011	0.043	1.621	0.127
1502	WT	0.010	0.025	2.008	0.006
1503	WT	0.007	0.025	2.101	0.007
1504	WT	0.014	0.034	3.447	0.270
1505	L143F+G446S	0.162	0.157	2.161	0.306
1506	L143F+G446S	0.200	0.144	2.536	0.510
1507	L143F+G446S	0.287	0.166	4.316	0.563
1508	WT	0.009	0.022	2.210	0.019
1509	WT	0.014	0.038	5.753	0.352
1510	WT	0.012	0.027	4.115	1.660
1511	WT	0.012	0.029	3.725	0.403
1512	WT	0.010	0.027	4.311	0.479
1513	WT	0.014	0.044	3.856	0.020
1514	L143F+G446S	0.136	0.115	2.605	0.424
1515	L143F+G446S	0.212	0.175	4.084	0.563
1516	L143F+G446S	0.190	0.125	2.660	0.396
1517	L143F+G446S	0.248	0.140	3.112	0.550
1518	L143F+G446S	0.132	0.097	2.341	0.400
1519	WT	0.015	0.039	6.060	0.615
1520	WT	0.015	0.052	4.179	0.391
1521	WT	0.012	0.027	4.781	0.368
1522	WT	0.018	0.040	0.736	0.337
1523	WT	0.008	0.028	2.655	0.321
1524	WT	0.012	0.034	4.526	0.021
1525	WT	0.030	0.059	8.774	0.035
1526	WT	0.008	0.029	1.590	0.017
1527	WT	0.012	0.027	2.042	0.450
1528	G462S	0.030	0.033	9.873	0.366
1529	WT	0.015	0.028	6.265	0.012
1530	WT	0.014	0.033	5.981	0.016
1531	WT	0.012	0.035	10.000	0.445
1532	WT	0.004	0.021	3.939	0.616
1533	WT	0.010	0.019	2.074	0.011
1534	WT	0.009	0.026	4.484	0.368
1535	G462S	0.046	0.039	10.000	0.284
1536	WT	0.009	0.028	6.537	0.008
1537	WT	0.012	0.035	4.593	0.008
1538	WT	0.013	0.030	5.974	0.014
1539	WT	0.011	0.025	5.101	1.074
1540	WT	0.015	0.041	6.138	0.247
1541	L143F+G446S	0.146	0.170	5.560	0.318
1542	L143F+G446S	0.139	0.105	3.213	0.273
1543	L143F+G446S	0.157	0.098	4.494	0.307
1544	L143F+G446S	0.183	0.137	4.418	0.306
1545	L143F+G446S	0.161	0.101	5.103	0.267
1546	WT	0.010	0.032	5.623	0.420
1547	WT	0.013	0.030	5.941	0.512

1548	WT	0.014	0.037	5.620	0.488
1549	L143F+G446S	0.123	0.121	4.422	0.284
1550	L143F+G446S	0.184	0.140	0.685	0.406
1551	L143F+G446S	0.217	0.138	0.636	0.431
1552	L143F+G446S	0.180	0.144	0.646	0.368
1553	WT	0.013	0.031	1.156	0.489
1554	L143F+G446S	0.181	0.148	0.619	0.345
1555	WT	0.016	0.040	1.857	0.554
1556	WT	0.010	0.024	1.130	0.322
1557	WT	0.011	0.033	0.763	0.009
1558	WT	0.013	0.028	0.976	0.444
1559	WT	0.014	0.025	0.980	0.734
1560	WT	0.012	0.023	0.952	0.706
1561	WT	0.013	0.029	1.432	0.368
1562	WT	0.009	0.031	0.695	0.305
1563	WT	0.016	0.043	2.349	0.440
1564	WT	0.015	0.035	1.604	0.501
1565	WT	0.012	0.029	1.146	0.446
1566	WT	0.013	0.034	1.113	0.009
1567	WT	0.010	0.036	10.000	0.006
1568	WT	0.014	0.037	1.883	0.013
1569	WT	0.010	0.018	0.469	0.286
1570	WT	0.014	0.041	1.704	0.398
1571	L143F+G446S	0.134	0.112	0.535	0.256
1572	WT	0.016	0.024	1.886	0.474
1573	L143F+G446S	0.323	0.156	3.595	0.510
1574	WT	0.012	0.023	2.020	0.011
1575	WT	0.009	0.023	0.863	0.014
1576	WT	0.021	0.035	3.466	0.023
1577	WT	0.011	0.031	1.027	0.021
1578	WT	0.011	0.021	0.710	0.007
1579	WT	0.011	0.021	0.903	0.007
1580	L143F+G446S	0.232	0.119	1.969	0.434
1581	WT	0.013	0.027	1.643	0.553
1582	L143F+G446S	0.128	0.076	1.150	0.357
1583	WT	0.012	0.031	0.890	0.265
1584	WT	0.009	0.025	2.479	0.214
1585	WT	0.012	0.027	1.862	0.432
1586	L143F+G446S	0.159	0.130	1.780	0.444
1587	WT	0.013	0.035	2.425	0.019
1588	WT	0.005	0.018	1.811	0.298
1589	WT	0.013	0.049	1.570	0.156
1590	WT	0.011	0.020	1.615	0.297
1591	WT	0.009	0.029	10.000	0.245
1592	WT	0.013	0.021	2.519	0.190
1593	L143F+G446S	0.197	0.145	2.886	0.393
1594	WT	0.009	0.025	2.064	0.254
1595	WT	0.004	0.015	0.460	0.347
1596	WT	0.018	0.032	6.641	0.009
1597	WT	0.019	0.039	3.113	0.192
1598	WT	0.010	0.031	4.643	0.223

Ruchheim

1599	WT	0.011	0.031	5.895	0.238
1600	WT	0.013	0.039	7.333	0.011
1601	WT	0.010	0.026	6.075	0.011
1602	WT	0.010	0.036	5.341	0.012
1603	WT	0.013	0.034	3.328	0.239
1604	WT	0.012	0.041	3.224	0.192
1605	WT	0.013	0.034	5.650	0.011
1606	WT	0.012	0.034	6.736	0.010
1607	WT	0.014	0.039	4.802	0.289
1608	WT	0.011	0.034	5.384	0.298
1609	L143F+G446S	0.188	0.128	2.791	0.259
1610	WT	0.010	0.029	5.864	0.013
1611	WT	0.013	0.034	4.743	0.319
1612	WT	0.014	0.033	4.773	0.008
1613	WT	0.006	0.015	0.772	0.080
1614	WT	0.020	0.033	3.458	0.376
1615	WT	0.015	0.029	4.226	0.280
1616	WT	0.017	0.037	6.181	0.328
1617	G462S	0.051	0.046	9.955	0.264
1618	WT	0.008	0.019	4.590	0.009
1619	WT	0.015	0.031	6.319	0.008
1620	WT	0.013	0.040	3.170	0.018
1621	WT	0.016	0.041	2.657	0.017
1622	WT	0.014	0.043	5.197	0.016
1623	WT	0.008	0.032	3.117	0.010
1624	L143F+G446S	0.266	0.183	3.172	0.400
1625	L143F+G446S	0.153	0.151	1.411	0.318
1626	WT	0.015	0.046	3.666	0.016
1627	L143F+G446S	0.273	0.222	3.696	0.430
1628	WT	0.025	0.056	6.633	0.018
1629	WT	0.015	0.052	3.482	0.183
1630	WT	0.017	0.043	4.299	0.441
1631	WT	0.014	0.051	3.867	0.679
1632	WT	0.018	0.048	4.189	0.565
1633	WT	0.012	0.044	2.217	0.346
1634	WT	0.017	0.049	4.653	0.695
1635	WT	0.025	0.073	5.525	0.026
1636	L143F+G446S	0.120	0.179	1.680	0.403
1637	WT	0.013	0.051	3.825	0.384
1638	WT	0.013	0.038	3.350	0.013
1639	WT	0.014	0.042	3.960	0.016
1640	WT	0.013	0.032	2.077	0.020
1641	WT	0.015	0.044	5.185	0.020
1643	L143F+G446S	0.293	0.174	3.074	0.346
1645	L143F+G446S	0.123	0.083	0.656	0.269
1646	WT	0.010	0.024	0.794	0.240
1647	WT	0.013	0.034	1.033	0.017
1648	WT	0.012	0.031	1.702	0.350
1649	WT	0.012	0.033	1.223	0.575
1650	WT	0.016	0.028	10.000	0.135
1651	WT	0.010	0.017	0.729	0.379

1652	L143F+G446S	0.145	0.112	1.229	0.313
1653	L143F+G446S	0.164	0.141	0.867	0.323
1654	L143F+G446S	0.173	0.135	0.974	0.269
1655	WT	0.009	0.027	0.852	0.013
1656	WT	0.007	0.027	0.496	0.166
1657	WT	0.012	0.030	0.910	0.187
1658	WT	0.012	0.030	1.910	0.014
1659	WT	0.011	0.030	1.285	0.013
1660	WT	0.012	0.026	1.365	0.217
1661	WT	0.013	0.032	1.429	0.018
1662	WT	0.011	0.038	1.740	0.014
1664	L143F+G446S	0.147	0.164	1.032	0.285
1665	WT	0.015	0.040	1.956	0.025
1666	WT	0.010	0.028	1.857	0.015
1667	WT	0.008	0.036	1.419	0.213
1668	WT	0.013	0.041	3.608	0.304
1669	WT	0.020	0.039	4.279	0.364
1670	WT	0.013	0.023	2.606	0.265
1671	WT	0.015	0.032	3.933	0.014
1672	WT	0.018	0.042	5.642	0.265
1673	WT	0.015	0.035	4.565	0.135
1674	WT	0.024	0.028	3.911	0.012
1675	WT	0.019	0.036	3.254	0.433
1676	WT	0.025	0.044	3.675	0.461
1677	WT	0.014	0.038	3.089	0.013
1678	WT	0.011	0.033	4.062	0.019
1679	WT	0.015	0.035	3.395	0.013
1680	WT	0.013	0.026	2.841	0.015
1681	WT	0.029	0.044	4.663	0.730
1682	WT	0.013	0.035	2.762	0.016
1683	WT	0.017	0.038	3.393	0.664
1684	WT	0.030	0.061	5.604	0.745
1685	WT	0.017	0.042	3.317	0.018
1686	L143F+G446S	0.076	0.158	1.134	0.316
1687	WT	0.012	0.028	3.984	0.315
1688	WT	0.018	0.038	3.321	1.510
1689	WT	0.015	0.031	3.070	1.259
1690	WT	0.013	0.032	3.506	0.009
1691	L143F+G446S	0.126	0.124	1.655	0.242
1692	L143F+G446S	0.307	0.222	3.146	0.630
1693	WT	0.012	0.039	3.286	0.012
1694	L143F+G446S	0.186	0.148	1.790	0.425
1695	L143F+G446S	0.178	0.143	2.212	0.356
1696	WT	0.015	0.038	2.531	0.026
1697	WT	0.013	0.037	2.711	0.020
1698	WT	0.011	0.038	2.399	0.025
1699	WT	0.011	0.035	2.978	0.019
1700	WT	0.010	0.034	1.293	0.195

Table 23: Targeted mutation strains of *A. solani* and strains with ectopic integration used in this work.

Strain	<i>CYP51</i> haplotype
Li-0016	Parental WT strain
AsL143F-001	L143F
AsL143F-002	L143F
AsL143F-003	L143F
AsL143F-004	L143F
AsL143F-005	L143F
AsL143F-006	L143F
AsG446S-001	G446S
AsL143F+G446S-001	L143F+G446S
AsL143F+G446S-002	L143F+G446S
AsL143F+G446S-003	L143F+G446S
AsL143F+G446S-004	L143F+G446S
As001E	Ectopic integration
As002E	Ectopic integration

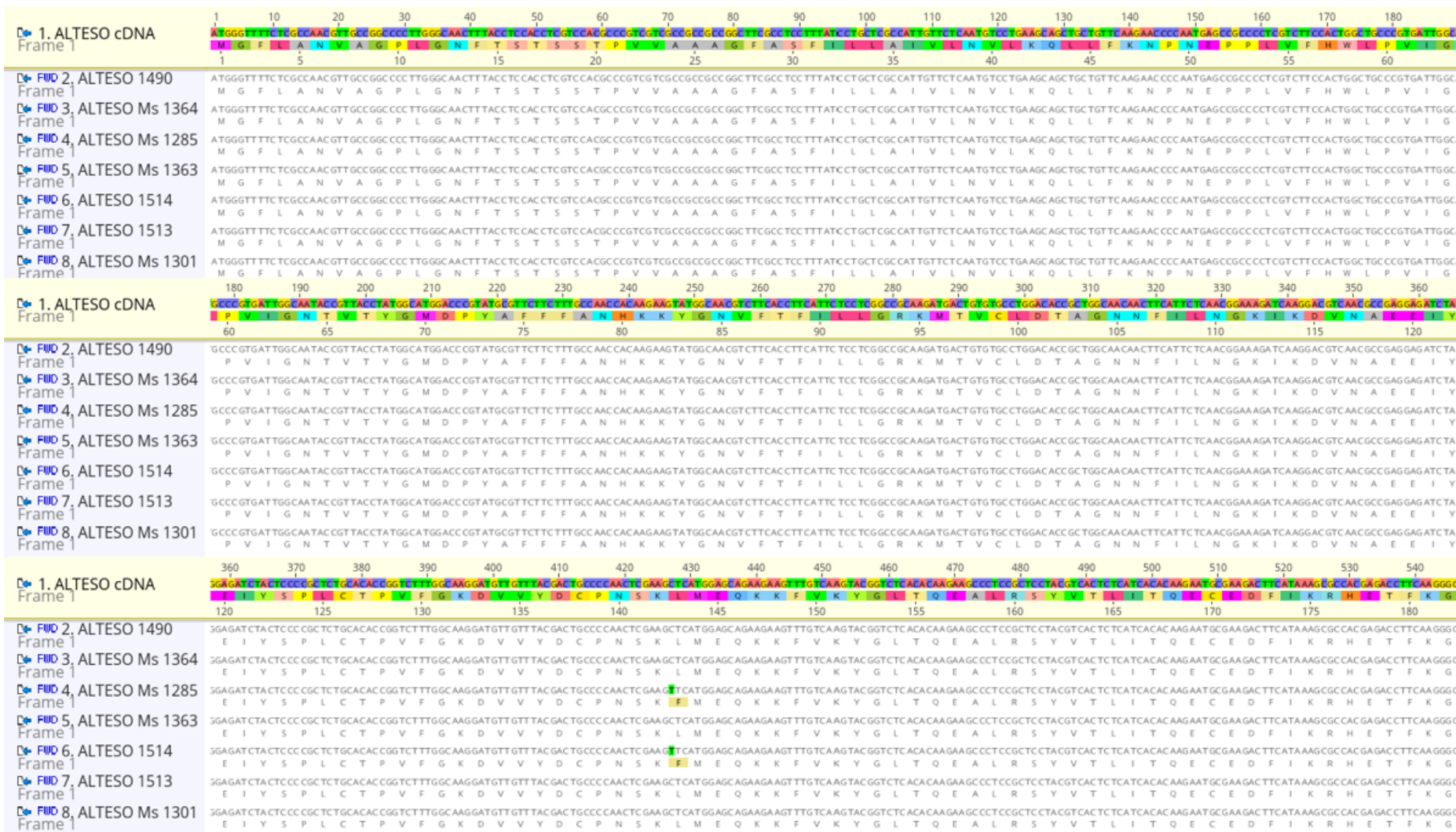


Figure 32: Amino acid sequence of all *CYP51* haplotypes identified in *A. solani* isolates of this work. Further information is given on page 129.



Figure 33: Amino acid sequence of all *CYP51* haplotypes identified in *A. solani* isolates of this work. Further information is given on page 129.



Figure 34: Amino acid sequence of all *CYP51* haplotypes identified in *A. solani* isolates of this work.

Alignment was performed with one *A. solani* single spore isolate and one *A. solani* isolate for each identified *CYP51* haplotype. Amino acids of the reference sequence of *A. solani* WT isolate and all disagreements to this sequence are highlighted in colour.

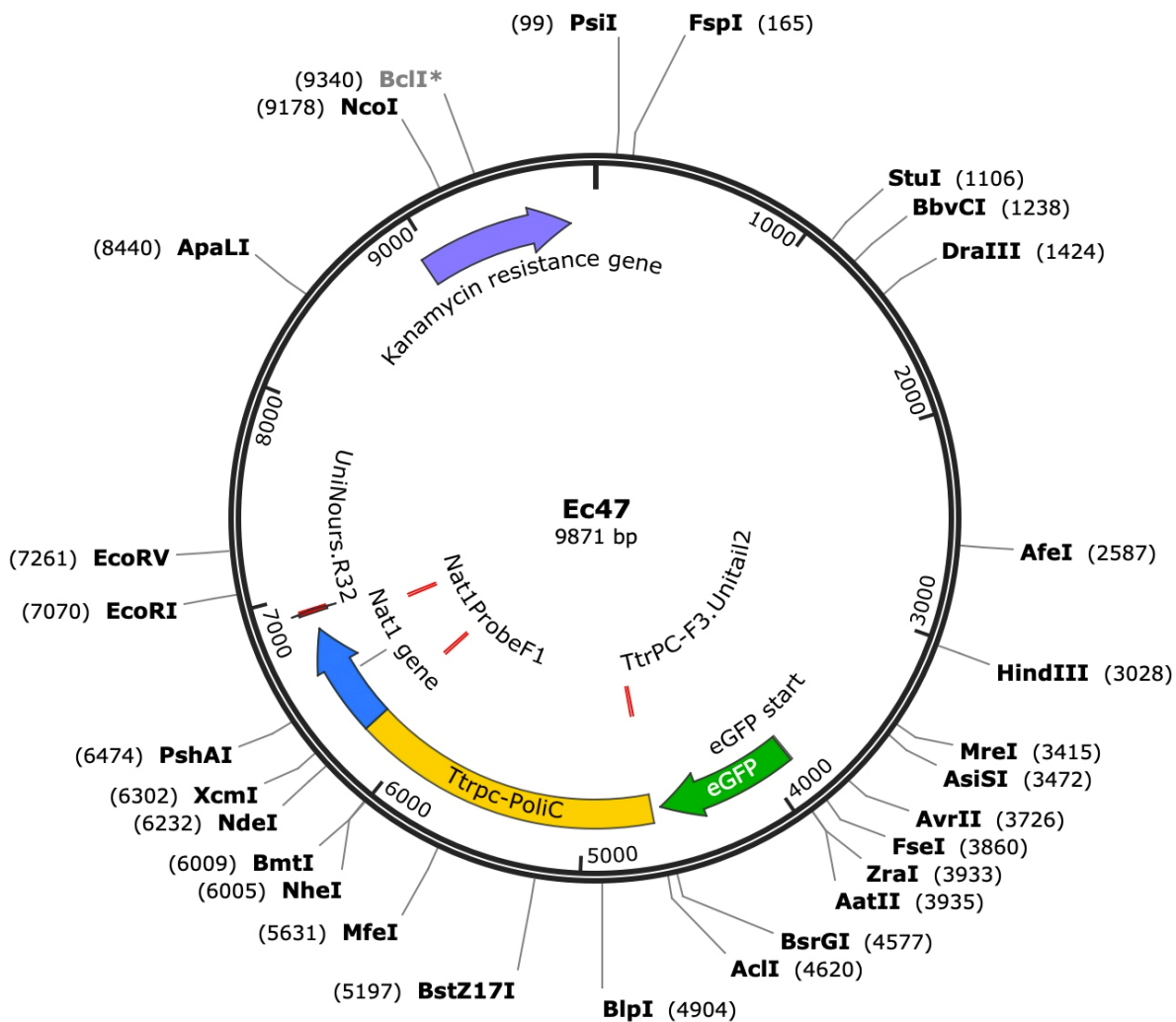


Figure 35: Plasmid with primer binding site.

Plasmid for amplification of the resistance cassette with *Aspergillus nidulans* *trpC* terminator (T_{trpC}), the *oliC* promoter (P_{oliC}) and the *Nourseothricin Phosphotransferase* (*nat1*) gene from *Streptomyces noursei* is illustrated with primer binding sites for primer pair Ttrpc-F3.Unitail and UniNours.R3.

7.2 List of figures

Figure 1: Disease cycle of <i>Alternaria solani</i> causing early blight on tomato (Agris, 2005).	4
Figure 2: Disease symptoms of <i>A. solani</i>	5
Figure 3: Experimental set up of a microtiter plate assay.	37
Figure 4: Map with completely randomized plots.....	39
Figure 5: Point mutations detected in <i>CYP51</i> gene of <i>A. solani</i>	48
Figure 6: Collection sites of <i>A. solani</i> isolates.....	48
Figure 7: Homology model of <i>A. solanis</i> sterol 14- α demethylase enzyme (Cyp51) representing the location of the WT amino acid identified as positions of new alterations.	49
Figure 8: Homology model of <i>A. solanis</i> Cyp51 representing the location L143, G446 and G462.	50
Figure 9: Cutout of the alignment of nucleotide and amino acid sequences from <i>A. solani</i> and other phytopathogenic fungi.....	52
Figure 10: <i>In vivo</i> competition studies of <i>CYP51</i> haplotype L143F+G446S and WT of <i>A. solani</i> under non-selective conditions.....	54
Figure 11: <i>A. solani</i> spore morphology and quantification of different <i>CYP51</i> haplotypes.....	55

Figure 12: <i>A. solani</i> infection of WT and haplotype L143F+G446S on treated and non-treated tomato leaves.	56
Figure 13: Inhibition of vegetative growth of <i>CYP51</i> haplotypes by mefentrifluconazole and difenoconazole.	57
Figure 14: DMI sensitivity in different <i>A. solani</i> <i>CYP51</i> haplotypes.	59
Figure 15: Correlation of EC ₅₀ values of <i>A. solani</i> haplotypes (WT, G462S, L143F+G446S) for mefentrifluconazole and difenoconazole.	60
Figure 16: Correlation of EC ₅₀ values of <i>A. solani</i> haplotypes (WT, G462S, L143F+G446S) for mefentrifluconazole and prothioconazole.	60
Figure 17: Correlation of EC ₅₀ values of <i>A. solani</i> haplotypes (WT, G462S, L143F+G446S) for difenoconazole and prothioconazole.	61
Figure 18: Distribution of EC ₅₀ values of <i>A. solani</i> haplotypes (WT, G462S, L143F+G446S) for azoxystrobin and mefentrifluconazole.	62
Figure 19: Distribution of EC ₅₀ values of <i>A. solani</i> haplotypes (WT, G462S, L143F+G446S) for azoxystrobin and difenoconazole.	62
Figure 20: Distribution of EC ₅₀ values of <i>A. solani</i> haplotypes (WT, G462S, L143F+G446S) for azoxystrobin and prothioconazole.	63
Figure 21: Fungicide efficacy of different compounds for <i>A. solani</i> population in 2023 on potato variety “Kuras”.	65
Figure 22: Fungicide efficacy of different compounds for <i>A. solani</i> population in 2023 on potato variety “Gala”.	66
Figure 23: <i>CYP51</i> haplotypes of <i>A. solani</i> and their relative frequency in field trials after application of fungicides.	68
Figure 24: Verification of transformed replacement construct.	70
Figure 25: Verification of replacement cassettes containing respective substitutions.	71
Figure 26: Cutout of the alignment of mutations introduced into <i>A. solani</i> WT.	72
Figure 27: DMI sensitivity of targeted mutation strains of <i>A. solani</i> carrying different mutations in <i>CYP51</i> gene.	73
Figure 28: Distribution of EC ₅₀ values in <i>CYP51</i> haplotype L143F+G446S and WT in <i>A. solani</i>	73
Figure 29: Vegetative growth of targeted mutation strains.	74
Figure 30: Efficacy of mefentrifluconazole (Revysol®), difenoconazole (Score®) and metiram (Polyram®) on targeted mutation strains of <i>A. solani</i> in greenhouse experiments.	76
Figure 31: Infection of targeted mutation strains of <i>A. solani</i> in the greenhouse.	76
Figure 32: Amino acid sequence of all <i>CYP51</i> haplotypes identified in <i>A. solani</i> isolates of this work. Further information is given on page 129.	127
Figure 33: Amino acid sequence of all <i>CYP51</i> haplotypes identified in <i>A. solani</i> isolates of this work. Further information is given on page 129.	128
Figure 34: Amino acid sequence of all <i>CYP51</i> haplotypes identified in <i>A. solani</i> isolates of this work.	129
Figure 35: Plasmid with primer binding site.	130

7.3 List of tables

Table 1: Taxonomy of <i>Alternaria solani</i> (EPPO 2024).	3
Table 2: Software used in this work.	20
Table 3: Components of PCR reactions.	24
Table 4: Schematic procedure of a standard PCR reaction program.	24
Table 5: Components of first reaction.	25
Table 6: Components of second and third reaction.	25
Table 7: Schematic procedure of a DJ-Nested-PCR reaction program.	26
Table 8: Components of Ligation.	27
Table 9: Components for pyrosequencing.	30
Table 10: Components of PCR reaction for probes.	33
Table 11: Schematic procedure of a PCR reaction program for amplification of probes.	33

Table 12: Preparation of fungicide dilutions.	36
Table 13: Fungicide treatments, product rate and active ingredient rate.....	39
Table 14: Single spore isolates used in competition studies of different <i>CYP51</i> haplotypes.	41
Table 15: Confirmation of the genetic identity of multicellular spores of <i>A. solani</i> through determination of quantitative mutation proportion (%).	46
Table 16: <i>CYP51</i> alterations found in <i>A. solani</i>	47
Table 17: Phytopathogenic fungi and point mutations in target gene <i>CYP51</i> responsible for sensitivity losses towards DMIs.	51
Table 18: EC ₅₀ values of <i>CYP51</i> haplotypes tested with difenoconazole and mefentrifluconazole in sensitivity agar plate tests.	57
Table 19: Sensitivity of <i>CYP51</i> haplotypes to azoxystrobin.	63
Table 20: Sensitivity of <i>CYP51</i> haplotypes to fluopyram.	64
Table 21: RFs of targeted mutation strains of <i>A. solani</i> for mefentrifluconazole and difenoconazole.	74
Table 22: <i>A. solani</i> isolates used in this work, their origin, year and EC ₅₀ values for different fungicides.....	116
Table 23: Targeted mutation strains of <i>A. solani</i> and strains with ectopic integration used in this work.	126
Table 24: Technical equipment used.	132
Table 25: Fungicides used in this work.	134
Table 26: Chemicals and consumables used in this work.	136
Table 27: Buffers, solutions and growth media used in this work.	137
Table 28: Oligonucleotides used.	140

7.4 Technical Equipment

In Table 24, technical equipment used during the present study is listed. Devices, such as centrifuges, incubators, thermomixer and pipettes, typically used in laboratories are not included.

Table 24: Technical equipment used.

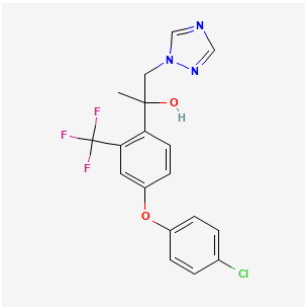
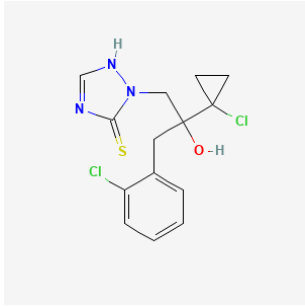
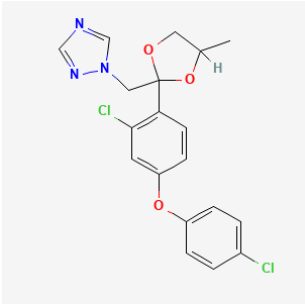
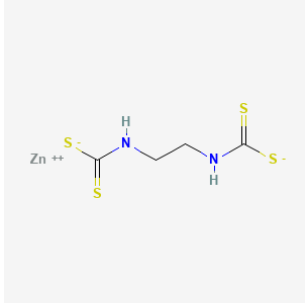
Equipment	Company
Analytical balance, MC 410S	Sartorius AG, Göttingen, DE
Blue light transillumination, UVT-28 BE Herolab GmbH Laborgeräte, Wiesloch, DE	Herolab GmbH Laborgeräte, Wiesloch, DE
Camera, Canon EOS 600D	Canon Deutschland GmbH, Krefeld, DE
ChemiDoc™ MP Imaging System	Bio-Rad Laboratories Inc., Hercules, US
Digital platform shaker, New Brunswick™ Innova® 2000	Eppendorf AG, Hamburg, DE
Electrophoresis Power Supply, PowerEase 500 W, Invitrogen	Thermo Fisher Scientific Inc., Waltham, US
Gel electrophoresis system	Martin-Luther-Universität, Halle, DE
Gel electrophoresis, Mini-Sub-Cell GT Basic System	Bio-Rad Laboratories Inc., Hercules, US
Gel electrophoresis, Sub-Cell GT Basic System	Bio-Rad Laboratories Inc., Hercules, US
Gel System, Peqlab, Perfect Blue Midi S	VWR International GmbH, Darmstadt, DE
IKA® ROCKER 3D digital shaker	IKA®-Werke GmbH & CO. KG, Staufen, DE
Impulse sealer	Allpax GmbH & CO. KG., Papenburg, DE

Inoculation station	BASF SE, Ludwigshafen, DE
Laminar airflow bench, Hersafe KS	Thermo Fisher Scientific Inc., Waltham, US
Laminar airflow bench, Holten LaminAir	Heto-Holten A/S, Allerød, DK
Laminar airflow bench, Holten PCR Mini	Heto-Holten A/S, Allerød, DK
Cold light source KL1500 LCD	Leica Mikrosysteme Vertrieb GmbH, Wetzlar, DE
Magnetic stirrer, IKA-RO 15	IKA®-Werke GmbH & Co. KG, Staufen, DE
Microscope, Leica DMLB	Leica Mikrosysteme Vertrieb GmbH, Wetzlar, DE
Microscope, Rebel	Echo Inc., San Diego, US
Microwave, R-941 INW	Sharp Electronics GmbH, Hamburg, DE
Nebulizer NS 19/26	witeg Labortechnik GmbH, Wertheim DE
Power Source 300V Power Supply	VWR International GmbH, Darmstadt, DE
PowerPac™ Basic Power Supply	Bio-Rad Laboratories Inc., Hercules, US
Small shaker, Vortex 4 Basic	IKA®-Werke GmbH & Co. KG, Staufen, DE
Stereomicroscope	Leica Mikrosysteme Vertrieb GmbH, Wetzlar, DE
Sunrise™ absorbance reader	TECAN Group AG, Männerdorf, CH
Thermal cycler, Mastercycler X50a	Eppendorf AG, Hamburg, DE
Thermal cycler, peqSTAR 96X Universal Gradient	VWR International GmbH, Darmstadt, DE
Tissue lyser, Mixer Mill MM200	Retsch GmbH, Haan, DE
TProfessional Basic Thermocycler	Analytik Jena GmbH & CO. KG., Jena, DE
Ultrapure water remote dispenser, Q-POD® Milli-Q	Merck KGaA, Darmstadt, DE
UVP Crosslinker CL-3000	Analytik Jena GmbH & CO. KG., Jena, DE
UVsolo TS Imaging System	Analytik Jena GmbH & CO. KG., Jena, DE
Vacuubrand™ Chemistry pumping unit, PC3001 VARIO Pro	Thermo Fisher Scientific Inc., Waltham, US
Vacuum-Concentrator BA-VC-300H	BACHOFER GmbH, Reutlingen, DE
Water bath, Typ WB10	P-D Industriegesellschaft GmbH, Dresden, DE

7.5 Fungicides

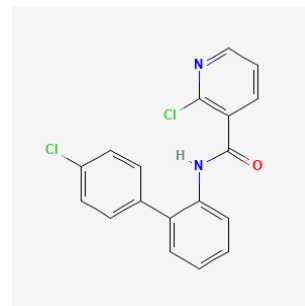
The sensitivity of *A. solani* was tested with different DMIs available on the market (Table 25).

Table 25: Fungicides used in this work.

Technical a. i. (trade name)	Company (market launch in Europe/further information)	Structural formula ¹
Mefentrifluconazole (Revysol®)	BASF SE (2019)	 <p>The chemical structure of Mefentrifluconazole consists of a central carbon atom bonded to a trifluoromethyl group, a hydroxyl group, a 1,2,4-triazole ring, and a 4-chlorophenoxy group.</p>
Prothioconazole (Proline®)	Bayer Crop Science (2004)	 <p>The chemical structure of Prothioconazole features a thiazole ring system connected to a chlorine-substituted benzene ring, which is further linked to a cyclopropylmethyl group and a hydroxyl group.</p>
Difenoconazole (Score®)	Syngenta Agro (2011)	 <p>The chemical structure of Difenoconazole includes a 1,2,4-triazole ring, a chlorine-substituted benzene ring, and a 4-chlorophenoxy group, all connected to a central carbon atom that also bears a hydroxyl group.</p>
Metiram (Polyram®)	BASF SE (2006)	 <p>The chemical structure of Metiram shows a zinc ion (Zn⁺⁺) coordinated to two sulfur atoms, which are part of a chain containing two nitrogen atoms and two sulfur atoms.</p>

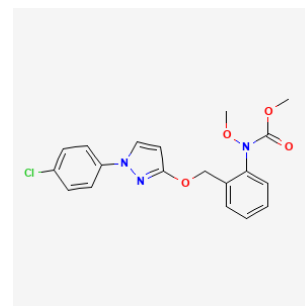
Boscalid
(Cantus®)

BASF SE (2003)



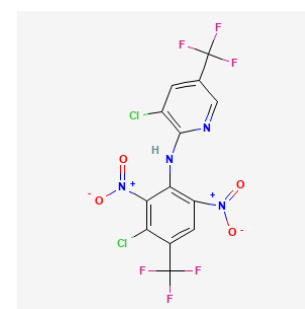
Pyraclostrobin
(Signum®)

BASF SE (2004)



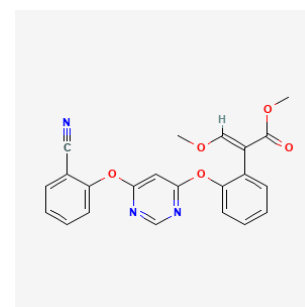
Fluazinam
(Shirlan®)

Syngenta Agro (2009)



Azoxystrobin
(Ortiva®)

Syngenta Agro (1998)



¹PubChem, 2023

7.6 Chemicals and consumable

Chemicals and consumables used in this study are shown in Table 26.

Table 26: Chemicals and consumables used in this work.

Chemicals/Consumables	Company
0.2 mL Thermo Strips	Thermo Fisher Scientific Inc., Waltham, US
96-well microtiter plates	VWR International GmbH, Darmstadt, DE
96-well PCR plates	4titude® Ltd., Wotton, UK
Aceton	Bernd Kraft GmbH, Duisburg, DE
Adhesive PCR Seal	4titude® Ltd., Wotton, UK
Agar-Agar	Carl Roth GmbH & CO. KG., Karlsruhe, DE
Ampicillin	Carl Roth GmbH & CO. KG., Karlsruhe, DE
Biozym LE Agarose	Biozym Biotech Trading GmbH, Wien, AT
Cell culture plate 12 well	Thermo Fisher Scientific Inc., Waltham, US
Deionized water, Milli-Q	Merck KGaA, Darmstadt, DE
Difco™ Agar	Becton, Dickinson and Company GmbH, Franklin Lakes, US
Dimethylsulfoxid (DMSO)	AppliChem GmbH, Darmstadt, DE
Eppendorf Safe-Lock Tubes	Eppendorf AG, Hamburg, DE
Erlenmeyer flask	Thermo Fisher Scientific Inc., Waltham, US
Ethanol	Sigma Aldrich, St. Louis, United States
Falcon tubes	Sarstedt AG & Co. KG, Nümbrecht, DE
Gel Blotting Papers Whatman® 3MM	Carl Roth GmbH & CO. KG., Karlsruhe, DE
Hybridization buffer, PerfectHyp™ Plus	Merck KGaA, Darmstadt, DE
Hydrochloric acid 1M (HCl)	VWR International GmbH, Darmstadt, DE
Kitalase	FUJIFILM Wako Pure Chemical Corporation, Tokyo, JP
Low-Plate, 96-Well	Qiagen GmbH, Hilden, DE
Mastercycler X50a	Eppendorf AG, Hamburg, DE
Microplate shaker, Variomag	Thermo Fisher Scientific Inc., Waltham, US
Nucleoside triphosphate (100 mM)	GeneONE GmbH, Ludwigshafen, DE
PyroMark Binding Buffer	Qiagen GmbH, Hilden, DE
PyroMark Gold Q96 Reagents	Qiagen GmbH, Hilden, DE
PyroMark Q96 Cartridge	Qiagen GmbH, Hilden, DE
Pyrosequencer, PyroMark® Q96	Qiagen GmbH, Hilden, DE
Small shaker Vortex 4 Basic IKA®	Werke GmbH & Co. KG, Staufen, DE
Sodium hydroxide solution (NaOH) 1 M	Bernd Kraft GmbH, Duisburg, DE
Sterile disposable filter units, Nalgene™ Rapid-Flow™	Thermo Fisher Scientific Inc., Waltham, US
Ultrapure water remote dispenser, Q-POD® Milli-Q	Merck KGaA, Darmstadt, DE
UltraPure™ TAE-Buffer, 50x	Thermo Fisher Scientific Inc., Waltham, US

7.7 Buffers, solutions and growth media

Buffers, solutions and growth media used in this work are listed in Table 27.

Table 27: Buffers, solutions and growth media used in this work.

Name	Composition	Notes
10x Blocking Reagent	10 g Blocking reagent 100 mL Malic acid buffer	autoclave at 121°C at 2 bar for 15 min
15% Glycerol	150 g glycerol 1000 mL deionized water	autoclave at 121°C at 2 bar for 15 min
2% malt extract medium	20 g malt extract 1000 mL deionized water	autoclave at 121°C at 2 bar for 15 min
Blocking solution	18 mL maleic acid buffer 2 mL 10% blocking reagent	
Detection buffer	6.057 g TRIS 2.922 g NaCl	adjust pH to 9.5 with HCl
HCl 0.25 M	125 mL HCl (1 M) 375 mL deionized water	
Kitalase suspension	60 mg Kitalase 6 mL 0.7 M NaCl	
Lysogeny broth (LB) medium	10 g peptone 10 g NaCl 5 g yeast extract	autoclave at 121°C at 2 bar for 15 min
Malt agar (2%)	20 g malt extract 20 g agar-agar 1000 mL deionized water	autoclave at 121°C at 2 bar for 15 min adjust pH to 6.8
Malt medium with glycerol	20 g malt extract 150 g glycerol (99%) 1000 mL deionized water	autoclave at 121°C at 2 bar for 15 min
Malt solution (2%)	20 g malt extract 1000 mL deionized water	autoclave at 121°C at 2 bar for 15 min adjust pH to 6.8
NaCl 0.7 M	40.9 g NaCl 1 L distilled water	
NaOH 0.4 M	200 mL sodium hydroxide solution 1 M 300 mL distilled water	
PEG solution	40 g PEG4000 (40%) 1 mL 1 M Tris-HCl pH 8 (10 mM) 4.4731 g KCL (0.6 M) 0.5549 g CaCl ₂ (50 mM) 100 mL distilled water	Sterile filtration (0.45 µm Millex-HA Filter, Millipore, Schwalbach, Germany)
Potato Dextrose Agar (PDA)	39 g potato dextrose agar 1000 mL deionized water	autoclave at 121°C at 2 bar for 15 min

		adjust pH to 5.7
Regeneration medium	137.2 g sucrose (1 M) 0.4 g yeast extract (0.1%) 0.4 g casein hydrolysate (0.1%) distilled water to 400 mL	mix well and divide into two fractions: in 100 mL add 0.6 g (0.6%) agar, in 300 mL add 4.5 g (1.5%) agar autoclave at 121°C at 2 bar for 15 min
Richard's liquid media	20 g Glucose 10 g KNO ₃ 5 g KH ₂ PO ₄ 2.5 g MgSO ₄ x 7 H ₂ O 1 g Yeast extract 1 L distilled water	autoclave at 121°C at 2 bar for 15 min
SOC medium	20 g Tryptone 5 g Yeast Extract 0.5 g NaCl 10 mL KCL 250 mM 18 mL glucose 20% 5 mL MgCl ₂ 2M 1000 mL deionized water	autoclave at 121°C at 2 bar for 15 min adjust pH to 7
SOC+AMP	20 g Tryptone 5 g Yeast Extract 0.5 g NaCl 10 mL KCL 250 mM 18 mL glucose 20% 5 mL MgCl ₂ 2M 15 g agar-agar 1000 mL deionized water	autoclave at 121°C at 2 bar for 15 min adjust pH to 7 cool down to 60°C add 100 µg/mL Ampicillin
Sodium hydroxide	80 g NaOH 1000 mL HPLC water	Used as 0.2 M concentration, diluted with Millipore water
STC buffer	18.217 g Sorbitol (1 M) 0.5549 g CaCl ₂ (50 mM) 1 mL 1M Tris-HCl pH 8.0 (10 mM) 100 mL distilled water	Sterile filtration (0.45 µm Millex-HA Filter, Millipore, Schwalbach, Germany)
TAE buffer 1x	UltraPure™ TAE-Puffer 50x	Dilution of stock solution to 1x working solution with deionized water
TSS buffer	5 g PEG 8000 0.30 g MgCl ₂ x6H ₂ O 2.5 mL DMSO Add LB medium to 50 mL	Sterile filtration (0.45 µm Millex-HA Filter, Millipore, Schwalbach, Germany)
Wash buffer 10x	100 mM (12.1 g) Tris Base 1000 mL HPLC water	Dilution of stock solution to 1x working solution with deionized water

		adjust pH to 7.6
Wash buffer M	997 mL Maleic Acid Buffer 3 mL Tween 20	autoclave at 121°C at 2 bar for 15 min cool down to room temperature add Tween 20
Wash solution 0.1x	5 mL SSC 20x 5 mL 20% SDS Ad 1 L water (VE)	
Wash solution 0.5x	12.5 mL SSC 20x 5 mL 20% SDS Ad 1 L water (VE)	
Wash solution 2x	100 mL SSC 20x 5 mL 20% SDS Ad 1 L water (VE)	
YBA medium d. c.	20 g yeast extract 20 g bacto peptone 40 g sodium acetate 1000 mL deionized water	autoclave at 121°C at 2 bar for 15 min

7.8 Vectors

pJET2.1/blunt (Fermentas, St. Leon-Rot, DE)

The plasmid pJET1.2/blunt was used for cloning of PCR products in *E. coli*. Because of the *eco47IR* gene, only transformants with insertions are viable. The presence of the ampicillin resistance gene the β -lactamase gene (*bla*) from *E. coli*, allows for the selection of transformants.

pNR1 (Malonek et al. 2004)

Under the control of the *A. nidulans* *oliC* promotor and the *B. cinerea* *tub1* terminator, the pNR1 plasmid contain the Nourseothricin N-acetyltransferase 1 gene (*NAT1*) from *Streptomyces noursei*. Additionally, it carries the resistance gene for ampicillin, the β -lactamase Gen (*bla*) from *E. coli*. This way, resistance to ampicillin in *E. coli* and nourseothricin in fungi is conferred, making this plasmid a "shuttle vector".

7.9 Oligonucleotides

In Table 28 oligonucleotides used as primers for PCR reactions and for Sanger sequencing are listed. Additionally, to the sequence, the annealing temperature (T_m), used polymerase, amplicon size and target/purpose are shown. Oligonucleotides were synthesized internally at BASF SE.

Table 28: Oligonucleotides used.

The sequence is provided in the 5' → 3' orientation.

Name	Sequence (5' → 3')	Orientation	T _m (°C)	Polymerase	Amplicon size (bp)	Target/purpose
KES 2285	AAGGCTGAGCGCCAGGAT	forward	60	DreamTaq	82	PCR primer for pyrosequencing (B-H278Y)
KES 2286	5'biotin- GACACGTCCTTGAGCAGTTGA	reverse				PCR primer for pyrosequencing (B-H278Y)
KES 2287	CATGAGCTTGTACCGAT	forward	57	DreamTaq	50	Sequencing primer for pyrosequencing (B-H278Y)
KES 2317	TTCTACGCTTTCCCCTTCTTCT	forward				PCR primer for pyrosequencing (C-H134R)
KES 2318	5'biotin-AGATGCCTCAAGCCGTTGAA	reverse				PCR primer for pyrosequencing (C-H134R)
KES 2319	TCCCCTTCTTCTTCC	forward				Sequencing primer for pyrosequencing (C-H134R)
KES 2345	CTTTATCTTAATGATGGCTACAGC	forward	52	DreamTaq	60	PCR primer for pyrosequencing (F129L)
KES 2346	5'biotin-TCAAACCATTTGGGCTATGT	reverse				
KES 2347	TTAATGATGGCTACAGCT	forward	49			Sequencing primer for pyrosequencing (F129L)
KES 2539	CGTCAAGACCGAAAGTGCGT	Reverse	65	Phusion	1702	Amplification of <i>CYP51</i>
KES 2592	CCCCGTCAACATTGCCCTT	Forward				
KES 2653	CGGTCTTTGGCAAGGATG	Forward	63	Phusion/ DreamTaq	1258	Amplification of fragment 1 (mutated region with L143F+G446S) and test- PCR with transformed strains
			(with KES 2654)		(with KES 2654)	
KES 2654 ²	gtgcaactgacagtcgtacaGAGGTCATTGC AGCTTCTAC	Reverse	56	Phusion	3441	Amplification of fragment 1 (mutated region with L143F+G446S, L143F, G446S)
			(with KES 2737)		(with KES 2737)	
			63		(with KES 2653)	
					1111	

						(with KES 2654) 1225 (with KES 2661)
KES 2655 ²	gtctggagtctcactagcttTTCGCCTTTTAAC GACGCAC	Forward	65	Phusion	1068	Amplification of fragment 3 (<i>CYP51</i> terminator)
KES 2656	CTCGACGGCTTCCATCACAC	Reverse				
KES 2657	GTTTACGACTGCCCAACTC	Forward	64	Phusion	4613 (with KES 2658)	Nested PCR for cassette with L143F+G446S
					4452 (with KES 2660)	
KES 2658	CCATCACACTGCCTACTTGG	Reverse	64 63 (with KES 2660)	Phusion	4613 (with KES 2657) 4594 (with KES 2662)	Nested PCR for cassette with L143F+G446S, G446S, L143F and sequencing of the final cassette
KES 2659	TCCTACGTCACTCTCATCAC	Forward	63	Phusion	1111 (with KES 2654)	Amplification of fragment 1 (mutated region with G446S)
KES 2660	ACTTCATAAAGCGCCACGAG	Forward	63	Phusion	4452 (with KES 2658)	Nested PCR for cassette with G446S and sequencing of the final cassette
KES 2661	CCAAGTTCATGGAGCAG	Forward	63	Phusion	1225 (with KES 2654)	Amplification of fragment 1 (mutated region with L143F)
KES 2662 ³	CGAAGTTCATGGAGCAGAAG	Forward	62	Phusion	4594 (with KES 2658)	Nested PCR for cassette with L143F
KES 2736	CTCTTGACGACACGGCTTAC	Forward	59	Taq	558 with (KES 2737)	Sequencing of the final cassette, Amplification of <i>nat1</i> probe
KES 2737	GGCAGGGCATGCTCATGTAG	Reverse	56	Taq, Phusion	3441 (with KES 2653) 558 (with KES 2736)	Sequencing of the final cassette and test-PCR with transformed strains, Amplification of <i>nat1</i> probe
KES 2749	CCAAGGTCATGGCCGAAGTTC	Forward	63	Taq	497	Amplification of <i>CYP51</i> probe

KES 2750	CTTCTGGAGGTCTTCGTAGG	Reverse				
KES 2893	TGTACGACTGTCAGTTGCAC	Forward	58			
KES 2894	CACTCCACATCTCCACTCGA	Reverse	59			Sequencing of the final cassette
KES 2895	TAGAGCCGCATTCCCGATTC	Forward	60			
KES 2899	GACTGCCCCAACCTCG	Forward	53			Sequencing primer for pyrosequencing (L143F)
KES 2917	GATCTACTCCCCGCTCT	Forward	55	DreamTaq	139	PCR primer for pyrosequencing (L143F)
KES 2918	5'biotin-ACAAACTGTCTTTGCGTTAG	Reverse	53			
KES 2920	CCCCGAGCACCAGCAATA	Forward				PCR primer for pyrosequencing (G446S)
KES 2921	5'biotin- TTTGTTCCTTGAAACGACA	Reverse	59	DreamTaq	90	
KES 2922	ACGAGGAGAAGATTGAC	Forward	50			Sequencing primer for pyrosequencing (G446S)
KES 2974	ATGGCTGGGGTGTGCTTTC	Forward	58	DreamTaq	132	PCR primer for pyrosequencing (G462S)
KES 2975	5'biotin-ACTCGCGCACGAATGCTA	Reverse				
KES 2976	TCCCTACCTGCCTTT	Forward	51			Sequencing primer for pyrosequencing (G462S)
pJET1.2F ¹	CRACTCACTATAGGGAG	Forward				Sequencing of the final cassette
pJET1.2R ¹	ATCGATTTTCCATGGCAG	Reverse				
TtrPC-F3. Unitail ²	tgtacgactgtcagttgcacCAAACAGCTTGA CGAATCTGG	Forward	63	Phusion	2278	Amplification of fragment 2 (resistance cassette)
UniNours.R3 ²	aagctagtgagactccagacAATCCAAGGG CTTGTGTACC	Reverse				

¹Thermo Fisher Scientific Inc., Waltham, US

²Lowercase nucleotides represent the complementary overhangs

³Red marked nucleotide mark nucleotide substitution C → T

7.10 Abbreviations

SI units and common abbreviations are not listed. Abbreviation for different countries were used according to ISO 3166-1 alpha-2 standard.

a.i.	active ingredient
aa	Amino acid
ABC	ATP-binding cassette
amp	Ampicillin
APS	Adenosine 5' phosphosulfate (an analogue of ATP)
ATP	Adenosine triphosphate
AZ	Azoxystrobin
BBCH	Biologische Bundesanstalt, Bundessortenamt und Chemische Industrie
BOS	Boscalid
bp	Base pair
cDNA	Complementary DNA
CSPD	Chemiluminescence substrate for phosphate detection
Cyp51	Sterol 14 α -demethylase enzyme of <i>A. solani</i>
<i>CYP51/ERG11</i>	Sterol 14 α -demethylase gene of <i>A. solani</i>
<i>CYTB</i>	Cytochrome <i>b</i> gene
d. c.	Double concentrated
dATP	Deoxyadenosine triphosphate
dCTP	Deoxycytidine triphosphate
DEPC	Diethyl pyrocarbonate
DFA	Difenoconazole
dGTP	Deoxyguanosine triphosphate
DIG	Digoxigenin
DJ-PCR	<i>Double joint</i> -PCR
DMI	Demethylation inhibitor
DMSO	Dimethylsulphoxide
DNA	Desoxyribonucleic acid
dNTP	Deoxyribonucleotide triphosphate
dpi	Days past infection
dTTP	Deoxythymidine triphosphate
dTTP	Deoxythymidine triphosphate
EC ₅₀	Effective concentration of 50% inhibition
EPPO	European and Mediterranean Plant Protection Organization
et al.	<i>et alii</i> , lat. and others
FAO	Food and Agriculture Organization of the United Nations
FRAC	Fungicide Resistance Action Committee
FZI	Fluazinam

gDNA	Genomic DNA
Hz	Hertz
kb	Kilo base pair
KRI	Keto-reductase inhibitors
LB	Lysogeny Broth
MDR	Multidrug resistance
MFA	Mefentrifluconazole
MFS	Major facility superfamily
Ms	Mono spore
N	Nitrogen
n	Number
NaCl	Sodium chloride
NaOH	Sodium hydroxide
NAT	Nourseothricin acetyltransferase (<i>NAT1</i>)
NCBI	National Centre for Biotechnology Information
NTC	No-template control
OD	Optical density
PCR	Polymerase Chain Reaction
PEG	Polyethyleneglycol
PTH	Prothioconazole
PYR	Pyraclostrobin
Qol	Quinone outside inhibitors
RF	Resistance factor
RNA	Ribonucleic acid
rpm	Revolution per minute
SBI	Sterol biosynthesis inhibitors
<i>SDH</i>	Succinate dehydrogenase gene
SDHI	Succinate dehydrogenase inhibitor
SDS	Sodium dodecyl sulfate
SNP	Single nucleotide polymorphism
SOC	Super Optimal broth with Catabolite repression
spp.	species pluralis
SSC	Sodium chloride/Sodium citrate
STC	Sorbitol-tris-calcium chloride
TAE	Tris-acetate-EDTA
T _m	Melting temperature
Tris	Tris(hydroxymethyl)aminomethane
UTC	Untreated control
UV	Ultraviolet
v/v	Volume by volume
VE water	Deminerlized water
w/v	Weight by volume
WT	Wildtype

7.11 Curriculum vitae

Beruflicher Werdegang

Seit 07/2024 Project Development Manager for North & Central Europe, BASF SE,
67117 Limburgerhof

Akademischer Werdegang

- 03/2021-07/2024 Doktorandin am Lehrstuhl für Phytopathologie und Pflanzenschutz an
der Martin-Luther-Universität Halle-Wittenberg mit dem Thema
„Mechanisms influencing the sensitivity of *Alternaria solani* causing
Early Blight on potato towards demethylation inhibitors“
- 07/2020 – 01/2021 Masterarbeit am Lehrstuhl für Pflanzenernährung an der Martin-Luther-
Universität Halle-Wittenberg mit dem Thema „Verlagerung und
Umverteilung von Mangan und Eisen in *Arabidopsis thaliana*- Die Rolle
des Metall-Transporters MTP10“
- 01/2020 – 06/2020 Erasmus Semester an der UPV Universitat Politècnica de València
- 10/2018 – 01/2021 Studium der Nutzpflanzenwissenschaften (M.Sc.) an der Martin-Luther-
Universität Halle-Wittenberg 06099 Halle (Saale)
- 07/2018 – 10/2018 Bachelorarbeit am Lehrstuhl für Pflanzenzüchtung an der Martin-
Luther-Universität Halle-Wittenberg mit dem Thema „Genetische
Analyse der alkoholunlöslichen Fraktion von Gerstenstängeln
hinsichtlich des Zellulosegehaltes anhand der multiparentalen
Wildgerstenpopulation HEB-25“
- 10/2015 – 10/2018 Studium der Agrarwissenschaften (B.Sc.) an der Martin-Luther-
Universität Halle-Wittenberg 06099 Halle (Saale)
- Fachrichtung: Pflanzenwissenschaften

Vorträge und Konferenzen

- 05/2024 19. EuroBlight Workshop in Lunteren, Niederlande

Title: Studies on the sensitivity status of *Alternaria solani* towards QoIs, SDHIs and DMIs
- 03/2024 15. NORBARAG Meeting in Helsinki, Finnland

Title: Studies on the sensitivity status of *Alternaria solani* towards QoIs, SDHIs and DMIs
- 09/2023 63. Deutschen Pflanzenschutztagung, Georg-August-Universität in Göttingen, Deutschland

Title: Sensitivity status of *Alternaria solani* towards different fungicides
- 03/2023 42. Jahrestagung der DPG-Arbeitskreise „Mykologie“ und „Wirts-Parasit-Beziehungen“ TU München in Freising, Deutschland

Title: Adaptation of the sensitivity of *Alternaria solani* towards different fungicides
- 05/2022 18. EuroBlight Workshop in Ascona, Schweiz

Poster

- 07/2023 XX International Plant Protection Congress in Athen, Griechenland

Title: Evaluation of the fungicide sensitivity of *Alternaria solani*

Datum

Unterschrift der Antragstellerin

7.12 Danksagung

Meinen besonderen Dank möchte ich Ihnen, Prof. Dr. Deising, aussprechen für die Betreuung meiner Promotion. Ich schätze sehr, wie viel Zeit Sie sich für mich genommen haben und wie Sie mir stets mit hilfreichen Gesprächen und Unterstützung zur Seite standen.

Im besonderen Maße möchte ich mich bei Dir, Dr. Gerd Stammler, bedanken, der mir dieses spannende Thema und die Möglichkeit bot, meine Promotion innerhalb seines Laborteams in der Fungizidresistenzforschung der BASF SE durchzuführen. Gerd, ich kann Dir gar nicht sagen, wie froh ich bin, in deinem Team gewesen sein zu dürfen. Danke für deine fachliche Unterstützung und Expertise. Danke für deine Ruhe, Gelassenheit und deinen Humor, sowie die Tagungen und Meetings, die Du mir ermöglicht hast. Durch deine Art hast Du dazu beigetragen, mich in turbulenten Zeiten wieder auf den Boden der Tatsachen zu holen und nicht vom Weg abzukommen.

Ein weiterer außerordentlicher Dank geht an dich, Dr. Mascha Hoffmeister, die mich während meiner Doktorarbeit betreut hat. Mascha, danke für deine Offenheit, Ehrlichkeit, Kompetenz und dein unglaubliches Fachwissen. Deine Unterstützung hat grundlegend zu meinen Erfolgen der letzten Jahre beigetragen. Danke ebenfalls, für die Korrektur meiner Arbeit.

Vielen Dank an Dr. Iain Proctor für die Unterstützung bei der statistischen Analyse und Dr. Iain Craig für die Unterstützung bei der Erstellung der Proteinmodelle.

Ein großes Dankeschön geht ebenfalls an das Laborteam der Fungizidresistenzforschung und Tino, die mich mit offenen Armen empfangen haben. Vielen Dank an Euch, Gabi, Birgit, Xenia, Sarah, Margit, Kerstin und Beate, die mich stets bei Laborarbeiten unterstützt haben und für ein angenehmes Arbeitsklima gesorgt haben. Ein besonderer Dank geht an Xenia, Gabi und Tino, die mir nicht nur bei fachlichen Fragen eine Unterstützung waren, sondern auch bei sonstigen Sorgen immer ein offenes Ohr für mich hatten. Ohne euch hätte ich so manche Krisen nicht so schnell überwinden können.

Danke ebenfalls an das Freilandteam, Gewächshausteam, Team der Nährbodenküche und allen anderen Kollegen der BASF, die mich bei der Umsetzung meiner Doktorarbeit unterstützt haben.

Des Weiteren möchte ich mich bei Euch, Andrea-Martin-Grand-Mazuir und Dr. Ulf Gröger bedanken. Danke für die Möglichkeit, an verschiedenen Meetings und Tagungen teilzunehmen und für die Bereitstellung des Themas. Liebe Andrea, lieber Ulf, ein ganz besonderer Dank geht jedoch an Euch für eure Unterstützung und Ratschläge bei persönlichen und zukunftsorientierten Fragestellungen. Danke für eure herzliche Art und die Gespräche, die ich mit euch führen durfte.

Zum Schluss möchte ich mich von ganzem Herzen bei meinen Eltern, Yaneth und Jochen, meinen Geschwistern, Paula und Lucas, meinem Freund Matthias und meiner besten Freundin Vanessa bedanken. Mit dem Glauben an mich und dem sicheren Hafen, den Ihr mir immer geboten habt, habt ihr den Grundstein für meine berufliche und persönliche Entwicklung gelegt. Danke für Eure offenen Arme und die Liebe, die aufmunternden Worte und den Rückhalt besonders in den

holprigen Phasen. Ein großer Dank dabei geht an meine Eltern, die mir immer alles ermöglicht haben und mich stets unterstützt haben.

7.13 Eidesstattliche Erklärung

Ich erkläre an Eides statt, dass ich die Arbeit selbstständig und ohne fremde Hilfe verfasst, keine anderen als die von mir angegebenen Quellen und Hilfsmittel benutzt und die den benutzten Werken wörtlich oder inhaltlich entnommenen Stellen als solche kenntlich gemacht habe.

Datum

Unterschrift der Antragstellerin